Contents

Studying the Impact of the Location of Air-Duct Lines on Methane Distribution and Concentration in Dog Headings

Magdalena Tutak[1]***, Jarosław Brodny***[2] *and* ***Kestutis Navickas***[3]

One of the basic issues associated with underground mining is providing a safe atmosphere in mine workings. This includes its chemical composition and reduction of hazardous concentrations of harmful gases. In particular, this applies to driven dog headings that have a one-sided connection to the central ventilation system in the mine. Therefore, it is necessary to use special ventilation systems in these areas. The widespread current methane hazard present in mine workings additionally increases the requirements of these systems. For this reason, the following paper presents the methodology and results of studies that looked at the ventilation system of driven dog headings. The aim of the study was to determine the impact of the location of air-duct lines on methane distribution and concentration in driven dog headings. The basis for the analysis were model studies carried out for the real system and for three additional location variants of air-duct lines forcing fresh air. The studies were carried out for the same real parameters of the air stream and methane emission in the studied dog heading. The results clearly show that the location of studied air-duct lines has an impact on the distribution and concentration of methane in individual points of the driven dog heading. The study also included the fracture zone as a porous centre around the driven dog heading, which enabled more accurate mapping of real conditions. The results broaden knowledge in the field of ventilation issues and should be used in practice.

Keywords: *underground coal mine, methane hazard, dog heading, ventilation, CFD.*

Introduction

An effective ventilation system is essential to ensure a safe and efficient process of underground exploitation of raw materials, including hard coal (Biały, 2013; 2014; 2018, Biały and Fries, 2019; Brodny et al., 2017; Brodny and Tutak, 2019). The main task of this system is to provide the right amount of fresh air, with a specific oxygen content, in the area of mining works, and thus ensuring the appropriate status (composition) of the mine atmosphere (Kurnia et al., 2016; Roghanchi et al., 2016; Tutak and Brodny, 2018; Tutak, 2020; Xiu et al., 2019; Cernecky et al., 2015). This condition should allow miners for free work and prevent the occurrence of dangerous concentrations of methane and other hazardous gases (Ordinance of the Minister of Energy, 2016). These requirements apply to all mine workings. However, for the workings of different specificity, the use of various ventilation systems is needed.

This mainly concerns dog headings driven in coal or gangue, which belong to the so-called "blind" or unidirectional mine workings. In other words, they have only one connection to the central (general) ventilation system of the mine (Brodny and Tutak, 2015). This, in turn, means that both fresh and used air is transported through the same heading (Brodny, 2010; 2011; 2012; Baranov et al., 2017). Fresh air must be supplied to the face zone, where the process of mining the rock mass is carried out, in such a way that it impedes neither the outflow of used air from this zone nor gases entering this heading from the rock mass. Due to their specificity, these headings require the use of a dedicated ventilation method.

For this purpose, the most commonly used method involves the so-called forced air-duct ventilation system, which consists of supplying fresh air to the face of a given dog heading. Through the face zone, this air flows all the way through the entire dog heading to later connect to the stream of used air from other headings and the mine's main ventilation network. A diagram of forced ventilation for the studied driven dog heading with the use of air-duct lines is shown in Figure 1.

This diagram also points to the fracture zone created during mining works (Małkowski et al., 2017; Masny et al., 2017; Prusek and Walentek, 2005; Prusek, 2008; Yang et al., 2019), which has a significant influence on the ventilation process.

In addition to ensuring an adequate composition of air in a dog heading necessary for miners to work in, the ventilation system must not allow for the exceedance of the permissible concentration levels of hazardous gases (Brodny et al., 2018, Krause, 2015; Tutak and Brodny, 2018). Methane is the most dangerous gas present during underground mining works, especially in coal (Zhao et al., 2019). Due to its flammable and explosive properties, methane is a huge threat to both safety and continuity of the mining process. Dog headings driven in coal are particularly vulnerable to the occurrence of hazardous methane concentrations. Methane is released into these dog headings from mined coal and exposed unmined coal as well as cracked ceilings, thills and side walls (Fig 1). Since this gas has a lower density than air, it usually accumulates in the ceiling zone of dog headings and in

[1] *Magdalena Tutak,* Silesian University of Technology, Faculty of Mining, Safety Engineering and Industrial Automation, Akademicka 2, 44-100 Gliwice, Poland, *magdalena.tutak@polsl.pl,*

[2] *Jarosław Brodny,* Silesian University of Technology, Faculty of Organization and Management, Roosevelta 26, 41-800 Zabrze, Poland, *jaroslaw.brodny@polsl.pl,*

[3] *Kestutis Navickas,* Institute of Sustainable Development, Aušros av. 66 A, 76233 Šiauliai, Lithuania, *info@univers.lt*

areas where the air supply is obstructed. They are referred to as dead zones. However, the phenomenon of methane accumulation in the ceilings is called methane layering (McPherson, 1993).

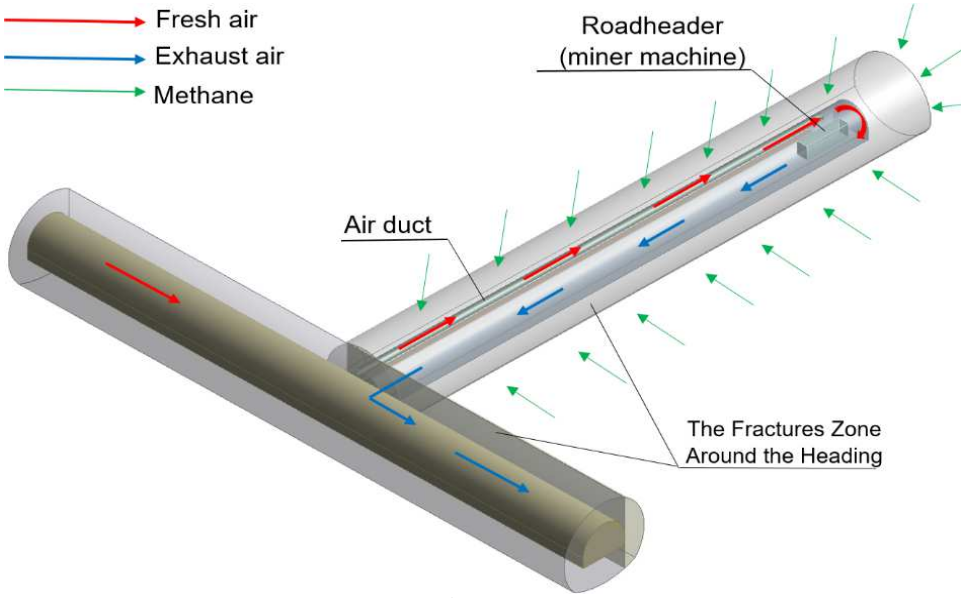

Fig. 1. A scheme of the excavated dog heading

In order to prevent the dangerous accumulation of methane and ensure an adequate atmosphere composition in driven dog headings, it is crucial to adapt the ventilation system and its parameters to the conditions in which mining works are performed. Therefore, the parameters of supplied air are selected depending on the geometry of driven dog headings, temperature and expected amount of methane released.

In addition to the parameters of supplied air, it is also important to properly locate air-duct lines supplying fresh air to dog headings. This mainly concerns headings into which large amounts of methane are released. The location of air-duct lines can affect the distribution of methane concentration in a given dog heading. Therefore, it is reasonable to determine what effect the location of air-duct lines supplying fresh air to a particular heading has on the distribution of methane concentration levels.

Literature on the ventilation systems in dog headings shows deficiencies in this respect although the subject area related to the study of airflows and mixtures of air and methane through dog headings has been presented in many papers (Kurnia et al., 2014a; Kurnia et al., 2014b; Sasimoto et al., 2013).

These papers, like many others, most frequently assumed that methane is released into dog headings from a given point, or from a surface, and only from the face area.

The analysis of literature proves that so far, there have been no studies which would determine the impact of the location of air-duct lines in dog headings on the distribution and concentration of methane. It was therefore assumed that from a scientific and practical point of view, this issue is relevant, and it is reasonable to conduct research in this area.

Therefore, in order to determine the impact of the location of air-duct lines on the distribution and concentration of methane in driven dog headings, model studies were performed in which the actual dog heading was mapped.

In the first stage of model studies, the actual ventilation system that was used in this dog heading was mapped (air-duct lines were located along the ceiling in the heading axis). This helped to establish the distribution of methane concentration. In order to assess the quality of the developed model, the findings were compared with the measurement results. A satisfactory correlation of these results (at three measuring points) enabled the analyses for additional three location variants of air-duct lines in the same heading. In total, four location variants of air-duct lines were analysed. The tests were carried out using numerical fluid mechanics (Kalentev et al. 2017). The calculations were made in the ANSYS Fluent program, based on the Finite Volume Method (FVM).

Due to significant difficulties in conducting studies in real conditions, the use of model studies seems fully justified in this case. The numerical method utilised for calculations enabled very accurate (for good mapping of geometry and reliable boundary conditions) determination of studied parameters, practically at every point of the studied area.

It should be emphasised that the study included the fracture zone around the dog heading. The size of this zone depends on many mining and geological factors. Its size was established based on the research presented in the literature on rock mass mechanics. It was also assumed that this zone is a porous medium with defined

permeability, which was determined using the results of strength tests of the rocks in which the dog heading was being driven. Undoubtedly, this is a new, unused so far approach, which more accurately reflects the real conditions that occur in the rock mass affected by mining activity.

The paper presents the applied methodology, obtained results, discussion and final conclusions.

Materials and Methods

The flow of air in the mine heading was analysed by means of the Finite Volume Method (FVM). This method involves discretisation (in physical space) of the computational domain (the spatial flow area) into a finite number of non-overlapping control volumes. A control volume may be created, depending on the research tool applied, inside the volume of the fluid element or around the volume element node.

The tests were conducted for a spatial model of the area under analysis, using CFD. The authors' experiences and the results presented by other researchers indicate that this method is widely applied for analysing phenomena related to the flows of fluids and dust, the transfer of mass and heat or the processes of combustion (Veersteg and Malalasekera, 2007).

The paper made use of the ANSYS Fluent software (Ansys, 2011), which is one of the most popular tools for the CFD method, whereas the discretisation process was carried out by means of the FVM. The methodology for conducting studies by means of this program encompasses the development of a mathematical model of the phenomenon in question, the adoption of boundary conditions, the performance of calculations, and the analysis of the results.

Mathematical models

The flow of the air and methane mixture is described by the conservation equations for mass, momentum, energy and species transport. The conservation equations for mass, momentum and energy can be expressed as (Kurnia et al., 2014a, 2014b; 2016; Sasmito et al., 2013; Zhou et al., 2017):

$$\nabla \cdot U = 0 \tag{1}$$

$$\rho\left(\frac{\partial U}{\partial t} + U \cdot \nabla U\right) = -\nabla p + \mu \nabla^2 U + F \tag{2}$$

$$\rho\left(\frac{\partial E}{\partial t} + E \cdot \nabla E\right) = k\nabla^2 T + W_s + S_E \tag{3}$$

where: ∇ is the divergence operator, ρ is the air density (kg/m^3), U is the air velocity vector (where $U=u_x, u_y, u_z$) (m/s), t is time (s), ∇p is pressure gradient (Pa), μ is the dynamic viscosity (Pa·s), F is the body force vector (where: $F=F_x, F_y, F_z$), E is energy (J), k is the coefficient of conductivity (W/(m·K)), T is the temperature (K), W_s is the work done by surface stress (J), and S_E is the source term energy (J).

The basis of the mathematical description of the transport process of the methane emission to the driven dog headings is a mass conservation principle related to this gas. Mathematical model of the transport, being a system of equations of advection-diffusion, which for the i-th substance it takes the following form (Ansys, 2011):

$$\frac{\partial}{\partial t}(\rho Y_i) + \nabla \cdot (\rho U Y_i) = -\nabla \cdot J_i + R_i + S_i \tag{4}$$

where: Y_i means the local mass fraction of each species, J_i is the diffusion flux of species i (kg/(m^{2}s)), R_i means the net rate of production of species i by chemical reaction and S_i is the rate of creation by addition from the dispersed phase plus any user-defined sources.

The flow of air-methane mixture through driven dog heading has turbulent character, in which there is an irregular movement of air molecules, and the parameters of its flow experience unpredictable random changes in space and time (Tuliszka–Sznitko, 2011).

Large Eddy Simulation (LES), Direct Numerical Simulation (DNS) and Reynold-Averaged Navier-Stokes (RANS) were used to describe turbulent flows (Fig. 2).

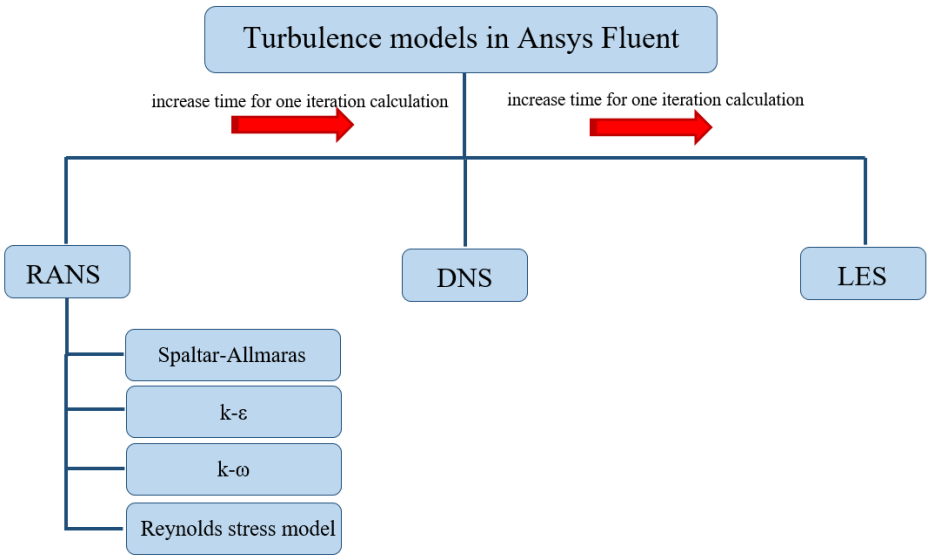

Fig. 2. Turbulence models in the Ansys Fluent software (RANS - Reynold Averaged Navier-Stokes; DNS - Direct Numerical Simulation; LES - Large Eddy Simulation)

For the numerical calculation, there was used the „*k-ε*" turbulence in standard variation model belonging to semi-empirical models, characterising by parameters determined based on experimental tests. This model describes components of Reynolds turbulent stress tensor according to the Boussinesq hypothesis.

Area of research

The basic calculation model was built by means of the real geometrical and ventilation parameters of the driven dog heading in one of the Polish hard coal mines. The basic geo-mining parameters of driven dog heading are as follows:

- Airflow rate: ~ 302 m^3/min;
- Gas emission: ~ 4,0 kg/min;
- The geometry of driven dog heading (height × length × width): 3,0 m × 60,0 m× 4,0 m;
- The length of air duct: 57,0 m;
- The diameter of auxiliary ventilation: 0,8 m.

As already mentioned in the introduction, the model also includes the fracture zone around the dog heading. Due to its permeability, methane migrates from this zone to the driven dog heading. The dog heading model also contains its technical equipment such as air-duct lines, a conveyor and a roadheader. The model of the studied dog heading with marked flow directions, the fracture zone, as well as measurement points and lines, are shown in Figure 3.

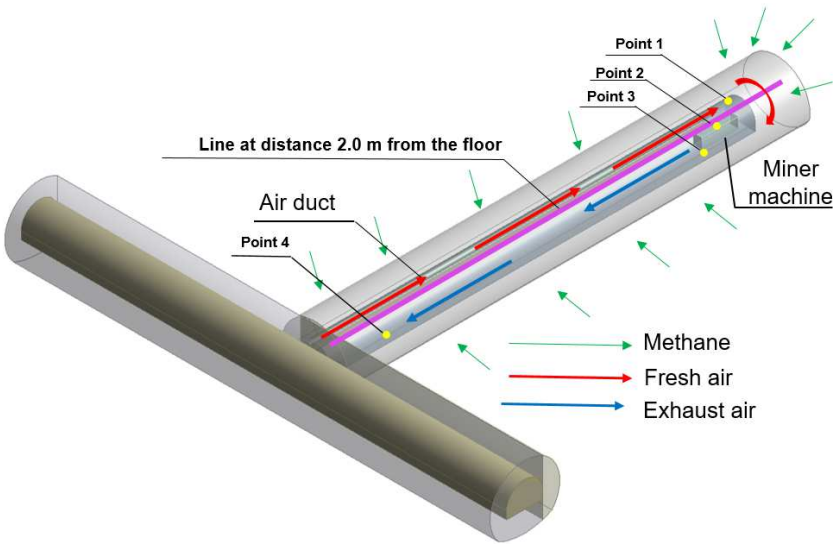

Fig. 3. The geometry of the computational domain of underground driven dog heading with equipment and measurement points and line

The studies were carried out for the real system (Fig. 4a) and three additional locations of air-duct lines in the studied dog heading. The distribution diagrams of the air-duct lines for the studied variants are shown in Figure 4.

The model, along with adopted simplifications, was subjected to numerical analysis. Calculations were made in the ANSYS Fluent 18.2 software. The pressure – velocity coupling and scheme Coupled algorithm, the second-order upwind discretization method and the algebraic multigrid method were used to solve the equations mass, momentum, energy and species transport.

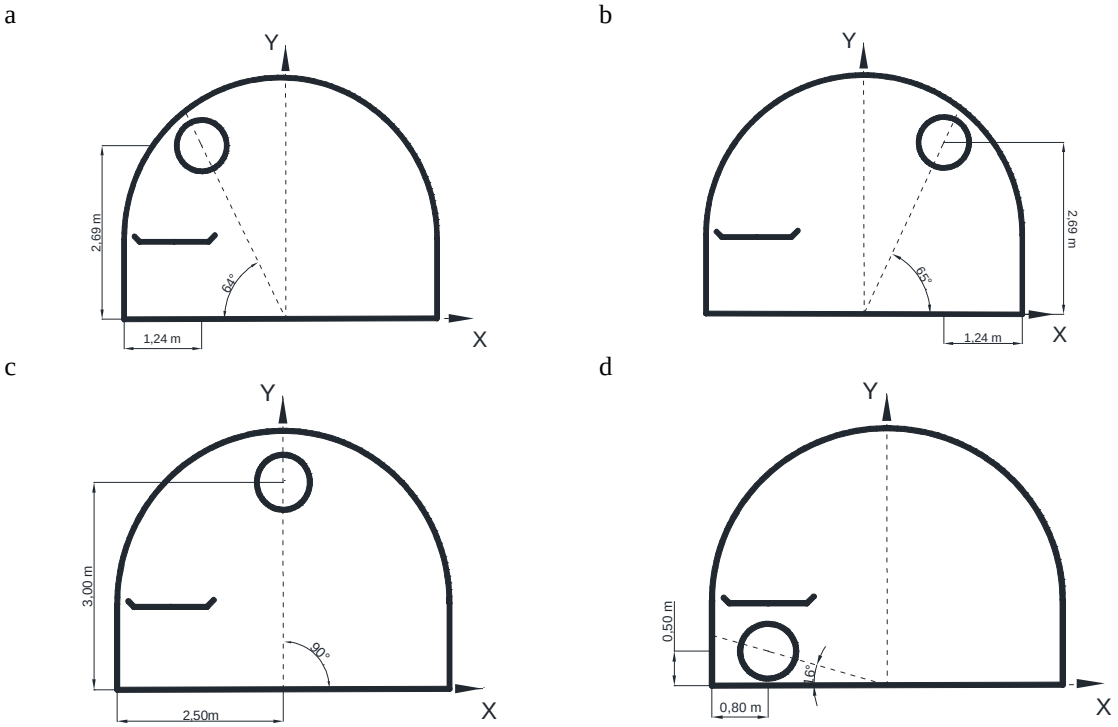

Fig. 4. Distribution diagrams of the air-duct lines for the studied variants (a - left side (constitutes real variants); b – right side; c – the central part of dog heading and d – under conveyor)

Results and Discussion

Based on the analyses, the number of parameters related to the flow of air and methane mixture in the studied dog heading were determined.

Airflow trajectories through the driven dog heading were determined in the first stage of studies for all analysed location variants of the air-duct lines. The way of airflow through this dog heading has a significant impact on the areas of local methane accumulations. The airflow trajectories through the driven dog heading for studied location variants of the air-duct lines are shown in Figure 5.

The analysis of the determined trajectories clearly shows that the largest flow disturbances were reported in the face zone of the driven dog heading (mining zone). An air stream flowing out of the air-duct lines hits the unmined coal being worked on. After bouncing off, it flows through the entire length of the underground dog heading. This creates a vortex movement and air recirculation in the face zone. The phenomenon of the impact of the airstream on the unmined coal leads to the creation of large curvatures of the current line.

The presented trajectories also reveal that taking into account the fracture zone around the driven dog heading leads to a situation where the small amounts of air forced into the face of the driven dog heading, regardless of the location of the air-duct lines, can migrate to the zone in question. This phenomenon disturbs the dog heading ventilation process, which may also be the reason for low-temperature coal oxidation in the fractured side wall (Szurgacz et al., 2019; Tutak and Brodny, 2019). This, in turn, can lead to the occurrence of endogenous fire, which is confirmed by the statistics of endogenous fires in the wall sides and ceilings of driven dog headings (Wyższy Urząd Górniczy, 2019).

On the other hand, the phenomenon of air migration deep into the rock mass through the fracture zone reduces the amount of methane released into the dog heading.

Distributions of methane concentration in cross-sections of the driven dog heading for individual variants are presented in Figure 6. These distributions were located every 10.0 m from the dog heading face. The distribution shown in Figure 6a corresponds to the real system.

a

b

c

d

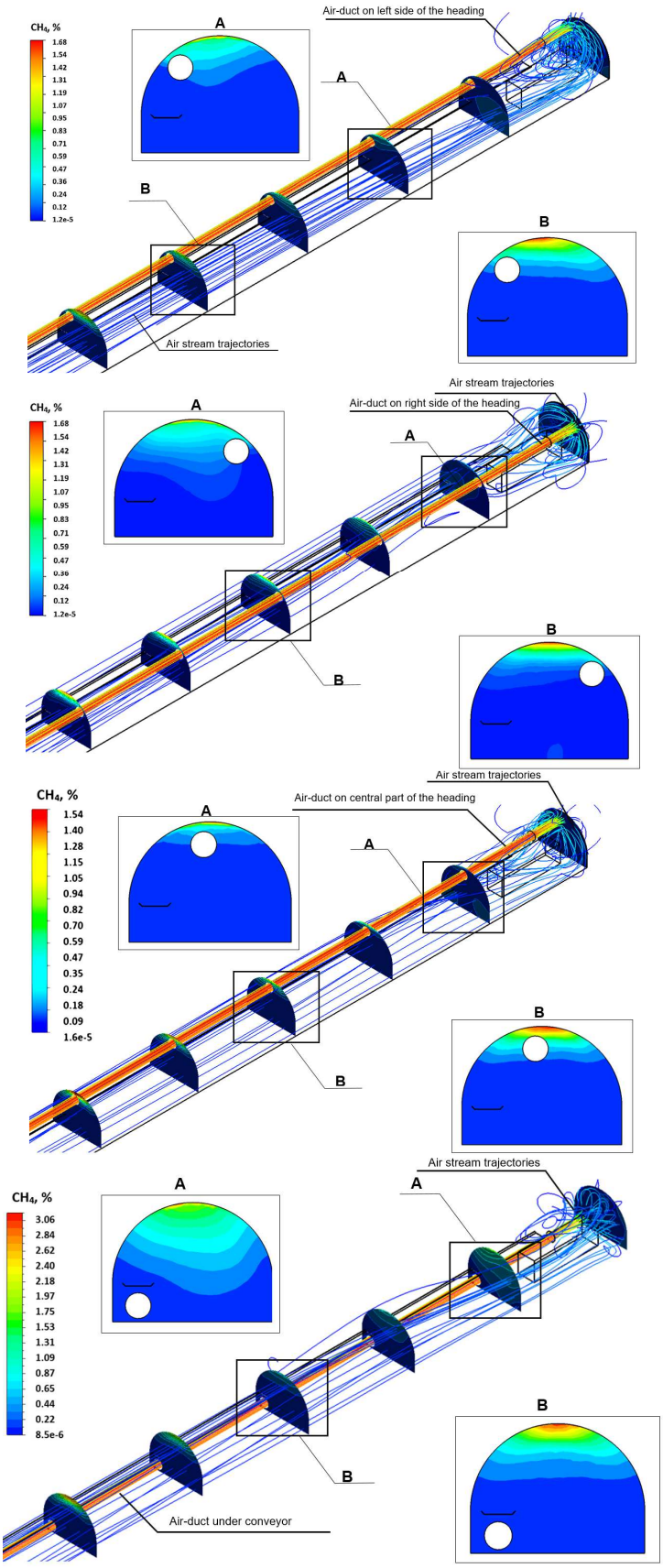

Fig. 5. Distribution of methane concentration in cross-sections of the driven dog heading for different location of air-duct (a - left side; b – right side; c – the central part of dog heading and d – under conveyor)

When analysing the obtained distributions, it can be stated that the location of the air-duct lines in the driven dog heading affects methane distribution and concentration in the studied dog heading. The conducted analyses showed that the most unfavourable situation occurs for the air-duct lines on the thill of the dog heading. For this variant, the local methane concentration levels may exceed 3% (Fig. 5d), while in other cases, these concentration levels do not exceed 1.66%.

The reason for this is the fact that methane, as a gas lighter than air, accumulates near the ceiling of the dog heading, and the air stream flowing out of the air-duct line located on the thill has less impact on the upper part of the dog heading, which creates a zone with higher methane concentration levels.

The most favourable location of the air-duct line in the dog heading is its central part, i.e. for case 3 (Fig. 5c).

The distribution of methane concentration levels in vertical sections of the driven dog heading was also found to be worth mentioning. The results obtained in the cross-sections for studied variants are shown in Figure 6. Due to the fact that during the calculations in the area of boundary conditions "outlet", the reserved flow phenomenon occurred.

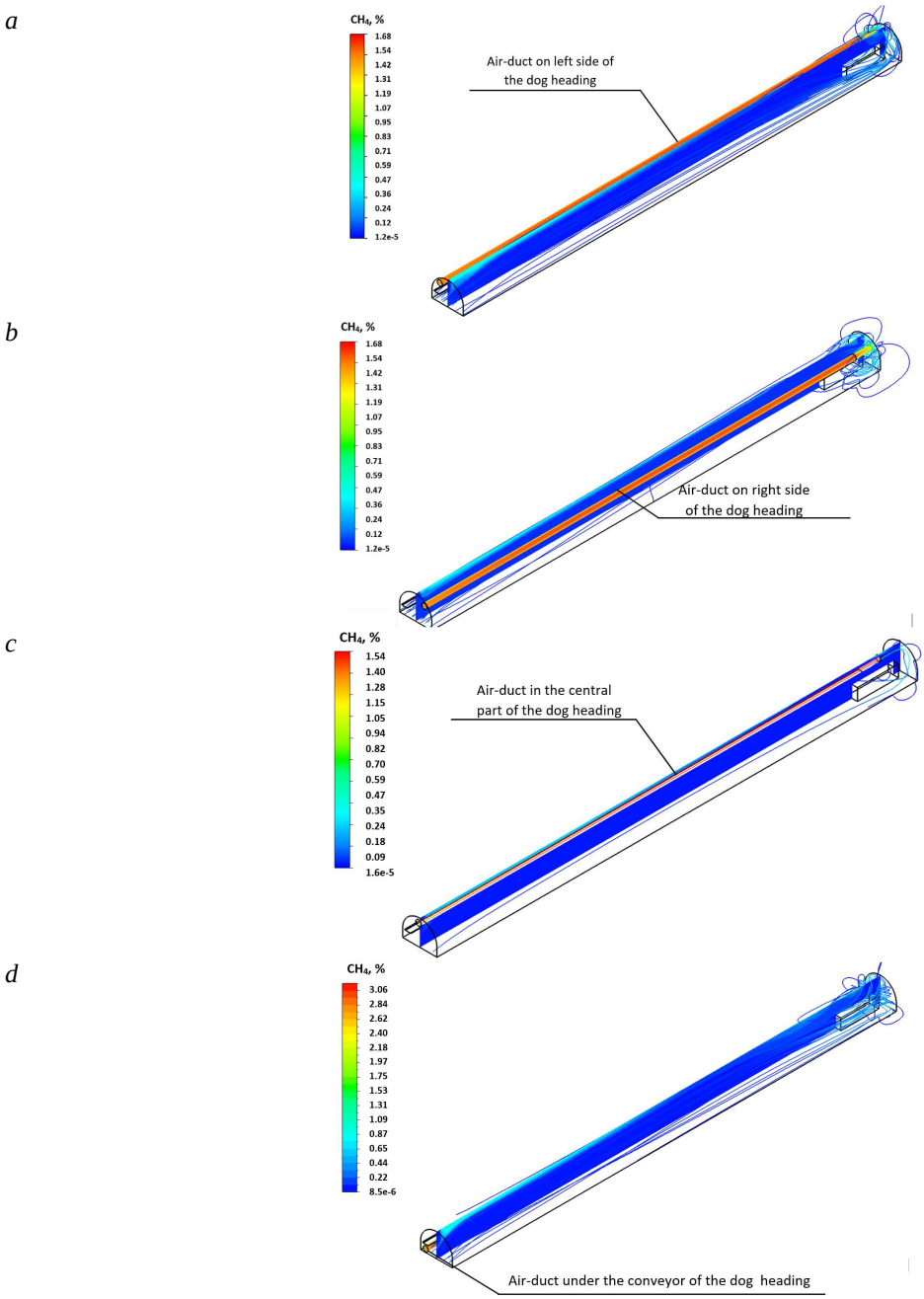

Fig. 6. Distribution of methane concentration in cross-sections of the driven dog heading for different location of air-duct (a - left side; b – right side; c – the central part of dog heading and d – under conveyor)

The results also enabled the determination of the methane concentration value at any point of the dog heading. In order to better illustrate the changes in the value of methane concentration in this dog heading, they were determined for the measurement line.

Figure 7 presents the values of methane concentration levels along the measurement line for studied location variants of the air-duct lines in the driven dog heading.

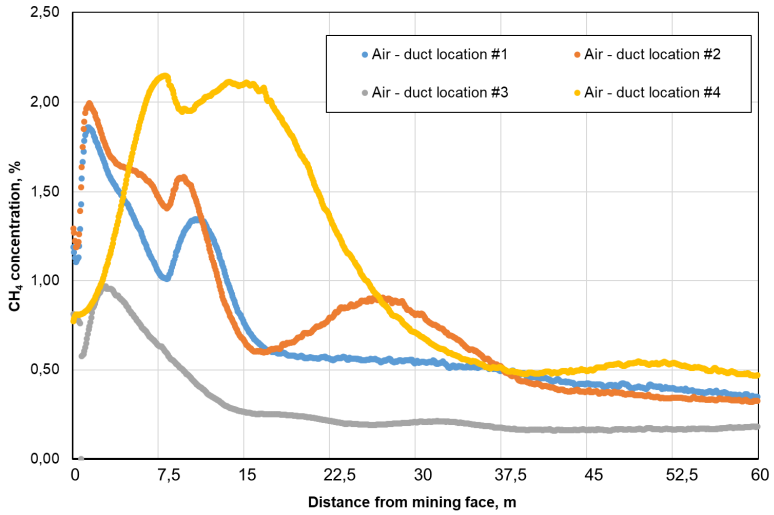

Fig. 7. The distribution of methane concentration along the measurement line in the heading for different location of air-duct (location #1-left side; location #2 – right side; location #3 – the central part of dog heading and location #4 – under conveyor)

Based on the analysis of the results, it can be concluded that the highest methane concentration levels were reported at an altitude of 2.0 m from the thill of the dog heading, along its entire length for all studied variants. These results confirmed that the location of the air-duct lines affects the distribution and, consequently, methane concentration levels in the dog heading.

The lowest methane concentration levels along the measurement lines were reported in the dog heading with air-duct lines located in the central part of the dog heading, under the ceiling (case 3). However, the highest methane concentration levels were observed in the dog heading with air-duct lines located on the thill, under the conveyor (case 4). This is clearly the most unfavourable location of the air-duct lines in the dog heading.

For the variant with air-duct lines located at the sidewall opposite the conveyor (case 2), at a level of around 20 meters, a local increase in methane concentration levels was noted. This phenomenon may be associated with the occurrence of intensive recirculation flow, which is confirmed by the airflow trajectories shown in Figure 5b. The recirculation phenomena can lead to the creation of a zone with weaker air exchange and local elevated methane concentration levels. Around 30 meters from the face, a decrease in the methane concentration values for this variant was shown. This increase applies especially to the measurement line located at a distance of 2.0 m from the thill of the dog heading.

The accuracy of the results was assessed by comparing them with the measurement values in real conditions (for variant 1). The measurement of methane concentration in Polish mines is a point (local) measurement, and it is carried out only in specified places (points). In this case, the location of control points in the numerical model coincided with the location of the automatic methane measurement sensors (Fig. 8).

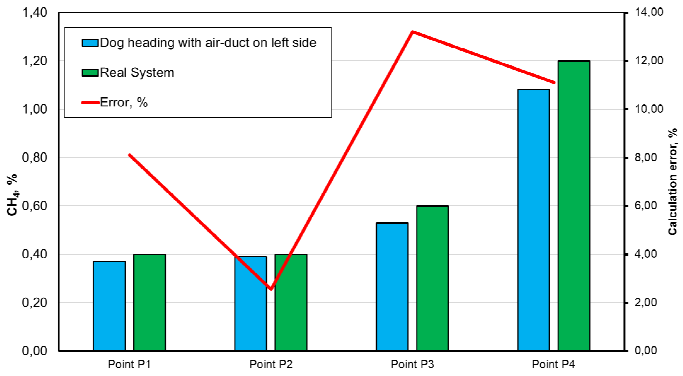

Fig. 8. The comparison of methane concentration values obtained from the measurements in real dog heading with air-duct on the left side and determined from the model studies for the variant with air-duct on left side

Conclusions

The methane hazard is one of the most common and dangerous threats reported in underground hard coal mines. Therefore, for the mining production process, the goal is to avoid a situation in which methane concentration levels in the mine atmosphere reach critical values that may result in either its ignition or explosion. This problem particularly applies to dog headings, which, due to the one-sided connection with the central ventilation system, are particularly exposed to the occurrence of hazardous methane concentration levels.

The methodology of model studies developed and presented in the paper, based on the results of measurements in real conditions, creates great possibilities for the analysis of ventilation conditions in mine headings. The publication focuses on the analysis of the impact of air-duct lines on the distribution and concentration of methane in driven dog headings. The results clearly indicate that the location of air-duct lines has an impact on the distribution of methane concentration in the studied dog heading. These results also enable the location of areas where hazardous concentrations of this gas may occur, which is a valuable source of information for ventilation services.

Both the studies and the results also point to potential areas where air-duct lines can be located and those where it is inadvisable. This is particularly important information when choosing a proper location for them (for example, if limited for technical reasons), or in the event where it is necessary to install an emergency air-duct. In such cases, the results clearly show locations where, for example, methane concentration values should be monitored.

The idea of taking into account the fracture zone around the studied dog heading is also a very essential and undoubtedly valuable achievement of this paper. Undoubtedly, the size of this zone and its permeability has an impact on the physical parameters of the air and gas stream in the dog heading. Its inclusion in the analysis enabled more accurate mapping of real conditions.

It should also be emphasised that the tests and the results broaden knowledge in the field of ventilation system studies. This is particularly crucial for underground mine workings, where ventilation hazards are still being reported, leading to immensely dangerous events.

Therefore, effective forecasting of methane concentration in mine workings is extremely important from the point of view of ensuring the safety of both miners and equipment. The results also prove that the use of model studies combined with the results of tests in real conditions can be successfully utilised for variant analyses of processes related to the ventilation of underground mine workings, as well as in analyses of emergency conditions. These activities should also support the forecasting of ventilation hazards in mine workings.

In addition, it needs to be highlighted that the developed methodology is universal and can be used to analyse other objects.

References

ANSYS. (2011). Ansys Theory Guide; ANSYS, Inc.: Canonsburg, PA 15317., USA.

Baranov, M., Bozek, P., Prajova, V., Ivanova, T., Novokshonov, D., and Korshunov, A. (2017). Constructing and calculating of multistage sucker rod string according to reduced stress. *Acta Montanistica Slovaca, Vol. 22, Issue: 2, pp. 107-115*.

Biały, W. (2013). New devices used in determining and assessing mechanical characteristics of coal. 13th SGEM GeoConference on Science and Technologies In Geology, Exploration and Mining, SGEM2013 Conference Proceedings, June 16-22, 2013, Vol. 1, BUŁGARIA ISBN 978-954-91818-7-6/ISSN 1314-2704. pp. 547-554.

Biały, W. (2014). Coal cutting force measurment systems - (CCFM). 14th SGEM GeoConference on Science and Technologies In Geology, Exploration and Mining, SGEM2014 Conference Proceedings, June 17-26, 2014, Vol. III, BUŁGARIA ISBN 978-619-7105-09-4/ISSN 1314-2704. pp. 91-98.

Biały, W. (2018) Application of quality management tools for evaluating the failure frequency of cutter-loader and plough mining systems. *Archives of Minning Sciences, Volume 62, issue 2, 2017. pp. 243-252*. ISSN 0860-7001. DOI 10.1515/amsc-2017-0018

Biały, W. and Fries, J. (2019) „Computer Systems Supporting the Management of Machines/Equipment in Hard Coal Mines. Case Study" *Management Systems in Production Engineering, Volume 27 issue 3/2019. pp. 138-143*. ISSN 2299□0461. DOI 10.1515/mspe-2019-0022

Brodny, J. (2010). Determining the working characteristic of a friction joint in a yielding support. *Archives of Mining Sciences, 55(4), pp. 733–746*.

Brodny, J. (2011). Tests of friction joints in mining yielding supports under dynamic load. *Archives of Mining Sciences, 56(2), pp. 303–318*.

Brodny, J. (2012). Analysis of operation of new construction of the frictional joint with the resistance wedge. *Archives of Mining Sciences, 57(1), pp. 209–227*.

Brodny, J. and Tutak, M. (2015). Numerical analysis of airflow and methane emitted from the mine face in a blind dog heading. *Management Systems in Production Engineering, 5(2), pp. 110-118.*

Brodny, J., Alszer, S., Krystek, J. and Tutak, M. (2017). Availability analysis of selected mining machinery. *Archives of Control Sciences, 27(2), pp. 197-209.*

Brodny, J., Tutak, M. and John, A. (2018). The impact of airway geometry on the distribution of methane concentrations at the outlet from a longwall. *Mechanika, 24(5), pp. 695-702*.

Brodny, J. and Tutak, M. (2019). Analysing the Utilisation Effectiveness of Mining Machines Using Independent Data Acquisition Systems: A Case Study. *Energies 12, 2505*.

Cernecky, J., Valentov, K., Pivarciova, E. and Bozek, P. (2015). Ionization Impact on the Air Cleaning Efficiency in the Interior. Measurement science review, Vol. 15, Issue 4, p. 156-166

Kalentev, E., Vaclav, S., Bozek, P., Tarasov, V. and Korshunov, A. (2017). Numerical analysis of the stress-strain state of a rope strand with linear contact under tension and torsion loading conditions. *Advances in science and technology-research journal, 11(2) 2, pp. 231-239.*

Krause, E. (2015). Short-term predictions of methane emissions during longwall mining. *Archives of Mining Sciences, 60(2), pp. 581–594*.

Kurnia, J.C., Sasmito, A.P. and Mujumdar, A.S. (2014a). CFD simulation of methane dispersion and innovative methane management in underground mining faces. *Applied Mathematical Modelling, 38(14), pp. 3467–3484.*

Kurnia, J.C., Sasmito, A.P. and Mujumdar; A.S. (2014b). Simulation of a novel intermittent ventilation system for underground mines. *Tunnelling and Underground Space Technology, 42, pp. 206–215.*

Kurnia, J.C., Xu, P. and Sasmito, A. (2016). A novel concept of enhanced gas recovery strategy from ventilation air methane in underground coal mines e A computational investigation. *Journal of Natural Gas Science and Engineering*, 35, pp. 661-672.

Ordinance of the Minister of Energy *On detailed requirements for conducting underground mining operations* of 23 November 2016 (Journal of Laws of 2016, No. 2017, item 1118, as amended).

Małkowski, P., Ostrowski, Ł. and Bachanek, P. (2017). Modelling the Small Throw Fault Effect on the Stability of a Mining Roadway and Its Verification by In Situ Investigation. *Energies, 10, 2082.*

Masny, W., Prusek, S., Mutke, G. (2017). Numerical Modeling of the Dynamic Load Changes Exerted on the Support in the Stress Concentration Zones. *Procedia Engineering, 191, pp. 894-899.*

Prusek, S. and Walantek, A. (2005). Wielkość strefy zniszczenia górotworu wokół wyrobiska korytarzowego w oparciu o kryteria Hoeka-Browna. *Prace Naukowe GIG. Seria Konferencje, 49, pp. 13–24*.

Prusek, S. (2008). Modification of parameters in the Hoek-Brown failure criterion for gate road deformation prediction by means of numerical modeling. *Glückauf*, 9, pp. 529-534.

McPherson, M.J. (1993). Subsurface Ventilation and Environmental Engineering. Chapman & Hall, New York.

Roghanchi, P., Kocsis, K. and Sunkpal, M. (2016). Sensitivity analysis of the effect of airflow velocity on the thermal comfort in underground mines. *Journal of Sustainable Mining, 15(4), pp. 175–180*.

Sasmito, A.P., Birgersson E., Hung C. and Mujumdar, A.S. (2013). Some approaches to improve ventilation system in underground coal mines environment – A computational fluid dynamic study. *Tunneling and Underground Space Technology, 34, pp.82–95.*

Szurgacz, D., Sobik, L. and Brodny, J. (2019). Integrated method of reducing the threat of endogenous fires in hard coal mines. *E3S Web of Conferences, 105, 01013.*

Tuliszka–Sznitko, E. (2011). Wybrane zagadnienia z mechaniki płynów wirujących. WPP, Poznań.

Tutak, M. and Brodny, J. (2018). Analysis of the impact of auxiliary ventilation equipment on the distribution and concentration of methane in the tailgate. *Energies 11*, 3076.

Tutak, M. and Brodny, J. (2019). The Impact of the Strength of Roof Rocks on the Extent of the Zone with a High Risk of Spontaneous Coal Combustion for Fully Powered Longwalls Ventilated with the Y-Type System—A Case Study. *Applied Sciences, 9, 531*.

Tutak, M. (2020). The Influence of the Permeability of the Fractures Zone Around the Heading on the Concentration and Distribution of Methane. *Sustainability, 12, 16.*

Veersteg, K.K. and Malalasekera, W. (2007). An Introduction to Computational Fluid Dynamics. The Finite Volumne Method; Pearson Education: London, UK.

Wyższy Urząd Górniczy. (2019) Available online http://www.wug.gov.pl/bhp/stan_bhp_w_gornictwie (accessed on 15 November 2019).

Xiu, Z., Nie, W., Yan, J., Chen, D., Cai, P., Liu, Q., Du, T. and Yang, B. (2019). Numerical simulation study on dust pollution characteristics and optimal dust control air flow rates during coal mine production. *Journal of Cleaner Production*, 119197.

Yang, H., Han, C., Zhang, N., Sun, C., Pan, D. and Dong, M. (2019). Stability Control of a Goaf-Side Roadway under the Mining Disturbance of an Adjacent Coal Working Face in an Underground Mine. *Sustainability, 11, 6398*.

Zhao, J., Qin, Y., Shen, J., Zhou, B., Li, C. and Li, G. (2019). Effects of Pore Structures of Different Maceral Compositions on Methane Adsorption and Diffusion in Anthracite. *Applied Sciences, 9, 5130*.

Zhou, G., Zhang, Q., Bai, R., Fan, T., Wang, T. (2017). The diffusion behavior law of respirable dust at fully mechanized caving face in coal mine: CFD numerical simulation and engineering application. *Process Safety and Environmental Protection*, 106, pp. 117-128.

Comparison of 2.5D Volume Calculation Methods and Software Solutions Using Point Clouds Scanned Before and After Mining

***Martin Štroner*[1], *Tomáš Křemen*[1], *Jaroslav Braun*[1], *Rudolf Urban*[1], *Peter Blistan*[2] *and* *Ludovít Kovanič*[2]**

The development of contactless mass data collection methods such as laser scanning or digital photogrammetry leads to the development of a wide variety of algorithms and calculations that can be applied to such data. The volume calculation of material that was mined away is one of such applications. This paper compares available software solutions capable of calculating volume, namely commercially available programs Atlas DMT, 3D Reshaper, Leica Cyclone and Trimble RealWorks, and an open-source program CloudCompare. All of these are commonly applicable for general point cloud processing, and volume calculation is just one of the functions offered by the programs. Two principal types of algorithms are used by those software solutions – grid-based algorithms and algorithms based on a triangular irregular network created from the point cloud. Some of the tested programs offer both calculation methods. The experimental testing of the accuracy of those programs was performed on real data from a quarry where laser scanning was used in combination with a GNSS method. The individual software solutions were used to calculate the scanned area, volume calculations using various settings and processing demands (expressed as processing time). Besides, the algorithms used in individual programs, their limitations and specific problems are discussed. Grid-based methods turned out to be very effective due to the low processing time and very good provided results even for relatively large grid cells. TIN-based methods, on the other hand, also provide very accurate results, the processing time is, however, substantially higher. In some cases, the quality of the results also depends on the algorithm constructing the triangular network itself.

Keywords: *volume, comparison, Atlas DMT, 3D Reshaper, Leica Cyclone, Trimble RealWorks, CloudCompare.*

Introduction

The availability and practical utilization of mass data collection technologies such as 3D scanning (terrestrial, airborne) or multi-image intersection photogrammetry from terrestrial or airborne images (acquired, for example, using fixed-wing aircraft or multicopters) processed by SfM (Structure from Motion) grows (Bartos et al., 2019; Blistan et al., 2016; Blistan et al., 2019; Kršák et al., 2016; Pukanská et al., 2014; Rusnák et al., 2018; Blistan et al. 2020). Thus acquired point clouds are subsequently utilized for various purposes, including volume calculations, for example, for heaps of loose material (Tucci et al., 2019; Salagean et al., 2019), determining the volume of material that has been mined away (Stojcsics et al., 2018; Zápalková et al., 2011), of concrete (Martínez-Sánchez et al., 2016), quantification of morphological changes (Medjkane et al., 2018), pinpointing landslides (Tang et al., 2019), determining the amount of transported loose material (He et al., 2019), and many others.

For volume calculations, it is often necessary to combine such dense data with data acquired using geodetic methods such as GNSS or total station. Such methods provide significantly lower data density but are irreplaceable where, for example, dense vegetation or other obstacles to laser scanning are present.

Multiple algorithms of determining volume from the above-described data have been developed. For practical usage, it is, however, necessary to know the degree to which a selection of an algorithm or settings affects the results.

Many of the above mentioned (and other) papers describe the methods used for determining volume in detail, but the accuracy of the results (and comparison with reality) is not sufficiently discussed, despite the fact that many authors dilute the point clouds massively prior to the volume calculations, which may impact the accuracy. Few studies have compared methods of point cloud-based volume calculations. One of the few was published by Urbancic et al. (2015), where the authors analyse their own calculation methods and methods of interpolation on the resulting volumes. Nevertheless, using own scripts/software is not feasible for everyone and often not for high volume data, and hence, the use of ready-made software solution is in practice usually the preferred method.

In our study, multiple algorithms implemented in various freely or commercially available software solutions have been applied to the same point cloud to quantify the effects of individual algorithms on the

[1] *Martin Štroner, Tomáš Křemen, Jaroslav Braun, Rudolf Urban*, Czech Technical University in Prague, Faculty of Civil Engineering, Department of Special Geodesy, Thákurova 7, Prague 6, 166 29, Czech Republic, *martin.stroner@fsv.cvut.cz, tomas.kremen@fsv.cvut.cz, jaroslav.braun@fsv.cvut.cz, rudolf.urban@fsv.cvut.cz*

[2] *Peter Blistan, Ludovít Kovanič*, Institute of Geodesy, Cartography and Geographical Information Systems, Faculty of Mining, Ecology, Process Control and Geotechnology, Technical University Kosice, Park Komenského 19, 04001 Košice, Slovak Republic, *peter.blistan@tuke.sk, ludovit.kovanic.2@tuke.sk*

calculation. Namely, we will apply various methods for volume calculation on data from real 3D scanning that are non-homogenous in density (due to the necessity to manually determine coordinates of some areas by GNSS), and compare their results. Limitations of individual software solutions and settings as well as algorithms used in the individual methods as well as the temporal and economic demands of individual software solutions will be discussed. Both commercially and freely available software solutions utilising triangular network as well as grid-based 2.5D algorithms (which are the most commonly used for groundworks volume calculations) will be tested. Of the commercially available software solutions, Atlas DMT, 3D Reshaper, Leica Cyclone and Trimble RealWorks have been chosen for testing; CloudCompare was used as a representative of freely available software solutions.

Data

The utilised data have been acquired in the Trebejov quarry in Eastern Slovakia, between Prešov and Košice (Fig. 1). In this quarry, dolomite is being mined in a five-level quarry with the height of individual mining walls between 16 and 25 metres. The top of the quarry is covered by mature beeches and oaks that are being gradually removed in line with the needs of mining progress.

The data was acquired by terrestrial scanning using 3D scanning system Leica C10 in two time epochs; the first scanning was performed in October 2011, the other after rock blasting in February 2012. A geodetic network was permanently stabilized using bolts and used for pinpointing control points. Scanner settings were identical during both scannings, i.e., 20 mm spacing at 50 m.

The data was complemented by a ground survey of the top of the quarry before and after blasting using GNSS RTK in places where scanning would not provide reliable data. As far as the data density is concerned, the data is, therefore, non-homogeneous. The accuracy of the points surveyed using GNSS is lower than that of data measured by laser scanning, with standard deviations of approx. 25mm horizontally and 50mm vertically. This, however, represents no problem for our study as the crucial consideration here is that the data was identical for all methods of calculation. In other words, we needed to compare all algorithms on the same real data; the accuracy of the actual volume calculation is only secondary.

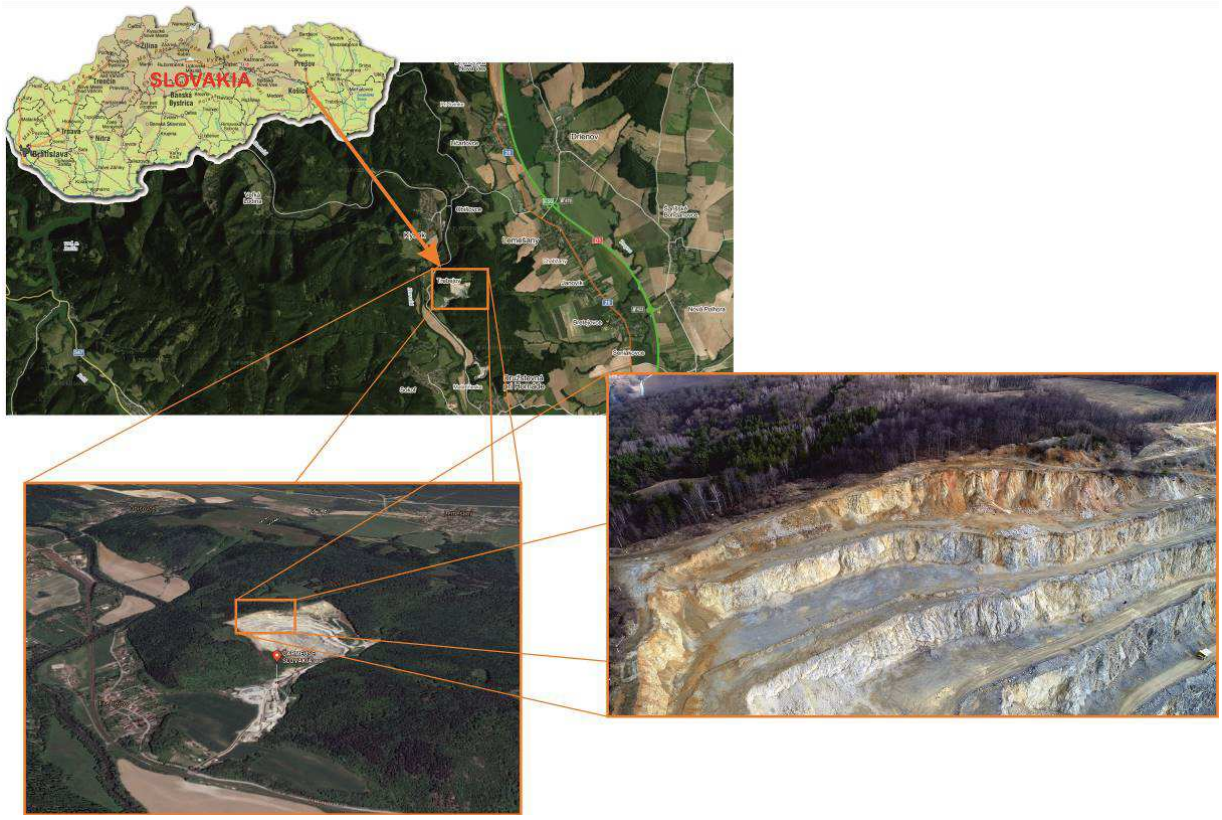

***Fig. 1**: The Trebejov quarry*

Firstly, the original point clouds were adjusted to allow their processing in all tested software solutions. Fig. 2 shows a visualization of the point clouds (top – October 2011, middle – February 2012, bottom – cropped overlay).

The points that were not on the ground (mining equipment, stabilization of control points, etc.) were removed from the cloud. Further, all data were tilted in the same way to remove vertical overlaps, which is necessary for using 2.5D algorithms, and cropped to cover the same area in the XY plane.

The images obviate that our data indeed represent real data, including all common imperfections and problems such as non-homogeneity, holes caused by obstacles, etc. Data 1 (from 2011) contain altogether 6,220,168 points while data from 2012 (Data 2) comprise 3,213,671 points (both including GNSS points). The difference in the number of points is caused by the fact that Data 1 was scanned approximately from half the distance than Data 2, utilising the same scanner settings (the same angle spacing).

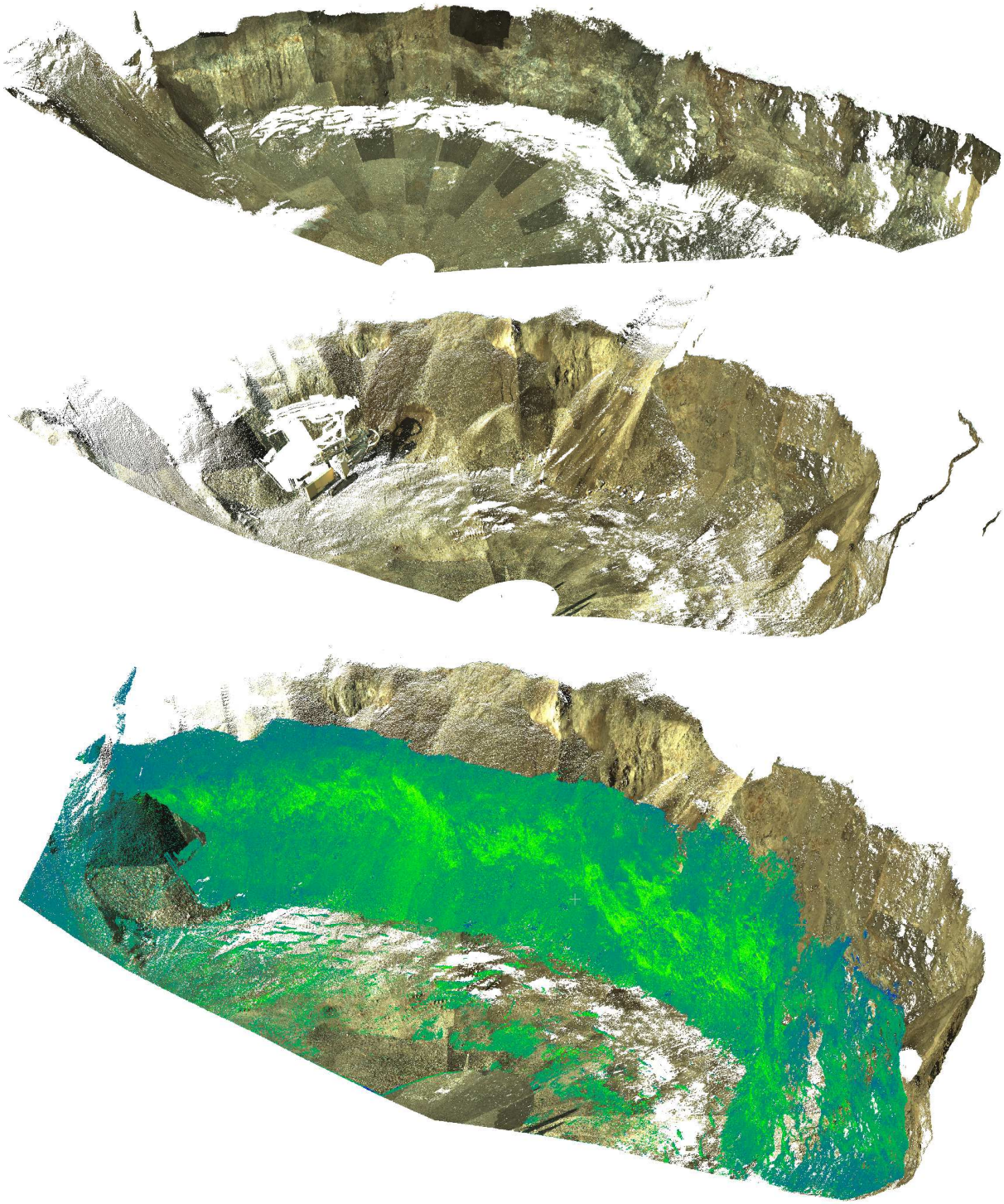

Fig. 2. Used data: top – Data 1 (2011); middle – Data 2 (2012); bottom – cropped overlay

Used software and calculation algorithms

Below, the individual software solutions used for testing and their volume calculation algorithms will be described. All used software solutions utilize 2.5D algorithms, which means that for the correct calculation, no vertical overlaps of the data in the individual models are allowed. The results of the computation in individual programs usually produce summation of values with a positive sign (i.e., volume increase, added material), of those with a negative sign (volume decrease, material mined away) and the total summation providing the overall balance.

Atlas DMT ver. 19.08.1

The primary purpose of the commercially available software Atlas DMT (Atlas, spol. s.r.o., Czech Republic) is processing elevation data (both individually surveyed points or point clouds) and transforming them into digital terrain models that can be subsequently further analysed or used for generating graphical outputs.

The term Digital Terrain Model (DTM) means a model of a surface area covering the surveyed terrain. The model is constructed as a 3D combination of points, lines and faces from the input data. Where such data is missing, estimation of the additional surface is calculated to estimate the real surface. The calculation between the points is not based on linear interpolation but uses terrain smoothing. The version used for analysis in this study allows work with up to 666 mils. points and costs, including the volume calculation module, approx. 3850 Eur (http://www.atlasltd.cz/atlas-dmt.html).

The input point cloud and, if applicable, predefined compulsory lines are used to generate an irregular triangular network (TIN), which is used for all Atlas DMT applications and computations. When generating the model, the data are first sorted according to the positions of the points, named and checked for duplicities. Where there are two points too close to each other, one of them is excluded from the following steps. In the presented case, the default settings considering points within 1mm of space as duplicates were kept. In the next step, the triangular network is created and optimized in the projection into the XY plane. A convex model envelope is created as well, which however may lead to creating triangles with acute angles and to generating connecting lines between points that are not associated in the terrain. This is prevented setting up criteria which, when met, mark the triangle as an envelope and is not used further for the actual calculation. In standard settings, the criteria for envelope triangles are an angle opposite the envelope edge greater than 140º or a ratio of the envelope edge and the neighbouring side greater than 2.5. Here, the settings were amended to consider only the condition of an angle greater than 170º. Envelope triangles were manually edited after generalization to achieve a maximum area of the model. This setting was selected to make the model comparable with models from other software solutions, although we are aware that this is not correct from the perspective of land surveying.

ATLAS DMT offers two methods for calculating the volumes of the triangular terrain model against a comparison plane or against another triangular network.

The first one is a regular grid method. The volume is calculated only over the area of model overlap. A regular square grid with a set resolution (step) covering the entire area of interest is created, and the elevation value from the centre of each square (bottom square – one model, top square – the other one) is taken for calculation of the volume of the individual prisms (base area x elevation difference). The elevations are determined from smoothed out triangular models.

The other method uses the blending of the triangular networks in the overlap area (envelope triangles are excluded from the calculation). As the original triangles of the two DTMs are not identical in their positions and angles, they are broken into smaller (secondary) triangles with matching base areas. The heights of individual vertices of the triangular prisms are determined as the elevation difference of the individual vertices, which in turn are calculated from the original unsmoothed triangles. The total volume is calculated as a sum of volumes of all individual secondary triangular prisms.

CloudCompare ver. 2.9.1

A freely available open-source software for working with point clouds and triangular meshes can be downloaded from www.cloudcompare.org (Version 2.9.1 was used in this study). This software allows a wide range of operations, including point cloud transformations, their filtering, classification, mutual comparison, etc. It also allows volume calculations both against a comparison plane and against another point cloud. The first step is rasterization of the point cloud, splitting it with a set step into square cells in the XY plane (although XZ or YZ planes are also possible). Subsequently, an average elevation value from all points in the square is calculated. Where there are no points in the cell, the elevation value can be determined as a minimum value from the whole grid, average value from the whole grid, user-defined value, or interpolation from the surrounding cells (only within the convex envelope). The volume calculation itself is then elementary – an elevation difference of

surfaces in individual cells is multiplied by the cell base area to acquire the volume differences of individual prisms.

Leica Cyclone ver. 9.4.2

The commercially available software by Leica (https://leica-geosystems.com/products/laser-scanners/software/leica-cyclone), originally developed for processing data acquired using their 3D scanners, costs 13850 Eur. Leica Cyclone uses the method of prisms for calculation. The two TINs are blended and based on the combination of the triangles from both networks, new (secondary) triangular bases are formed, similar to the second method used in Atlas DMT. This huge number of formed triangles also, of course, increases the number of prisms and the necessary processing time and memory demands. Before the TINs are blended, a normal for the new network can be set in either of the X, Y, Z axes. Should a normal in another direction be needed, the full data must be tilted prior to combining models. When creating a TIN network, it is possible to set the number of points for generating the network. The standard setting shows 500,000 points; the maximum recommended number is 2 mil. points. It is possible to generate an even greater network, however considering its further use for calculating differences and processing demands associated with such network, it cannot be recommended as even high-performing computers often end up with memory overflow or, best case scenario, is taking many hours to perform this task. Once both networks with secondary triangles are created, the original and secondary (new condition, in our case after blasting) TINs are selected by the user, and the calculation is performed (algorithm not made public by the software producer).

3D Reshaper ver. 18.0.7.28912

This software, originally costing approx. 11,500 Eur, is by now sold under the new brand Leica Cyclone 3DR (10,000 Eur). This software only allows volume computation between two networks. The manufacturer's description of the algorithm is as follows: „For the computation of the volume of two surfaces, the software uses a direction for the calculation of the cubature. This direction will be used to calculate projections that will generate elementary objects (tetrahedrons) from which we can calculate an overall volume. The direction must be the direction according to which you see the best the mesh with the minimum of hidden parts (usually according to Z). We create a tetrahedron by a triangle, taking as the vertex the centre of gravity of the mesh, and we add each volume to have the total volume. In the example of a sphere, it seems trivial. But in the case of more complex shapes, this calculation may seem to be false; but some tetrahedrons are found with a negative volume (depending on the orientation of the triangle of the base) which compensates the whole result and makes the calculation accurate no matter the shape of the model." (Acquired by personal communication from representatives of 3D Reshaper).

Trimble RealWorks ver. 11.1.1.442

The commercial RealWorks software (approx. 6900 Eur) serves for processing and analyses of point clouds acquired from 3D laser scanning (https://geospatial.trimble.com/products-and-solutions/trimble-realworks). This software uses 2.5D algorithms (a) calculating the volume directly from the point clouds or (b) a hybrid algorithm calculating the change of volume using a grid overlaying a triangular network. In the first case, the calculation utilizes a regular square grid of customizable size (step/grid size and direction of the calculation can be set). After the calculation, the software creates a graphical representation of individual cuboids. If the point clouds are not homogenous, the volume difference in the grid cells containing points from one point cloud only is not approximated – the software does not perform any automatic interpolation between the points. It is, therefore, necessary to edit such calculation to make the software calculate the differences in these areas as well. Such "holes" must be manually delimited and filled using the tool "Fill holes". The results detail the added (+) and mined away (-) volumes as well as the size of the areas where any volume was added or removed.

The other method uses a hybrid algorithm. The software allows the operator to set a normal for computing a triangular network. It is possible to choose the main axes, ideal point cloud fitting, or other options. The point clouds are transformed into two triangular networks used for volume calculation in the direction of the selected normal. However, for the computation itself, the software uses a grid with an optional cell size again; it is, therefore, a combined calculation method based on a created triangular network representing the surface, but the points for the volume calculation itself are acquired using a grid projected on the triangular network.

Testing methods

The respective methods of volume calculation were applied to the data processed as described above. Where the particular software allowed multiple settings or algorithms, all realistically applicable ones were used.

As each software has a different interface and allows different settings, at least some criteria were adhered to where possible to simplify the evaluation of the results. In principle, we can distinguish between algorithms using grid and TIN. For grid solutions, the raster size represents the principal setting, hence multiple cell sizes have been used, namely: 0.005; 0.010; 0.020; 0.050; 0.100; 0.200; 0.500; 1.000; 2.000; 5.000; and 10.000 m cell size. Besides, the interpolation of empty cells from the surrounding cells was applied. It is, however, not possible to unify the settings of triangular networks in a similar way; therefore, the settings were individual and are detailed in the description of the particular software solutions. Comparing the resulting values can then provide information on the magnitude of error associated with the use of particular software, algorithm and setting, as well as its pros and cons. A question remains, which of the methods (if any) can be considered as the most accurate. Considering the principles of the methods, it appears that the TIN-based method used in Atlas DMT makes no or only minimum simplification and uses practically all points for constructing the triangular mesh (except for the practically duplicate points); hence, the value calculated by this method should be the most accurate.

All computations were made using a laptop with Intel i7, 32 GB RAM and a graphics card with a dedicated memory of 6GB.

Results

Atlas DMT

Table 1 shows the results of the grid computation using Atlas DMT. In our case, a difference model with 27,578,415 points, 80,986,334 edges (connecting lines) and 53,990,888 triangles was constructed. The import of the point clouds, generalization and optimization of the triangular network took approx. 1.5 hour; the volume calculation using the triangular networks 3 hours while only using the raster method, the calculation was completed within a few minutes.

Tab. 1. Atlas DMT – results of grid-based volume calculations

Raster size [m]	Number of cells	Surface [m²]	Volume⁺ [m³]	Volume⁻ [m³]	Volume^{total} [m³]	Difference [%]
0.005	*83,840,800*	2,096.02	72.94	-4,280.02	-4,207.08	0.00
0.010	*20,960,100*	2,096.01	72.94	-4,280.02	-4,207.08	0.00
0.020	*5,240,050*	2,096.02	72.94	-4,280.02	-4,207.08	0.00
0.050	*838,416*	2,096.04	72.94	-4,280.01	-4,207.07	0.00
0.100	*209,614*	2,096.14	72.93	-4,280.10	-4,207.17	0.00
0.200	*52,394*	2,095.76	72.94	-4,280.30	-4,207.36	0.01
0.500	*8,384*	2,096.00	72.93	-4,279.78	-4,206.84	0.01
1.000	*2,097*	2,097.00	73.17	-4,282.43	-4,209.27	0.05
2.000	*523*	2,092.00	73.74	-4,285.93	-4,212.20	0.12
5.000	*83*	2,075.00	71.58	-4,244.68	-4,173.10	0.81
10.000	*21*	2,100.00	15.93	-3,622.04	-3,606.11	14.28

The calculation from the triangular method yielded the following results: Area 2096,02 m^2, volume$^+$ 72,94 m^3, volume$^-$ -4280,02 m^3, volume ^{total} -4207,08 m^3. As mentioned above, this result can be considered as the most accurate due to the use of (almost) all points with minimum simplification.

The grid-based calculations reveal that, surprisingly, there is no change in the accuracy of the results up to the 2.0 raster size (results are presented in Tab. 1, where Difference column shows relative (percentage) changes to the most accurate value (first) in this table). For better comprehension, 10m^3 represents approx. 0.2 % of the total volume. The results acquired using the TIN and grid method, therefore, correspond very well to each other.

CloudCompare

Volumes were calculated using the above-described method within several minutes. The results are shown in Table 2. Here, we again observe that some grid coarsening (in this case, up to 0.2m) preserves the same result accuracy; from the grid size of 0.5 m, the error slightly grows, but even for a 1.0 m grid, the error represents only approx. 1.4 % of the total volume.

Tab. 2. CloudCompare – results of grid-based volume calculation

Raster size [m]	Number of cells	Surface [m²]	Volume⁺ [m³]	Volume⁻ [m³]	Volume^{total} [m³]	Difference [%]
0.005	84,038,480	2,100.96	73.000	4,280.09	-4,207.09	0.00
0.010	21,010,210	2,101.02	73.13	4,279.88	-4,206.75	0.01
0.020	5,253,430	2,101.37	73.04	4,279.76	-4,206.72	0.01
0.050	841,085	2,102.71	73.45	4,279.87	-4,206.42	0.02
0.100	210,453	2,104.53	72.92	4,287.80	-4,214.88	0.19
0.200	52,815	2,112.60	73.75	4,282.21	-4,208.46	0.03
0.500	8,479	2,119.75	75.22	4,299.95	-4,224.73	0.42
1.000	2,155	2,155.00	73.72	4,338.25	-4,264.54	1.37
2.000	562	2,248.00	71.21	4,402.10	-4,330.88	2.94
5.000	106	2,650.00	107.59	4,595.00	-4,487.41	6.66
10.000	32	3,200.00	216.33	4,853.66	-4,637.34	10.23

Leica Cyclone

Two calculations with different maximum numbers of points for TIN construction were performed, namely with 500,000 and 2mil. points. The processing time for 500,000 points was approx. 5 minutes, for 2 mils. points approx. 4 hours. The results are shown in Table 3; the difference is negligible.

Tab. 3. Results of volume difference calculation in Leica Cyclone

Raster size [m]	Volume⁺ [m³]	Volume⁻ [m³]	Volume ^{total} [m³]	Difference [%]
2000000	*4,280.60*	*72.90*	*-4,207.70*	*0.00*
500000	*4,283.70*	*72.70*	*-4,211.00*	*-0.08*

3D Reshaper

The software only allows the calculation of the difference between two meshes; no customizable settings are available. The results indicate that 4251.47 m^3 was mined away, 76.26 m^3 added and the total balance is therefore -4175.21 m^3. The TIN generation took several minutes and the volume calculation tens of seconds.

Trimble RealWorks

The calculation was performed three times, using various settings. The first calculation used two triangular meshes (Table 4), the second two point clouds with factory settings (without filling holes; Table 5) and the last one for two point clouds with holes filled prior to the computation (Table 6). The computing time was several seconds for grids of 0.02m and more, several minutes for a grid of 0.01 and approx. 15 minutes for a grid of 0.005m. The calculation for generating TIN took several minutes..

Tab. 4. Results of Trimble RealWorks – a direct calculation from two TINs

Raster size [m]	Number of cells	Surface [m²]	Volume⁺ [m³]	Volume⁻ [m³]	Volume^{total} [m³]	Difference [%]
0.005	*83,501,400*	*2,087.54*	*-4,268.96*	*72.16*	*-4,196.80*	*0.00*
0.010	*20,875,360*	*2,087.54*	*-4,268.97*	*72.16*	*-4,196.80*	*0.00*
0.020	*5,218,825*	*2,087.53*	*-4,268.95*	*72.16*	*-4,196.79*	*0.00*
0.050	*835,020*	*2,087.55*	*-4,268.95*	*72.16*	*-4,196.79*	*0.00*
0.100	*208,760*	*2,087.60*	*-4,268.93*	*72.17*	*-4,196.76*	*0.00*
0.200	*52,188*	*2,087.52*	*-4,268.95*	*72.16*	*-4,196.78*	*0.00*
0.500	*8,343*	*2,085.75*	*-4,267.62*	*72.13*	*-4,195.49*	*-0.03*
1.000	*2,084*	*2,084.00*	*-4,267.22*	*72.34*	*-4,194.88*	*-0.05*
2.000	*516*	*2,064.00*	*-4,269.20*	*72.74*	*-4,196.46*	*-0.01*
5.000	*79*	*1,975.00*	*-4,234.29*	*67.00*	*-4,167.30*	*-0.70*
10.000	*19*	*1,900.00*	*-4,484.82*	*32.85*	*-4,451.97*	*6.08*

Results of the hybrid TIN + grid calculation (Table 4) indicate that no or only minimal changes in results were observed up to the grid size of 2.0 m, after which, the accuracy begins to decrease more significantly.

Tab. 5. Results of Trimble RealWorks – calculation from point clouds without filling the holes

Raster size [m]	Number of cells	Surface [m²]	Volume⁺ [m³]	Volume⁻ [m³]	Volume^total [m³]	Difference [%]
0.005	*41,274,280*	*1,031.86*	*-2,079.19*	*54.48*	*-2,024.71*	*0.00*
0.010	*10,603,110*	*1,060.31*	*-2,118.02*	*55.90*	*-2,062.12*	*1.85*
0.020	*2,688,772*	*1,075.51*	*-2,143.47*	*56.55*	*-2,086.92*	*3.07*
0.050	*435,674*	*1,089.19*	*-2,178.92*	*56.78*	*-2,122.14*	*4.81*
0.100	*110,191*	*1,101.91*	*-2,223.91*	*56.95*	*-2,166.96*	*7.03*
0.200	*28,056.*	*1,122.24*	*-2,291.96*	*57.31*	*-2,234.65*	*10.37*
0.500	*4,772*	*1,193.00*	*-2,574.94*	*57.88*	*-2,517.06*	*24.32*
1.000	*1,344*	*1,344.00*	*-3,044.61*	*60.97*	*-2,983.64*	*47.36*
2.000	*412*	*1,648.00*	*-3,730.83*	*71.37*	*-3,659.46*	*80.74*
5.000	*71*	*1,773.76*	*-4,443.70*	*98.76*	*-4,344.94*	*114.60*
10.000	*30*	*3,000.00*	*-4,850.43*	*224.64*	*-4,625.79*	*128.47*

Results without interpolating (filling) the holes in data are obviously incorrect (Table 5) when compared to other software solutions and methods. This algorithm is therefore not suitable for this type of data.

Tab. 6. Results of Trimble RealWorks – calculation from point clouds with hole interpolation

Raster size [m]	Number of cells	Surface [m²]	Volume+ [m³]	Volume- [m³]	Volume [m³]	Difference [%]
0.005	*74,874,080*	*1,871.85*	*-4,407.98*	*97.63*	*-4,310.35*	*0.00*
0.010	*18,394,970*	*1,839.50*	*-4,395.39*	*76.34*	*-4,319.05*	*0.20*
0.020	*4,657,250*	*1,862.90*	*-4,400.21*	*122.02*	*-4,278.19*	*-0.75*
0.050	*751,024*	*1,877.56*	*-4,353.44*	*121.42*	*-4,232.02*	*-1.82*
0.100	*187,901*	*1,879.01*	*-4,369.72*	*120.34*	*-4,249.38*	*-1.41*
0.200	*47,565*	*1,902.60*	*-4,386.66*	*122.22*	*-4,264.44*	*-1.07*
0.500	*7,753*	*1,938.25*	*-4,445.60*	*116.59*	*-4,329.01*	*0.43*
1.000	*2,073*	*2,073.00*	*-4,489.93*	*137.15*	*-4,352.78*	*0.98*
2.000	*531*	*2,124.00*	*-4,429.91*	*106.12*	*-4,323.79*	*0.31*
5.000	*91*	*2,275.00*	*-4,725.00*	*98.76*	*-4,626.24*	*7.33*
10.000	*30*	*3,000,00*	*-4,850,43*	*224,64*	*-4,625,79*	*7,32*

When the point clouds were manually edited and holes filled, however (Table 6), the results are better; it is nevertheless still obvious that both the areas and volumes change more significantly with grid size than the other methods.

Discussion

For software comparison, the best achievable results were selected, i.e., grid (step) 0.005m where grid solutions were concerned and the highest allowed number of points where TIN meshes were concerned (to allow a comparison of Leica Cyclone with others, the results for both 500,000 and 2 mils. points are shown as the calculation time differ significantly). Resulting in total volumes, differences when compared to Atlas DMT-TIN method and total computing times are shown in Table 7. The Atlas DMT TIN method was, as mentioned above, considered as a reference method due to using minimum simplification and all points, practically without diluting the point cloud in any way. This, however, goes hand in hand with the computing demands of several hours, which is true even for the grid method but even more so for the TIN method.

It is, however, also obvious that results of the best grid algorithms provide comparable accuracy of the results to those of the best TIN algorithms much faster than the TIN methods. This is in all likelihood caused by the high density of the point cloud used for calculations. We can not, however, extend this conclusion to sparse point clouds (e.g. data cully collected using GNSS or total station survey).

Very good results, actually the best when considering the time demand/accuracy ratio were achieved by CloudCompare, which only allows a grid computation. Moreover, CloudCompare is the only tested software available free of charge; hence the price/performance ratio is absolutely unmatched among the tested software solutions.

Tab. 7. Overview of resulting (most accurate) volumes for individual programs

software	method	Volume ^{total} [m^3]	Difference [%]	Total time
Atlas DMT	TIN	-4,207.08	0.00	4.5 hour
	grid	-4,207.08	0.00	1.5 hour
CloudCompare	grid	-4,207.09	0.00	10 minutes
Leica Cyclone	TIN (2 mils. points)	-4,207.70	0.01	4 hours
	TIN (500,000 points)	-4,211.00	0.09	5 minutes
3D Reshaper	TIN	-4,175.21	-0.76	10 minutes
Trimble RealWorks	TIN/grid	-4,196.80	-0.24	15 minutes
	grid	-4,310.35	2.45	15 minutes

Fig. 3 compares the results of programs with respect to the various raster sizes. The graph shows that up to the step of approx. 1m, the volume calculation yields a minimum deviation for most software solutions (in our case, approximately 2,000 squares forming the grid). When increasing the step (lowering the grid resolution) further, both the area (Table 1,2,5,6) and volume change significantly. This may possibly be caused by the grid cells on the edges of the point cloud where a substantial portion of the area may be outside the data (Fig. 4 right) and therefore confound the calculation. For example, in Table 2, we can observe the growth of the area with the grid raster. In general, almost all grid algorithms yielded near identical results; the only exception is the Trimble RealWorks software providing different results in all grid sizes (Fig. 3).

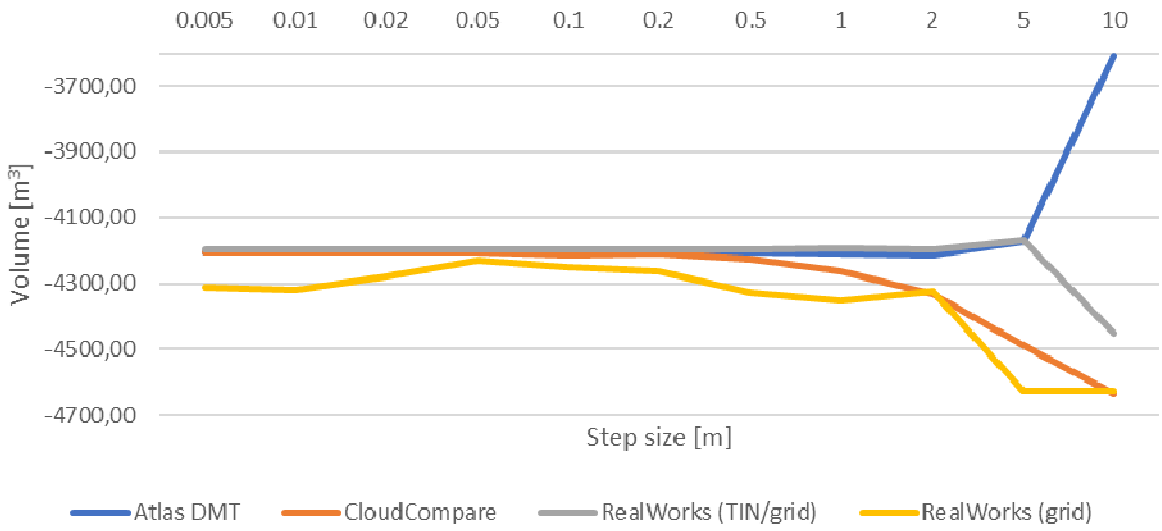

Fig. 3. Comparison of the grid methods

From the perspective of the calculation methods, grid algorithms are very simple and fast when compared with the TIN algorithms, where the TIN mesh must be generated first, and only then the volume can be calculated. This usually requires a dilution of the input point cloud to prevent excessive demands on the computer processing capacity and memory. This can be demonstrated on the Atlas DMT, which does not perform such dilution and the resulting processing time is then extremely high (see Table 7). Curiously enough, however, the processing time using Leica Cyclone, which dilutes the point cloud significantly even with the highest settings (2 mils. points), was almost as high as that of Atlas DMT (using full 6.2 mil. and 3.2 mil. points for individual networks), which suggests that the algorithm in Atlas DMT is less demanding on the processing power than Leica Cyclone. Further dilution of the point cloud in Leica Cyclone (to 500,000) however significantly reduced the processing time.

The processing time and results of TIN-based methods are directly dependent on the constructed TIN mesh, which does not have to be identical for individual programs as each software uses a different method for diluting the point cloud. In some programs, rules for generating the TIN triangles can be set up while others use a fixed algorithm without giving the user a possibility to interfere. For example, the Atlas DMT allows relatively detailed settings of parameters for creating TIN and of manual correction of the automatically generated mesh, Leica Cyclone allows one parameter (the number of points) while 3D Reshaper allows almost no customization.

The volume calculation can also be affected by the convex envelope (Fig. 4) interpolating surrounding data, despite the fact that the real surface can be different.

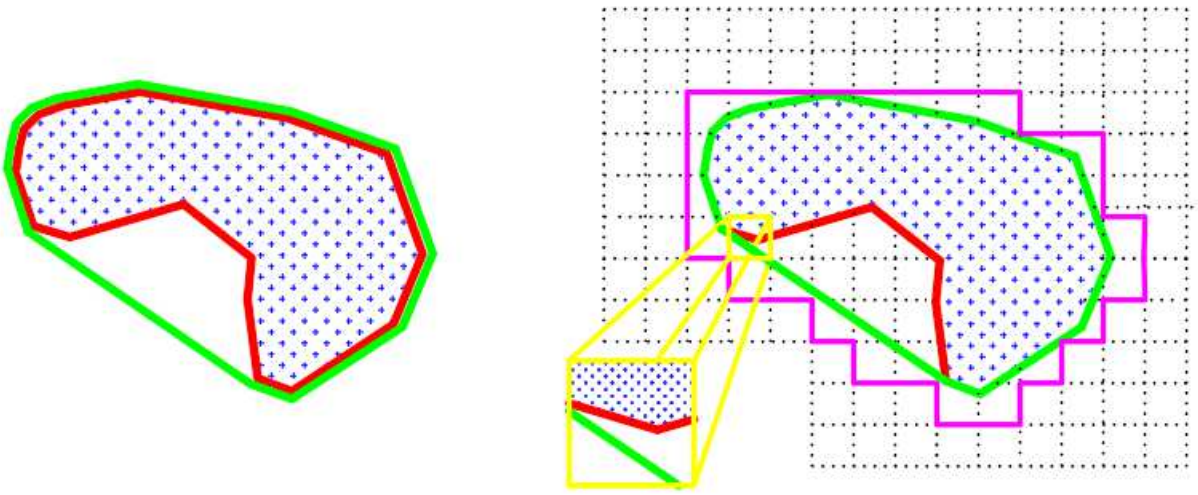

Fig. 4. Convex area (left) and rasterization (right) in CloudCompare (blue points = point cloud; red line – real data borders; green line (left) – delimiting the area for computation using convex envelope, (right) rasterization of the convex envelope with grid cells containing only partial data on the edge of the point cloud; when using a finer grid, the peripheral cells would stick more closely to the edges

Conclusion

This study reports volume calculation and comparison between two states in several software solutions using various algorithms and settings. The data used for the experiment originate from a real TLS scanning in a quarry, complemented by GNSS survey.

Both grid-based and TIN-based algorithms were used. The obtained results were compared to find out how a method of calculation (algorithm, settings, software) affects the resulting volume. Principally, the most accurate results should be those from Atlas DMT, which uses no simplification and utilizes all points (except for duplicate points) for the calculation. However, most raster methods yielded practically identical results up to the grid size of 1 m. Most of the other TIN-based algorithms also yield very similar results.

In conclusion, we can state that the practical effect of the selected software or algorithm is minimal as long as a reasonable raster size or number of TIN points are used. The only exception is represented by Trimble RealWorks, the results of which are mildly different from those provided by all other programs. For raster methods, we can say that dividing the area of our size into 2,000 cells is generally sufficient if dense data is used (as in our case).

Where we can see a significant difference, however, is the necessary processing time. Raster methods are generally significantly faster than TIN methods. If diluting the point cloud sufficiently, the time can be nevertheless similar for both types of algorithms, with only a mild decrease in results accuracy (see Leica Cyclone).

The tested software solutions are designed for various applications. If however only considering volume calculations, the freeware CloudCompare is absolutely sufficient and provides results identical to those computed by the best commercial solutions. The only caveat when using this software lies in the method of calculating the convex envelope, which can potentially distort the results.

Acknowledgement: *This research was funded by the Grant Agency of CTU in Prague — grant number SGS19/047/OHK1/1T/11. and by the Scientific Grant Agency of the Slovak Republic (VEGA – MŠVVaŠ SR) through the project. No. 1/0844/18 and the Cultural and Educational Grant Agency of the Slovak Republic (KEGA – MŠVVaŠ SR) through the project. No. 004TUKE-4/2019.*

References

Bartos, K., Pukanska, K., Repan, P., Ksenak, L., Sabova, J. (2019) Modelling the Surface of Racing Vessel's Hull by Laser Scanning and Digital Photogrammetry. *REMOTE SENSING*, Vol. 11 (13), DOI: 10.3390/rs11131526

Blistan, P.; Jacko, S.; Kovanič, Ľ.; Kondela, J.; Pukanská, K.; Bartoš, K. TLS and SfM Approach for Bulk Density Determination of Excavated Heterogeneous Raw Materials. *Minerals* 2020, *10*, 174

Blistan, P., Kovanič, Ľ., Patera, M. and Hurčík, T. (2019) Evaluation quality parameters of DEM generated with low-cost UAV photogrammetry and Structure-from-Motion (SfM) approach for topographic surveying of small areas. *Acta Montanistica Slovaca*, Vol 24(3), 198-212

Blistan, P., Kovanič, Ľ., Zelizňaková, V., and Palková, J. (2016). Using UAV photogrammetry to document rock outcrops. *Acta Montanistica Slovaca, 21* (2), 154-161

He, H., Chen, T., Zeng, H., Huang, S. (2019) Ground Control Point-Free Unmanned Aerial Vehicle-Based Photogrammetry for Volume Estimation of Stockpiles Carried on Barges. *Sensors* 2019, 19,

Kršák, B., Blišťan, P., Pauliková, A., Puškárová, P., Kovanič, L., Palková, J., & Zelizňaková, V. (2016). Use of low-cost UAV photogrammetry to analyze the accuracy of a digital elevation model in a case study. *Measurement: Journal of the International Measurement Confederation, 91*, 276-287. doi:10.1016/j.measurement.2016.05.028

Martínez-Sánchez, J., Puente, I., González-Jorge, H., Riveiro, B., Arias, P. (2016). Automatic Thickness and Volume Estimation of Sprayed Concrete on Anchored Retaining Walls from Terrestrial Lidar Data. In: T*he International Archives of the Photogrammetry, Remote Sensing and Spatial Information Sciences*, Volume XLI-B5, 2016. XXIII ISPRS Congress, 12–19 July 2016, Prague, Czech Republic.

Medjkane, M., Maquaire, O., Costa, S., Roulland, T., Letortu, P., Fauchard, C., Antoine, R., Davidson, R. (2018) High-resolution monitoring of complex coastal morphology changes: cross-efficiency of SfM and TLS-based survey (Vaches-Noires cliffs, Normandy, France). *LANDSLIDES.* Volume: 15 Issue: 6 Pages: 1097-1108, DOI: 10.1007/s10346-017-0942-4

Pukanská, K., Bartoš, K., & Sabová, J. (2014). Comparison of survey results of the surface quarry spišské tomášovce by the use of photogrammetry and terrestrial laser scanning. *Inzynieria Mineralna, 15*(1), 47-54

Rusnák, M., Sládek, J., Kidova, A., Lehotský, M. (2018) Template for high-resolution river landscape mapping using UAV technology. *Measurement* 2018, 115.

Salagean, T., Suba, EE., Pop, ID., Matei, F., Deak, J. (2019) Determining stockpile volumes using photogrammetric methods. *Scientific papers-series e-land reclamation earth observation & surveying environmental engineering.* Volume: 8 Pages: 114-119. Published: 2019

Stojcsics, D., Domozi, Z., Molnar, A. (2018). Automated Volume Analysis of Open Pit Mining Productions Based on Time Series Aerial Survey. In: UKSim-AMSS 20th International Conference on Modelling & Simulation 20th UKSim-AMSS International Conference on Computer Modelling and Simulation, UKSim 2018, Cambridge, United Kingdom, March 27-29, 2018. IEEE 2018, ISBN 978-1-5386-5877-2.

Tang, Ch., Tanyas, H., Westen, CJ., Tang, Ch., Fan, X., Jetten, VG. (2019) Analysing post-earthquake mass movement volume dynamics with multisource DEMs. *Engineering Geology* 248 (2019) 89–101, https://doi.org/10.1016/j.enggeo.2018.11.010

Tucci, G., Gebbia, A., Conti, A., Fiorini, L., Lubello, C. (2019) Monitoring and Computation of the Volumes of Stockpiles of Bulk Material by Means of UAV Photogrammetric Surveying. *Remote Sensing* 2019, 11(12), 1471; https://doi.org/10.3390/rs11121471

Urbancic, T., Grahor, V., Koler, B. (2015) Impact Of The Grid Cell Size And Interpolation Methods On Earthwork Volume Calculation. *GEODETSKI VESTNIK*. Volume: 59 Issue: 2 Pages: 231-245. DOI: 10.15292/geodetski-vestnik.2015.02.231-245

Zápalková, P., Smítka, V., Mikoláš, M. (2011). Comparison of Tacheometry and Laser Scanning Methods for Measuring the Quarry in Jakubčovice Nad Odrou. *GeoScience Engineering*. 57. 10.2478/gse-2014-0030.

Computer simulation as a means of efficiency of transport processes of raw materials in relation to a cargo rail terminal: A case study

Martin Straka[1]***, Janka Šaderová***[1]*, **Peter Bindzár***[1]***, Tomasz Małkus***[2] *and* ***Marcin Lis***[3]

The article deals with the use of computer simulation for the solution of a streamline of transport processes in relation to the cargo rail terminal. The case study is focused on the job sequence problem of transport processes at the rail terminal. The rail terminal serves as a means of the mineral resources delivery support with the necessity of scheduling a lot of means of transport. Unloading time of a wagon with a capacity of 60-70 t based on observations and measurements in practice varies on average from 30 to 45 minutes. Time for unloading the wagons affects their length of stay at the loading track as well as the waiting charges that affect operational efficiency. The problem is related to the utilization of concrete computer simulation system EXTENDSIM for the necessity of simulation and more effectivity of the whole transport system with his processes. The aim of the solution is the practical application of computer simulation for the needs of effective activities of concrete transport processes of a concrete company. The intention is to show the practical role of simulation systems and to use EXTENDSIM as concrete simulation system for the needs of a streamline of transport processes and activities of a concrete company. The objective of this study is to compare the several possibilities of alternative solutions of activity concrete system, which is created from unloading the mineral resources from railway wagons by cyclically working grab and the transport of mineral resources to places of storing. The simulation was performed for different variants of the unloading process. The simulations in this article simulate the process of unloading of ten railway wagons and one unloader by a different number of trucks (2, 3 and 4) providing a transfer of mineral resources. The simulation results show that the lowest unloading time is reached when unloading by one unloader working with three or four lorries; this represents a decrease of 10% when compared use two lorries. The simulation results show that the effective unloading time is reached in dependence on the number of working means of transport and scheduling of the whole system.

Keywords: *Computer Simulation, Transport Processes, EXTENDSIM, Rail Terminal, Efficiency of Processes, Case Study*

Introduction

Dynamic changes in the business environment require a well-organized supply chain, and this requires a proper organization of logistics processes within the enterprise (Groover, 2007; Kot, 2015; Oláh et al., 2018).

The transport of minerals is carried out by various types of vehicles. Most often, for on and off-site transport of bulk raw materials are used road trucks, wagons, ships, long-distance belt transport and other (Marasova et al., 2007). Choosing an appropriate means of transport depends on several factors. Besides the raw materials property, the factors include route length and the amount of transported material. For the transport of smaller amount of raw materials within company's premises (quarries) and short-distance transport (for example, construction, mining, agriculture, food industry) are mostly used trucks and various types of conveyors (belt, bulk-conveyor). For the horizontal transport in the mining conditions, mining rail transport and belt conveyors are used. Vertical mining transport uses transport cage towing equipment and conveyors (Marasova et al., 2009; Šimková et al., 2019). Wagons are used for transporting a huge amount of materials over long distances, and ships transport bulk material. Before the actual transportation takes place, it is necessary to load and unload the suitable means of transport at the intended destination. The method of loading and unloading is again dependent on the type of minerals, means of transport and unloading facilities available (Toomey, 1996).

Several authors deal with the loading and unloading process in the literature, and it is not only for the bulk materials. That issue is most elaborated for port terminals; articles are dedicated to modelling and simulation of bulk material or containers (Bugaric and Petrovic, 2007; Demirici, 2003; Carteni and de Luca, 2012; Kia et al., 2002; Janič et al., 2019). Wagon unloading is wide because this type of transportation uses various types of wagons for which different unloading equipment.

Literature review

The modelling process can serve as a basis for selecting unloading process or rationalization of the existing system, which has a significant impact on the evaluation of the performance of the transport system or the entire enterprise (Rosova and Balog, 2012; Ho et al., 2010; Pan et al., 2014; Markulik et al., 2018; Kovács and Kot, 2016).

The problem is related to the utilization of concrete simulation system EXTENDSIM for the necessity of simulation and more effectivity of the whole transport system with his processes. It is the product of the Imagine

[1] *Martin Straka, Janka Šaderová, Peter Bindzár,* Technical University of Košice, Faculty of Mining, Ecology, Process Control and Geotechnology, Institute of Logistics and Transport, Letná 9, 042 00 Košice , Slovakia, *martin.straka@tuke.sk, janka.saderova@tuke.sk, peter.bindzar@tuke.sk,*

[2] *Tomasz Małkus,* Cracow University of Economics, Department of Management Process, 31-510 Cracow, ul. Rakowicka 27, Poland, *malkust@uek.krakow.pl*

[3] *Marcin Lis,* Department of Management, Faculty of Applied Sciences, WSB University, 41-300 Dąbrowa Górnicza, Poland

That, Inc. USA company. A simulation language that is used belongs to advanced simulation capabilities where the simulation model consists of blocks that are grouped in the libraries. Its use is simple and intuitive. System of implementation of transport processes is limited by a lack of suitable means of transport, creates a lot of downtime and restriction of planning for the needs of the efficient use of means of transport and of logistics ensuring. The aim is to streamline and configure the transport system to a level that would be effective as economically, technically and also by side the logistics. The aim of the solution is the practical application of computer simulation for the needs of effective activities of concrete transport processes of a concrete company. The intention is to show the practical side of simulation systems and to use EXTENDSIM as concrete simulation system for the needs of a streamline of transport processes and activities of a concrete company.

For the transport of mineral resources by rail, there are used the types of wagons marked by capital letters as follows:

E - Open Top (High wall) wagon of ordinary construction with a flat floor and the possibility of frontal or side tipping (wagons are designed to carry the bulk and general cargo goods that doesn't require the carriage of covered space and protection from the weather).

F - Open wagon of special construction (wagons are designed for the carriage of the bulk of powdered bulk goods like coal, limestone, gravel, etc.). Wagon construction enables double-sided gravity unloading of goods.

G - Covered wagon of normal construction (wagons are designed to carry the palletized goods, general cargo, bulk grain or another bulk substrate like industrial salt that must be protected from the weather. The wagons allow the transport of live animals).

T - Wagon with an openable roof (Tds) - wagon of special construction with a convertible roof (wagon is designed to transport bulk goods requiring weather protection). The wagon construction enables double-sided gravity unloading of goods.

Conceptualization of traffic flow pattern is one of the influential factors on traffic simulation modeling (Kim, 2011; Bohács et al., 2018). The same idea is necessary for the creation of a simulation model of our transport system.

Unloading of minerals from railway wagons under real conditions can be carried out in various ways depending on the type of rail wagon, type of minerals, loading mechanisms to be available and forms of trans-loading. The Slovak Republic is specific in that its territory features normal and broad railway gauge, and besides classic wagon unloading also loading and unloading of minerals from normal to broad railway gauge takes place (Saderova and Bindzar, 2014). Thus there are three dimensions of the process:

1. Unloading of minerals from the standard gauge railway wagons using different types of unloading systems.
2. Unloading of minerals from broad gauge rail wagons using different types of unloading systems.
3. The transhipment mineral resources from railway wagons on a broad gauge to standard gauge railway wagons that may be realized as direct transhipment or indirect transhipment.

In the direct transhipment, minerals are directly transferred from broad gauge wagons to parallel wagons that are then shipped to customers. In the case of indirect transhipment, the minerals are not transferred directly from wagon to wagon, but minerals are firstly unloaded using unloading devices to another type of vehicle and moved to storage or to an open dump. Then, when the time comes, its loading is carried out in the required quantity.

Unloading of mineral resources in all forms can be realized in four ways – by shovelling, scooping, tipping or by self-unloading. Self-unloading requires the special construction of railway wagons allowing double-sided gravity discharge of raw material (series F and Tds). The first three forms are used for the unloading of mineral resources from high-wall opened or closed wagons (series E and G). It is important to use suitable unloaders depending on the form of unloading. There are 2 groups of unloaders for shovelling, scooping and tipping (Saderova and Bindzar, 2014):

- Means of "small mechanization" are considered as mechanisms where human effort remains an essential factor (mechanical shovel),
- Means of "complete mechanization" like mobile and bridge grab cranes, bucket unloaders, front and rotary tipplers.

Modelling and model creation is one of the basic cybernetic approaches to study, analysis, design and design of systems. The modelling is the process of replacing a dynamic system by its model. The model represents a simplified object or process and is created on a computer, physical or real object (Malindzak, 2009; Straka et al., 2016). Several authors deal with the modelling and model creation in various sectors across process technology, transport, handling, services, etc. (Vilamova et al., 2016; Gracanin et al., 2013; Šaderová et al., 2018; Pekarcikova et al., 2019; Urzúa et al., 2019).

Simulation is an experimental method in which the real system is replaced by a computer model. It is possible to make a number of experiments with such a model, to evaluate and to optimize it and then results can be applied to the real system. The first step in the simulation is to build a simulation model of the real system. The next step is to provide experiments with the simulation model by which there are achieved results, which

need to be correctly interpreted and applied. Application possibilities of computer simulation can be applied in designing manufacturing processes and systems (Lu et al., 2015; Ba et al., 2016).

The modelling of unloading the mineral resources is composed of two subsequent parts. The first preparatory phase is targeted on creating the algorithm as a basis for the second part. The second modelling part consists of two types of model for a selected time period based on the algorithm graphic and simulation models.

Simulation is not a tool for getting the optimal solution, but it is a tool that allows you to test different outputs decision on simulation models. The model allows performing experiments to evaluate, analyse, and to optimize the results that can be subsequently used for the real system. Risk reduction can be examined in advance, by "replaying" the system run whilst observing the performance and behaviour of the system, then after applying the required changes, examine the future behaviour of the system, where any potential problems and bottlenecks can be removed in advance (Straka et al., 2019). Animations of manufacturing processes allow greater clarity and understanding of the production processes, thus allowing to prevent failures, which could exist in practice if a system is not testing on mistakes and deficiencies (Straka, 2007).

The simulation model created by EXTENDSIM is defined by a specific sequence of modelling blocks connected by lines representing the processing flow directions. The block position, icon and name, the connector blocks, the links as well as the user interface dialogues with operands and flows are the main properties of individual blocks. The blocks themselves represent individual processes or subsystems, thus creating the actual representation of the real-life system under examination. The icons and block names are the graphic representation of each block, with their exact unique name that describes their defined function and the primary purpose of the particular block within the model. The block labelled "create" represents the generation of input requirements while the model block labelled "queue" defines the creation of a series of demands, with the input to the queue and the subsequent output. The block labelled "exit" represents the simulation model output. The blocks connectors enable connecting each block with others in accordance with a rule that one connector can only connect the input with output slot. The connectors of two different blocks form a logical sequence of blocks, which reflects the real system and forms the basis for forcing the flows. The connected blocks form flows representing the real sequence of units and facilities within the examined system. User interface windows and operands represent specific items and the block properties characteristic for the particular blocks. By opening a user interface window, the parameters and properties of each block can be displayed and specified for each modelling block (Straka, 2007).

Researched transport system

Type of minerals in the railway wagon and its physical and chemical properties should be considered as input data for individual sub-processes.

The first activity in the process of unloading is the "in-feed motion" – supplying the wagons at the place of unloading (unloading ramp). Before this activity, there should be done operations such as an announcement about the arrival of wagons to be unloaded. When doing transhipment between railway wagons (form 3 - direct transhipment), it is also necessary to make an order for rail wagons that will be loaded.

After wagons are ported, wagon unloading takes place. During the unloading process, wagons are either still, or move in certain times or continuously depending on the type of unloading equipment - device. The unloading process consists of several activities. Figure 1 shows the simple formalized scheme of the process of unloading (Fig. 1).

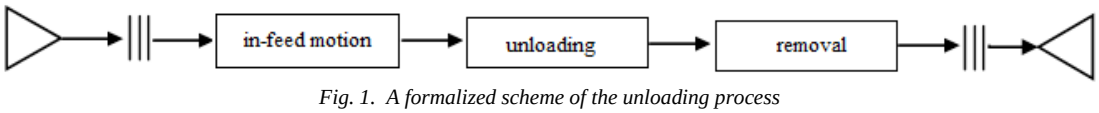

Fig. 1. A formalized scheme of the unloading process

When unloading with a gripper crane a wagon is still, and the unloaded raw material is unloaded directly to another means of transport (for example, right on the truck, through the hopper onto a conveyor belt, etc.). When unloading with a wagon tippler wagons are shifted to the rotary tilter where they are disconnected from the set, tilted, put out of the tilter, and subsequently joined to the wagon set again. Material falls from the rotary tilter into the containers that are then moved by conveyors. When using bucket unloaders, the wagons are still or continuously move depending on unloaders' construction.

Unloading of minerals is followed by its removal (displacement) to the destination such as operational stock, to the customer, stock for input materials, to the manufacturing process, etc. Figure 2 shows an example of a simplified flow chart of unloading of minerals from the railway wagons (Fig. 2).

The modeling of any process is based on pre-defined steps - an algorithm. The proposed algorithm is for unloading open wagons to trucks that are to be unloaded at a temporary landfill using portable gripper cranes. The results obtained from the model made according to the proposed algorithm can serve for assessing the

current state of unloading and rationalization in order to increase the capacity of the existing system. During the rail wagon loading, the train set will remain at rest so that unloading equipment will move only.

Figure 3 shows the basic algorithm for unloading the mineral resources from railway wagons (Fig. 3). There must be known some input parameters to perform the unloading, such as (Fig. 3, a):

"*n*" - the number of railway wagons to be unloaded of the train set;
"*M*" - the volume of mineral resources in one railway wagon in tons;
"*N*" - the volume of mineral resources unloaded by one grab unloader in tons.

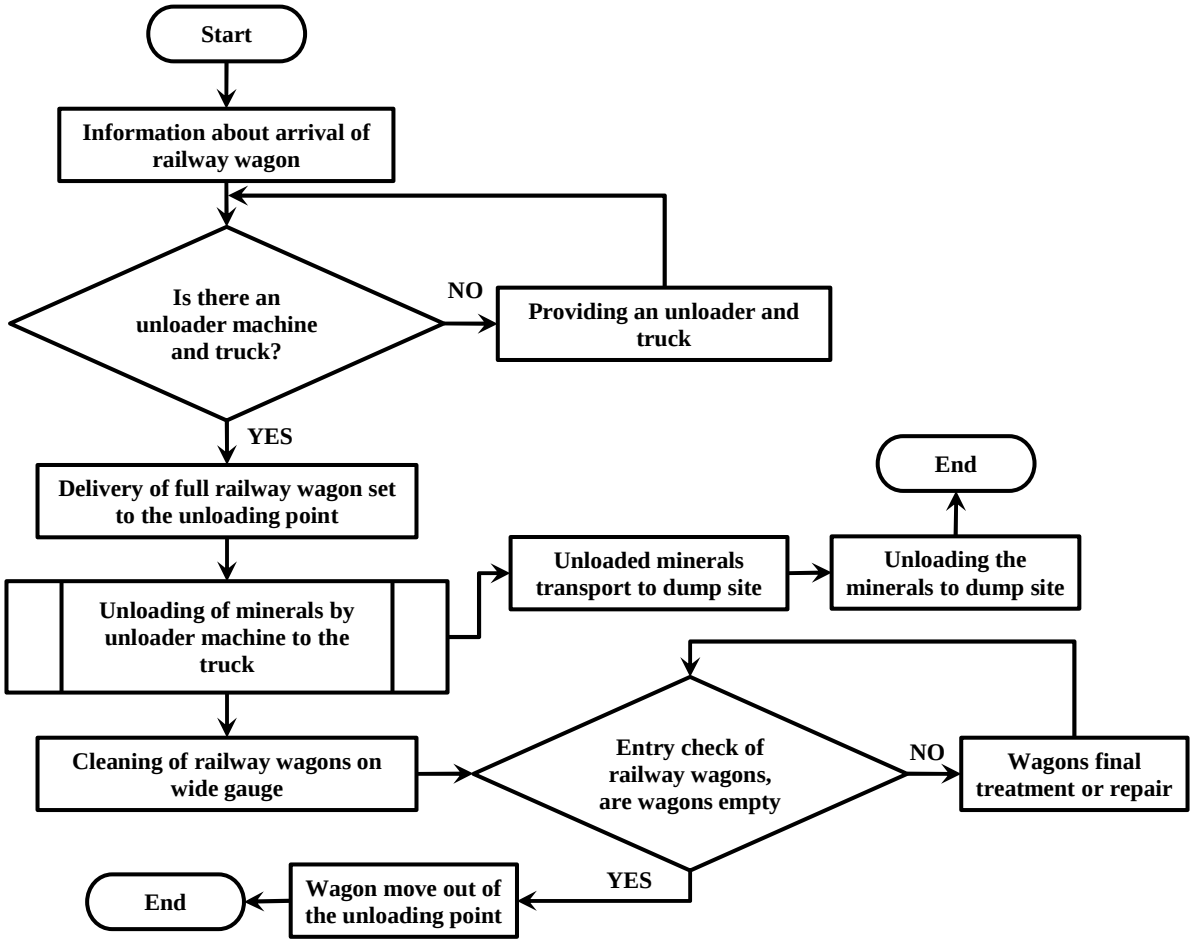

Fig. 2. A flow chart representing direct unloading of mineral resources from a railway wagon

The unloading process begins when rail wagons are furnished at the unloading point (Fig. 3, b). Subsequently, the unloading is carried out by cycle (Fig. 3, c) (step by step - wagon after wagon if we have a single unloader; in parallel – it is used in case of more unloaders) that begins by furnishing the unloader to the railway wagon (Fig. 3, d).

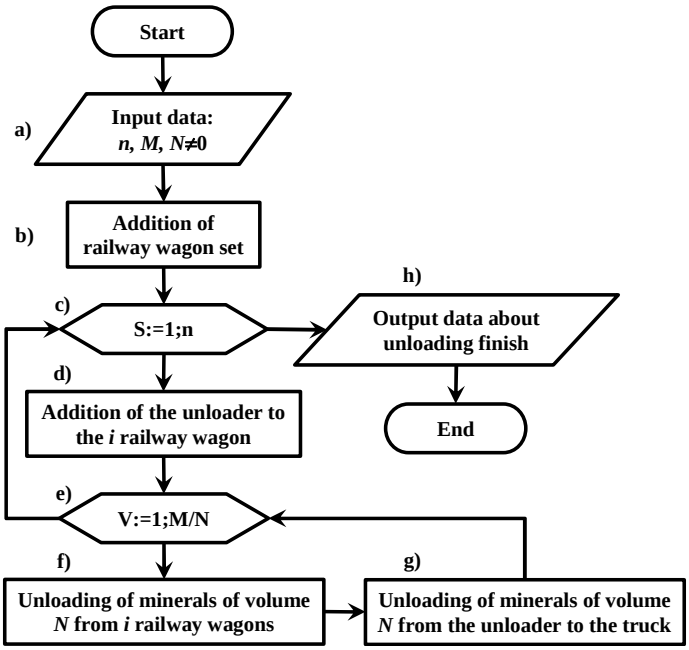

Fig. 3. A basic algorithm of unloading minerals from train set

Unloading of a single wagon is represented by cycle (Fig. 3, e-g) consisting from operations (Fig. 3, f) "Unloading of mineral resources of volume "*N*" from railway wagon by unloading means and its deposit into a transport vehicle" (Fig. 3, g) until the discharged amount of "*M*" isn't unloaded. After unloading a single wagon, the loader means is moved to the next wagon (Fig. 3, c, d) followed by unloading of the wagon by cycle (Fig. 3, e). After unloading the mineral resources of all railway wagons, the information about the completion of unloading of train set is interpreted by cycle (Fig. 3, h) and the unloading process is finished.
Figure 4 shows the secondary algorithm representing the realization of transport of unloaded mineral resources by trucks (Fig. 4). Input parameters (Fig. 4, a) in this case are: "*N*" - the volume of mineral resources unloaded by grab unloader [t]; "*K*" – truck capacity. The first step is an addition of a truck to the unloading equipment (Fig. 4, a). Consequently, the truck is loaded with suitable equipment (Fig. 4, d). After loading the volume of "*K*" to the truck, it is moved and unloaded (Fig. 4, e, f). After emptying (Fig. 4, g) the truck returns to the loading point, or its work is finished with that train set (Fig. 4, h).

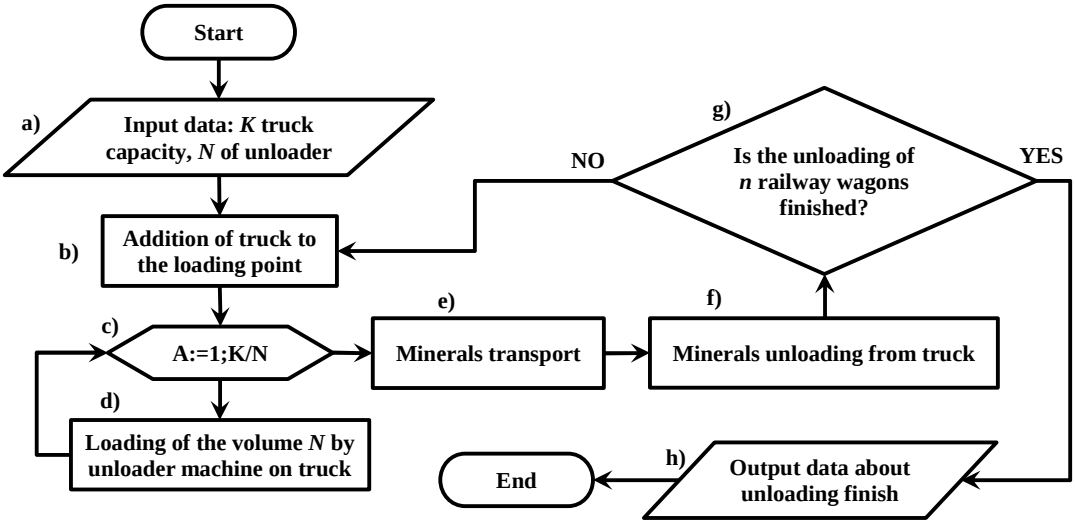

Fig. 4. Algorithm of transport of unloaded mineral resources

The creation of a simulation model by EXTENDSIM

Modelling requires some input data. Input data are dependent on questions like „What I want to achieve by the modelling? The modelling should result in:

- Project of the system of unloading.
- Rationalization of the existing system.
- Improving the capacity of the existing system and so on.

Input data can be categorized by these groups:

1. The type and properties of the mineral resources.
2. Operating conditions data in which the unloading will be carried out like intervals for wagons to be in feed, the number of wagons in the train set, the capacity of wagons, the distance between the place of unloading to the stock and so on.
3. Performance of the unloading equipment (per year, per hour) and related transport equipment.
4. The form and method of unloading.

All input data from all groups above are required when designing a new system from the beginning. While doing a rationalization of the existing system only or trying to improve the capacity of the existing system, the input data to be required are mainly from the groups 1-3. The performance of unloading equipment and related transport systems can be obtained from the prospectus, by calculation according to the known relationship or directly by observing under real conditions (just for existing mechanisms).

Input data (Table. 1) are required when creating a model of the process of unloading that is based on the algorithms above. Data (Table. 1) also lists other parameters closely connected with the formation of a model.

The model of the unloading process was created based on algorithms above (Fig. 3 and Fig. 4). Data connected with the formation of a model are listed in Table 1 (input data).

The model's result is to determine the time of unloading of the specified number of wagons under the given conditions, provided that the grab unloader has already been present at the first rail wagon of the set (excluding the initial presence of the grab unloader). That time of unloading serves as a basis for calculating the cost of demurrage of wagons.

Under real conditions, the number of railway wagons in one train set mainly depends on the length of the so-called handling (the loading) track. Quantity of mineral resources in the railway wagon depends mainly on the type of mineral resource and parameters of the wagon. The volume of mineral resources to be unloaded by unloading equipment during one unloading cycle depends on the type of the mineral resources, the volume capacity of an unloader and a coefficient of grab unloader's loading.

Tab. 1. Input data for modelling of the unloading process

Parameter	**Value**
Number of rail wagons in trains [-]	$n = 10$
Volume of mineral resource in the wagon [t]	$M = 70$ t
Volume of mineral resource unloaded during one cycle by a grab unloader [t]	$N = 0.86$ t
Operating cycle time of the loader [s]	$T_{pcv} = 27$ s
Number of operating cycles to unload 10 wagons by the claws of a grab unloader	810 cycles
The time needed for loader moving between the wagons [s]	90 s

The run time of the hydraulic operation of the grab unloader is specified by the manufacturer, or it can be set on the basis of practical measurements – the operation then may vary depending on the type of raw material and the size of the work equipment - the grab. The run time consists of the following partial steps: dropping down the grab into the wagon→ loading the material (opening the grab + loading + closing) → lifting up the grab and moving over the truck → opening the grab (unloading the material) → lifting up the grab and moving over to the wagon.

Another model parameter is the time it takes the grab to move to the next wagon and the number of loaders used for loading. Based on the parameters (Table 1) and simple calculations, we can determine the so-called "starting" - the technical time of unloading of 10 wagons "T_T" by one unloading grab. Unloading time consists of the sum of individual times for unloading of wagons and relocation times needed for the grab to move from one unloaded wagon to a full wagon. 81 unloading cycles are needed to unload one wagon at given capacity, unloading time of one cycle is 27 seconds, for all cycles it is 2187 seconds or 36.45 minutes. Net time of unloading 10 wagons is 364.5 minutes and can be reduced using multiple unloaders. Time of movement of loader between two successive wagons, also considering a safe operation, is 90 seconds as can be seen in Table 1. Movement of a loader in order to unload 10 wagons will be performed 9 times; it is 13.5 minutes. Based on these values, the time of unloading 10 wagons is $T_T = 378$ minutes or 6.3 hours.

Thus the specified time of unloading does not take into account the process of raw material transportation which depends on the distance to which the raw material is being transported, the number of used trucks and their capacity.

The capacity of a truck is again given by the type of raw material and truck's parameters. In practice, the capacity of a truck can be determined by the number of unloader's operations as determined by the ratio of the truck's volume to the volume of the unloader and the truck's capacity to the amount of raw materials. The transport distance affects the turnaround time of the truck, the time it takes for the truck to return, the number of truck needed for the continuous work. An insufficient number of trucks may result in long unloader downtime

and increased unloading time, which could have a negative economic effect. Other additional input data listed in Table 2 were required during the creation of the model.

The model of unloading of the mineral resource has been developed according to the algorithms previously described and for input data as in Table 1 and Table 2.

Tab. 2. Input data for modelling of the unloading process

Parameter	Value
Truck capacity	K = 7.77 t (capacity of 9 claws)
Time for loading a one truck	t_n = 243 s
Route length for the transport of mineral resource	L = 450 m
Truck cycle time (transport, unloading, return journey to loading point)	t_o = 270 s

Before the model itself was created, it had to be determined based on Table 2. A number of trucks (N_T) is able to manage the performance of unloader. Based on the capacitive conversion of truck transportation, the required number of trucks on a distance of 450 m is N_T = 2,1. Figure 5 shows the model of unloading where transport of unloaded mineral resources will be done by two trucks (Fig. 5). The model was made on the basis of the assumption that the loading process starts at the moment the unloader has arrived to the first wagon, as indicated above. It can be seen on the graphic model a process of wagon unloading RW_1 to RW_{10}. The unloading of each railway wagon consists of two lines that are represented by trucks T_1 and T_2 providing removal of the mineral resource to the destination. Black stripes represent unloading activities that alternate depending on the truck to be loaded. Red stripes represent down-time "t_i" of an unloader that is caused by waiting for the trucks in operation (T_1 or T_2). Green stripes represent moving of an unloader to the next wagon. Grey stripes represent truck circulation (driving time out and back, time of unloading and its bringing again to rail wagon). Blue colour stripes are a truck waiting for loading.

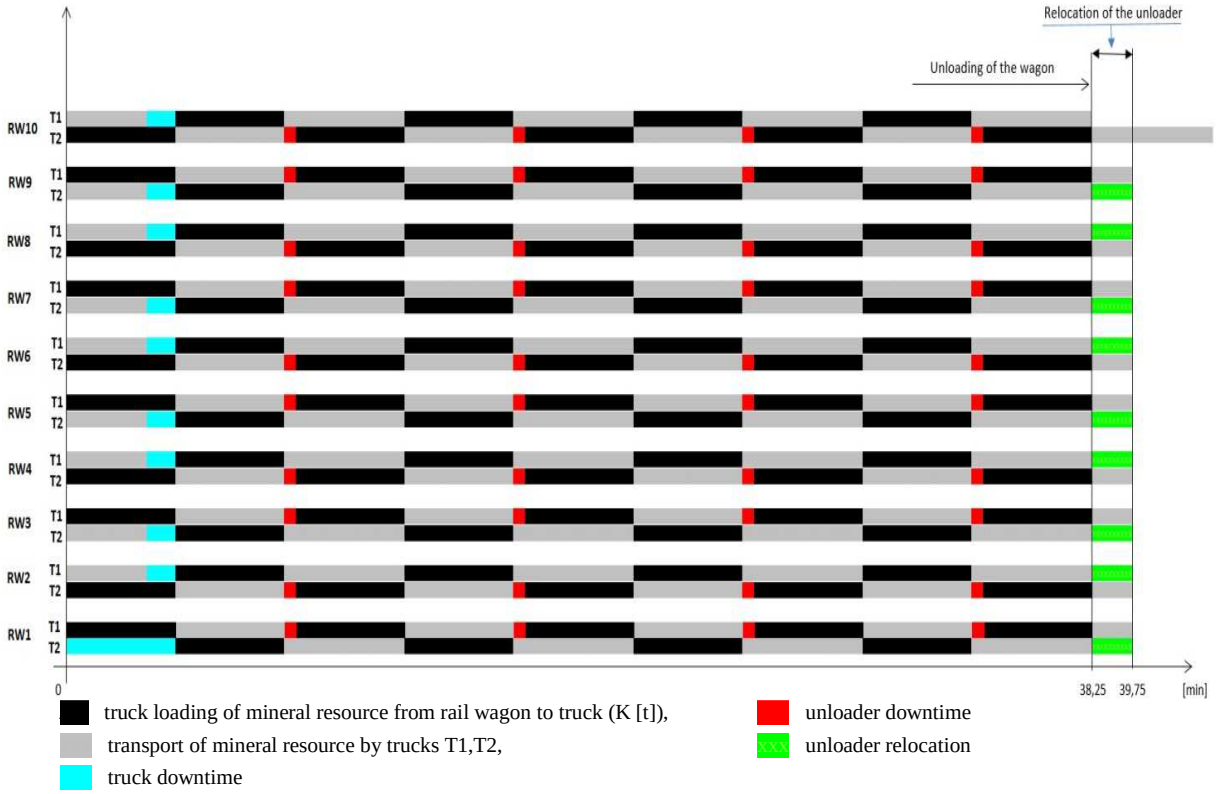

Fig. 5. The graphic model of unloading with the transport of unloaded mineral resources

The simulation model of the transport processes (Fig. 6) of the mineral resource has been created in the simulation system called EXTENDSIM. It is the product of the Imagine That, Inc. USA company. A simulation language that is used belongs to advanced simulation capabilities where the simulation model consists of blocks that are grouped in the libraries. Its use is simple and intuitive. The simulation model is a model of discrete simulation and is built from the blocks of the library "Discreet Event" and "Plotter" (Straka, 2007). The upper part of the model represents the unloading of wagons; the lower part shows the transportation of mineral resource.

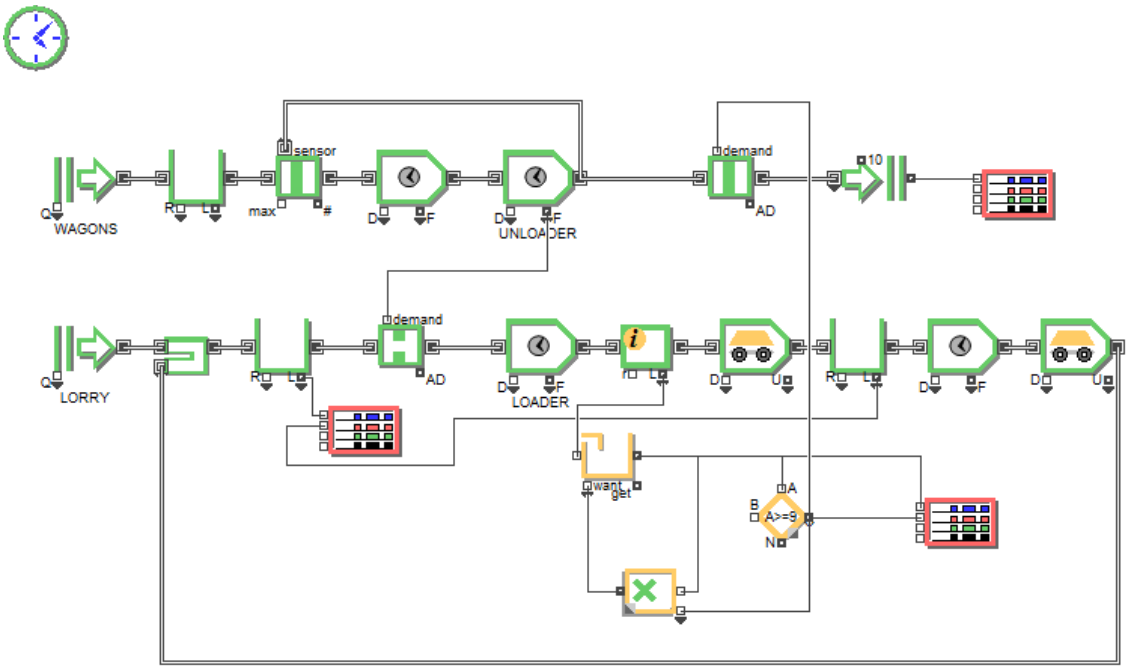

Fig. 6. The simulation model of the transport processes by EXTENDSIM computer simulation system

Results and discussion

The graphic model on Figure 5 results in the following: 9 trucks are needed to unload 1 rail wagon, every wagon can be unloaded within 2295 s = 38.25 minutes, this time includes 4 unloader downtimes (totally 108 s) caused by waiting of trucks T_1 (resp. T2), 90 trucks are needed to unload mineral resource from 10 rail wagons, 6.075 hours netto is needed to unload 10 rail wagons, totally 40 downtimes is formed while unloading 10 wagons; it is 0.3 hours (18 minutes), the unloader is moved – times during the unloading; it is 0.25 hours (15 minutes), time of unloading T_T is 6.60 hours.

Time for unloading a train set can be reduced by deploying multiple loaders and the corresponding number of means of transport. Losses caused by waiting for a truck can be eliminated in several ways:

1. By deploying multiple trucks (Option 2).
2. By increasing a truck capacity (Option 3 and 4).
3. By increasing a loader capacity (Option 5 – 8).

Similar models have also been developed for these options, and the results are found in Table 3. In option 2 (deploying a 3 trucks) each wagon is unloaded in t_u = 2187 seconds = 36.15 minutes. It is similar to Option 1, but there are no downtimes caused by waiting for a truck. Unloading time T_T is reduced to 6.3 hours. The deployment of three cars will reduce unloading time by unloader downtime, but on the other hand, there is downtime on average 3.60 minutes per vehicle turnover, which is on one side. For the same time, it landed raft even with Option 3 and 4, since the time of loading one car is equal to or greater than the circulation time of the car, resulting in downtime remained in a car with a capacity of 9.5 tons.

In Option 5 and 6 by increasing the volume of claws to 1.2 m^3 the time of unloading compared to other options will rise up to 6.43 hours or up to 6.64 hours by increasing the volume of claws to 1.30 m^3 in options 7 and 8. The increase, in this case, is due to the time increase in the unloading cycle and not by unloader's downtime. Deploying grabs with a larger volume negatively impacts the time utilization of trucks. However, such downtime provides enough time in case the route needed for unloading the material takes longer than expected. Table 3 shows recommended color-coded options which should be applied when unloading at given input data.

Tab. 3. Results of modelling

Parameter	Option 1	Option 2	Option 3	Option 4	Option 5	Option 6	Option 7	Option 8
V_D	1.1				1.2		1.3	
N [t]	0.86				0.94		1	
K [t]	7.77	7.77	8.64	9.50	8.46	9.40	9	10
t_n [s]	243	243	270	297	270	300	297	330
t_o [t]	270	270	270	270	270	270	270	270
N_T [-]	2	3	2	2	2	2	2	2
t_u [s]	2187	2187	2187	2187	2234	2234	2310	2310
t_i [min]	18	0	0	0	0	0	0	0
T_T [h]	6.60	6.30	6.30	6.30	6.43	6.43	6.64	6.64

We can assume based on the values for option 2 that during the 12-hour shift, one unloader unloads about 12 wagons, i.e. 840 t. 70% of the time shift of 12-hour shift represents the time of unloading; for example, 504 minutes (8.4 hours). The time needed for moving will account for 8.3 hours.
Unloading time is greatly influenced by the time wagons remain at the loading track and time needed for moving the wagons, thus affecting the cost of wagons demurrage.
If the cost of staying for a single wagon is 3 EUR / hour, the total cost of the stay for 12 wagons will be 12x8,3x3 = € 298.8 or 0.356 euros/tone of unloaded mineral resource. Using multiple unloaders will lead to reducing not only unloading time but the costs also (Table 4).

Tab. 4. Modifications to the parameters when deploying multiple loaders

Number of wagons	12	12	12
Number of deployed loaders	2	3	4
Unloading time [h]	4.15	2.77	2.05
Costs per stay for 12 wagons [€]	149.40	99.72	74.70
Costs per 1t of handled mineral resource [€]	0.18	0.12	0.09

Unloading time of a wagon with a capacity of 60-70 t based on observations and measurements in practice varies on average from 30 to 45 minutes. The same is confirmed by our graphical model.
The simulation was performed for different variants of the unloading process. The simulations in this article simulate the process of unloading of ten railway wagons and one unloader (SIM1 to SIM3) by a different number of trucks providing a transfer of mineral resources. The output data and the results obtained by simulation are shown in Table 5. The truck circulation time for all the simulations is taken from Table 3.

Tab. 5. Output data and simulation results

Parameter	SIM1	SIM2	SIM3
Number of wagons	10	10	10
Number of unloaders	1	1	1
Number of trucks	2	3	4
t_u [s]	47.58	36.45	36.45
T_T [min]	417.58	379.50	379.50

A graphical representation of simulation SIM2 is shown in Figure 7. It is unloading of 10 wagons by one unloader using 3 trucks (Lorries). The blue line represents the unloading of a wagon to 9 trucks while the red line represents the completion of unloading the wagon from the train set.

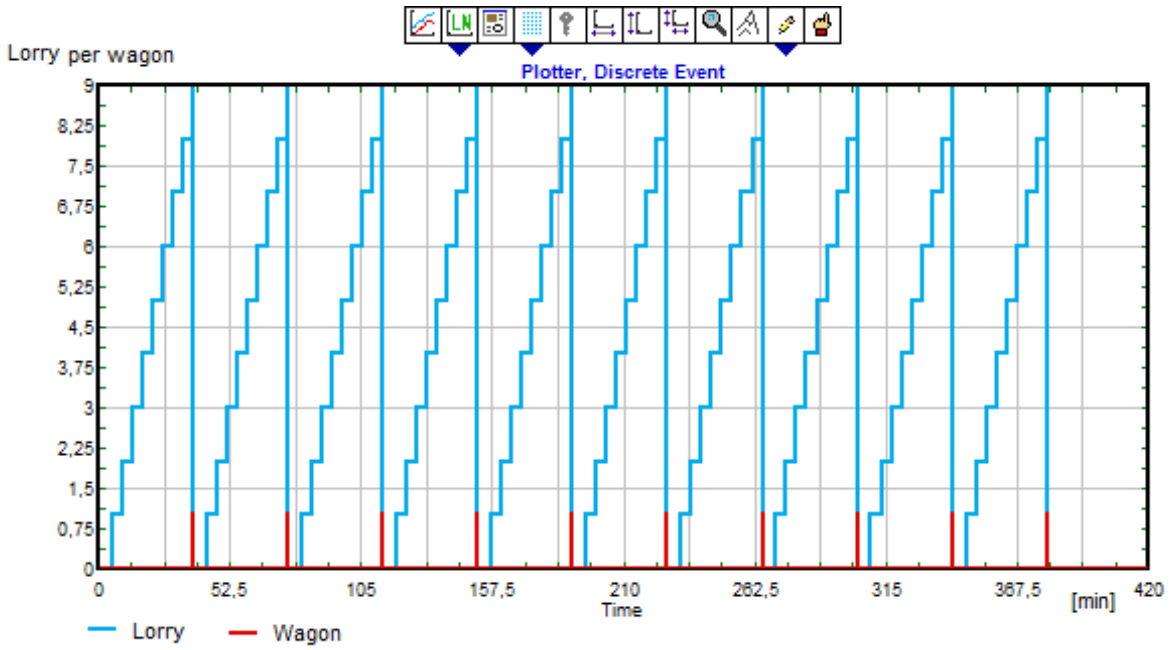

Fig. 7. Graph of the simulation of the transport processes

The simulation results show that the lowest unloading time is reached when unloading by one unloader working with three or four lorries. Extra downtimes are present when using four lorries.

Summary

This paper was aimed to use a model approach create an algorithm and creation of graphic and simulation model by EXTENDSIM for the needs of modelling the unload process from railway wagons using the grab unloader followed by transfer of minerals by trucks. In order to create an algorithm, there was a short overview of the process of unloading described in the article's introduction: forms, methods, types of unloading facilities and types of wagons used to transport raw materials. We can allege that the aim of the study solution was reached.

This algorithm forms a basis for the creation of the specific model in graphic form as well as a simulation model. The algorithm can be modified easily for any way and form of unloading. This is only one of many procedures which can be used to address the problem. The other methods such as simulation, software applications can be used to solve the problem and the decision-making process with the use of multi-criteria analysis. That job does not end with the creation of the algorithm and forming specific actions that are necessary. Next, it is necessary to monitor and evaluate the process using the tools of controlling as well as to ensure the efficiency of the operation. The future research should focus on the extension of the existing model and the application thereof to other unloader types and unloading methods, either underground or on the surface.

Acknowledgement: *This work was supported by the Slovak Research and Development Grant Agency, VEGA grant number 1/0317/19.*

References

Ba, L., Li, Y., Yang, M.S., Gao, X.Q., Liu, Y. (2016). Modelling and simulation of a multi-resource flexible job-shop scheduling. *International Journal of Simulation Modelling*, 15(1):157-169. doi:10.2507/IJSIMM15(1)CO3

Bohács, G., Gáspár, D., Kánya, D. (2018). Conception an intelligent node architecture for intralogistics. *Acta logistica*, 5(2):31-37. doi:10.22306/al.v5i2.82

Bugaric, U., Petrovic, D. (2007). Increasing the capacity of terminal for bulk cargo unloading. *Simulation Modelling Practice and Theory*, 15(10):1366-1381. doi:10.1016/j.simpat.2007.09.006

Cartenì, A., de Luca, S. (2012). Tactical and strategic planning for a container terminal: Modelling issues within a discrete event simulation approach. *Simulation Modelling Practice and Theory*, 21(1):123-145. doi:10.1016/j.simpat.2011.10.005

Demirci, E. (2003). Simulation Modelling and Analysis of a Port Investment. *SIMULATION*, 79(2):94-105. doi:10.1177/0037549703254523

Gracanin, D., Lalic, B., Beker, I., Lalic, D., Buchmeister, B. (2013). Cost-time profile simulation for job shop scheduling decisions, *International Journal of Simulation Modelling*, 12(4):213-224. doi:10.2507/IJSIMM12(4)1.237

Groover, M. P. (2007). *Automation, Production Systems and Computer-Integrated Manufacturing*, 3rd edition, Prentice Hall, Upper Saddle River.

Ho, W., Xu, X. W., Dey, P. K. (2010). Multi-criteria decision making approaches for supplier evaluation and selection: A literature review. *European Journal of Operational Research*, Vol. 202, No. 1, 16-24, doi:10.1016/j.ejor.2009.05.009

Janič, P., Jadlovská, S., Zápach, J., Koska, L. (2019). Modeling of underground mining processes in the environment of MATLAB / Simulink. *Acta Montanistica Slovaca*, 24(1):44-52.

Kia, M., Shayan, E., Ghotb, F. (2002). Investigation of port capacity under a new approach by computer simulation. *Computers & Industrial Engineering*, 42(2-4):553-540. doi:10.1016/S0360-8352(02)00051-7

Kim, B.J. (2011). Conceptualization of traffic flow for designing toll plaza configuration: A case study using simulation with estimated traffic volume. *International Journal of Industrial Engineering*, 18(1):51-57.

Kot, S. (2015). Cost structure in relation to the size of road transport enterprises. *Promet - Traffic - Traffico*, 27(5):387-394. doi:10.7307/ptt.v27i5.1687

Kovács, G., Kot, S. (2016). New logistics and production trends as the effect of global economy changes. *Polish Journal of Management Studies*, 14(2):115-126. doi:10.17512/pjms.2016.14.2.11

Lu, J.T., Yang, N.D., Ye, J.F., Liu, X.G., Mahmood, N. (2015). Connectionsim strategy for industrial accident-oriented emergency decision-making: a simulation study based on PCS model. *International Journal of Simulation Modelling*, 14(4):633-646. doi:10.2507/IJSIMM14(4)6.315

Malindzak, D., Strakoš, V., Koštial, I., Lenort, R., Straka, M., Macurová, P., Rosová, A., Cibulka, V. (2009). *Modelovanie a simulácia v logistike, teória modelovania a simulácie, Modelling and simulation in logistics, theory of modelling and simulation*, 1st edition, Karnat, Kosice. (Original in Slovak)

Marasova, D., Petruf, M., Taraba, V., Šaderová, J., Fedorko, G., Bindzár, P., Husáková, N. (2007). *Logistika dopravy, Logistics of transport,* 1st edition, TUKE, Kosice. (Original in Slovak)

Marasova, D., Mikušová, N., Boroška, J., Strakoš, V., Lukáč, S. (2009). *Vnútropodniková doprava v ťažobnom priemysle, In-plant transport in the extractive industry,* 1st edition, TUKE, Kosice. (Original in Slovak)

Markulik, Š., Cehlár, M., Kozel, R. (2018). Process approach in the mining conditions. *Acta Montanistica Slovaca,* 23(1):46-52.

Oláh, J., Sadaf, R., Máté, D., Popp, J. (2018). The influence of the management success factors of logistics service providers on firms' competitiveness. *Polish Journal of Management Studies,* 17(1):175-193. doi:10.17512/pjms.2018.17.1.15

Pan, R., Zhang, W., Yang, S., Xiao, Y. (2014). A state entropy model integrated with BSC and ANP for supplier evaluation and selection. *International Journal of Simulation Modelling,* 13(3):348-363. doi:10.2507/IJSIMM13(3)CO13

Pekarcikova, M., Trebuna, P., Kliment, M. (2019). Digitalization effects on the usability of lean tools. *Acta logistica,* 6(1):9-13. doi:10.22306/al.v6i1.112

Rosova, A., Balog, M., (2012). Traditional and modern methods and approaches to the evaluation of company performance. *Proceedings of the Carpathian Logistics Congress,* Jeseník, Czech Republic.

Saderova, J., Bindzar, P. (2014). Using a model to approach the process of loading and unloading of mining output at a quarry. *Gospodarka Surowcami Mineralnymi,* 30(4):97-112. doi:10.2478/gospo-2014-0033

Saniuk, S., Saniuk, A., Cagáňová, D., (2019). Cyber Industry Networks as an environment of the Industry 4.0 implementation. *Wireless Networks*. 2019(7): 1-7. doi:10.1007/s11276-019-02079-3

Straka, M., Hurna, S., Bozogan, M., Spirkova, D. (2019). Using continuous simulation for identifying bottlenecks in specific operation, *International Journal of Simulation Modelling,* 18(3):408-419. doi:10.2507/IJSIMM18(3)477

Straka, M. (2017). *Teoretické východiská simulácie - simulačný systém EXTENDSIM 9.x, Theoretical basis of simulation – simulation system EXTENDSIM 9.x,* 1st edition, Faculty BERG, TUKE, Kosice. (Original in Slovak)

Straka, M., Malindzakova, M., Rosova, A., Trebuna, P. (2016). The simulation model of the material flow of municipal waste recovery. *Przemysl chemiczny,* 95(4):773-777. doi:10.15199/62.2016.4.12

Šaderová J., Marasová D., Galliková J. (2018) Simulation as logistic support to handling in the warehouse: case study, *TEM Journal*. 7(1):112-117.

Šimková, M., Očenášová, M., Tudoš, D., Róth, B. (2019). The political frame of the European Union for mining of non-energetic raw materials. *Acta Montanistica Slovaca,* 24(1):35-43.

Toomey, J. W. (1996). *MRP II: Planning for Manufacturing Excellence,* Chapman & Hall, NY.

Urzúa, M., Mendoza, A., González, A. O. (2019). Evaluating the impact of order picking strategies on the order fulfilment time: a simulation study, *Acta logistica,* 6(4):103-114. doi:10.22306/al.v6i4.129

Vilamova, S., Besta, P., Kozel, R., Janovska, K., Piecha, M., Levit, A., Straka, M., Sanda, M. (2016). Quality quantification model of basic raw materials, *Metalurgija,* 55(3):375-378.

New seismic station Pražmo in Silesia and Northeast Moravia, Czech Republic - initial seismological observations

Markéta Lednická[1]***, Jana Rušajová***[1] *and* ***Pavel Kalenda***[2]

Analysis of initial seismological observations at the newly established seismic station at Pražmo in Beskydy Mountains is presented in this study. The PRAZ station represents the easternmost station at the territory of the Czech Republic currently and it is supposed that this station will contribute to detection of mining induced events from the Upper Silesian Coal Basin and to local tectonic events in the eastern part of Moravian-Silesian region, where significant seismic source zones of historical earthquakes are located – e.g. Český Těšín and Opava. Seismological recordings obtained at PRAZ station during six months of continual monitoring since December 2018 were analysed not only from the seismological point of view, but the local geology effect has been considered as well. Achieved results proved that the PRAZ station contributes especially to the detection of mining induced events from the Ostrava-Karviná Coal Basin. Evaluation of local site effect by spectral ratio methods, namely the HVNR and the HVSR, confirmed low amplification at an investigated place due to first meters of Quaternary sediments covering the sandstone bedrock. Performed detail analysis of three local tectonic events and one mining-induced event proved that the PRAZ station provides good-quality data for the foci location.

Keywords: *Silesia and Northeast Moravia, seismic monitoring, seismic network, earthquake.*

Introduction

The study presents the first results of initial seismological observations made between the beginning of December 2018 and the end of May 2019 at the newly established seismic station at Pražmo (Beskydy Mountains, Frýdek-Místek district). The Pražmo seismic station (signed as PRAZ) representing the easternmost station in the territory of the Czech Republic is operated by the Institute of Geonics of the CAS (IGN CAS), and it has been established within the frame of the CzechGeo/EPOS-Sci project. The main aim of this station is an expansion of the actual seismic network of the IGN CAS and consequently also local seismic network MONET (MOravia NETwork) operated by the Institute of Physics of the Earth, Masaryk University of Brno (IPE MU). Nowadays, the IGN seismic network consists of the following stations - Ostrava-Krásné Pole (OKC), Stěbořice (STEB), Klokočov (KLOK) and Zlaté Hory (ZLHC). The OKC station is included in the Czech Regional Seismological Network (CRSN), and it is jointly operated by the IGN CAS, the Institute of Geophysics of the CAS (IG CAS) and the VSB-Technical University of Ostrava (VSB-TUO). Stations STEB, KLOK and ZLHC are included into MONET since 2016 for the purpose of the project CzechGeo/EPOS. All stations excepting the OKC have been equipped with the new data acquisition system and seismometer thanks to the financial support of above mentioned CzechGeo/EPOS-Sci project. Interpretation of seismograms carried out by the IGN CAS is focused on picking up Pn, Pg and Sg phases corresponding to local tectonic events, seismic events induced by coal mining in the Czech and Polish mines within the Upper Silesian Coal Basin (USCB), seismic events induced by ore mining in the Legnica-Glogów Copper Belt area (Poland), quarry blasts and other seismic phenomena. Readings are available at the website of the IGN CAS in local bulletins (IGN bulletin, 2019). Data recorded at the OKC and the STEB stations are transmitted online to the data centres at IG CAS and IPE MU, and they are thus available for primary determination of seismic event location. Readings are also included in bulletins of seismic events recorded by the CRSN which are available at the data portal CzechGeo (CzechGeo, 2019). More detailed information about seismic monitoring activities at Silesia and Northeast Moravia, actual and historical seismicity, development of local seismic networks and other studies like, for example, 3D regional velocity model determination are presented in following papers - (Holub et al., 2004; Špaček et al., 2006; Holub et al., 2007; Kaláb et al., 2007; Holub et al., 2009; Holub and Rušajová, 2011; Růžek et al., 2011; Zedník and Pazdírková, 2014; Špaček et al., 2015).

It is assumed that the PRAZ seismic station will contribute to the detection of local tectonic events in the eastern part of Moravian-Silesian region and also to detection of induced seismic events caused by mining activities in the Czech and the Polish part of USCB. The lack of seismic station distribution in the eastern part of the discussed region became evident in the case of mechanism reconstruction of the strongly felt earthquake originated near Hlučín on December 10, 2017, with local magnitude M_L = 3.5 (Hrubcová et al., 2018; Šílený and Zedník, 2018). Authors present class of acceptable and forbidden mechanisms instead of the single best solution due to insufficient density and regularity of nearby seismic stations and they compare the results with the direction of local faults to find related tectonics. The PRAZ station is expected to provide valuable data for

[1] *Markéta Lednická, Jana Rušajová,* The Czech Academy of Sciences, Institute of Geonics, Studentská 1768, CZ-70800, Ostrava - Poruba, Czech Republic, *marketa.lednicka@ugn.cas.cz; jana.rusajova@ugn.cas.cz*

[2] *Pavel Kalenda,* CoalExp, Pražmo, Czech Republic, *p.kalenda@volny.cz*

mechanism reconstruction in such cases of strong local tectonic events. Three seismic source zones are located within the perimeter of 60 km from the PRAZ station where historical earthquakes were documented with the intensity 6 ^{o} MSK and higher - Opava area, Český Těšín area (for example, Schenk et al., 1997) and Žilina area (Slovakia, part of the Pieniny Klippen Belt zone; for example, Kováč et al., 2002). The earthquake near Český Těšín originated on February 27, 1786 (Io = 7-8^{o}, Mw = 5.44) and belongs to the strongest documented earthquakes in the territory of the Czech Republic within the last centuries. Several historical earthquakes have been documented near Žilina since 17th century – three strongest originated on December 11, 1613 (Io = 8^{o}, Mw = 5.77), January 15, 1858 (Io = 7-8^{o}, Mw = 5.44) and October 24, 1858 (Io = 6^{o}, Mw = 4.46). Next earthquake felt in discussed territory occurred on April 12, 1931, near Opava (Io = 6^{o}, Mw = 3.9). Epicentral macroseismic intensity Io and moment magnitude Mw were taken from The SHARE European Earthquake Catalogue (SHEEC**)** 1000-1899 (Stucchi et al., 2013; Locati et al., 2014) and from The SHARE European Earthquake Catalogue (SHEEC**)** 1900-2006 (Grünthal et al., 2013).

Analysed period of six months of monitoring at the PRAZ station provides enough data to perform statistical analysis of recorded events in given categories defined in local bulletins. These results are compared with events recorded at another station located in the territory of Silesia and Northeast Moravia equipped with the same data acquisition system and seismometer – the STEB seismic station. The study also provides brief information about local geology and related site effect investigated using spectral ratio methods, namely the HVNR method for ambient noise records and the HVSR method for records of seismic events. Few examples of recorded seismic events, both the tectonic and mining-induced, originated during the analysed period in the discussed territory are presented including their foci location using data from seismic stations operated by the IGN CAS.

Locality – seismic stations and geology

The situation of current seismic stations operated by the IGN CAS in the territory of Silesia and Northeast Moravia is presented in the Fig. 1 together with temporary stations operated within the CzechGeo/EPOS-Sci project and with the newly established PRAZ station discussed in the paper. Other surrounding seismic stations operated at the territory of the Czech Republic, Slovakia and Poland are also displayed to see how the PRAZ station will contribute to existing national seismic networks at the boundary of these three countries. Seismic stations of IG CAS included in CRSN and stations of IPE MU included in CRSN and MONET are located at the territory of Czech Republic. The National Network of Seismic Stations of Slovakia (NNSS) is operated by the Earth Science Institute of the Slovak Academy of Sciences (ESI SAS), and stations of the Polish Seismological Network (PLSN) are operated by the Institute of Geophysics of Polish Academy of Sciences (IG PAS). Detailed information about all mentioned seismic networks (including local and temporary networks) can be found on the web pages of individual institutions (www.ig.cas.cz; www.ipe.muni.cz; www.igf.edu.pl; www.seismology.sk) and in published papers, for example, Trojanowski et al., 2015; Zedník and Špaček, 2016; Csicsay et al., 2018.

The PRAZ seismic station is installed in a cellar of a small building at a depth of approximately 2 meters below the surface, and its position is defined by geographical coordinates φ = 49.6069^{o} N, λ = 18.4861^{o}E and altitude of 459 m. Local geology represents a layer of Quaternary sediments in the thickness of the first meters covering the sandstone bedrock (for details see Table 1). Local geology can significantly influence the seismic response, and therefore local site effect was evaluated in detail to know possible amplification and the resonant frequency of near-surface layers at the locality. Information about local geology is briefly described in Table 1 also for all permanent stations of the IGN seismic network. The STEB and the KLOK stations are situated in similar conditions as the PRAZ station because all three stations are installed in masonry objects on the surface. Seismometers of the OKC station are installed at a depth of 10 m below the surface directly on the bedrock outcrop in the experimental gallery driven in the weathered slates (Lednická and Rušajová, 2016). The seismic pillar of the ZLHC station is located at a depth of 90 m below the surface in quartzite rock (Zimák and Štelcl, 2000) in restricted underground spaces of speleotherapy that is operated by the private medical institution for children with respiratory diseases – Sanatorium EDEL, Ltd.

The PRAZ station is equipped with the data acquisition system GAIA Q (Vistec company, Prague) and three-component seismometer Lennartz LE3D/5s (Lennartz, Germany) with the frequency range 0.2 – 50 Hz (Fig. 2). The station with a continuous record and GPS synchronization of time operates now in the offline regime. Nevertheless, the data acquisition system enables also on-line data transmission to the centre of the CRSN. Recorded data in MiniSEED format are sampled at 100 Hz frequency, and they are stored on SD card.

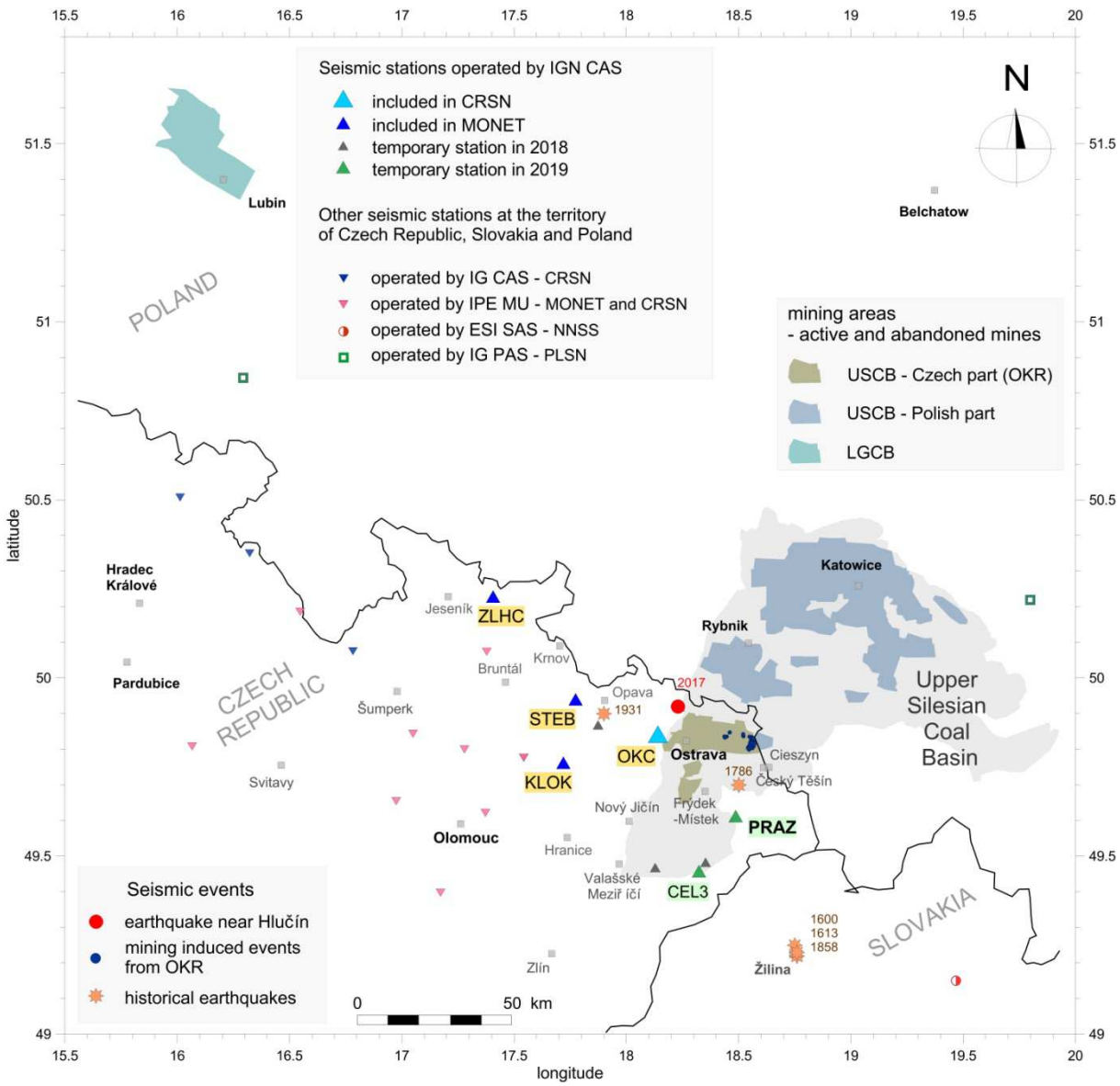

Fig. 1. The situation of seismic stations operated by the IGN CAS in the territory of Silesia and Northeast Moravia in the years 2018 – 2019 and situation of other surrounding seismic stations operated by the IG CAS, IPE MU, ESI SAS and IG PAS at the territory of Czech Republic, Slovakia and Poland. The OKC station is jointly operated by the IGN CAS, IG CAS and VSB-TUO. Temporary station – seismic station tested within the project CzechGeo/EPOS-Sci, CRSN – Czech Regional Seismological Network; MONET – Moravia NETwork, NNSS - National Network of Seismic Stations of Slovakia, PLSN - Polish Seismological Network. Displayed mining areas at the territory of Czech Republic (according to Martinec et al., 2006) and Poland (according Dubiński et al., 2019; Bartlett et al., 2013) represent focal zones of mining-induced seismic events included in the regional bulletins – USCB (Upper Silesian Coal Basin), OKR (Ostrava-Karviná Coalfield), LGCB (Legnica-Glogów Copper Belt). Examples of local seismic events are also presented – historical earthquakes originated near Opava, Český Těšín and Žilina; earthquake originated near Hlučín on December 10, 2017; mining-induced events originated in OKR from December 2018 to May 2019 with released energy more than 1.0E+04 J (GreenGas database, 2019).

*Tab. 1. Brief information about the depth of sediments and type of underlying bedrock at the places of individual seismic stations was compiled based on the Map applications of the Czech Geological Survey. Available boreholes closest to the stations and reaching underlying bedrock were selected from the descriptive database of geological objects (Borehole surveys, 2019). Each borehole is described by the reference ID in the borehole inventory, thickness of Quaternary sediments and type of underlying bedrock. Characterization of Quaternary sediments results from the geological map (Geological map 1:500,000, Quaternary cover 1:500,000, 2019). *Geological map was used for local geology specification directly at the place of KLOK station due to lack of boreholes in the vicinity of the investigated place.*

Station	Borehole ID	Borehole distance from the station	Quaternary sediments	Thickness of QS	Underlying bedrock
PRAZ	487268	326 m	Sandy silts up to silty sands	4.0 m	Sandstone
	487269	345 m	Sandy silts up to silty sands	4.6 m	Sandstone
	487392	201 m	Silty sediments with cobbles	7.5 m	Sandstone
STEB	313120	77 m	Sandy silts up to silty sands	6.0 m	Slates
	313121	22 m	Sandy silts up to silty sands	5.5 m	Slates
	313122	41 m	Sandy silts up to silty sands	8.4 m	Slates
KLOK	317079	927 m	Sandy silts up to silty sands	3.6 m	Slates
	317080	995 m	Sandy silts up to silty sands	2.8 m	Slates
	317082	983 m	Sandy silts up to silty sands	2.6 m	Slates
	Geol. map*	0 m	_	0 m	Slates
OKC	325041	20 m	Clay loam, detritus	4.5 m	Slates
ZLHC	305402	20 m	_	0 m	Quartzite
	305454	20 m	_	0 m	Quartzite

Fig. 2. Apparatus GAIA Q with seismometer Lennartz LE-3D/5s is installed in the cellar of a small masonry building at a depth of approximately 2 meters below the surface.

Used data and methods

Statistical analysis of events recorded at the PRAZ station and comparison with the STEB station

The database of seismic events detected at the PRAZ station was compiled using those events with apparent body wave onsets so that the arrival times of seismic phases Pn, Pg and Sg could be interpreted. All events from this database were compared to events detected at the STEB station that is equipped with the same instrumentation, and that is located in similar conditions – it means masonry object on the surface where underlying bedrock is covered by the first meters of Quaternary sediments. There was no interruption of recording during the analysed period of six months for both stations, so the data are fully acceptable for the analysis. Mutual comparison of the number of detected events was performed for individual categories classified in the bulletins of the IGN CAS:

- **Poland** – mining-induced events from the Polish part of USCB (for example, Stec, 2007); mainly events from the mines near Rybnik and Katowice; epicentral distances usually from 40 to 100 km (PRAZ) and from 35 to 105 km (STEB)
- **OKCB** – mining-induced events from Ostrava-Karviná Coal Basin including destress rock blasting for rockburst control (Koníček et al., 2013; Koníček and Schreiber, 2018); epicentral distances usually from 15 to 25 km (PRAZ) and from 50 to 60 km (STEB)
- **Lubin** – mining-induced events from the mines near Lubin in Legnica-Glogów Copper Belt area in southwestern Poland (for example, Lasocki and Orlecka-Sikora, 2008); epicentral distances from 245 to 275 km (PRAZ) and from 190 to 215 km (STEB)
- **explosions** – quarry blasts from adjacent quarries;

- **tectonic events –** tectonic events at the territory of Silesia and Northeast Moravia (for example, focal zones near Opava, Suchdol, Vítkov and other) and tectonic events from adjacent areas in Poland and Slovakia;
- **other** - for example, events from the open-pits of the brown coal district near Belchatow (Poland), rest of unidentified seismic events, …

Location of events using data from the IGN seismic stations

Several local tectonic events were recorded at the PRAZ seismic station within the analysed period, and three of them were selected for detail analysis of event foci location using only stations of the IGN network – OKC, STEB, KLOK, ZLHC, temporary station CEL3 and discussed station PRAZ. Moreover, one mining-induced event from the OKCB (locality of CSM Mine, released energy 4.13E+05 J; GreenGas database, 2019) has been analysed in the same way using only data from the IGN stations.

Analysis of seismic recordings has been realized using the Seismic Handler software package (Stammler, 1993; http://www.seismic-handler.org/). Foci location computation within Seismic Handler was performed by external program LocSat. Precise manual picking of P and S-wave arrival times is a fundamental part of the computation process. Example of graphical output from the software is presented in Figs. 3 and 4 for the local tectonic event originated near Vítkov on March 27, 2019, and for the mining-induced event originated at CSM Mine on April 15, 2019.

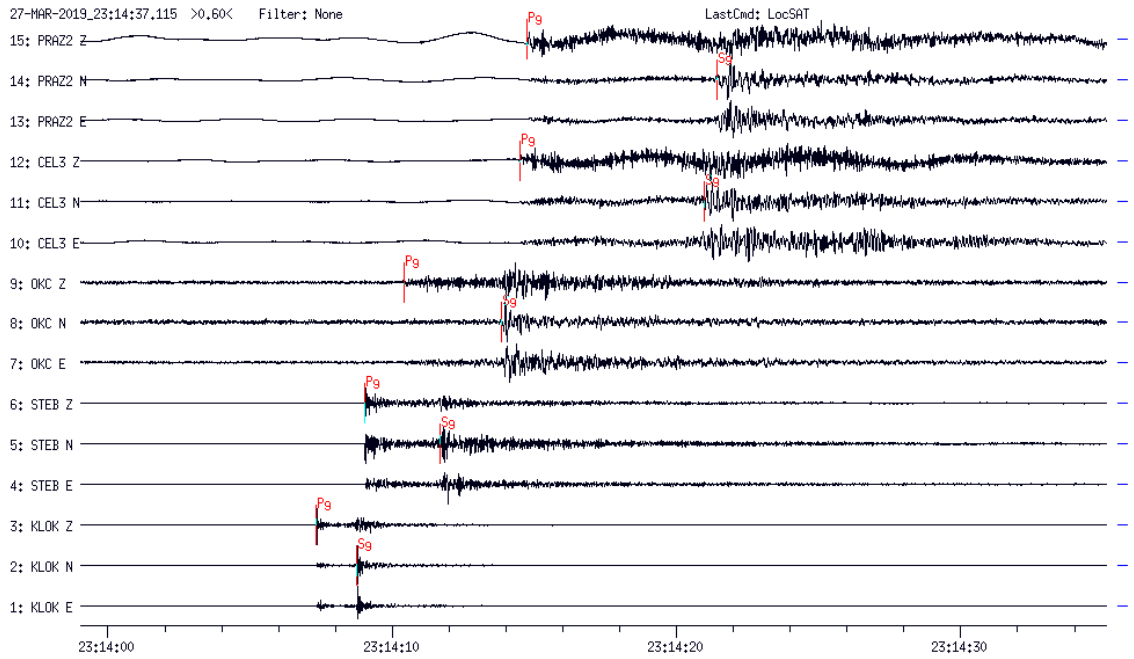

Fig. 3. Graphical output from the Seismic Handler software – manual picking of P and S-wave arrival time; local tectonic event originated near Vítkov on March 27, 2019, with the local magnitude M_L 1.9 (bulletins of seismic events recorded by the CRSN; CzechGeo, 2019).

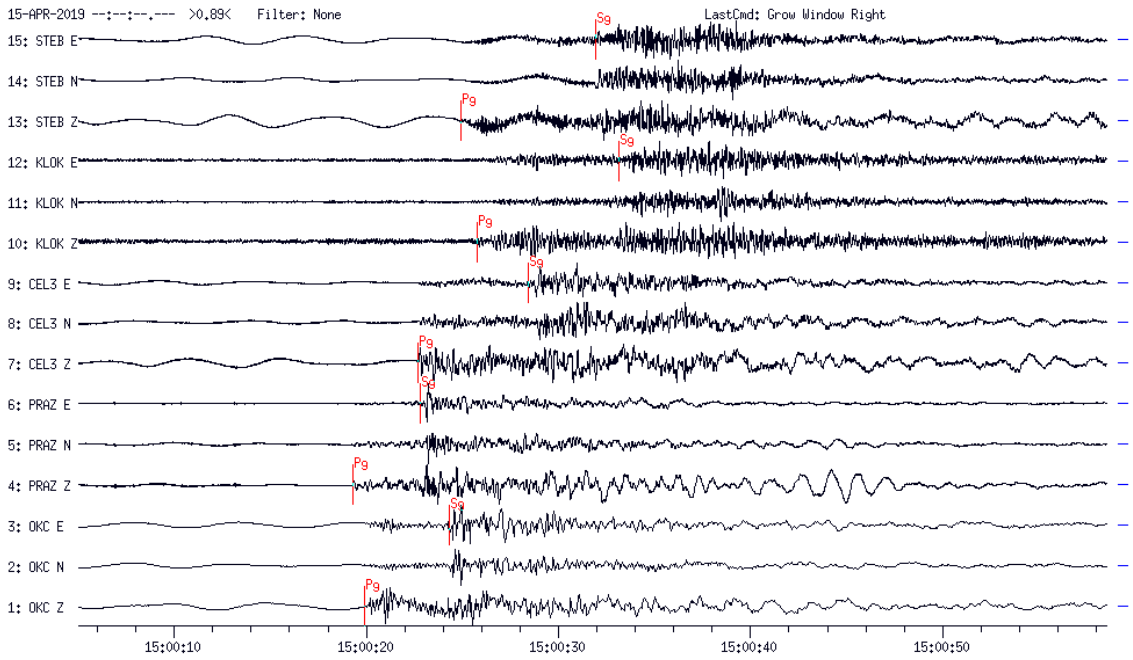

Fig. 4. Graphical output from the Seismic Handler software – manual picking of P and S-wave arrival time; mining-induced event originated at CSM Mine on April 15, 2019, with released energy 4.13E+05 J (GreenGas database, 2019).

Evaluation of local site effect using spectral ratio methods

Local site effect, it means the resonant frequency of sedimentary layers and the amplification factor, was analysed using spectral ratio methods – the HVNR "horizontal to vertical noise ratio method" and the HVSR "horizontal to vertical spectral ratio method" (e.g. Nakamura,1989; Lermo and Chávez-García, 1993). Resonant frequency ***f*** depends on average shear-wave velocity $\boldsymbol{v_s}$ and the thickness of sedimentary layers ***h,*** and it can be described using the following formula:

$$f = v_s (4\,h)^{-1} \qquad (1)$$

The amplitude of the fundamental resonant peak depends on the impedance contrast between soil layers and underlying bedrock (for example, Pitilakis, 2004).

Records of the ambient seismic noise were analysed by the HVNR method separately for stations PRAZ, STEB, KLOK, OKC and ZLHC to have the possibility to compare site effect at newly established PRAZ station with permanent IGN stations. The HVNR method uses seismic noise as an input and computes the horizontal to the vertical spectral ratio between the horizontal and vertical components. The data were analysed using the H/V tool of Geopsy software (Wathelet et al., 2011; www.geopsy.org). The duration of selected records of seismic noise measured during the night was approximately 2 hours and more than 100 windows of the length of 60 s were analysed in each record. Before computing the spectral ratio, Fourier spectra amplitudes of individual components were smoothed with the Konno-Ohmachi smoothing function with a smoothing constant equal to 40 and the spectra of two horizontal components were averaged using a quadratic mean. Resulting averaged spectral ratio curve, and its standard deviation was computed for all selected windows.

The HVSR method was applied only for seismic events recorded at the PRAZ station to confirm the results obtained by the HVNR method for this newly investigated locality. Dataset of 14 mining-induced events from OKCB was used for this analysis. The H/V tool of Geopsy software was used for the spectral ratio curve computation again. The length of windows was 40 s, and each window included the part of the seismic record corresponding to S-wave phase, so the total number of selected windows corresponds to the number of elaborated events.

Results and discussion

Statistical analysis and comparison with the STEB station

The number of interpreted events corresponding to individual categories classified in the bulletins of the IGN CAS for the PRAZ and the STEB stations is presented in Fig. 5. The total number of interpreted events per month was from 245 to 375 for the STEB station and from 227 to 334 for the PRAZ station. Mining induced events from the Polish part of USCB represent the substantial part of each data set. Mining induced events from the OKCB represent the second group considering the number of interpreted events.

The STEB station represents the best seismic station of the IGN network for detection of local tectonic events and mining-induced events in the territory of Silesia and Northeast Moravia considering the number of interpreted events in local bulletins (IGN bulletin, 2019). Majority of events from the Polish part of the USCB have a similar epicentral distance to both seismic stations. The lesser number of these events registered at the PRAZ station is related to the higher level of seismic noise at this place, which is approximately by 20 % higher than the noise level at the STEB station. When evaluating mining-induced events from the OKCB, the PRAZ station has detected more events than the STEB station, which corresponds to the location of the PRAZ station, which is much closer to the Ostrava-Karviná Coal Basin than the STEB station.

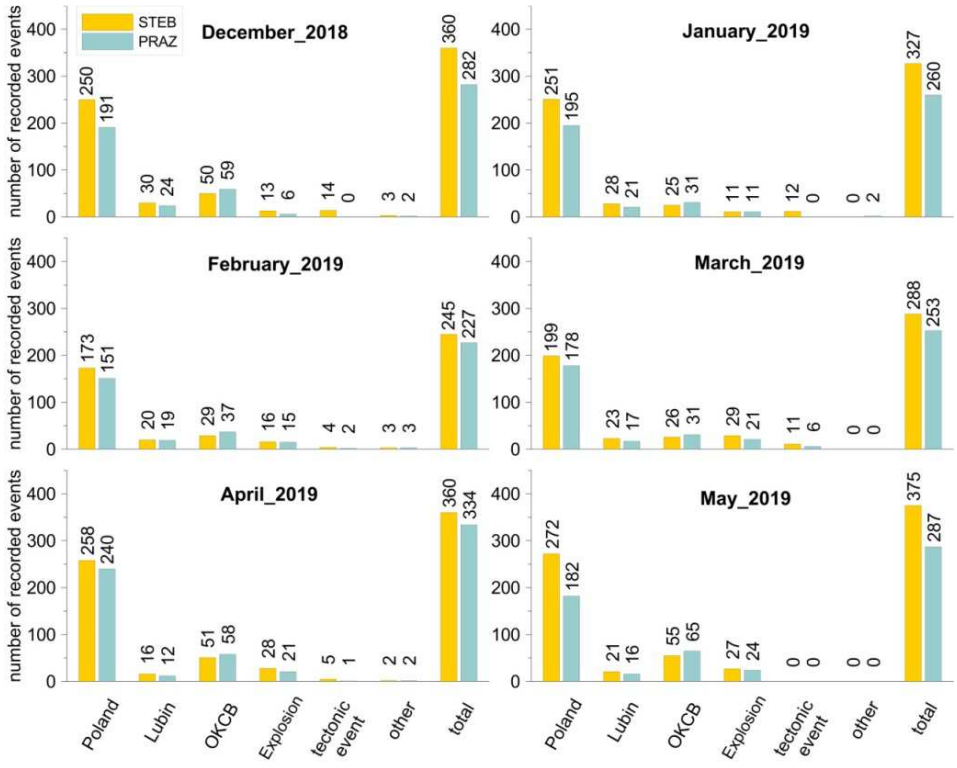

Fig. 5. The number of interpreted events corresponding to individual categories classified in the bulletins of the IGN CAS for the PRAZ and the STEB stations within the period from December 2018 to May 2019.

Location of events using data from the IGN seismic stations

Foci location of four seismic events elaborated by using the Seismic Handler software package is displayed in Fig. 6 – three local tectonics and one mining-induced event from OKCB. Results of foci location computation using LocSat program are summarized in Table 2 for all elaborated events.

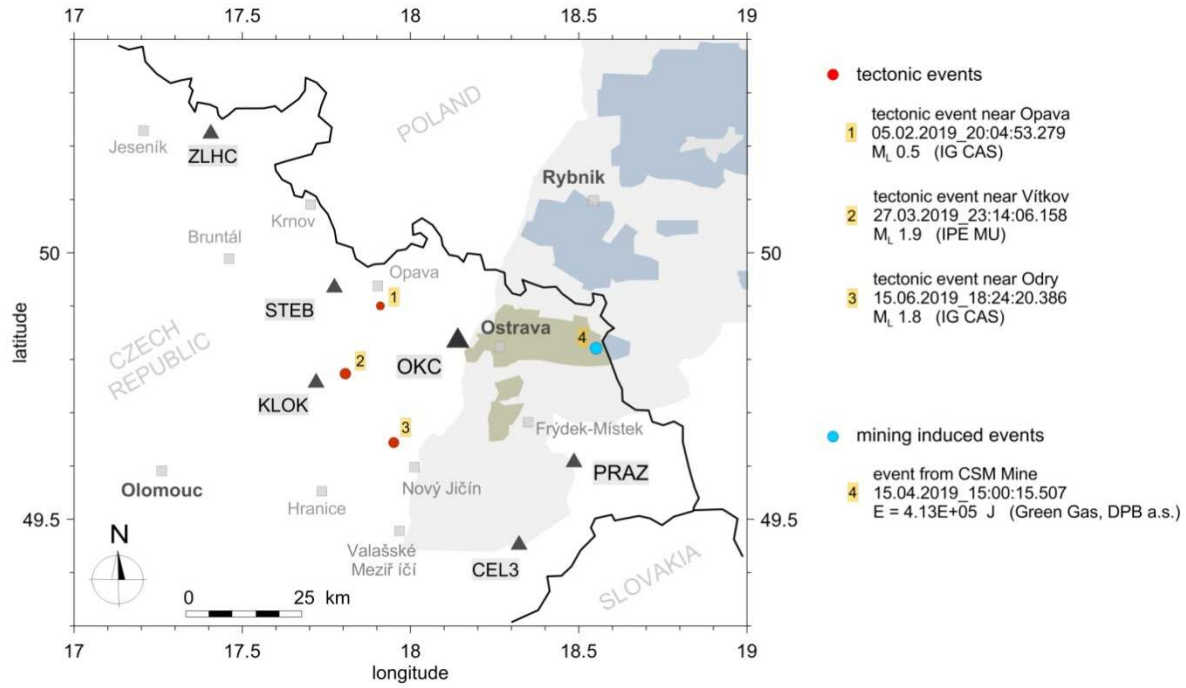

Fig. 6. Foci location of three local tectonic events and one mining-induced event from OKCB. Displayed seismic stations operated by the IGN CAS were used for the foci location computation performed by the Seismic Handler software package.

Tab. 2. Results of foci location computation using LocSat program within Seismic Handler for all elaborated events

Tectonic event near Opava	Origin time: 5-FEB-2019_20:04:53.279			
Latitude: 49.900 deg. N	Longitude: 17.910 deg. E		Depth: 2.347 km	
Station	Phase	Residuals	Distance (deg.)	Azimuth (deg.)
STEB	Pg	-0.1	0.095	291.65
STEB	Sg	0.1	0.094	291.65
OKC	Pg	0.0	0.163	113.54
OKC	Sg	0.0	0.163	113.54
KLOK	Pg	0.0	0.189	220.77
KLOK	Sg	0.0	0.189	220.77
PRAZ	**Pg**	**0.1**	**0.475**	**127.87**
PRAZ	**Sg**	**0.0**	**0.475**	**127.87**

Tectonic event near Vítkov	Origin time: 27-MAR-2019_23:14:06.158			
Latitude: 49.773 deg. N	Longitude: 17.806 deg. E		Depth: 1.902 km	
Station	Phase	Residuals	Distance (deg.)	Azimuth (deg.)
KLOK	Pg	-0.1	0.059	253.52
KLOK	Sg	0.2	0.059	253.52
STEB	Pg	-0.1	0.163	352.57
STEB	Sg	-0.1	0.163	352.57
OKC	Pg	0.2	0.225	73.98
OKC	Sg	0.1	0.225	73.98
CEL3	Pg	0.0	0.465	133.56
CEL3	Sg	-0.3	0.465	133.56
PRAZ	**Pg**	**0.1**	**0.472**	**110.39**
PRAZ	**Sg**	**0.0**	**0.472**	**110.39**

Tectonic event near Odry		Origin time: 15-JUN-2019_18:24:20.386		
Latitude: 49.644 deg. N		Longitude: 17.950 deg. E	Depth: 3.780 km	
Station	Phase	Residuals	Distance (deg.)	Azimuth (deg.)
KLOK	Pg	-0.2	0.219	191.27
KLOK	Sg	0.1	0.219	191.27
OKC	Pg	-0.4	0.267	273.02
OKC	Sg	0.1	0.267	273.02
CEL3	Pg	0.1	0.399	202.03
CEL3	Sg	-0.1	0.399	202.03
STEB	Pg	0.1	0.516	282.98
STEB	Sg	-0.1	0.516	282.98
PRAZ	**Pg**	**0.4**	**0.543**	**263.45**
PRAZ	**Sg**	**0.0**	**0.543**	**263.45**
ZLHC	Pg	-0.1	0.627	337.97
ZLHC	Sg	0.0	0.627	337.97

Mining-induced event from the CSM Mine		Origin time: 15-APR-2019_15:00:15.507		
Latitude: 49.821 deg. N		Longitude: 18.552 deg. E	Depth: 1.765 km	
Station	Phase	Residuals	Distance (deg.)	Azimuth (deg.)
PRAZ	**Pg**	**-0.2**	**0.219**	**191.27**
PRAZ	**Sg**	**0.1**	**0.219**	**191.27**
OKC	Pg	-0.4	0.267	273.02
OKC	Sg	0.1	0.267	273.02
CEL3	Pg	0.1	0.399	202.03
CEL3	Sg	-0.1	0.399	202.03
STEB	Pg	0.1	0.516	282.98
STEB	Sg	-0.1	0.516	282.98
KLOK	Pg	0.4	0.543	263.45
KLOK	Sg	0.0	0.543	263.45

When we compare results of foci location for the mining-induced event using LocSat program with the information listed in the database of GreenGas DPB a.s. (49.831^{o}N; 18.561^{o}E; depth of 986 m; GreenGas database, 2019), the difference in epicentre position is 1.26 km, and the difference in the depth is 0.98 km. The LocSat program used for the computation within the SeismicHandler software uses the simplified velocity model IASP91. This velocity model is sufficient for preliminary computation of the foci location. Nevertheless, it doesn´t correspond to the complex local geological conditions in the Ostrava-Karviná Coal Basin. More precise information about the foci location can be obtained using a representative velocity model determined for given locality (i.e. Kalenda, 1992). In the case of tectonic events originated at the locality of Silesia and Northeast Moravia, more precise location can be obtained by using, for example, 3D velocity model defined by Růžek et al. (2011**).**

Evaluation of local site effect using spectral ratio methods

Resulting spectral ratio curves determined by the HVNR method are presented in Fig. 7 for all investigated stations PRAZ, STEB, KLOK, OKC and ZLHC. Displayed spectral ratio curves show the averaged curve and its standard deviation computed for all selected windows. The flattest shape of the curve with no amplification corresponds to the ZLHC station located in quartzite rock massif 90 meters below the surface. The stations OKC and KLOK show almost flat shape of spectral ratio with amplification lower than 1.5 and no one clear peak. According to Steidl et al. (1996), the existence of weathered rock layers may result in the site effect. According to borehole 325041, which is located almost at the place of the OKC station, there is a layer of weathered slates of the Carboniferous age at a depth of 10 m below the surface where seismometers are installed. The fresh rock is located below the depth of 23 meters (Lednická and Rušajová, 2016). According to the geological map, there are no layers of Quaternary sediments directly at the place of the KLOK station. The station is situated in small masonry object on the surface, so the slight site effect corresponds most probably to the layers of weathered slates near the surface. Remaining two spectral ratio curves exhibit low amplification within the frequency range 2 – 20 Hz for the STEB station and 1.5 – 10 Hz for the PRAZ station. Maximum amplification up to 2.0 falls within the frequency range 5.5 – 7.5 Hz for the STEB and 2.5 - 6.5 Hz for the PRAZ station. The significant peak at frequency 20 Hz on the spectral ratio curve for the PRAZ station do not correspond to the effect of local geology. The amplification is caused most probably by some artificial source of harmonic vibrations in the

vicinity of station, because changes of the amplification factor corresponding to 20 Hz are evident on spectral ratio curves calculated for different time periods (Fig. 7) while the amplification below 10 Hz corresponding to site effect is similar for all elaborated curves. In addition, there is not the same peak on the spectral ratio curve calculated for seismic events using the HVSR method presented in Fig. 8. On the other hand, the frequency range of amplification 1.5 – 10 Hz corresponds well to results of the HVNR method. There is only a small difference in the amplification factor close to the frequency of 5 Hz.

Analysis of local site effect proved slight amplification due to Quaternary sediments at Pražmo and Stěbořice locality. Considering the same type of sediments at both localities (sandy silts up to silty sands) with the same values of s-wave velocities, the thickness of sediments at Pražmo locality should be few meters more than at Stěbořice based on obtained resonant frequencies. These results of spectral ratio methods can help to specify local geology, especially at places where there is lack of boreholes and other geological documentation.

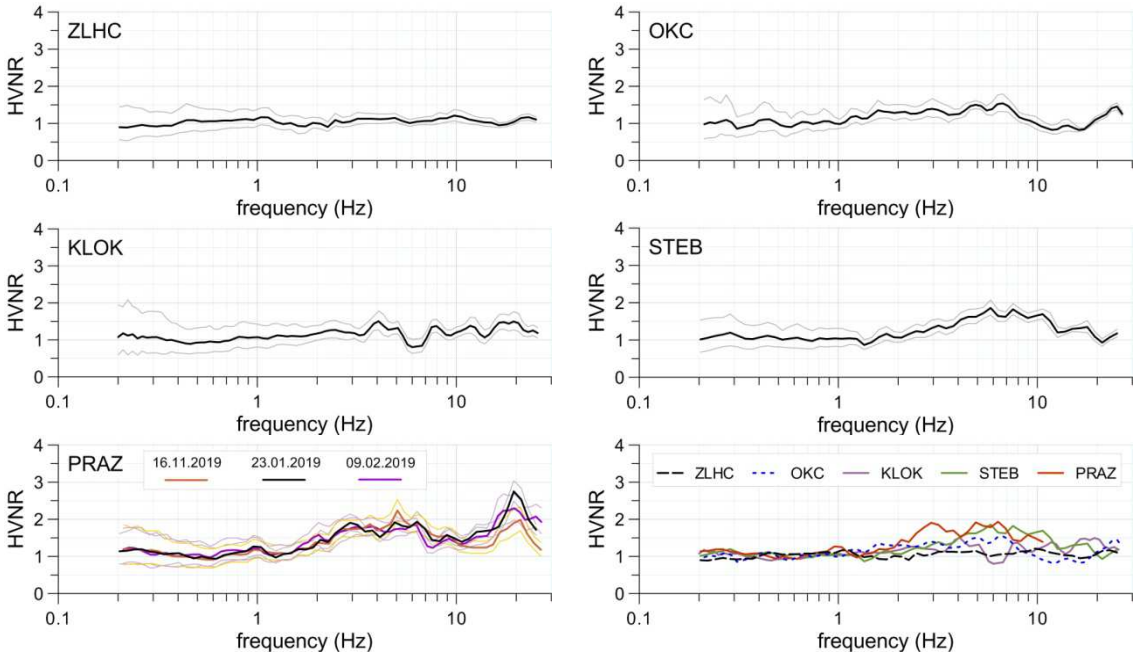

Fig. 7. Spectral ratio curves calculated for stations of the IGN network and for newly established PRAZ station using HVNR method; spectral ratio curves show the averaged curve and its standard deviation computed for all selected windows.

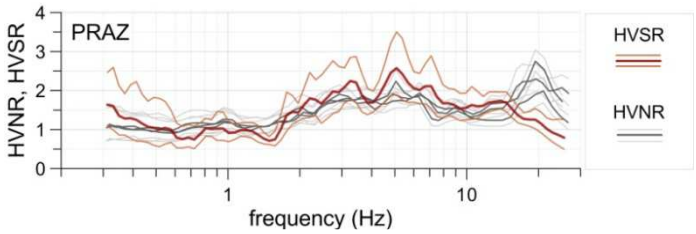

Fig. 8. Spectral ratio curves calculated for the PRAZ station using HVSR and HVNR method; spectral ratio curves show the averaged curve and its standard deviation computed for all selected windows

Conclusion

The main aim of the presented paper was to provide detail information about the newly established seismic station at Pražmo (Silesia and Northeast Moravia, Frýdek-Místek district) representing the easternmost station at the territory of the Czech Republic. Seismological recordings obtained during six months of continual monitoring were analysed not only from the seismological point of view, but the effect of local geology has also been considered. Conclusions resulting from the initial seismological observations at the PRAZ seismic station can be characterized as follows:

- the station has a suitable location for the expansion of the IGN seismic network to the east. Its position near the boundaries between the Czech Republic, Slovakia and Poland will contribute to complement data from Slovak and Polish seismic stations in the case of earthquakes occurring at boundary of these three countries, especially from both regions Český Těšín and Žilina, where macroseismically felt historical earthquakes occurred.
- site effect evaluation by spectral ratio methods confirmed low amplification due to local geology similar to other stations of the IGN seismic network located in similar geological conditions.
- statistical analysis of all interpreted events proved that the PRAZ station contributes especially to the detection of mining induced events from the Ostrava-Karviná Coal Basin.
- nine tectonic events originated at the territory of Silesia, Northeast Moravia and adjacent area in Poland have been detected during the analysed period at the PRAZ seismic station. Performed analysis of selected seismic recordings using the Seismic Handler software package proved that the PRAZ station provides good-quality data for preliminary computation of the foci location.

Acknowledgements*: We thank anonymous reviewers for their comments, which improved the clarity of this paper. This research is supported by the project of large research infrastructure CzechGeo/EPOS (LM2015079) and by the project CzechGeo/EPOS-Sci (CZ.02.1.01/0.0/0.0/16_013/0001800) and it is partly performed with the long-term conceptual development support of research organizations RVO: 68145535.*

References

Bartlett, S.C., Burgess, H., Damjanović, B., Gowans, R.M., Lattanzi, C.R. (2013). Technical report on the copper-silver production operations of KGHM Polska Miedź S.A. in the Legnica-Glogów copper belt area of southwestern Poland. Technical report, Canada: Micon International Ltd., 159 p. Available from: https://kghm.com/sites/kghm2014/files/document-attachments/kghm_technical_report_micon.pdf.

Borehole surveys (2019). In: Borehole surveys [online]. Praha: Czech Geological Survey [cit. 2019-05-03]. Available from: https://mapy.geology.cz/vrtna_prozkoumanost/.

Csicsay, K., Cipciar, A., Fojtíková, L., Kristeková, M., Gális, M., Srbecký, M., Chovanová, Z., Bystrický, E., Kysel, R. (2018). The National Network of Seismic Stations of Slovakia – Current state after 13 years in operation from the project of modernization and enhancement. *Contributions to Geophysics and Geodesy, Vol. 48, no. 4*, p. 337 – 348. DOI: 10.2478/congeo-2018-0016.

CzechGeo (2019). Seismic data portal. Available from: http://www.czechgeo.cz/en/article/default/seismic-data-portal.

Dubiński, J., Stec, K., Bukowska, M. (2019). Geomechanical and tectonophysical conditions of mining-induced seismicity in the Upper Silesian Coal Basin in Poland: a case study. *Archives of Mining Sciences, Vol. 64, no. 1*, p. 163 – 180. DOI: 10.24425/ams.2019.126278.

Geological map 1:500,000, Quaternary cover 1:500,000 (2019). In: Geoscience maps 1:500,000 [online]. Praha: Czech Geological Survey [cit. 2019-05-06]. Available from: https://mapy.geology.cz/geocr500/.

GreenGas database (2019). Database of Green Gas, DPB a.s. Available from: https://www.dpb.cz/seismologicky-informacni-system-archiv-jevu/?rok=2019.

Grünthal, G., Wahlström, R., Stromeyer, D. (2013). The SHARE European Earthquake Catalogue (SHEEC) for the time period 1900-2006 and its comparison to the European-Mediterranean Earthquake Catalogue (EMEC). *Journal of Seismology, Vol. 17, no. 4*, p. 1339 – 1344. DOI: 10.1007/s10950-013-9379-y.

Holub, K., Kaláb, Z, Knejzlík, J. and Rušajová, J. (2004). Frenštát seismic network and its contribution to observations of the natural and induced seismicity on the territory of Northern Moravia and Silesia. *Acta Geodynamica et Geomaterialia, Vol. 1, no. 1 (133)*, p. 59 – 71.

Holub, K., Kaláb, Z., Knejzlík, J., Rušajová, J. (2009). Contribution of the Institute of Geonics of the ASCR Ostrava to Seismological monitoring in Silesia and Northern Moravia. *Acta Geodynamica et Geomaterialia, Vol. 6, no. 3 (155)*, p. 391–398.

Holub, K., Rušajová, J., Pazdírková, J. (2007). Re-opening of the temporary seismic station at Klokočov (KLOK). *Transactions of the VŠB – Technical University of Ostrava, Civil Engineering series, Vol. VII, No. 2*, p. 83 – 90.

Holub, K., Rušajová, J. (2011). Re-established seismic station at Stěbořice in the Nový Dvůr arboretum Near Opava. *EGRSE. Exploration Geophysics, Remote Sensing and Environment, Vol. XVIII, no. 2*, p. 24 – 31.

Hrubcová, P., Šílený, J., Zedník, J (2018). Earthquake at Hlučín. *Vesmír, Vol. 97, no. 3*, p. 158 – 159. (in Czech)

IGN bulletin (2019). Local bulletins of the stations operated by the IGN. Available from: http://ugn.cas.cz/?l=en&a=&v=&p=bulletin/bulletin.php.

Kaláb, Z., Knejzlík, J., Holub, K. (2007). Decade of seismological observations in the northern Part of Moravo-Silesian region. *Acta Geodynamica et Geomaterialia, Vol. 4, no. 4 (148)*, p. 43 – 49.

Kalenda, P. (1992). Zhodnocení závislosti vyzařované seismické energie na parametrech horninového prostředí a technologii dobývání. PhD Theses, GFÚ ČSAV, Praha.

Koníček, P., Schreiber, J. (2018). Rockburst prevention via destress blasting of competent roof rocks in hard coal longwall mining. *The journal of the Southern African Institute of Mining and Metallurgy, Vol. 118, no. 3*, p. 235 - 242. DOI: 10.17159/2411-9717/2018/v118n3a6.

Koníček, P., Souček, K., Staš, L., Singh, R. (2013). Long-hole destress blasting for rockburst control during deep underground coal mining. *International Journal of Rock Mechanics and Mining Sciences, Vol. 61*, p. 141–153. DOI: 10.1016/j.ijrmms.2013.02.001.

Kováč, M., Bielik, M., Hók, J., Kováč, P., Kronome, B., Labák, P., Moczo, P., Plašienka, D., Šefara, J., Šujan, M. (2002). Seismic activity and neotectonic evolution of theWestern Carpathians (Slovakia). *Stephan Mueller Special Publication Series, 3*, p. 167 – 184.

Lasocki, S., Orlecka-Sikora, B. (2008). Seismic hazard assessment under complex source size distribution of mining-induced seismicity. *Tectonophysics, Vol. 456, no. 1-2*, p. 28–37. DOI:10.1016/j.tecto.2006.08.013.

Lednická, M., Rušajová, J. (2016). Experimental measurement at the seismic station Ostrava-Krásné Pole (OKC): preliminary results and remarks on site effect at the studied locality. *Acta Geodynamica et Geomaterialia, Vol. 13, no. 2 (182)*, p. 137 – 147. DOI: 10.13168/AGG.2015.0051.

Lermo, J., Chávez-García, F. J. (1993). Site effect evaluation using spectral ratios with only one station. *Bulletin of the Seismological Society of America, Vol. 83, no. 5*, p. 1574 – 1594.

Locati, M., Rovida, A., Albini, P., Stucchi, M. (2014). The AHEAD portal: A gateway to European historical earthquake data. Seismological Research Letters, Vol. 85, no. 3, p. 727 – 734. DOI: 10.1785/0220130113.

Martinec, P. et al. (2006). *Termination of underground coal mining and its impact on the environment*. Ostrava: Anagram.

Nakamura, Y. (1989). A method for dynamic characteristics estimation of subsurface using microtremor on the ground surface. *Quarterly Reports of Railway Technical Research Institute, Vol. 30, no. 1*, 25 **–** 33.

Pitilakis, K. (2004). Site effect, In A. Ansal (Ed.), *Recent advance in earthquake geotechnical engineering and microzonation* (pp. 139 – 197). Dordrecht: Kluwer Academic Publisher.

Růžek, B., Holub, K., Rušajová, J. (2011). Three-dimensional crustal model of the Moravo-silesian region obtained by seismic tomography. *Studia Geophysica et Geodaetica, Vol. 55, no. 1*, p. 87 – 107.

Schenk, V., Schenková, Z., Kottnauer, P. (1997). Categorisation and harmonisation of probabilistic earthquake hazard assessment with respect to statistic representation of input data. *Natural Hazards, Vol. 15, no. 2-3*, p. 121 – 137.

Stammler, K. (1993). SeismicHandler - Programmable multichannel data handler for interactive and automatic processing of seismological analyses. *Computers and Geosciences, Vol. 19, no. 2*, p. 135 – 140.

Stec, K. (2007). Characteristics of seismic activity in the Upper Silesian Coal Basin in Poland. *Geophysical Journal International, Vol. 168, no. 2*, p. 757 – 768. DOI: 10.1111/j.1365-246X.2006.03227.x.

Steidl, J. H., Tumarkin, A. G. and Archuleta, R. J. (1996). What is a reference site? *Bulletin of the Seismological Society of America, Vol. 86, no. 6*, p. 1733 – 1748.

Stucchi, M., Rovida, A., Gomez Capera, A.A., Alexandre, P., Camelbeeck, T., Demircioglu, M.B., Gasperini, P., Kouskouna, V., Musson, R.M.W., Radulian, M., Sesetyan, K., Vilanova, S., Baumont, D., Bungum, H., Fäh, D., Lenhardt, W., Makropoulos, K., Martinez Solares, J.M., Scotti, O., Živčić, M., Albini, P., Batllo, J., Papaioannou, C., Tatevossian, R., Locati, M., Meletti, C.,Viganò, D., Giardini, D. (2013). The SHARE European Earthquake Catalogue (SHEEC) 1000-1899. *Journal of Seismology, Vol. 17, no. 2*, p. 523-544. DOI:10.1007/s10950-012-9335-2.

Šílený, J., Zedník, J. (2018). Mechanism of the earthquake at Hlučín near Ostrava, Czech Republic, on December 10, 2017. *EGRSE. Exploration Geophysics, Remote Sensing and Environment, Vol. XXV, no. 1*, p. 83 – 91. DOI: 10.26345/EGRSE-083-18-107. (in Czech)

Špaček, P., Bábek, O., Štěpančíková, P., Švancara, J., Pazdírková, J., Sedláček, J. (2015). The Nysa‑Morava Zone: an active tectonic domain with Late Cenozoic sedimentary grabens in the Western Carpathians' foreland (NE Bohemian Massif). *International Journal of Earth Sciences, Vol. 104, no. 4*, p. 963 – 990. DOI: 10.1007/s00531-014-1121-7.

Špaček, P., Sýkorová, Z., Pazdírková, J., Švancara, J., Havíř, J. (2006). Present-day seismicity of the south-eastern Elbe Fault System (NE Bohemian massif). *Studia Geophysica et Geodaetica, Vol. 50, no. 2*, p. 233 − 258.

Trojanowski, J., Plesiewicz, B., Wiszniowski, J. (2015). Seismic monitoring of Poland - description and results of temporary seismic project with mobile seismic network. *Acta Geophysica, Vol. 63, no. 1*, p. 17 – 44. DOI:10.2478/s11600-014-0255-0.

Wathelet, M. et al. (2011). Geophysical signal database for noise array processing (GEOPSY), free download available at the web-site: http://www.geopsy.org/download.php.

Zedník, J., Pazdírková, J. (2014). Seismic activity in the Czech Republic in 2012. *Studia Geophysica et Geodaetica, Vol. 58, no. 2*, p. 342 – 348. DOI: 10.1007/s11200-013-1290-z.

Zedník, J., Špaček, P. (2016). Czech Regional Seismic Network and local seismic network MONET. In: CzechGeo/EPOS Workshop [online]. Available from: http://czechgeo.ig.cas.cz/data/CRSN_MONET_2016.pdf.

Zimák, J., Štelcl, J. (2000). Geological conditions and rock radioactivity in the speleotherapy medical facility in the Zlaté Hory ore district (the Czech Republic). *Geologica Carpathica, Vol. 51, no. 6*, p. 407 – 412.

The influence of extraction speed on the value of the coefficient of subsidence rate

***Piotr Strzałkowski*[1], *Wiesław Piwowarski*[2] *and* *Roman Ścigała*[1]**

The presented paper discusses the issues of prediction of land surface transient deformation state caused by underground mining, using Budryk-Knothe theory, which is still the most popular solution in this field in Poland. The research results known from the literature and authors' own observations indicate the relationship between the value of the coefficient of subsidence rate "c" and the speed of extraction progress as well as the depth of underground mining works. Firstly in this paper, a short description of present knowledge state in this field has been presented. As the next part of this work, an empirical formula (9) has been proposed, that links the value of parameter "c" with the depth of mining works and the extraction speed. The formula (9) has been worked out on the basis of 9 cases, where extraction was led with the different speed at different depths. Then, the obtained formula was compared with some research results known from the literature. Presented calculations results are consistent with them, concerning analyses of surveys conducted above underground mining extraction carried out with high speed. This allows considering the proposed empirical relationship (9) as valid and useful for the practice of mining in the field of prediction of land surface transient deformation state. In the final part of the paper, some suggestions have been pointed, regarding the further possible development of the research toward increasing the accuracy of predictions of transient deformation state caused by underground mining.

Key words: *prediction of post-mining transient deformations, geometric-integral theories, speed of extraction front.*

Introduction

As it is well known, underground mining generates many adverse changes to the natural environment as well as constructions in urbanized areas (Peng, 2015; Stojiljkovic et al., 2014; Strzałkowski, 2010a; Mikulenka, 2007; Bell, Genske, 2001). Economic indicators of Polish hard coal mining industry inspire to seek new strategies for increasing the efficiency of underground mining with taking into account issues of minimization of its influence on the environment by using different methods, for example, described in (Wang et al., 2016). One of the possible solutions for improving efficiency is the concentration of extraction by, among others, increasing the speed of extraction advance, as the simplest solution – especially that the existing mining machinery has some power reserves. The impact of high–speed progress of mining extraction on the land surface deformation state was a subject of many publications (Dżegniuk, Sroka, 2002; Chudek, 2010; Hejmanowski, 1997; Kowalski, 1993, 2007; Smolnik, 2009; Sroka, 1974, 1999; Strzałkowski, 2010a). On the other hand, it should be noted that high extraction speed causes a significant increase in deformation rates over time, which negatively affects the construction of buildings and is an important factor causing mining damages.

A. Sroka (1999) concluded, basing on the experience of the Ruhr Coal Basin, that the cost of mining damages increases with the square of the extraction advance speed. The need for continuous extraction advance, without weekend breaks, was also pointed in his work. As an expression of this finding, there was a proposal of defining the categories of mining areas basing on the subsidence rate and its acceleration.

Extraction speed should, of course, be adopted to specific conditions, with particular emphasis on the resistance of surface building objects to mining damages. It is worthy to mention that the research results published in (Kratzsch, 1983) indicate (based on the experiences of the Ruhr area) that the extraction speed close to 5 m/day did not result in typical building objects damages, while in case of objects with low resistance, safe was the speed of 3 m/day.

In Poland, extraction is usually led with a moderate speed at about 3–5 m/day. Only in the case of "Staszic" coal mine, the speed of extraction was significantly greater – up to 20m/day (Kowalski, 1993; Kowalski, 2007). Presently, in the Lublin Coal Basin, "Bogdanka" mine operates with extraction speed at about 10 m/day, while the total longwalls advance reaches several kilometres.

In the USA ("Twentymile" mine, Colorado) average extraction speed amounts about 40 m/day, but maximum reaches up to 80 m/day (Smolnik, 2009). German experiences come from the extraction speed at the maximum level of 20m/day.

[1] *Piotr Strzałkowski, Roman Ścigała*, Silesian University of Technology, Faculty of Mining, Safety Engineering and Industrial Automation, Akademicka 2, 44-100 Gliwice, Poland. *piotr.strzalkowski@polsl.pl, roman.scigala@polsl.pl*

[2] *Wiesław Piwowarski*, AGH University of Science and Technology, ul. Mickiewicza 30, 30-059 Krakow, Poland

All analyses concerning deformation state changes over time with consideration of high-speed extraction must be founded on the mathematical models verified by surveys. Most of such models based on the proposed by S.Knothe solution of a differential equation, expressing the law of limited growth (Knothe, 1953):

$$\frac{dw(t)}{dt} = c \cdot (w_k(t) - w(t)) \tag{1}$$

where :

$w_k(t)$ – final (asymptotic) value of subsidence,
$w(t)$ – transient value of subsidence,
c – the coefficient of subsidence rate (often called: „time factor").

S.Knothe gave the solution of equation (1) for a theoretical case of instantaneous extraction of elementary field (with the assumption: $w_k(t,x)=w_k=const.$), with the initial condition $t=0 \Rightarrow w(t)=0$, as follows:

$$w(t) = w_k \cdot (1 - e^{-ct}) \tag{2}$$

In work (Piwowarski et al., 1995) there was pointed, that for given mining–geological conditions: $w_k = const$ and $c = const$, $w(t)$ – trajectory in the z direction, the subsidence rate is estimated according to:

$$\frac{dw(t)}{dt} = c \cdot w_k \cdot e^{-c \cdot t} \tag{3}$$

for $t \to 0$ one has the speed of subsidence expressed as:

$$\frac{dw(t)}{dt} = c \cdot w_k \Rightarrow max \tag{4}$$

In practice, subsidence process $w(t)$ cannot start with its maximum rate, as it goes from the equation (4), so it is necessary to take into account the condition: $w_k=w_k(t)\neq const$. Such assumption means that final subsidence w_k varies along with extraction front development. With this assumption, the solution of the inhomogeneous differential equation (1), with the condition: $w(t=0)=0$ has the form:

$$\left.\begin{aligned} w(t) &= A \cdot e^{-c \cdot t} + c \int_0^t w_k(\tau) d\tau \\ &= e^{-ct} \left[A + c \int_0^t w_k(\tau) \cdot e^{c \cdot \tau} d\tau \right] \\ w(t) &= c \cdot e^{-c \cdot \cdot t} \cdot \int_0^t w_k(\tau) \cdot e^{c \cdot \tau} d\tau \end{aligned}\right\} \to A = 0 \tag{5}$$

where:

τ – independent time variable.

Assuming that extraction field is of rectangular shape and active extraction edge moves with constant speed v, one obtains, according to S.Knothe theory, final subsidence expressed by the formula:

$$w_k(t) = \frac{w_{\max}}{r^2} \int_{x_0}^{x_t} \int_{y_1}^{y2} \exp\left[-\pi \left(\frac{\xi^2(\tau) + \eta^2}{r^2} \right) \right] d\xi(\tau) d\eta \tag{6}$$

where:

w_{max} – maximum possible value of subsidence,
r – parameter (so–called the radius of major influence range),
y_1, y_2 – space coordinates describing the size of the extraction field in the Y direction,
x_o – x coordinate of longwall's starting roadway,

x_t – x coordinate describing the location of active (moving) longwall edge at time t: $x_t = x_0 \pm v \cdot t$,

v – the speed of extraction,

t – the extraction lasting time,

ξ,η – independent space variables,

τ – independent time variable.

It is necessary to point here, that parameter c cannot be measured directly. It is important, therefore, to plan the optimal location of displacement field sensors for its identification purposes. Such analysis should concern space kinematics of the process. The process model in the R^{3+1} space is a formal structure involving four independent variables, and the description is usually given by employing differential equations. Classical techniques of identification are not effective here, which goes from the necessity of recalculation of the information matrix.

Characteristics of the problem and research state

Aiming at determining the deformation state of rock mass and land surface, several models have been worked out for predicting the displacement of transformed subspace and procedures of displacement field observation have been developed. Solutions should be distinguished here: based on the S. Knothe model and other concepts described, for example, in works (Piwowarski et al., 1995; Sroka, 1999). Other works which come from developing equation (1) with the assumption that c≠const. were presented, among others, by P.Strzałkowski (Strzałkowski, 1998) and J.Białek (Białek, 1991), which additionally modified function describing asymptotic deformation state by introducing two radii of influence range. Interesting discussion on this idea is given in work (Orwat, Mielimąka 2016). There is also a solution that bases on the phenomenon of diffusion (Piwowarski, 1989). In the 70s, the theory of dynamical systems was considered, which expanded the possibilities of describing the phenomena encountered in nature (Piwowarski et al., 1995). In a transient process, the value of a given variable at the time t depends on the value of this variable at the time *(t–1)*, and also determines its value at the time *(t+1)*. The same variable can be treated as both – a cause and consequence. Such approach stays in contradiction with the traditional way of unidirectional thinking about the relationship between cause and effect and creates a kind of causal loop.

The results of analyses performed by different authors (Hejmanowski 1997; Kowalski 1993, 2007; Sroka, 1974) point, that in case of extraction led with high speed, not always significant decrease in values of deformation indices is observed, as it was judged earlier. Discussions of survey results from Niederberg coal mine presented in (Sroka, 1999) show the ratio of transient tilt decrease in relation to its maximum values at the level of 0.95, which refers to so-called "dynamic variable" u ($u=c \cdot r/v$) value of about 7.5. The coefficient of deformation reduction – f_B, one should understand as :

$$B_{\max} = f_B \cdot B^k_{\max} \tag{7}$$

where:

B_{max} – maximum value of given deformation index in a transient state,

B^k_{max} – maximum value of the given deformation index in the asymptotic (final) state.

The same author in work (Sroka, 1999) gives the following reduction coefficients, characteristic for central part of Upper Silesian Basin:

- for tilt: $f_t = 0.60$,
- for horizontal extensive strain: $f_{\varepsilon+} = 0.50$,
- for horizontal compressive strain: $f_{\varepsilon-} = 0.28$.

One can find similar values in (Kowalski, 2007):

- for tilt: $f_t = 0.51 \pm 0.12$,
- for horizontal extensive strain: $f_{\varepsilon+} = 0.50 \pm 0.20$,
- for horizontal compressive strain: $f_{\varepsilon-} = 0.84 \pm 0.15$.

In work (Sroka, 1999) Author states, that on the basis of mentioned above findings, it may be presumed, that relation between values: $\{c, r, v\}$ exists. It was further found, that the impact of the extraction speed on the parameter characterizing influence range leads to different profiles of asymptotic troughs for the same extraction field mined out with different speed. It was also noted that the value of parameter c depends on the speed of extraction, recalling the results of (Sroka, 1974).

In the framework of this work, the empirical function which binds values of parameter c with the extraction speed – v has been worked out. Next, the results of transient deformation state calculations obtained with using the proposed formula along with the analysis of their agreement with values known from the literature have been presented.

An attempt to establish the relation between parameter c values and the speed of extraction

First, the identification of S.Knothe parameters, on the basis of asymptotic subsidence trough profile taken from surveys led in one of Upper Silesia Basin coal mine had been performed. The extraction was led at the depth *H=500 m* with caving. The thickness of the extracted deposit was *g=1.7 m*. The sketch of the mining field against observing line location is shown in Fig.1. The following values of parameters were identified: coefficient of roof control: $a \approx 0.6$, parameter describing influence dispersion: $tg\beta \approx 2.0$. Next, using these parameters, values of *c* were determined on the basis of trajectories of chosen observing points with using dedicated software (Ścigała, 2008). An exemplary course of subsidence over time for observing point No 17 is presented in Fig.1, along with the obtained value of parameter *c* and percentage fit error.

In Table 1 the values of *c* parameters are given, obtained on the basis of survey for different extraction depths – *H* and the speed of extraction front – *v*. Values of *c* for extraction speeds of *v=8 m/day* and *v=14.2 m/day* have been taken from works (Kowalski, 1993; Sroka, 1999). In Table 1, the values of time factor $c_{calc.}$ have been added, that were obtained by calculating them from the empirical formula (9) presented below.

The empirical formula has been worked out with the assumption, that the dependence between extraction speed *v*, its depth *H* and the value of parameter *c* exists.

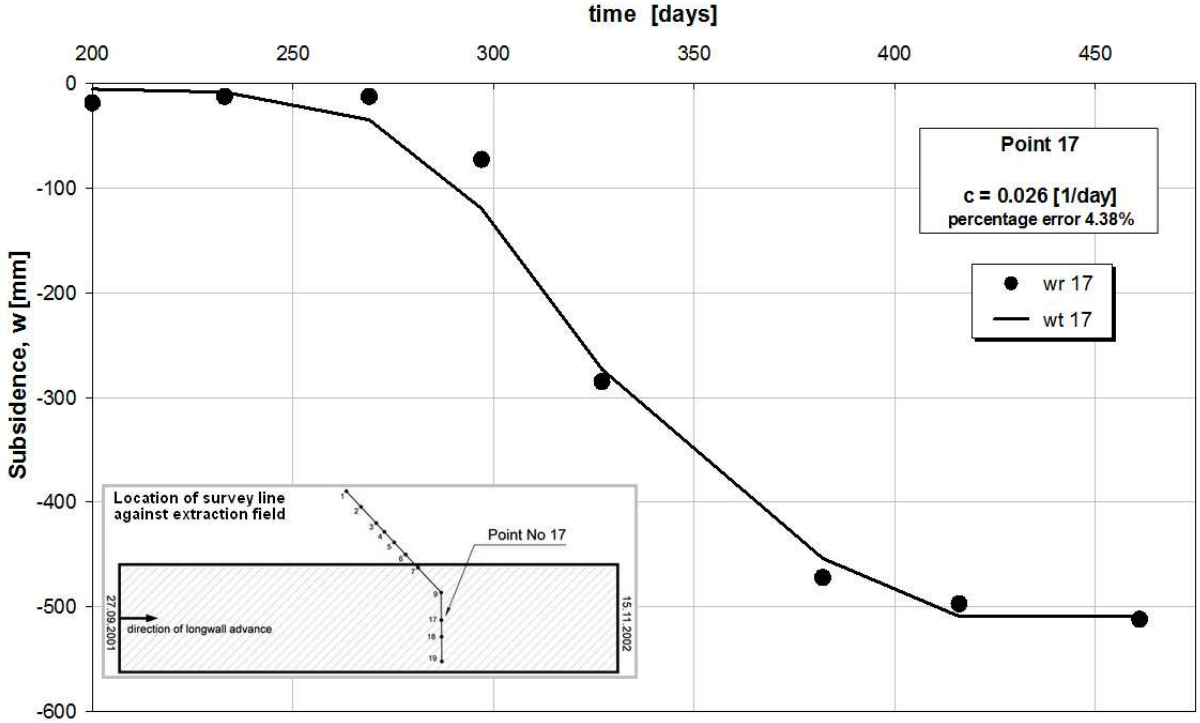

*Fig.1. The exemplary course of subsidence over time – measurement **wr** and calculation results with using S.Knothe model – **wt***

Tab. 1. Obtained values of parameter c for different considered cases of extraction

No	H	v	c	$c_{calc.}$
	[m]	[m/day]	[1/day]	[1/day]
1	840	14.20	0.040	0.045
2	500	5.25	0.026	0.030
3	500	4.60	0.033	0.027
4	495	8.00	0.052	0.044
5	440	1.50	0.011	0.012
6	440	2.40	0.014	0.018
7	360	1.30	0.015	0.012
8	330	2.60	0.022	0.024
9	310	2.00	0.023	0.020

The following regression formula has been used for estimation:

$$c = f(\{\Xi\}, H, v) \tag{8}$$

where: $\{\Xi\}$ – vector of model parameters.

As an effect of regression analysis performed using Mathematica software, the following formula has been obtained:

$$c = 1.463 \cdot \left(\frac{v}{H}\right)^{0.847} \tag{9}$$

For the formula (9), the value of determination coefficient amounts to $R^2=0.976$. In Fig.2 the course of parameter c value according to formula (9) is presented with a thick black line, as well as source data for estimation (Table 1) – dots. Additionally, the confidence intervals at the level of 0.95 are marked on the graph as greyed bands.

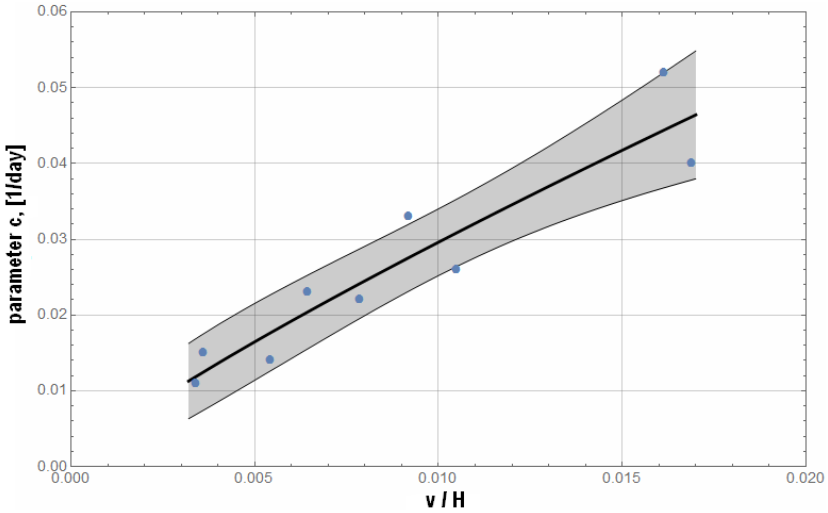

Fig. 2. The graph of empirical formula (9) with confidence intervals at the level of 0.95

The analysis of post–mining deformations changes over time with using an obtained regression formula

For analysis purposes of formula (9) practical use, some testing calculations were performed. Theoretical case of single longwall extraction was assumed, with the length of 250m and the total advance of 1000m. It was also assumed that maximum subsidence equals to $w_{max} = -a \cdot g = 1\ m$. Extraction was located at a depth of $H=600\ m$; coal seam is horizontal and planar. Different speeds of extraction were considered v: 3, 5, 7, 10 i 14 [m/day]. The following values of S.Knothe model parameters were used:

- Parameter $tg\beta = 2.0$ (typical for Upper Silesia Basin),
- Coefficient of proportionality in the Awiershin's relationship $B = 0{,}32r$.

Values of parameter c were calculated by using formula (9), proposed in this paper. So, according to this formula, they were different for diverse extraction speeds – not fixed as it was assumed in work (Strzałkowski, 2010b). Used values of parameter c are presented in Table 3.

For calculation point located at the surface level exactly above the centre of the longwall, the values of deformation indices were calculated, with using DEFK–Win software (Ścigała, 2008) – Fig.3. Calculations were performed in a special way – it was a simulation of extraction advance in the eastern direction, assuming the start of extraction on January 1st, 2017 and 5–day step of extraction advance. As an effect, the distributions of deformation indices over time (along with extraction development) were obtained.

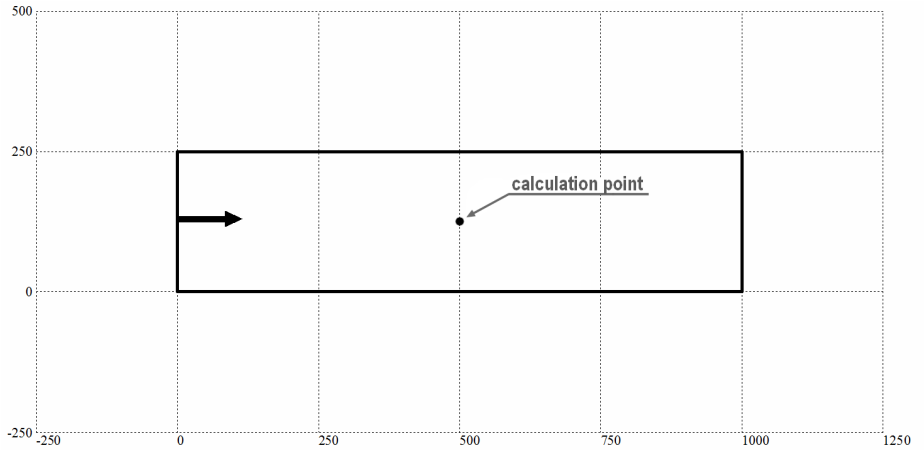

Fig. 3. The sketch of extraction location against calculation point

The following deformation indices were calculated : subsidence *w*, maximum tilt T_{max}, extreme horizontal strain E_{max}. The course over time for these deformation indices are shown in figures 4–6. In Table 3, their extreme values are presented with subsidence rate value *dw/dt* added. Every row in the table presents deformation indices for different value of parameter *c* and "dynamic variable" $c \cdot r/v$.

Tab. 3. Extreme values of deformation indices obtained for considered extraction speeds

v	c	$\frac{c \cdot r}{v}$	T_{max}	E_{max} +	dw/dt
[m/day]	[1/day]		[mm/m]	[mm/m]	[mm/day]
3	0.016	1.600	1.57	0,66	4,68
5	0.025	1.500	1.52	0.63	7.58
7	0.034	1.457	1.50	0.62	10.48
10	0.046	1.380	1.47	0.61	14.50
14	0.069	1.307	1.42	0.56	19.68

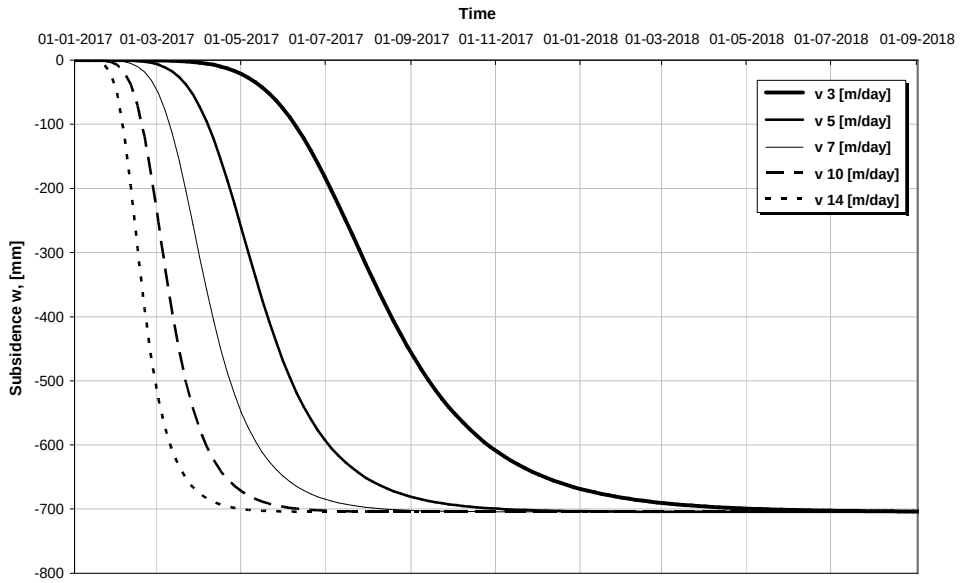

Fig. 4. The course of subsidence over time for different extraction speeds

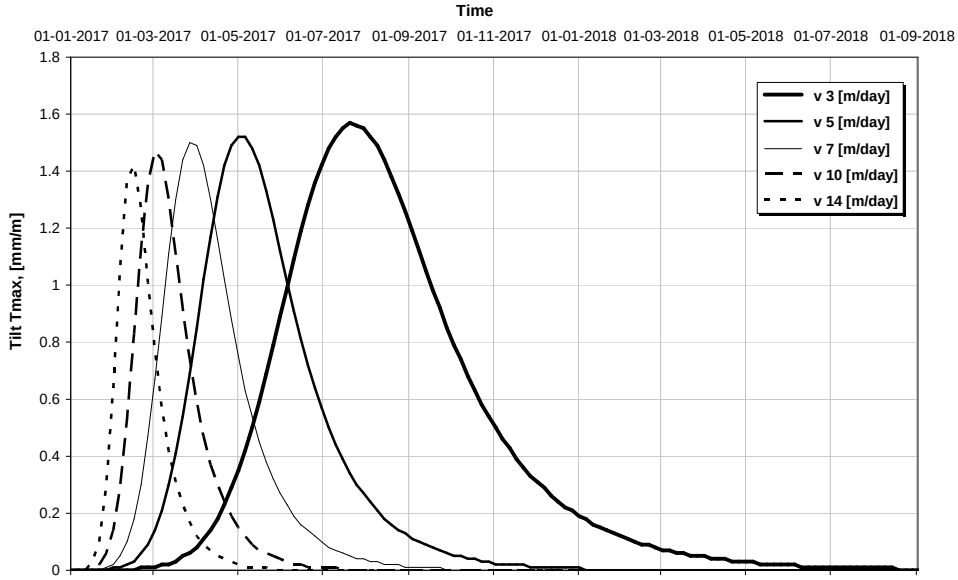

Fig. 5. The course of maximum tilt over time for different extraction speeds

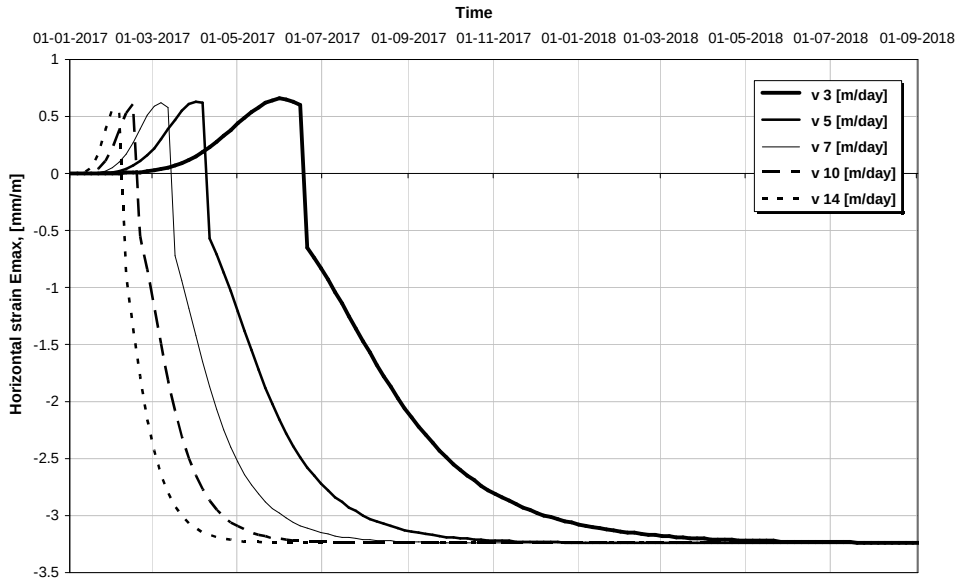

Fig. 6. The course of extreme horizontal strain over time for different extraction speed

As it is apparent from the foregoing drawings and Table 3, an increase in extraction speed does not reduce significantly – in the light of the results of calculations – the values of the deformation indices relative to the predetermined minimum speed of extraction – 3 m/day. It can be concluded, that increasing the extraction speed did not result – in the light of presented calculations results – in a significant reduction of the deformation indices. On the other hand, the subsidence rates *dw/dt* were significantly greater, from approximately 5 mm/day (for v = 3 m/day) to nearly 20 mm/day (for v = 14 m/day).

Further calculations were carried out for 33 points located along a straight line on the surface above the same extraction field – Fig. 7. Calculation points were positioned at mutual distances of 25 m. The calculations were performed for the last day of the given extraction period with the same set of different speeds as used above. The profiles of transient subsidence troughs and asymptotic one are shown in Fig. 8. In Table 4, the maximum values of instantaneous and final: tilt – T_{max} and horizontal strain – E_{max} (positive and negative).

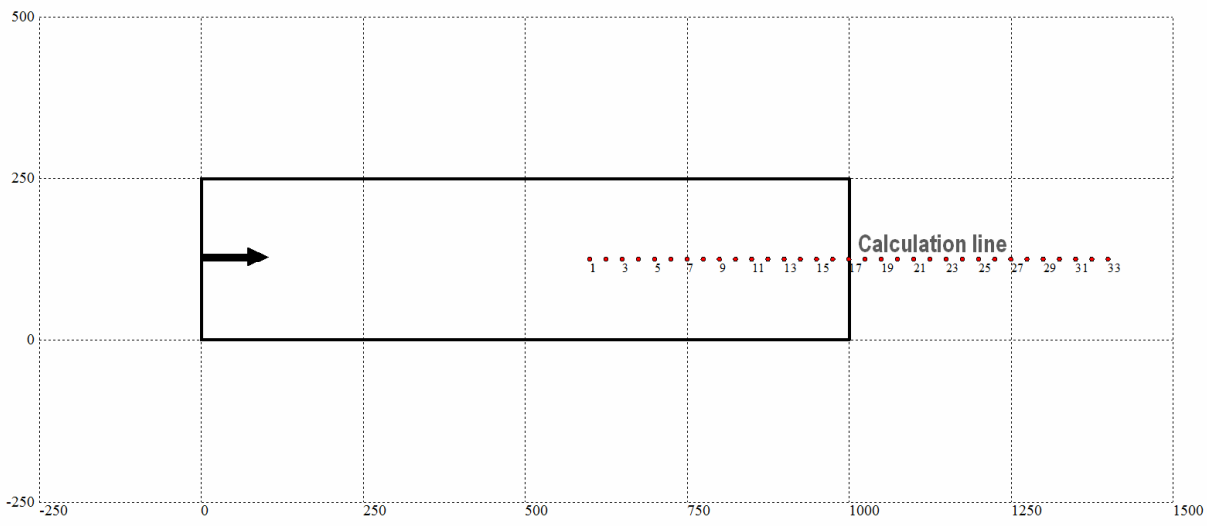

Fig. 7. The sketch of extraction location against calculation line

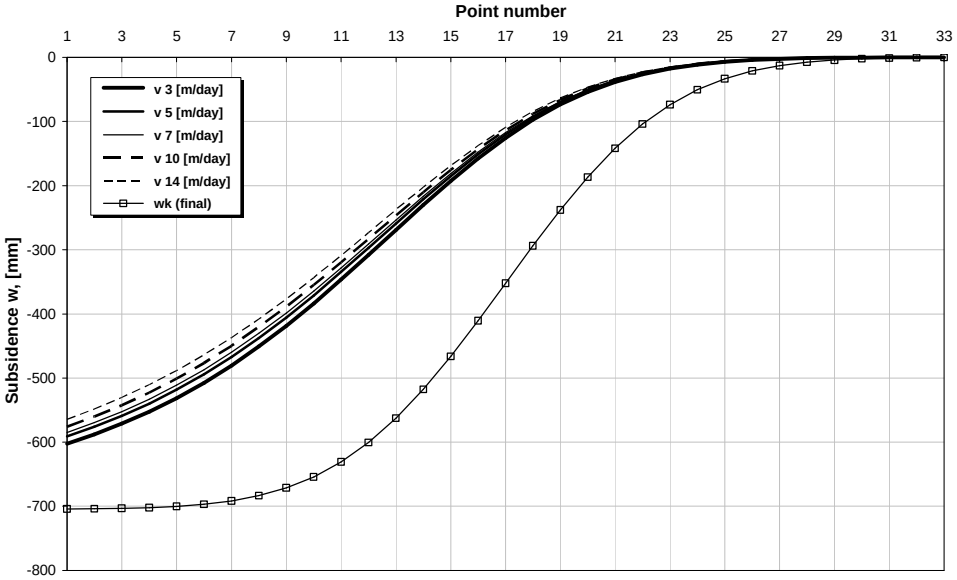

Fig.8. The profiles of transient subsidence troughs obtained with different extraction speed and the profile of asymptotic trough – w_k

Tab. 4. Maximum values of transient and asymptotic values of considered deformation indices and reduction coefficients

v	T_{max}	E_{max+}	E_{max-}	Reduction coefficients		
[m/day]	[mm/m]	[mm/m]	[mm/m]	f_T	f_{E+}	f_{E-}
3	1.56	0.65	-2.77	0.664	0.570	0.855
5	1.52	0.63	-2.72	0.647	0.553	0.840
7	1.50	0.62	-2.69	0.638	0.544	0.830
10	1.47	0.60	-2.65	0.626	0.526	0.818
14	1.43	0.58	-2.60	0.609	0.509	0.802
asymptotic values	2.35	1.14	-3.24	1.000	1.000	1.000

In Table 4, the coefficients of deformation reduction f_i are given – for tilt and horizontal strain (compressive and tensile). It is worthy to emphasize here, that there is an agreement of their values with those cited from publications in the introductory part of the paper. The agreement is clear when referring to A. Kowalski work (1993), whereas some differences one can find in relation to work (Sroka, 1999), regarding compressive strain.

Suggested directions for further research

The analyzed problem of mining displacement process approximation by solutions of differential equations in the form (1) needs to assess whether the process has the trajectories of locally finite *p–variation*. Equation (1) was examined separately as homogeneous and inhomogeneous, as they require different solution definitions as well as various parameters. It can be seen that empirical trajectories of displacement are equivalent to the so–called problem with stochastic disturbance. It seems that it would be advisable to consider the employment of the deterministic equivalent for the stochastic inclusion for a convex, time–varying set of observations of the process.

It can be proved (Skorochod, 1961), that for any continuous functions: y, y_0 and x_0, functions exist: x, k such that:

$$A\,x_t = y_t + k_t \geq 0 \qquad \text{for} \qquad t \in R^+ \tag{10}$$

$k_0 = 0$, k is non–decreasing

$$\int_0^t x_s dk_s = 0 \qquad t \in R^+ \tag{11}$$

Function k is given as follows:

$$k_t = \sup_{s \leq t}(y_s)^- \tag{12}$$

It can be proved, that above-mentioned lemma stays true if instead of continuous functions, one employs the Càdlàg functions (right–continuous with left limits – RCLL) of type:

$$x_t = y_t + k_t \geq l_t \;; \qquad t \in R^+ \tag{13}$$

So, for every $t \in R^+$ we have:

$$\left.\begin{aligned} x_t &= max\left\{min\left| x_t^- + \Delta y_t \right|, l_t \right\} \\ k_t &= max\left\{min\left| k_t^-, u_t - y_t \right|, l_t - y_t \right\} \end{aligned}\right\} \tag{14}$$

Hence the problem arises of existence and uniqueness of solutions to deterministic equations of the form:

$$x_t = x_0 + \int_0^t f\left(s, x_s^-\right) db(s) + \int_0^t g\left(s, x_s^-\right) da(s) + k_t \,; t \in R^+ \tag{15}$$

where integral with respect to a is a generalized Riemann–Stieltjes integral.

A solution to the problem (15) has a finite *p–variation* for any function y of locally finite *p–variation*, which goes from the equation (16):

$$\left| \nabla_x g(t,x) \right| \leq C_{g,N} \tag{16}$$

where: C – is a constant

The solutions of the equation (15) one can approximate by series of iterations in the form:

$$\left(x_0, k_0\right) = ESP\left(x_0, l, u\right)$$

This issue seems to be important, prompting the authors to undertake further research in this field.

Conclusions

Presented in this paper recognition of literature, carried out calculations and analysis of their results entitle to formulate the following statements and conclusions :

1. It should be considered, both in the view of findings known from the literature as well as authors' research, that value of the coefficient of subsidence rate *c* is a function of, among others, the speed of extraction. One possible way of taking this variability into account is the formula (9) presented in this work.
2. A linear relationship between the extraction speed and coefficient of subsidence rate *c* entails coherence in the form of obtaining in predictions the transient subsidence troughs with the same maximum tilt for different extraction speeds. Therefore, it was decided to seek empirical formula (9), basing on a power function.
3. The results of calculations contained in this work confirm the validity of the proposed formula, as obtained transient values of deformation indices stay in similar relations to their final maximum values, as those known from the literature.
4. As a part of the work, the need has been noted for research related to the estimation of whether the mining displacement process described by solutions of the differential equation (1) is the process having the trajectories with locally finite *p–variation*. This issue authors intend to devote more attention in a separate publication.

References

Bell, F.G., Genske, D.D. (2001) The influence of subsidence attributable to coal mining on the environment, development and restoration: Some examples from western Europe and South Africa. *Environmental and Engineering Geoscience 7(1), pp. 81-99.*

Białek J. (1991) Opis nieustalonej fazy obniżeń terenu górniczego z uwzględnieniem asymetrii wpływów końcowych. *Zeszyty Naukowe Pol. Śl., s. Górnictwo, nr 194, Gliwice.*

Chudek M. (2010) Mechanika górotworu z podstawami zarządzania ochroną środowiska w obszarach górniczych i pogórniczych. *Wydawnictwo Politechniki Śląskiej, Gliwice.*

Dżegniuk B., Sroka A. (2002) Prędkość i przyśpieszenie procesu osiadania w aspekcie przerw w prowadzeniu eksploatacji. *Prace Naukowe GIG. Seria Konferencje nr 41. Problemy Ochrony Terenów Górniczych, Katowice.*

Hejmanowski R. (1997) Optymalizacja prędkości eksploatacji górniczej i przerw eksploatacyjnych – oprogramowanie komputerowe. *Conference Proceedings: IV Dni Miernictwa Górniczego i Ochrony Terenów Górniczych, Rytro.*

Knothe S. (1953) Wpływ czasu na kształtowanie się niecki osiadania. *Archiwum Górnictwa i Hutnictwa, Vol 1, Issue 1, Kraków.*

Kowalski A. (1993) Deformacje terenu powstałe w wyniku szybkiej eksploatacji górniczej. Nowe doświadczenia. *Conference Proceedings: II Dni Miernictwa Górniczego i Ochrony Terenów Górniczych, Ustroń..*

Kowalski A. (2007) Nieustalone górnicze deformacje powierzchni w aspekcie dokładności prognoz. *Prace naukowe Głównego Instytutu Górnictwa, nr 871, Katowice.*

Kratzsch H. (1983) Mining Subsidence Engineering. *Springer-Verlag. Berlin, Heidelberg, New York.*

Mikulenka V. (2007) Influence of the mining works on the roads in Ostrava-Karviná´s distrikt. *Acta Montanistica Slovaca, Vol.12, issue 3, p.465-470.*

Orwat, J., Mielimąka, R. (2016) Approximation of average course of measured curvatures of mining area with reference to their forecast values by Bialek's formulas, *Proceedings of 14th International Conference of Numerical Analysis and Applied Mathematics, pp. 130003-1 - 130003-4, ISBN 978-0-7354-1538-6; AIP Conference Proceedings, Volume: 186, Rhodes (Greece).*

Peng S. (2015) Topical areas of research needs in ground control - A state of the art review on coal mine ground control. *International Journal of Mining Science and Technology 25(1), pp. 1-6.*

Piwowarski W. (1989) Opis przemieszczeń pionowych aktywnego procesu deformacji górotworu w warunkach eksploatacji górniczej. *Zeszyty Naukowe Akademii Górniczo – Hutniczej, Vol. Geodezja, Issue No 106, Kraków.*

Piwowarski W., Dżegniuk B., Niedojadło Z. (1995) *Współczesne teorie ruchów górotworu i ich zastosowania. Wydawnictwo AGH, Kraków.*

Skorochod A. V. (1961) Stochastic equations for diffusion processes in a bounded region. *Theory of Probability and its Appllications, Vol. 6 Issue 3,264-274. Society for Industrial and Applied Mathematics, Philadelphia.*

Smolnik G. (2009) Najnowsze trendy w badaniu interakcji górotworu i ścianowej obudowy zmechanizowanej. *Maszyny Górnicze 4/2009, 31-37. Quarterly by KOMAG Mining Mechanization Centre, Gliwice.*

Sroka A. (1999) Dynamika eksploatacji górniczej z punktu widzenia szkód górniczych. *Polska Akademia Nauk, seria Studia, rozprawy, monografie, nr 58, Kraków.*

Sroka A. (1974) Wpływ postępu frontu eksploatacji górniczej na kształtowanie się wskaźników deformacji górotworu. *Phd thesis, AGH Univ. of Science and Technology, Kraków.*

Stojiljkovic E., Grozdanovic M., Marjanovic D. (2014) Impact of the undergroud coal mining on the environment. *Acta Montanistica Slovaca, Vol.19, issue 1, p.6-14.*

Strzałkowski P. (1998) Model nieustalonych przemieszczeń pionowych górotworu w obszarze objętym oddziaływaniem eksploatacji górniczej. *Zeszyty Naukowe Pol. Śl., s. Górnictwo, nr 237, Gliwice.*

Strzałkowski P. (2010a) Zarys ochrony terenów górniczych. *Wydawnictwo Politechniki Śląskiej, Gliwice.*

Strzałkowski P. (2010b) Forecasts of mine-induced land deformations in consideration of the variability of the parameter describing the process kinematics. *Archives of Mining Science. Volume 55. Issue 4, Kraków.*

Ścigała R. (2008) Komputerowe wspomaganie prognozowania deformacji górotworu i powierzchni wywołanych podziemną eksploatacją górniczą. *Wydawnictwo Politechniki Śląskiej, Gliwice.*

Wang X., Zhang D., Sun C., Wang Y. (2016) Surface subsidence control during bag filling mining of super high-water content material in the Handan mining area. *International journal of oil gas and coal technology Vol. 13, issue 1, p. 87-102 DOI: 10.1504/IJOGCT.2016.078049*

Aerodynamics of the Flow Paths of the Vacuum Unit of a Special Cleaning Vehicle in Mining Areas

***Boris Benderskiy*[1], *Pavol Božek*[2], *Afanasij Kolotov*[1], *Nikola Abo Issa*[3], *Aleksey Terentyev*[1] *and* *Alena Chernova*[1]**

The aerodynamic processes occurring in the flow paths of the vacuum device in a special hybrid vehicle intended for mine rail cleaning and the preliminary evaluation of air parameters in the flow paths of the vacuum device are studied. Mathematical modelling of aerodynamic processes was carried out to confirm its performance of rail and air cleaning. The spatial problem of aerohydrodynamics for a single-phase medium by means of a fixed computational grid is solved. Modern computer packages are used for numerical simulation. As a result of the numerical calculations, the pressure losses and maximum flow rate values in the flow paths were determined when the airflow rate varied from 0.5 m^3 / s to 0.27 m^3 / s. The distribution fields of the velocity and pressure module in the intake duct, tank, filter element and silencer are given. It has been shown that at different capacities of the system, the pressure drop in the suction channel ranges from 185 Pa to 300 Pa, the total pressure path loss is 2000 Pa. A mathematical simulation of the filtration and exhaust air damping processes in the filter unit and a vacuum unit muffler was performed. It is shown that the flow rate is reduced to 80%. Analysis of the resulting flow diagrams and aerohydrodynamic parameters confirming the performance of the vacuum unit, which manages flawlessly the mine cleaning.

Keywords: *Special universal vehicle, mine cleaning, attachments, vacuum installation, aerohydrodynamics, mathematical modelling.*

Introduction

Human life activity is mostly the reason for environment pollution. Main places of waste accumulation are public amenities. Such places are public transport route stops and inter-rail space as well as water drainage and sanitary manholes that are often littered with fine wastes (cigarette butts, candy wrappers, paper, small packages and fallen leaves in a mid-season) (Ivanov, 1999), (Murray-Smith, 2019) as well as industrial infrastructure objects, for example, operation (Bołoz & Castañeda, 2018) and sealed off coal mines (Qazizada, 2018).

First railway and train line cleaning devices were designed within the period starting from the end of the 19th century (Herrera, 1880) - to the beginning of the 20th century (Pringle, 1906) and they were self-propelled railway cars with almost no functions and poor manoeuvring performance. These devices were significantly updated during the 20th century and by 70-80s became big vehicles with performance and design similar to the diesel locomotives (Lasser, 1973) and trams (Perrin, 1989) depending on the time period. The last decade of the 20th century and the first decades of the 21st century showed great interest in ecological matters that lead to new special vehicles design promotion. Such devices have very focused specialization due to the strict standards for railway ballast removal procedure.

Today there are not enough universal and environment-friendly samples of special vehicles for railway and tram lines inter-rail space cleaning on the market. A special type of similar devices is designed for railway track ballast removing (Valditerra, 2013) but such devices not just have big size but also are equipped only with railway undercarriage.

The second major group of special railway track cleaning vehicles are railway undercarriage vehicles (Jiyannpieeru, 1996). This group is characterized by considerable size (Theurer and Oellerer, 1991). Such special vehicles are focused ones and are almost impossible to be applied outside the railway track conditions, especially when talking about the urban infrastructure.

Another group of tram line inter-rail space cleaning vehicles that is a wheel mounted and diesel motor driven can be pointed out, for example, Raymond, 1980. Such devices have a smaller size and more functions, but they have a limited size of the collected waste (very small pieces less than 50 grams) and are harmful to the environment due to the diesel engine emission.

Thus, we can point out that the main disadvantages of the existing devices are big size, low functionality and insufficient ecological compatibility of the engines. Consequently, it can be said that the market shows a limited

[1] *Boris Benderskiy, Afanasij Kolotov, Aleksey Terentyev, Alena Chernova*, Kalashnikov Izhevsk State Technical University, Department of Heat Engines and Plants, 7 Studencheskaya st., Izhevsk, Russia, *bib@istu.ru, kolotoff.afanasy2015@yandex.ru, tdu_teran@mail.ru, alicaaa@gmail.com*

[2] *Pavol Božek*, Slovak University of Technology in Bratislava, Faculty of Materials Science and Technology, J. Bottu 25, 917 24 Trnava, Slovakia, *pavol.bozek@stuba.sk*

[3] *Nikola Abo Issa*, Damascus University, Faculty of Mechanical and Electrical Engineering, P.O.Box 86 Damascus, Syria, *nicolanu@scs-net.org*

range of vehicle designs for rail tracks, yard space and public roads cleaning that combine wheel and rail undercarriage for moving by regular roads as well as by railway tracks.

Analysis of main disadvantages of current devices allowed to develop the list of requirements for special vehicles designed for inter rail cleaning. Such requirements include small size, levity and versatility.

Special vehicles shall be equipped with a waste collection device (Attachment, 2010; Kolotov and Benderskiy, 2019; GOST 27478-87, 1987). Newly designed or upgraded installations require waste grip of maximum volume (GOST 27415-87, 1987; GOST 27478-87, 1987). The analysis of the current designs (Kolotov, 2019) discovered a number of major deficiencies of vacuum-cleaning vehicles thus in order to clean the inter-rail space of the tram lines and streets a special hybrid vehicle for tram line and streets cleaning was designed (Fig. 1).

Fig. 1. Hybrid special vehicle with attachable equipment set.

Main characteristics of special vehicle

The proposed vehicle is equipped with a hybrid drive and motor-wheels. The power for electromotor is supplied from the acid accumulator batteries unit that is charged by diesel-generator, mounted on the vehicle frame or by current collector through step-down transformer while the vehicle moves along the tramline. The combined power of four motor-wheels induces motive force of 5000 N (Sleptsov et al., 2006) enough for special vehicle movement across the country with various landform and angle up to 30° (Kolotov and Benderskiy, 2019). The vehicle is mounted on a chassis with a double undercarriage that allows moving both by roads and by rails however road wheels are driven ones. In order to reduce the weight of the vehicle, its double undercarriage is performed as a frame structure made of composite materials. The quick-turn railway carriage is mounted on a frame, and it gives the direction of the vehicle movement along the rails. Thus the designed vehicle has small size, low weight due to the composite frame materials and mobile as it can move along the rails as well as the road track.

Such a special vehicle (Attachment, 2010) design and dimensions provide the ability to turn within a 20m radius without leaving the rails.

The special vehicle configuration (Fig. 2) includes a waste-collecting tank with special structure (Kolotov and Benderskiy, 2019), vacuum-heating unit and portable attachments of various applications in addition to the above the given vehicle is environmentally friendly and multifunctional.

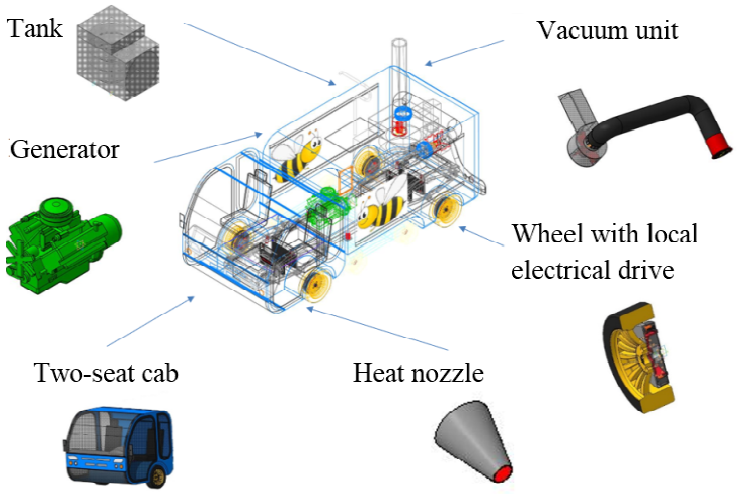

Fig. 2. Special vehicle scheme

A dry weight of the vehicle is 800 kilograms. The weight is uniformly distributed by axles. Each vehicle axle can receive additional load up to 200 kilograms. Removable attachable equipment quickly transforms special vehicle from vacuum cleaning vehicle to filter-exhauster for coal mines cleaning, snow blower, sweeping device, washing or sprinkling machine using the multifunctional drive common for the corresponding unit such as snowblower screw, cleaner brushes, water pump unit of washing or sprinkling machine. The fan included in the vacuum unit generates airflow. Such modifications provide the air supply from the outside and then it is transferred to the operating mechanisms.

The attached equipment of the special vehicle also includes a washing unit that consists of 100 litres tank designed as small volume accumulator used in situations when there is no fire hydrant or water pits. The second main unit is low pressure pumping unit with a capacity of 10 l/min. The drive of attached equipment is a pneumatic one. The main application area of the special vehicle is a tram or railway tracks with stops, yard or near road areas (sidewalks), park areas and cross-country terrain, surfaces with asphalt concrete pavement (parking lots, squares).

The special vehicle module-type construction allows performing various operations. Attachable side trimmers allow for cutting lawns and near-rail territories. Air heated to a certain temperature blown through nozzles maintains the railway switches safe performance during the winter period.

Moreover, the special vehicle can be applied for maintenance/cleaning of the railway tracks in closed coal mines and air filtration in mines. In order to clean the railway track from coal dust, the vacuum unit can be upgraded using the Rainbow exhauster operation principle. The special vehicle attached equipment set is added with a water filter that collects the most part of fine dust. Thus, a designed special vehicle with module accessories has wide effective implication in urban areas as well as specific objects.

One of the main fictions of the device is cleaning of the surrounding space from the garbage. The vacuum-heated unit sucking the waste ensures the environment safety of waste collecting process.

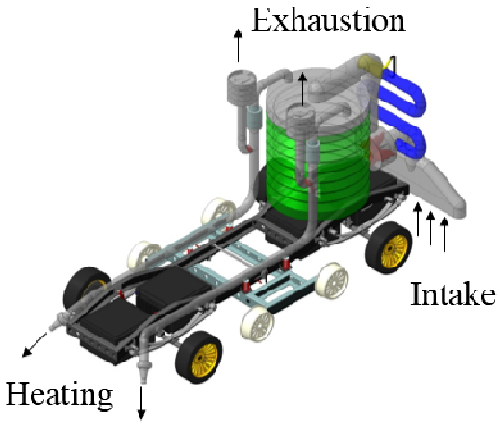

Fig. 3. Vacuum-heating unit of a special vehicle

The vacuum-heated unit of the special vehicle.

Vacuum unit (Fig. 3) design required the calculation of fan power (Kolotov, 2019) that can provide required under pressure that allows sucking waste up to 0.1 kg. Reynolds number estimation (Re> 10^5) indicates the turbulent mode of air circulation.

Figure 4 shows the vacuum unit (Kolotov, 2019) air duct. The radial-flow-fan mounted behind an inlet nozzle sets up required pressure differential that results in low-pressure zone generation upstream the fan and high-pressure zone downstream the fan. The airflow passes through the tank, filter and then out to the atmosphere. The radial-flow-fan with the capacity of Q = 0.5 m^3/s is used as the vacuum unit drive.

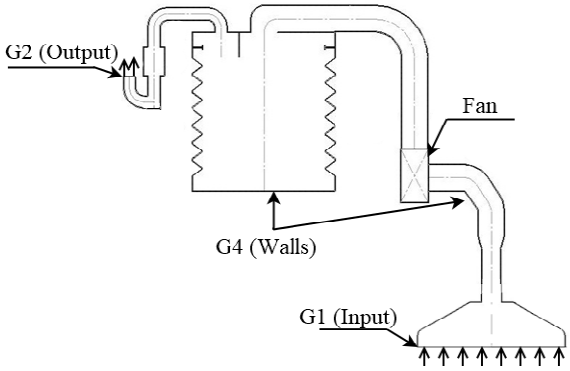

Fig. 4. Vacuum unit air duct

In order to specify the flow structure, gas flow speed rate, hydrodynamic losses the mathematical modelling of aerodynamics processes proceeding in unit flow ducts was performed.

Considering low speeds of air movement in the unit dust (Mach number $M < 0{,}3$) incompressible liquid was chosen as a mathematical model. In this case, the Navier Stokes equation will have the following form:

$$\nabla \boldsymbol{v} = 0 \tag{1}$$

$$\rho \frac{\mathrm{d}\boldsymbol{v}}{\mathrm{d}t} = \rho \boldsymbol{F} - \nabla p + \nabla(\mu \nabla \boldsymbol{v}) \tag{2}$$

where ρ – gas velocity, p – pressure, v – velocity vector, F – bulk force, μ – dynamic viscosity. Airflow in a unit ducts does not consider fan rotation.

The computational grip is shown in Figure 5. It consists of more than 1 million elements with a maximal dimension of 0.02 mm. Hexahedral elements are used.

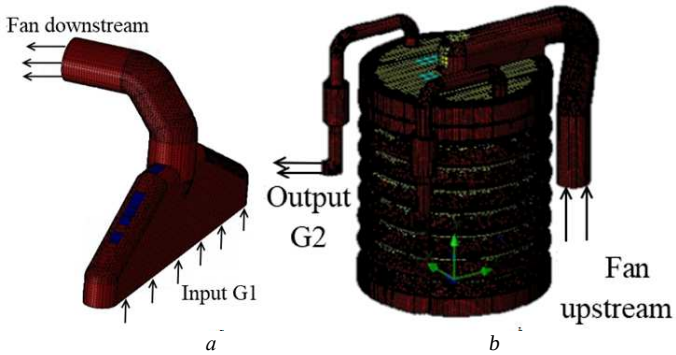

Fig. 5. Computational grip
(a) for decompression zone (b) for over-pressure zone

Boundary conditions are set up in the following way:

for the input zone (G_1 – boundary) gas flow rate and initial turbulence intensity are specified, $G_1 = 0{,}27 \div 0{,}5\, m^3/s$ $Tu_1 = 5\,\%$;

for air bleeding to the atmosphere zone (G_2 boundary) atmosphere pressure is set, $P_{2,3} = 101350$ Pa;

for the walls (G_4 boundary) – no-slip and no-leak conditions;

when calculating the flow in a vacuum zone, the physical parameters received in the output section upstream the fan (Fan downstream boundary) become the input parameters (boundary conditions) for the inflow boundary (Fan upstream boundary) for overpressure area downstream the fan;

the airflow passes through the ducts of damper and air filter for better noise damping and environment pollution protection.

Equation system (1)-(2) is averaged by Reynolds number ($R_e > 105$). In order to loop up the obtained system (1)-(2) (Volkov and Emelyanov, 2008) Menter SST (Menter, 1994) turbulence model was applied (empirical factor of dynamic viscosity $c_\mu = 0{,}09$).

The calculations discovered flow structures in unit working ducts, pressure and velocity fields.

Figure 6 shows the flow structure in the unit intake manifold that demonstrates a dead zone with dimensions 0.18x0.048 m.

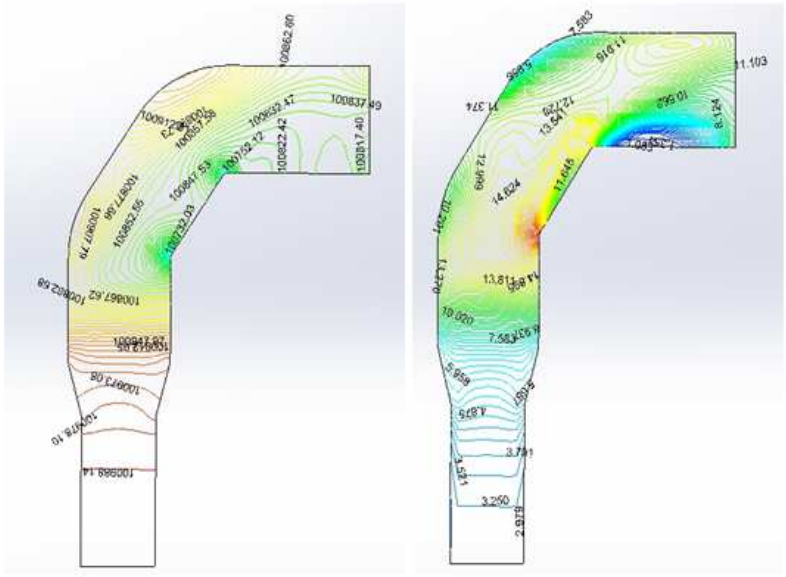

a *b*

Fig. 6. Airflow structure in an intake manifold
(a) isobars; (b) isotaches

Figure 7 shows the flow structure in the intake convergent short tube. Fig. 7a shows that differential pressure is 300 Pa, provided that maximum speed does not exceed 20 m/s.

Local separation zone in a transition area of unit intake into the tube has the following dimensions: from 0.03x0.02 m in the intake manifold up to 0.1x0.4m in the tube (Elbakian, 2018; Kalentev et al., 2017).

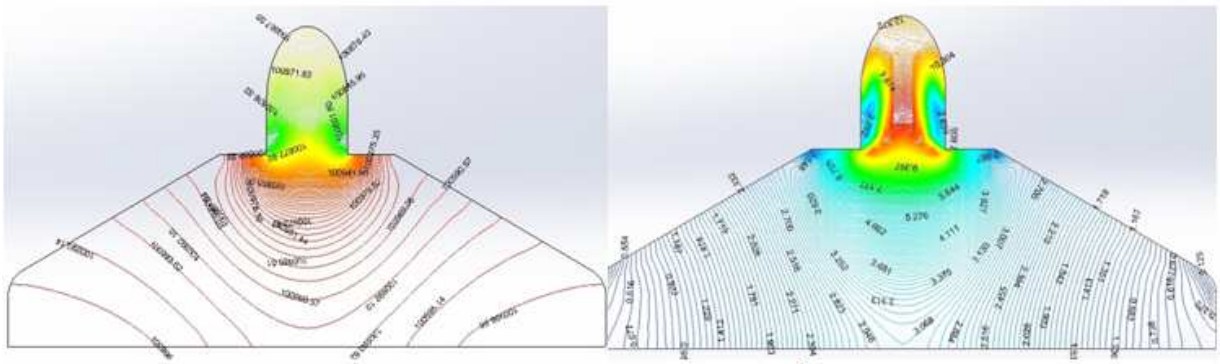

a *b*

Fig. 7. Airflow structure in a unit intake
(a) isobars; (b) isotaches

Flow variation form $G_1 = 0{,}5\ m^3/s$ $G_1 = 0{,}27\ m^3/s$ leads to pressure difference reduction up to 185 Pa.

Results prove that decompression in the output area of the duct required for lifting and collection of up to 0.1 kg of waste into the tank is generated.

The flow structure, isobars and isotaches in the collector are shown in Figure 8.

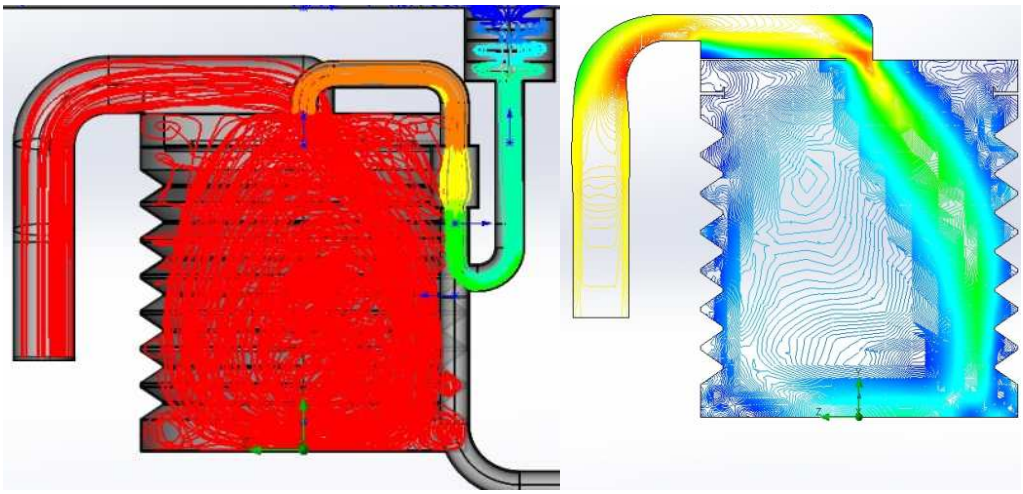

a *b*

Fig. 8. Flow structure in the collector
(a) space flow lines (b) isotaches

Fig 8,b shows that the flow going upstream the collector is of stream-like type. Air exhaustion is performed through an outlet on the cover of the collector. Circulation zone (Fig. 8, a) with dimensions of (0.4x05m) is generated in the central area of the collector. Air velocity in the tank is reduced due to interaction with sidewalls and bottom. Airflow turn makes the waste settle down on the tank bottom.

Air from the tank gets into the filter and then to the damper to reduce the noise. Airflow structure in filter and damper ducts is shown in Figure 9.

Exhausted air filtration process demonstrates the flow pressure reduction ($\Delta p = 767\ \ Pa$) and pocketing near the filter walls caused by the sudden widening of the channel.

After the air leaves, the filter flow velocity increases up to 20 m/s. The damper is essentially a cylinder with labyrinth type working space arrangement. Airflow velocity 80% reduction to $v = 1 \div 3\ \ m/s$ has been observed.

Common resistance losses in the channel are equal to 2000 Pa.

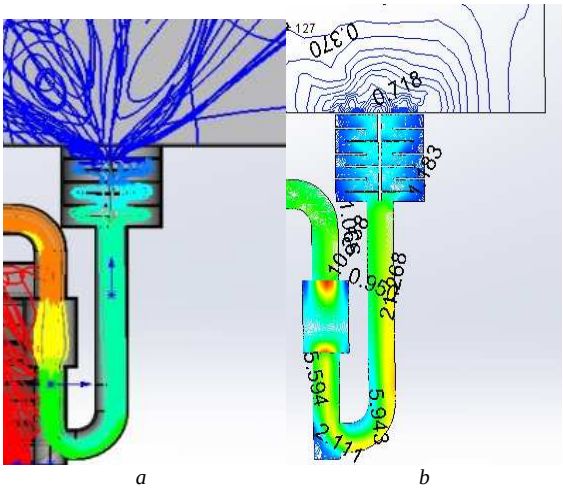

a *b*

Fig. 9. Airflow structure in filter and damper ducts:
(a) space flow lines (b) isotaches

The railway switches can be covered with ice during the winter period due to the low temperatures. The special vehicle vacuum- heated unit can redirect the exhaust airflow from the filtering and dumping system into

the railway heating system that contains air duct, turbular heating element and nozzle from each feeding side (Fig. 3).

Basing on the theoretical calculation spiral type turbular heating element with a power of 1.8 kWt was selected. In order to check the efficiency of the designed system and approve the turbular heating element power mathematical simulation of aerodynamic and thermophysical processes generated in air ducts, nozzle and near the heated surface, was performed (Bako, 2016). Couples heat transfer stationary problem was solved. Gas escape structure from the nozzle and its interaction process with the rail is shown in Figure 10.

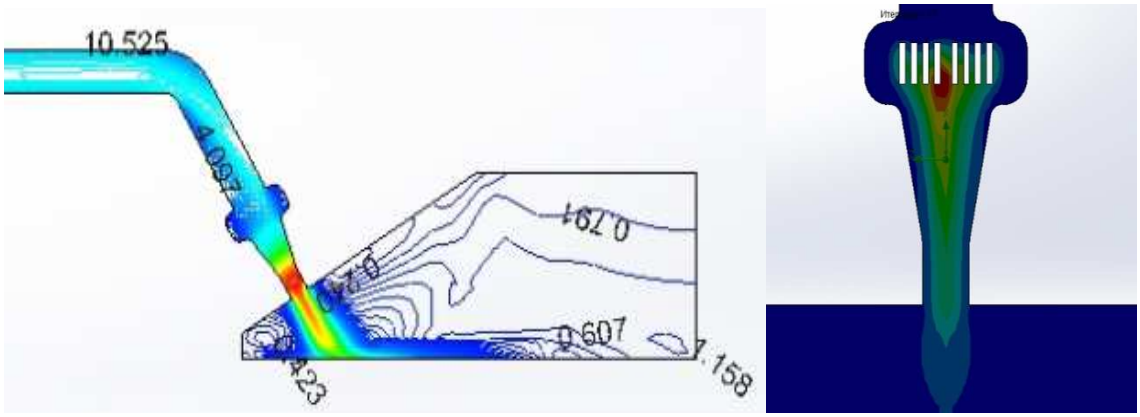

a *b*

Fig. 10. Gas escape structure from the nozzle: isotachs (a) and temperature field (b)

Isotach structure analysis is indicative of the heated gas escape from the nozzle of a stream like type. In order to provide exhausted air continuous heating, the turbular heating element construction was corrected considering preliminary calculations. Nozzle area temperature field analysis approves the heating process uniformity and temperature distribution in the flow- rail contact zone (5 ÷ 20 0C) indicates that the supplied heat is enough for railway switch heating (ice melting). Thus, the selected turbular heating element power was proved to be enough for the railway switch heating (Kolotov, 2019).

Results

1. The universal multi-functional special vehicle for inter-rail space waste cleaning was designed.
2. The outstanding feature is an application of the environment-friendly hybrid unit that include electrical motor-wheels and combustion engine. The designed vehicle has double undercarriage that allows moving along roads and railway tracks.
3. The capabilities of the vehicle are increased due to module accessories application. Particularly, beyond the waste cleaning, it is possible to install trimmers for railway lawn cutting, to clean the railway switches during the winter using heated gas streams and some other attachable devices.
4. Mathematical simulation of aerodynamic processes in the vacuum unit was performed. Pressure fields, velocities and flow structure calculation analysis confirms the vacuum unit working efficiency. It was discovered that unit intake fan operation mode ensures pressure difference in the range from 185 Pa up to 300 Pa that allows lifting the waste weighing up to 100 gr. Total resistance losses are smoothed by fan power and do not influence the efficiency of the structure (Cernecky, 2015).
5. Mathematical simulation of exhausted air filtration and damping processes in the filtering unit and vacuum unit damper was performed. It is showed that the flow velocity is reduced to 80%.
6. Numerical computation of the turbular heating element power enough to heat the ice up to 0.2 m height appearing on the railway switches during winter was performed. The selected turbular heating element power of 1.8 kWt and nozzle heating flow uniformity was computationally proved enough It was shown that if the turbular heating element surface temperature is 650^0C the spiral form of the turbular heating element allows to heat the air up to 60^0C in the flow middle, that ensures the nozzle outflow air temperature from 5^0C to 20^0C. Heated air exposure during 5 minutes allows to melt up to 16 kg of ice and totally heat the railway switch.
7. It is shown that if the vacuum unit is upgraded (water cleaning), the vehicle can be used in closed mine installations to clean the space form coal dust and coal coarse fragmenting.

Acknowledgements: *The research is funded by researchers' grant FSBEI of Higher Education "Kalashnikov ISTU" 13.04.03/18BBYA.*

The contribution is sponsored by the project 015STU-4/2018 Specialised laboratory supported by multimedia textbook for subject "Production systems design and operation" for STU Bratislava and by the project 013TUKE-4/2019: Modern educational tools and methods for forming creativity and increasing practical skills and habits for graduates of technical university study programmes.

References

Attachment (2010) N 25 to Customs Union CD dated 20th September, 2010 . N 378.

Bako, B., Bozek, P. (2016) Trends in Simulation and Planning of Manufacturing Companies. International Conference on Manufacturing Engineering and Materials (ICMEM), Procedia Engineering Vol. 149 Pages: 571-575

Bołoz Ł., Castañeda Leonel F., (2018) Computer-Aided Support for the Rapid Creation of Parametric Models of Milling Units for Longwall Shearers. Management Systems in Production Engineering. Volume 26, Issue 4, pp. 193-199. DOI: 10.1515/mspe-2018-0031.

Elbakian, A., Sentyakov, B., Bozek, P., et al. (2018) Automated separation of basalt fiber and other earth resources by the means of acoustic vibrations. Acta Montanistica Slovaca, Vol. 23 Issue: 3 Pages: 271-281

Cernecký, J., Valentová, K., Pivarčiová, E. et al. (2015) Ionization impact on the air cleaning efficiency in the interior. Measurement Science Review, Vol. 15, Issue 4, Pages 156-166.

GOST 27415-87 (1987) Garbage removal trucks. General technical requirements. – M.: The USSR State Committee for standards, 1987.

GOST 27478-87 (1987) Machines for cities cleaning. General technical requirements. – M.: The USSR State Committee for standards, 1987.

Herrera G. A. M. (1880) Máquina limpiadora de vías férreas, con particular aplicación a la limpieza de los raíles de los tranvías ES621 (A1) ― 1880-01-11

Ivanov M. D. (1999) Moscow tram: chapters of history. Moscow, Nauka

James, J., Wilson, J., Jetto, J., Thomas, A., Dhahabiya, V. K. (2016). Intelligent track cleaning robot. 2016 IEEE International Conference on Mechatronics and Automation.

Jiyannpieeru J. (1996) Machinary for cleaning railroad LINE JPH08338012 (A), 1996-12-24.

Kalentev, E., Václav, Š., Božek, P., Korshunov, A. and Tarasov, V. (2017). Numerical analysis of the stress-strain state of a rope strand with linear contact under tension and torsion loading conditions. In Advances in Science and Technology Research Journal. Vol. 11, iss. 2, pp. 231-239.

Kolotov A. A., Benderskiy B. Ya. (2019) Special vehicle with hybrid system (SV with HS) Vestnik of Vologda state university. Series: Technical science.1 (3).

Kolotov A. A. (2019) Rail-wheel vehicle with hybrid system. Graduation master's thesis for the specialization of 13.04.03 «Power engineering». Kalashnikov Izhevsk State Technical University

Kolotov A. A., Benderskiy B. Ya (2019) Utility model application in class MPK E01H1/08.

Lasser B. F. (1973) Method and apparatus for continuously exchanging or renewing the sleepers and optionally the rails of railway track GB1322545 (A), 1973-07-04

Menter F. R. (1994) Two-Equation Eddy-Viscosity Turbulence Models for Engineering Applications. AIAA Journal. 32 (8)

Murray-Smith D. (2019) Future Transport in Scotland A Review for the Scottish Association for Public Transport Honorary Senior Research Fellow and Emeritus Professor of Engineering Systems and Control, James Watt School of Engineering, University of Glasgow

Qazizada, E., Pivarčiová, E. (2018) Reliability of parallel and serial centrifugal pumps for dewatering in mining process. Acta Montanistica Slovaca, Vol. 23, Issue 2, pages: 141-152.

Nehal D. Jadhao and M.S. Tufail (2017) Review Paper on Automatic Railway Track Cleaning Machine Journal of Basic and Applied Engineering Research, 4 (1).

Neil R. F., Arun.M., Sudheer A.Pb. (2018) Design, modelling and fabrication of railway track cleaning bot, International Conference on Robotics and Smart Manufacturing (RoSMa2018), Procedia Computer Science 133.

Perrin J. (1989) Cleansing machine for tramway rails - comprises mobile bogie with suction system drawing air current across rail surface to remove and collect debris FR2628457 (A1), 1989-09-15

Pringle P. J. (1906) Apparatus for cleansing the rails of tramways and railways. Application filed june 18,1906. US916015 (A), 1909-03-23

Raymond U (1980) Machine for cleaning railway tracks US4235029 (A), 1980-11-25

Sleptsov M. A., Dolaberidze G. P., Prokopovich A. V. (2006) Basic principles of electric transport: a study book for high education students,.Moscow, Publishing center «Academia».

Theurer J., Oellerer F. (1991) Machine driveable on track and method for cleaning the permanent way of track HU203798 (B) — 1991-09-30

Valditerra E. (2013) Machine for restoring track beds with an excavating chain having a changeable end face ITGE20120055 (A1) — 2013-12-01

Volkov K. N., Emelyanov V. N. (2008) Large eddy simulation in turbulent flows calculation, Moscow, PHYSMATLIT.

GIS-based Analysis of Relative Tectonic Activity in Southeast of Iran with a focus on Taftan volcano

***Mohsen Jami*[1], *Ali Solgi*[2], *Mohsen Pourkermani*[3] *and* *Ali Asghar Moridi Farimani*[4]**

Taftan volcano has been located in southeastern of Iran and zone of Nehbandan-Khash (Iran Eastern Mountains). It seems that both the young volcano and active tectonic have played an important role in morphometry in this area. Geomorphic indices have been used to study tectonics in this area. These Indices include Drainage Basin Asymmetry (AF), Transverse Topography Symmetry (T), Mountain Front Sinuosity (Smf), River Slope Length (SL), Floor Width to Valley Height (VF), Hypsometric Integral (Hi), and Drainage Basin Shape (BS). These Indices have been used to evaluate Relative Active Tectonic (IAT) of basins and sub-basins of the area. Recently, it is found that Neo - Tectonic has played an important role in geomorphic evolution. On the basis of this model, three tectonic zones are recognizable in that area: (Zone with High Relative Tectonic) that found in sub-basins of 4-B and 9-C. (Zone with moderate Relative Tectonic) that found in the wide-area (northeast) including Dargiyaban and Sadabad Faults. (Zone with Low Relative Tectonic) that only found in sub-basins 5-C and 8.

Keywords: *Active Tectonic, Tectonic, Volcano, Morphometric, Taftan Volcano, Iran.*

Introduction

Taftan volcano aged Pliocene-Quaternary has a young and semi-active volcanic system that located at a distance of 50km from north of Khash city. This volcano has been considered by geologists. Effects of tectonics are different in various area of the volcano. Regarding the northern part of Saravan Fault which has been located near this area, it is important to calculate the level of Relative tectonic activity in that area. It seems that both young volcano and active tectonics have played an important role in morphometry of this area (Aghanabati, 2004).

Quantitative methods have been used to study rates of relative tectonic in Taftan volcano and around it (Keller and Pinter, 2002), as well as geomorphic indices have been used to study tectonics. These indices include Drainage Basin Asymmetry (AF), Sinuosity Mountain Front (Smf), River Slope Length (SL), Floor Width to Valley Height (VF), Hypsometric Integral (Hi) and Drainage Basin (BS). They are determined on the basis of a single useful index to study relative active tectonic (Keller and Pinter, 2002; Azor et al., 2002; Silva et al., 2003; Molin et al., 2004). The investigations of tectonic geomorphology is important because the results of regional studies on neotectonics are significant for evaluating natural hazards as well as land-use development and management in the crowd areas (Cloetingh et al., 2006; Pedrera et al., 2009; Pérez-Peña et al., 2010; Mahmood and Gloaguen, 2012; Faghih et al., 2015). In addition to the role of tectonic action of the area, it can be considered as the effect of quaternary actions of Taftan volcano in changing morphotectonic parameters can be considered.

These indices have been used to evaluate Relative Active Tectonic (IAT), basins and sub-basins of that area. This method has been used to calculate rate of tectonic activities in the areas such as southeastern of USA (Rockwell et al., 1985), Pacific Coast in Costa Rica (Wells et al., 1988), North China Plain (Han et al., 2003), Mediterranean Beach in Spain (El-Hamdouni et al., 2008), Sarvestan in the central Zagros (Dehbozorgi et al., 2010), Rudbar Lorestan dam site (Alipoor et al., 2011) and Tehran in the central Alborz (Bagha et al., 2014). Relative Category of active tectonics has been performed on the basis of studies done a basin of Taftan volcano and Surrounding areas (El-Hamdouni et al., 2008). The results gained from analyzing the indices have been compared with field observations. This research can be helpful to solve the problems of tectonics in this area. In an area surrounding the young volcano(s), structures such as Saravan and Mirjaveh faults, Khan Mohammad Chah, Sa'ad Abad, Dar Giaban, etc., are visible. By reason of the activity of these faults, the morphometric parameters will be changed. Due to the existence of active structures, such as the above mentioned faults and the history of the tectonic activities in this region, the probability of the occurrence of natural disasters (such as earthquakes, landslides and …) associated with the tectonic processes is inevitable. Therefore, any developmental activities such as dams' construction for developing the villages and the cities, the road-

[1] *Mohsen Jami*, Faculty of Industry & Mining (Khash), University of Sistan and Baluchestan, Zahedan, Iran, *M.jami@eng.usb.ac.ir*
[2] *Ali Solgi*, Department of Geology, Science and Research Branch, Islamic Azad University, Tehran, Iran, *A.Solgi@srbiau.ac.ir*
[3] *Mohsen Pourkermani*, Department of Geology, North Tehran Branch, Islamic Azad University, Tehran, Iran, *M pourkermani@iau-tnb.ac.ir*
[4] *Ali Asghar Moridi Farimani*, Department of Geology, Sistan and Baluchestan University, Zahedan, Iran, *amoridi@science.usb.ac.ir*

construction, mining, surface water's management in this area should be done based on the tectonic activity levels in order to prevent the financial damages and the rate of deaths in the near future.

Geological overview

Taftan volcano aged Pliocene-Quaternary (Aghanabati, 2004) has a young and semi-active volcanic system that located at a distance of 50 km from northeast of Khash city (Biabangard, 2009) (Fig. 1). This volcano, 1300 sq. m^2, has been acted last time since 1970-71. Taftan volcano is located at an altitude of 4050 meters above the sea level and 2000m, from the surrounding plains (Ganser, 1971).

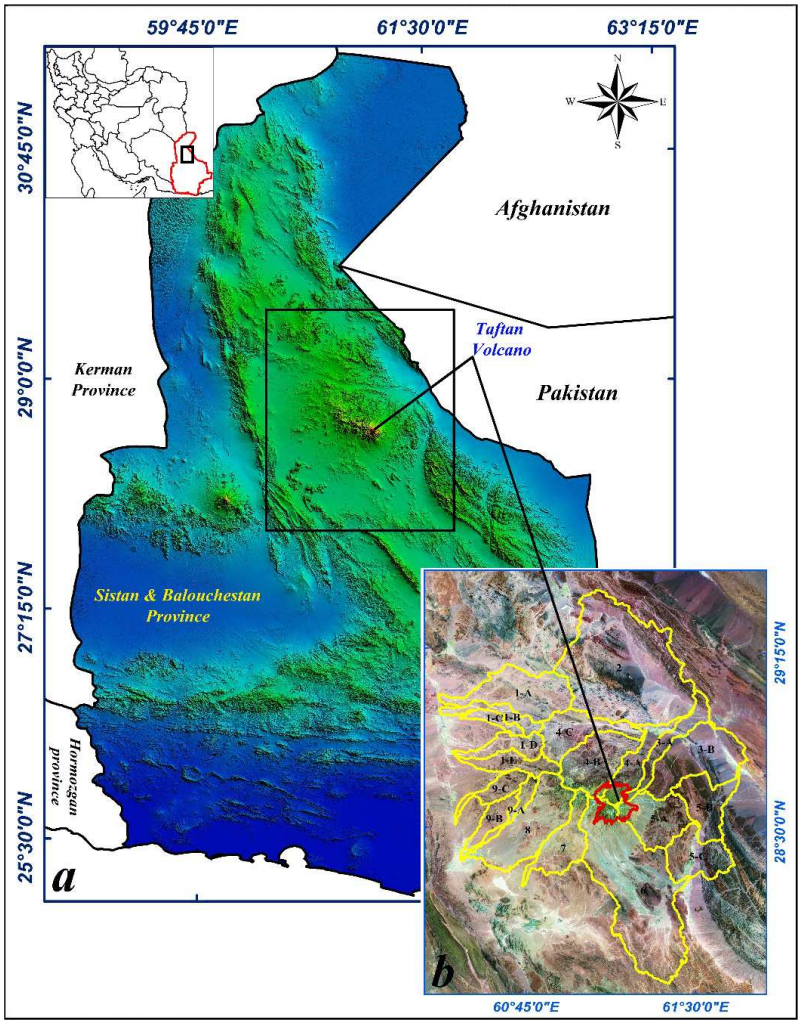

Fig. 1. Position of the area, Position of Volcanic Cone, Position of basins and sub-basins. a) SRTM data from Sistan and Balouchestan provinces, b) Satellite Image of the study area and Position of Volcanic Cone.

It is noted that Taftan volcano is one of the volcanic centres of the magmatic arc that originated from subduction of Oman Oceanic Crust under the Continental Accretion Prism of Makran (Aghanabati, 2004). In addition to acidic magmatisms to the moderate level of middle oligocene (granodiorite and quartzdiorite), the frequent dykes and sills as their combination is hornblind diorite to quartzdiorite (which has been attributed to the magmatism after the middle oligocene), have been cut the middle oligocene in different directions in many points such as the Eocene flaccid sediments and the intrusive igneous rocks (Aghanabati, 2004).

Quaternary Units include old and young alluvial sediments (Qt_1 and Qt_2), alluvium that is forming in the bed of current rivers (Qa_l) in different levels. Taftan volcano is the major unite in quaternary that the main products are extended in the form of pyroclastic rocks, lavas and their tuff, epyclastic and ignimbrite materials (Fig. 2). (Aghanabati, 2004).

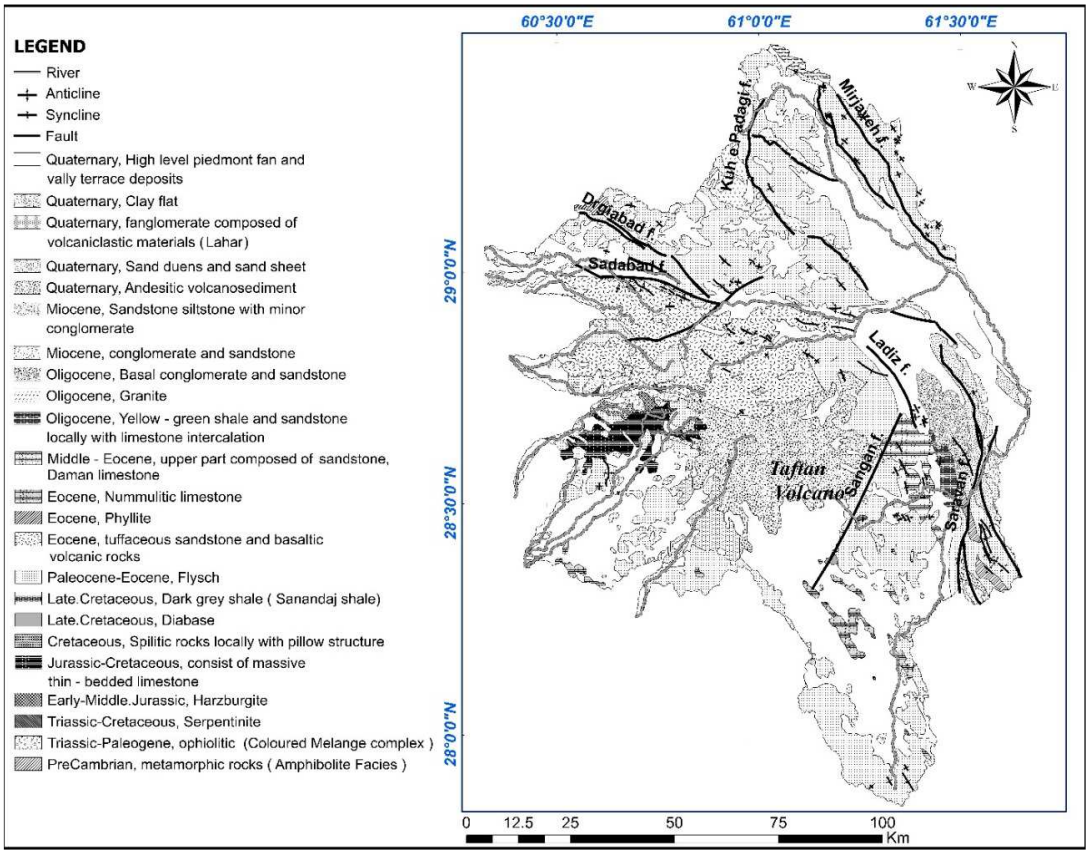

Fig. 2. Geological Map of Taftan. Geological Map of Taftan (Modified by Authors After Eftekhar Nejad and Aghanabati 1994).

Morphotectonics and Active Tectonics Indices

In morphometric and morphological studies, qualitative and quantitative indices are considerable. They are effective in order to get useful information about the tectonic position (active or passive) of the area. The results of several indices can be integrated and added to the other information such as uplift rat and determined category of tectonic activities; these categories suggest a relative level of activity in an area. Developed by several authors, these indices can be considered as tools for studying active tectonics because they provide rapid insights into specific area or sites in the study area that are adjusting to relatively rapid rate of active tectonic deformation (Bull and Mcfadden, 1977; Rockwell et al., 1985; Keller, 1986; Ramirez-Herrera, 1998; Silva et al., 2003). Some indices such as Drainage Basin Asymmetry (AF), Sinuosity Mountain Front (Smf), River Slope Length (SL), Floor Width to Valley Height (VF), Hypsometric Integral (Hi) and Drainage Basin (BS) have been calculated.

In this classification, the basins are separated from the dividing line of water as each of them (basin) is composed of the independent parts that are overlapped and divided into sub-basins, accordingly.

The study area is divided into 20 basins and sub-basins on the basis of Topographic maps 1:50000, Landsat satellite images in 15m, and 30m, IRS (5.5m), SRTM (30m), Topographic Maps1:50000, Satellite Images, SRTM (30m) and Geological Maps. Their positions have been drawn and determined on the basis of the Main River, slope, and topography. In order to determine the active tectonic area in the scale of drainage basin using morphometric indices of Taftan volcano and its surroundings, first, drainage basins were extracted using Arc Hydro tool in ArcGIS software, and then the main rivers' network in the study area were constructed and, finally, the morphometric indices have been measured on the basins and sub-basins.

Drainage Basin Asymmetries (Asymmetry Factor)

Active tectonics can cause deformations in drainage patterns, resulting in tilting of basins (Hare and Gardner, 1985; Keller and Pinter, 2002). Asymmetry Factor has been developed to show the tectonic tilting in drainage scale or large areas as follows:

$$Af = 100\ (Ar/At). \quad (1)$$

Where, *Ar*: Area of Right Basin of River, *At*: Total Area of Drainage Basin and *Af*: Basin Asymmetry. In this area, *Af* is calculated for 20 basins and sub-basins (Table 1). Amounts of $Af < 50$ and $Af > 50$ are tilted to the west and east, respectively. Drainage Basins Asymmetry evaluated by the symmetry factor of transverse

topography illustrates that there is tilting in many basins. Sub-basinn of “1-D (49.06)” is near the symmetrical position. And Sub-basins of “1-A, 1-E, 3-A, 3-B, 4-A” are associated with the have the highest slope due to the uplift resulted from the volcanic cone activity as well as the existing structures in this area. Among them, sub-basin of “4-A (92.02)” is the one which is along with tilts that can be related to the many small faults of this sub-basin (Fig. 3). Sub-basin “9-B” is the least tilting and extended from north to southwest.

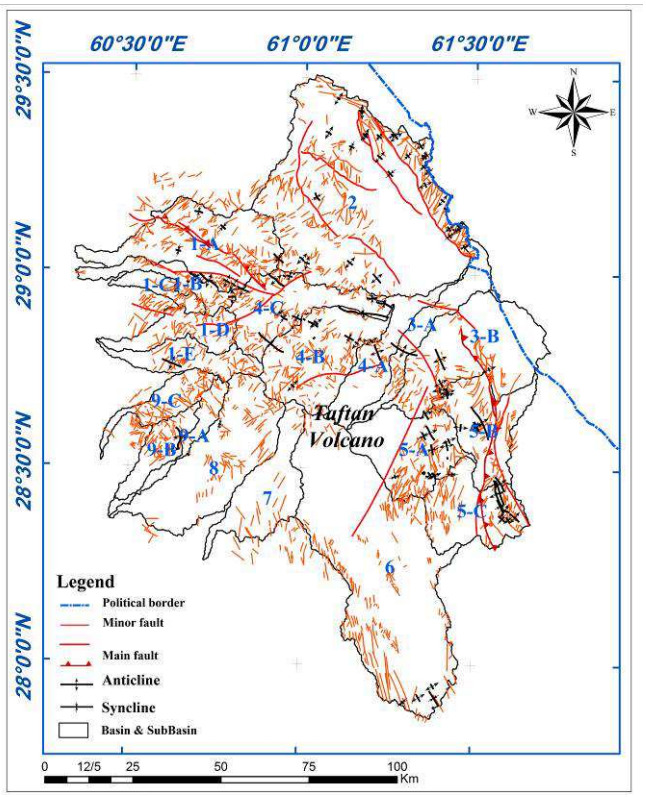

Fig. 3. Structures Map of Taftan.

Transverse Topography Symmetry

This index is used to evaluate and calculate Transverse Topography Asymmetry.

$$T = Da/Dd. \quad (2)$$

Where, *Da*: Distance from the middle line of the drainage basin to the middle line of Active Meander Belt and *Dd*: from the middle line of the basin-to-basin boundary. For a basin with complete symmetry $T = 0$, when the distance of asymmetry increases from the middle line, *T* also increases and becomes close to the amount of flow. It supposes that the slope of bedrock doesn't influence on channel movement, significantly. Then, *T* is a vector with direction and size of 0 and 1. Amounts of *T* are measurable with various parts of the valley and indicate vertical preferential movement, of the drainage basin axis.

$$Tave = T_1 + T_2 + T_3/3. \quad (3)$$

Amount of *T* is close to the *Af*, but it cannot be evaluated to determine tilting direction. While *Af* is a method that illustrates the amount and speed of tilting. For a basin with complete symmetry $T = 0$, when asymmetry increases, *T* also increases and becomes close to 1. Drainage basin symmetry evaluated by Transverse Topography Asymmetry indicates that there is tilting in many parts of the drainage basin and *T* ranges 0.16 and 8-0. 82 for basin and sub-basin "9-B", respectively. T index in the lower geographic latitudes shows a minor numerical value. But the values of this index will be increased in the geographical latitudes such as 24'280 'to 40'280 to the north (sub-basin of B-9), 36'280 to 01'290 to the north, and 38'280 to 55'280 to the north (sub-basins of A-4 and B-4), respectively, which indicates the asymmetry of a transverse topography in

these sub-basins. The increase of *T* in this part of the study area was related to the existing structures in this region, such as faults and active folds.

Sinuosity Mountain Front

Sinuosity Mountain Front is an index to reflect the between erosion forces that tend to make sinuosity and tectonics that tend to make a direct line in Sinuosity Mountain Front. Mountain Fronts related to active tectonics and uplift are direct relatives, and their *Smf* is low. The values equal to 1 (of this index) are specific to active tectonic areas. If the uplift level is decreased or stopped, the mountain front will be windswept by the erosion processes, and the value of this index (SMF)will be increased. The values of less than 1.4 indicate active tectonic fronts (Rockwell et al., 1985; Keller, 1986).

Regarding that geological maps don't outcrop any fault of mountain front in sub-basins of 1-C and 5-A sub-basins, then the index can't be calculated. All mountain fronts of this area are active, and three parts of 90, 109, and 125 are the most active of all and are related to Mirjaveh mountain front fault, a minor branch of Khan Mohammad Chah Fault and Saravan mountain front, respectively (Fig. 4). They indicate the high level of tectonic activities, and they are in one tectonic category which has been extended from the northwest of this area to the southeast one.

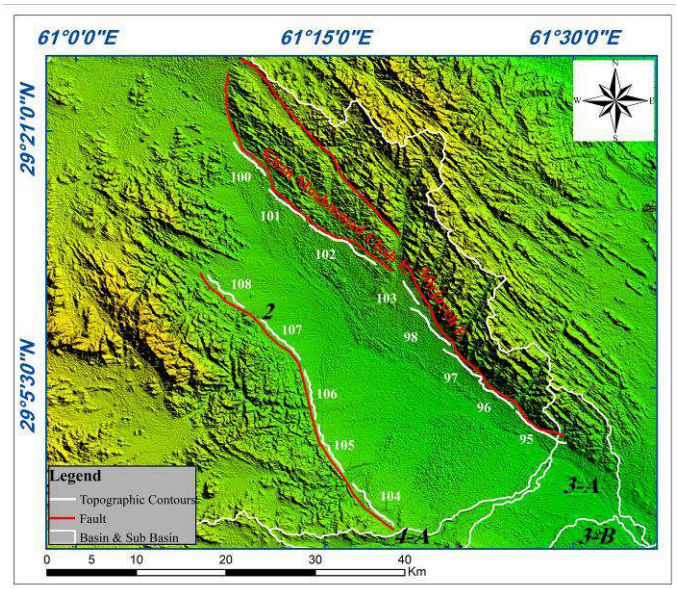

Fig. 4. Some calculated parts of Smf in the study area.

Stream Gradient Index

Defined Stream Gradient Index as follows:

$$SL = (\Delta H/\Delta L) \times L. \quad (4)$$

Where, SL: Stream Gradient Index, ($\Delta H/\Delta L$): Channel Slop or Gradient (ΔL: changes of channel length, ΔH: changes of channel height) and L: Total length of channel from the place of dividing stream to the middle area where the calculated index in it.

Slop-Length Index (*SL*) is one of the quantitative geomorphic parameters that used in morphotectonic studies. *SL* can be accounted as a useful tool to study the movements in active tectonic areas or areas in large scale (Chen et al., 2003; Zovoili et al., 2004). When streams and channels flow in the areas with a high uplift, *SL* will be increased, but when the streamflow is parallel with some structures such as valleys from right-slip faults, *SL* will be decreased (Keller and Pinter, 2002). In order to investigate the relationship between rock's strength and the aforementioned index, the rocks available in the study area have been classified based on their strength level toward various groups with very low level of strength (such as young alluvium deposits), low level of strength (such as sloping deposits), moderate level of strength (such as shale and siltstones), high level of strength (such as limestone, tuff, conglomerate, sandstone) and very high level of strength (such as andesite, granite, and basalt) (Memarian, 2001)

The most anomaly dispersion of *SL* is in the basins and sub-basins (that are in normal and resistant lithological category) located on the west and northwest of Taftan volcano. Due to anomaly areas, *SL* is only high in 4-C where its lithology is soft as young alluvial sediments and as its reason refers to the active and young tectonic structure (active fault). The remaining basins and sub-basins of the study area due to the lack of resistant lithology or the active and young structures in that area are associated with the low values of *SL*. As it can be seen, the lowest values of this index were related to the sub-basin of A-3 which mainly includes alluvial deposits of the present time, as well; the low level of strength of these rocks can be attributed to the low value of *SL* index in this sub-basin. (Fig. 5).

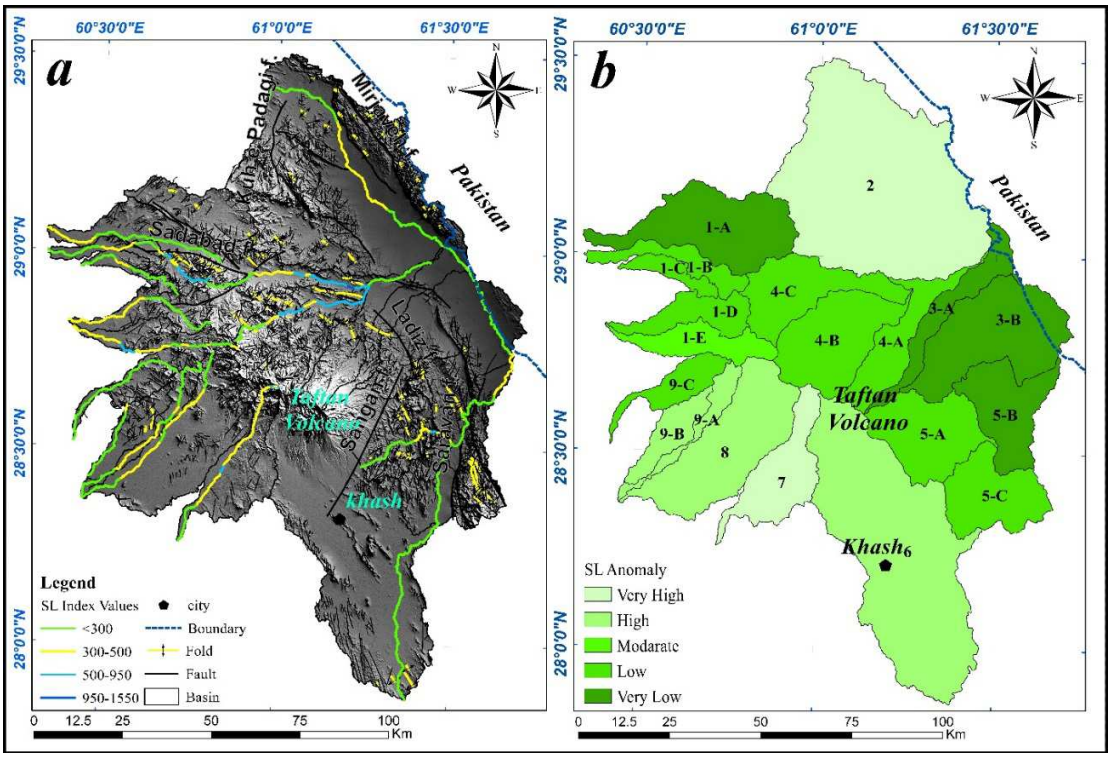

Fig. 5. a: SL for Drainage Net of River. b: Dispersion of anomaly areas of SL with resistance categorizing of the studied basins.

Additionally, this study area can be easily divided into several distinct sections grouped in regard to erosion. The high value of *SL* index in the sub-basin of E-1 and in the basin of 7 indicates the activity of the lower latitudes of the mentioned area; however, the highest values of *SL* due to the high level of lithologic resistance at that point are related to the basin of 7. Table 1 illustrates the category of *SL* in the area. *SL* has been considered to study the uplift effect of the main volcanic cone of Taftan; boundaries of the cone have been determined on the basis of geological maps, topography and ring structures of Taftan volcano In order to investigate the uplift – effect of the main cone of Taftan volcano, SL index has been studied. The boundaries of this cone have been determined based on the geological maps of the area, topography and catenary structure of the Taftan volcano. The measurements are carried out according to the topographic maps. Additionally, the height and the measuring intervals (regarding the cone and the plain boundaries) are considered equally for the aforementioned index to specify the uplift – effect of the cone (Relative activities of tectonics) to the surroundings. At this stage, the boundary of the cone and plane (its periphery) were studied separately in each basin. In the process, the boundaries of the cone and its plane have been considered, separately (Fig. 6).

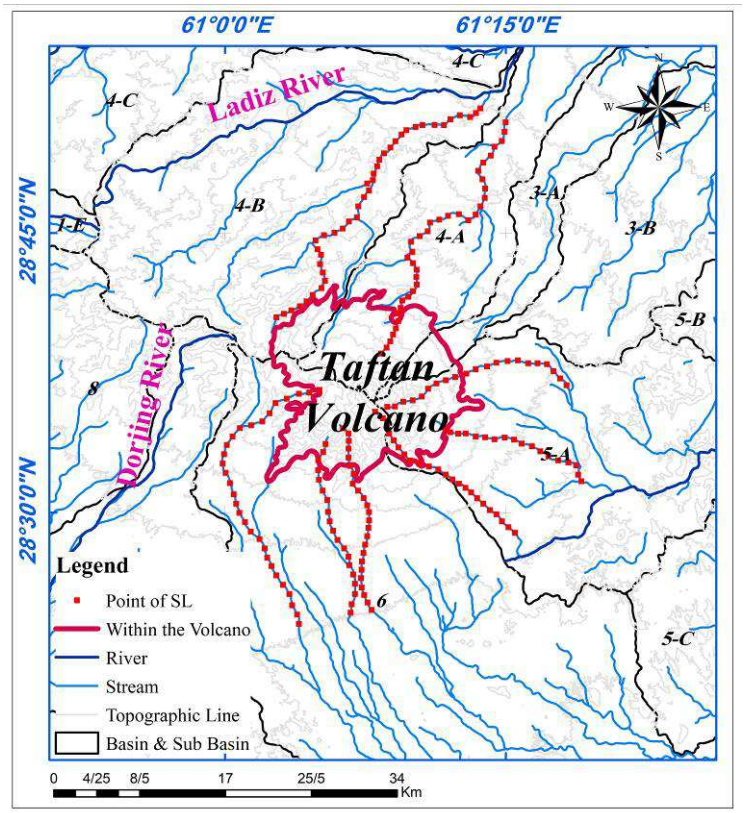

Fig. 6. Some measured places of SL around Taftan volcano.

These results suggest that uplift of the cone has influenced on active tectonic parameters, significantly *SL* is high around the cone. At a short distance, *SL* increases but decreases around the plane in spite of the long distance. Maximum amounts of *SL* around the cone in basins and sub-basins are 3A, 5A, 4A, 6,4B, respectively. But maximum amounts of *SL* around the plan are related to 5A, 6, 4A, 4B and 3A.

The ratio of Floor Width to Valley Height (VF)

Floor Width to Valley Height (VF) (Bull and Mc Fadden, 1977; Bull, 2007) is defined as follows:

$$Vf = 2Vfw/ (E1d - Esc) + (Erd - Esc). \quad (5)$$

Where, *Vf*: Ratio of Floor Width to Valley Height, *Vfw*: Floor Width, *E1d* and *Erd*: height of left and right walls then each other's and Esc: height of the floor. Valleys are often narrow upper than the mountain front (Ramirez-Herrara, 1998), and then SL should be an indefinite interval upper of the mountain front. Value of *Vf* will be changed according to the size of the basin, drainage discharge and kind of rock. Then amounts of *Vf* should be compared to similar geological conditions. Silva et al. (2003) calculated this index in the Eastern Cordillera (southwestern of Spain) and showed that V-shape valleys associated with a value of *Vf* less than 1 will be evolved in response to the active uplift, while U-shape valleys associated with a value of *Vf* more than 1 show a major lateral erosion due to the stability of the base surface or lack of tectonic performance.

According to geological maps of the area, any lineaments, main channel and minor branches don't cut 5-C, 3-B and A-3; and for this reason, this index can't be calculated for them. It is noticed that *Vf* is dependent on the drainage basins extent and bedrock lithology in addition to tectonic factors. In 19 active profiles in the area (Fig. 7), the value of *Vf* is low which has been determined on the basis of V-shape valleys Due the effect of uplift and the activity of Taftan volcano as well as the value of *Vf*, west, northwest and southeast of Taftan volcano can be considered or accounted as the youngest and most active parts along with high active tectonic relatives, So uplifting Taftan volcano has been influenced on tectonic structures of these parts. Figures 8 confirms results from this index as similar *SL* in Taftan Cone and Plane.

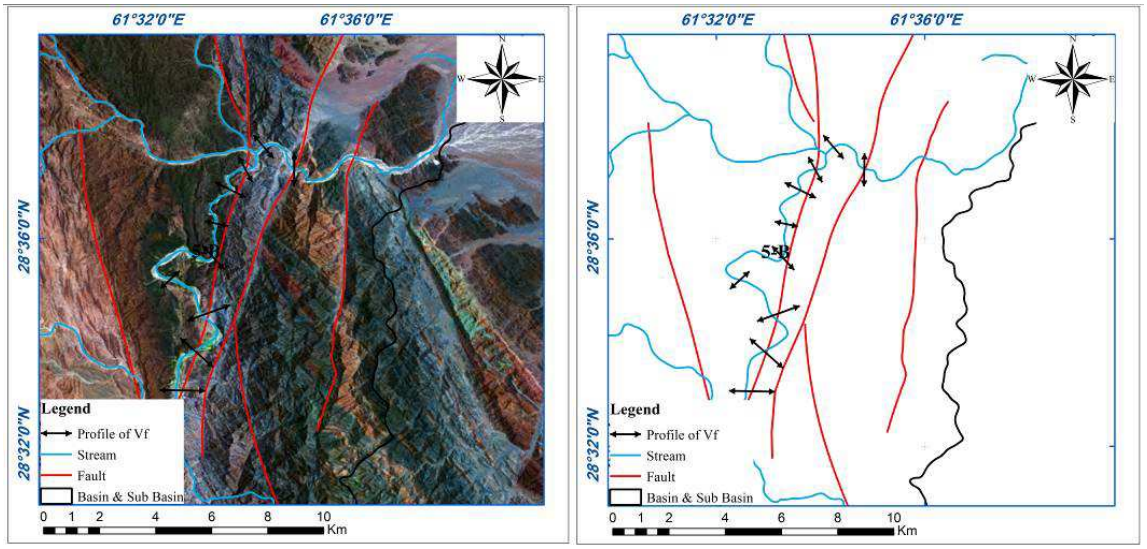

Fig. 7. Some measured place of Vf around Taftan volcano.

Hypsometric Integral (Hi)

The Altimetry Curve indicates the distribution of altitude in an area, a drainage basin to a complete plant (Strahler, 1952). This curve illustrates the results or the results gained from performing ratio of total basin height (relative height) to the total basin area (relative area), and it's a hypothetical altimetry curve for a drainage basin located on a monotone slope. The drainage basin includes 8 on the same line; total area (A) is the total area between a pair of lines of the same adjacent line. Area (a) is an area of the basin up to special height line (h). Amount of relative area a/A has ranged from 0 (the lowest area in the basin) to 1 (the highest area). Calculation of altimetry integral is a simple method to determine the altimetry curve in a special drainage basin as follows (Pike and Wilson, 1971; Keller and Pinter, 2002):

$$Hi = Average\ Altitude - Minimum\ Altitude / Maximum\ Altitude - Minimum\ Altitude. \quad (6)$$

Then, three amounts are necessary to calculate the Integral; two of them (Minimum and Maximum altitudes) are accessible from the topographic map, simply. High amounts of the Integral indicate young and active tectonic areas, but low ones indicate low tectonic and erosion (El-Hamdouni et al., 2008). (Maximum and Minimum altimetry Integral ranges between 0 and 1). It is necessary to note that the convex curve indicates the high activity of the area and activity of faults and uplifting related to folds currently, but cave curve indicates low tectonic activities in the area. In except of three sub-basins of 1-A, 9-A and 9-C as Hi is 0.53, 0.53 and 0.51, respectively (it shows a semi-active tectonic or maturity stage of Davies Pattern in three basins, average amount indicates geomorphic processes is balanced in three mentioned basins), other basins and sub-basinss indicate passive or old tectonic process or old stages of Davies Pattern because the amounts of *Hi* are lower than 0.50 and indicate high erosion in the sub-basins (Fig. 8).

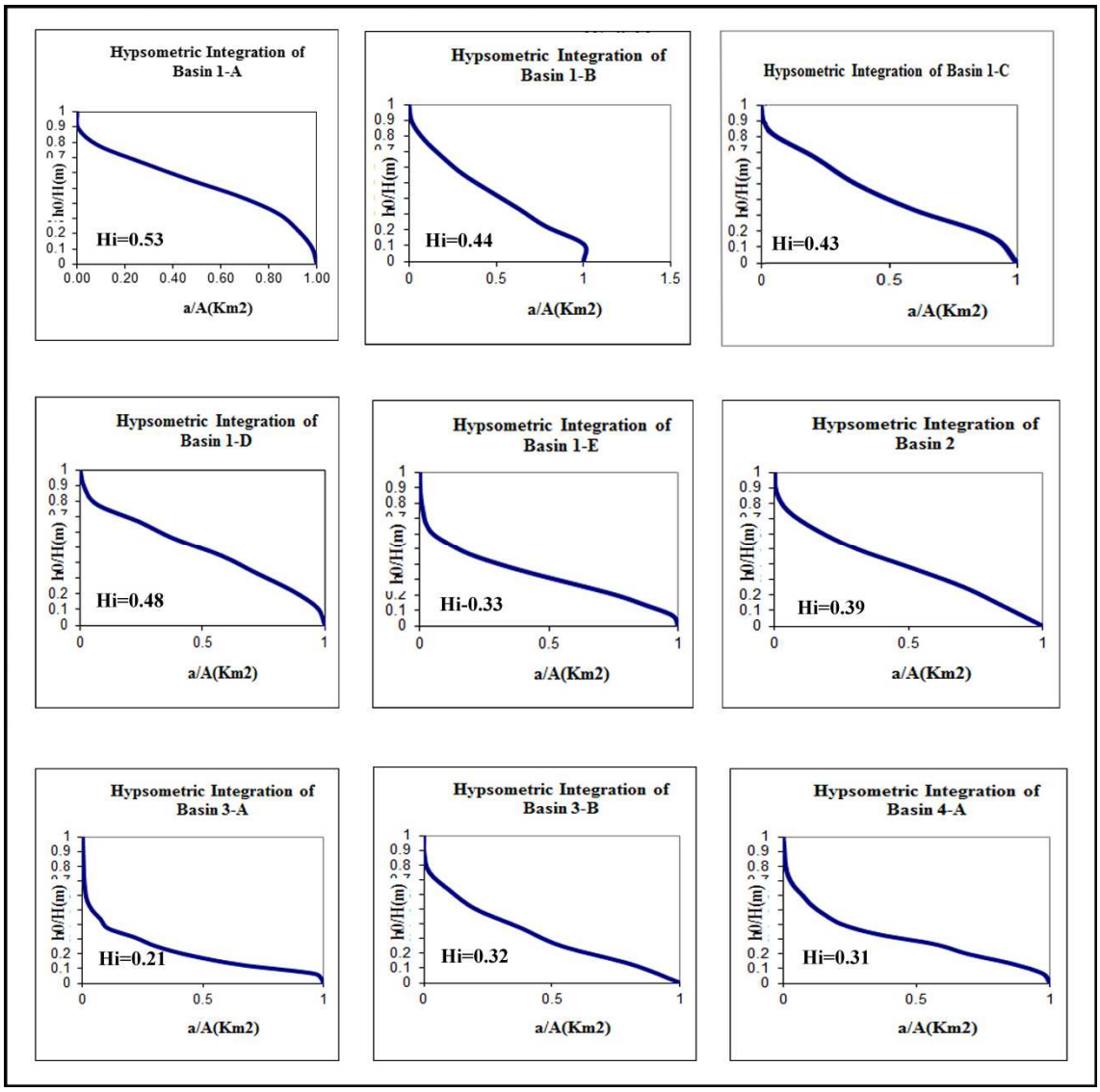

Fig 8. Hypsometric Curve of 20 Basins and Sub-basins.

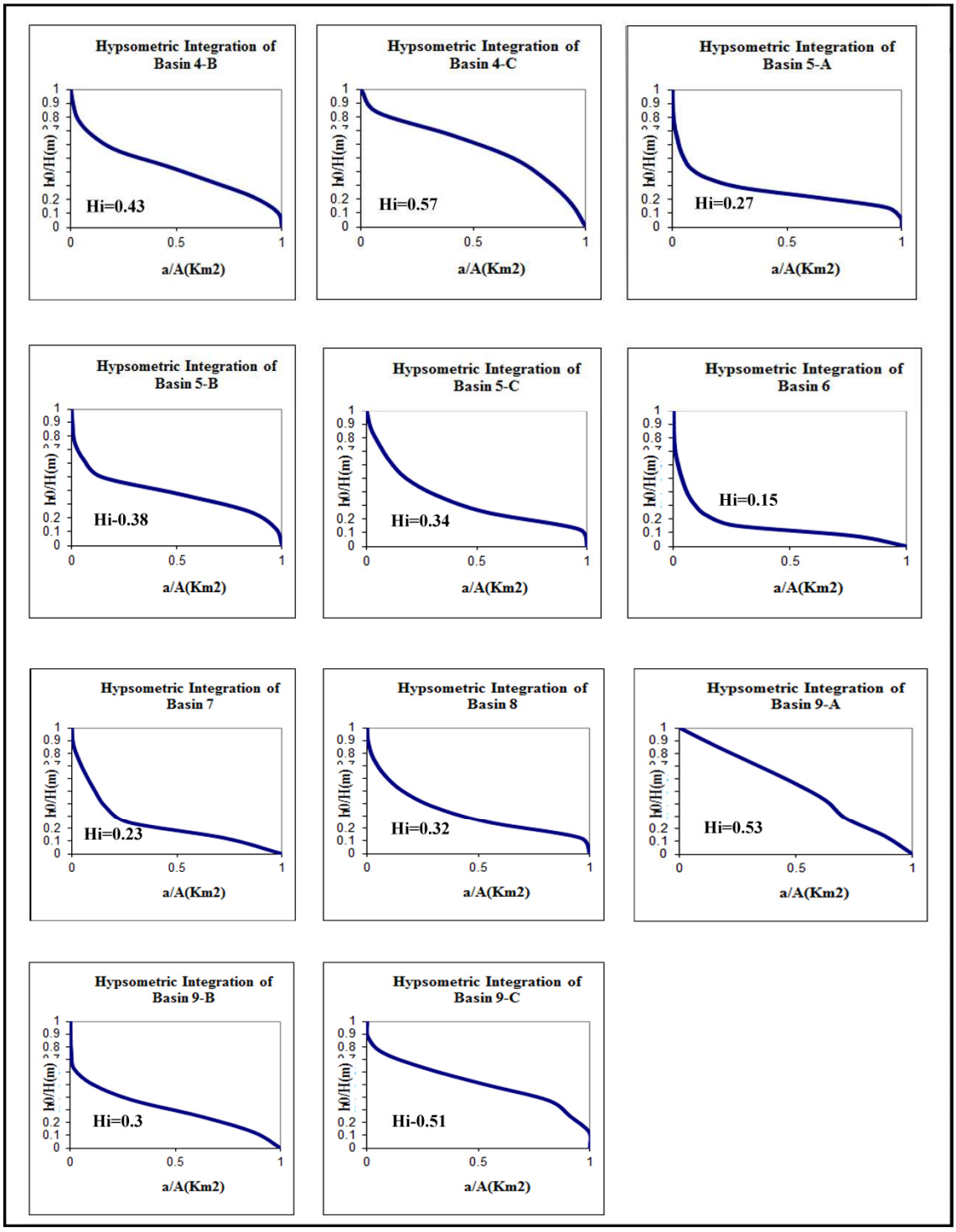

Continued Fig 8. Hypsometric Curve of 20 Basins and Sub-basins.

Index of Drainage Basin Form

It is calculated as follows (Ramirez-Herrera, 1998):

$$Bs = Bl/BW \quad (7)$$

Where, *Bs*: Drainage Basin Form, *Bl*: the length of Drainage Basin and *Bw*: the width of Drainage Basin. Young Drainage Basins in active tectonic areas tend to elongate in the direction with topographic slope. But along drainage basin evolution or decreasing the tectonic action, the basins have transformed from long to circular forms (Bull and Mc Fadden, 1977). This index illustrates the difference between long basins in high

amount and circular basins in low amount. Long basins are one of the specifications of the active tectonic area that has a river in a dig towards down. Mountain Fronts due to the fast uplifting are along with the steep and long basins. By decreasing or stopping the tectonic activities, basins will be extended, which will be started from the top of the mountain front (Ramirez-Herrera, 1998). It has been studied in Drainage Basin Form in the area (Table 1 and Fig. 9).

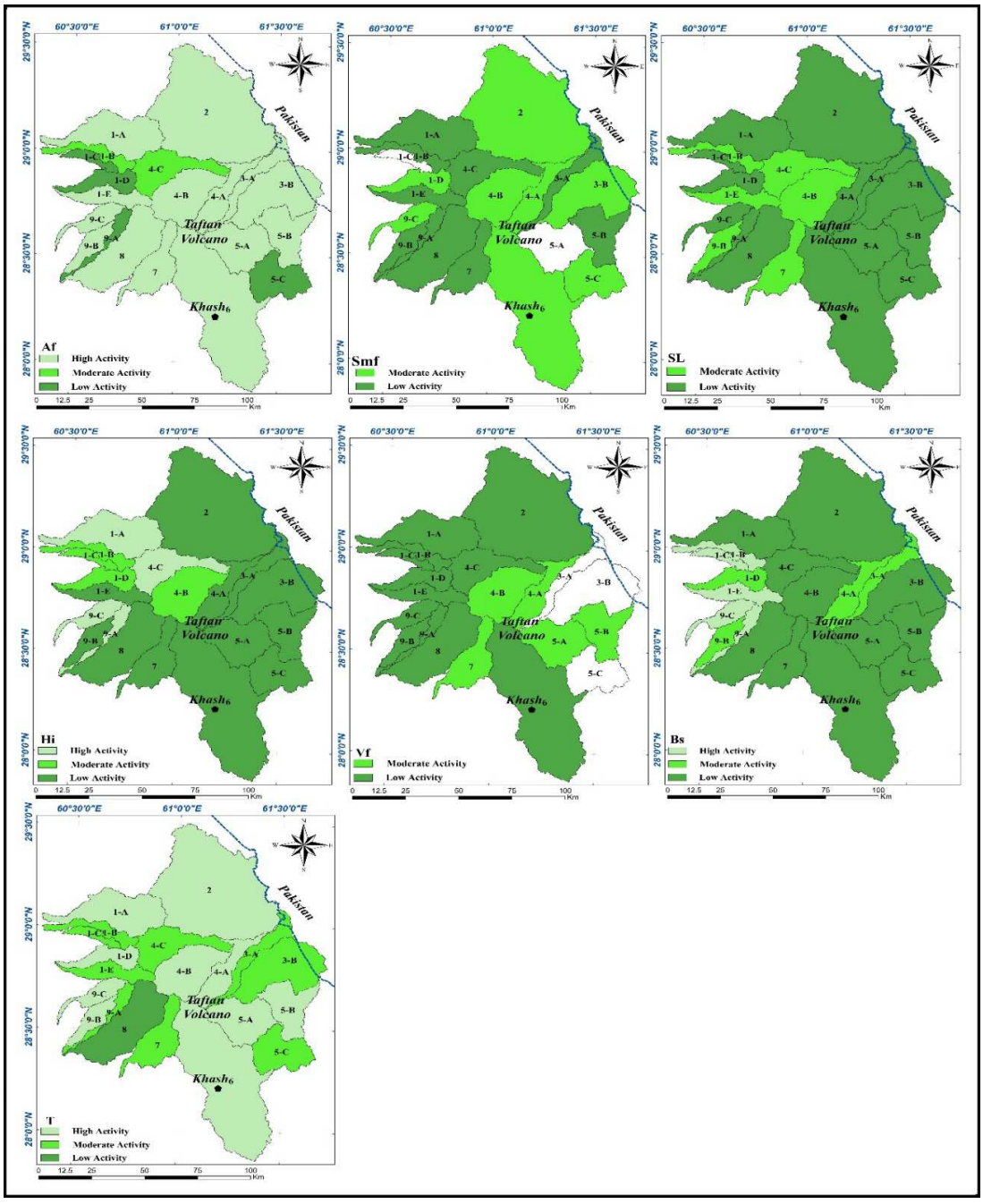

Fig. 9. Position of basins and their categorization in three groups of all Indices.

Categorizing Relative Tectonic Action

In this paper, categorization of Relative Active Tectonic introduced by the El Hamdouni et al. (2008) for the first time has been used to evaluate Relative Active Tectonic (IAT) of basins and sub-basins of that area. Various tectonic indices have been calculated for each basin and sub-basin and divided into three categories - 1, 2, and 3 - that indicate a high, middle, and low level of activities, respectively. Table 1 illustrates average Tectonic Indexes (S/n) and amounts of Relative Active Tectonic (Iat) for basins and sub-basins of the area. (Fig. 10).

Tab. 1. The categorization of Relative Active Tectonic in the area.

Ref.No	Basin	Class of:							S/n	Iat class	Assessment
		SL	AF	Hi	VF	Smf	T	Bs			
1	1a	3	1	1	3	3	1	3	2.14	3	Moderate
2	B1	2	2	2	3	3	2	1	2.14	3	Moderate
3	1c	3	3	2	3	-	2	1	2.33	3	Moderate
4	1d	3	3	2	3	2	1	2	2.29	3	Moderate
5	1e	2	1	3	3	3	1	1	2	3	Moderate
6	2	3	1	3	3	2	1	3	2.29	3	Moderate
7	3a	3	1	3	-	3	2	2	2.33	3	Moderate
8	3b	3	1	3	-	2	2	3	2.33	3	Moderate
9	4a	3	1	3	3	2	1	2	2.14	3	Moderate
10	4b	2	1	2	2	2	1	3	1.86	2	High
11	4c	2	2	1	3	3	2	3	2.29	3	Moderate
12	5a	3	1	3	2	-	1	3	2.17	3	Moderate
13	5b	3	1	3	2	3	1	3	2.29	3	Moderate
14	5c	3	3	3	-	2	2	3	2.67	4	Low
15	6	3	1	3	3	2	1	3	2.29	3	Moderate
16	7	2	1	3	2	3	2	3	2.29	3	Moderate
17	8	3	1	3	3	3	3	3	2.71	4	Low
18	9a	3	3	1	3	3	2	1	2.29	3	Moderate
19	9b	2	1	3	3	3	1	2	2.14	3	Moderate
20	9c	3	1	1	3	2	1	1	1.71	2	High

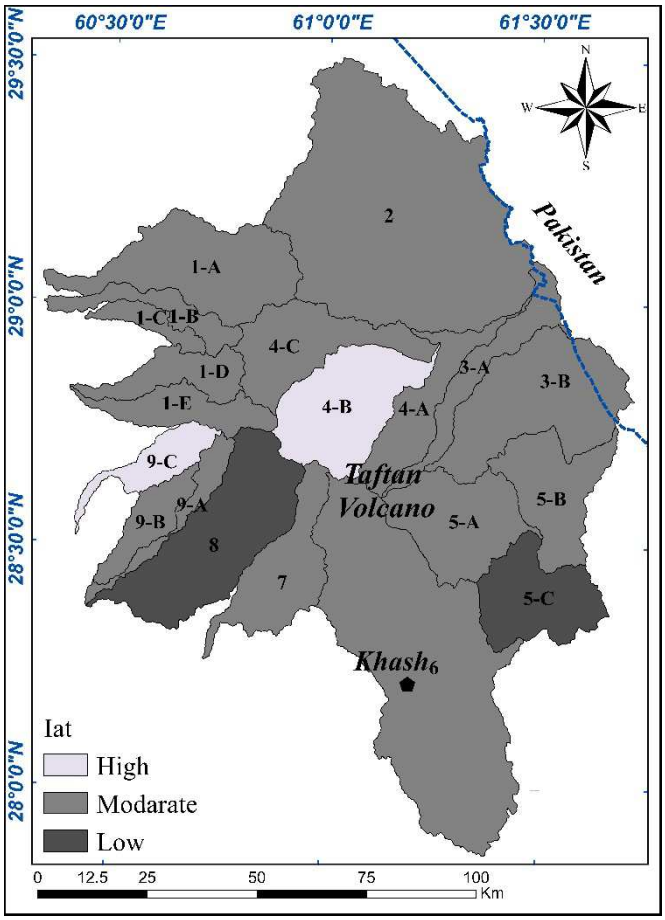

Fig. 10. Category of Relative Active Tectonic in the study area in terms of their separation.

1. The area in High Relative Active Tectonic: found in two sub-basins of 4-B and 9-C. Due to serious tilting of 4-B, amounts of Hi, and high extension of the drainage basin and tilting 9-C, these two sub-basins have high and young Relative Active Tectonic.

2. The area in Middle Relative Active Tectonic: It includes a large area. Important structures such as Dargiaban and Saadabad faults have been located in the area.

3. The area in Low Relative Active Tectonic: It is found in two sub-basins 5-C and 8. In terms of Lithology, there are Silt, clay, old and new alluviums in this area. Important structures include Saravan, Koohrud and Gazou faults located on the southeast of the area. Low level of activity of sub-basin 5-C is as the results of basin shape and the amount of uplifting and tilting (Fig. 8). Field studies have been considered in structures and morphologies areas located along the rivers, and some active tectonic parameters have been considered as follows (Fig. 11, 12).

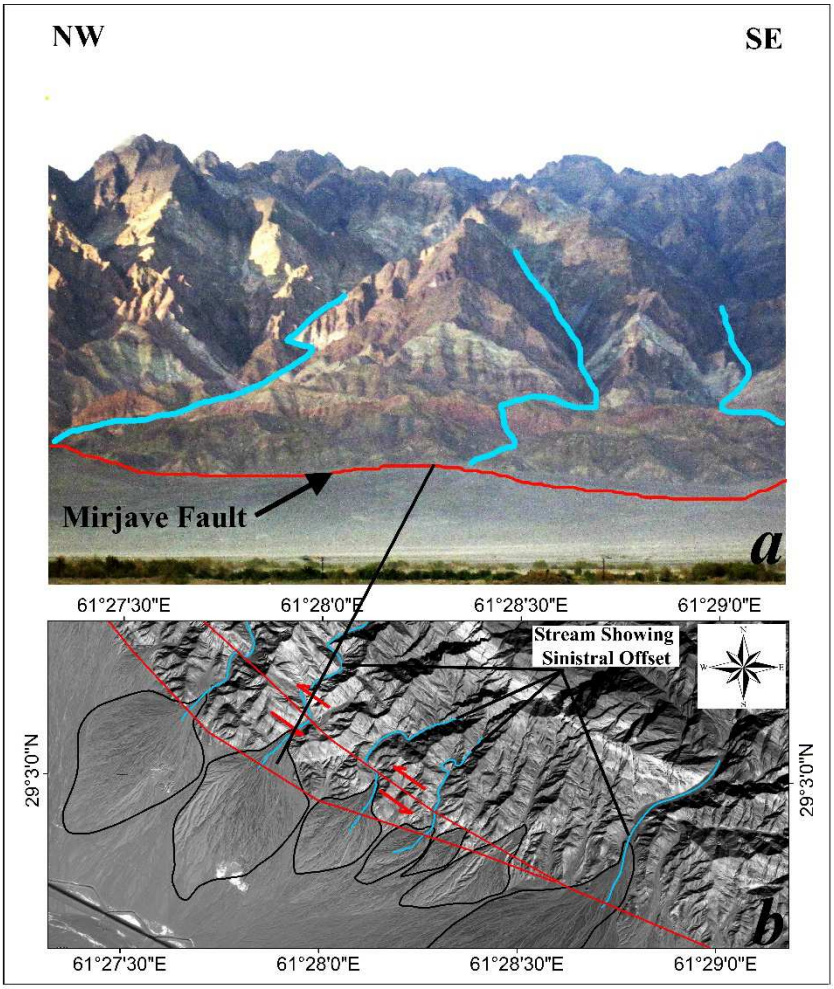

Fig. 11. a) Landsat Satellite images. It is found some transformations along the channel as a result of moving fault. Cones, located adjacent to the mountain front indicate active uplifting, b) Field picture of the area that illustrates Mirjaveh Fault and some geomorphic effects.

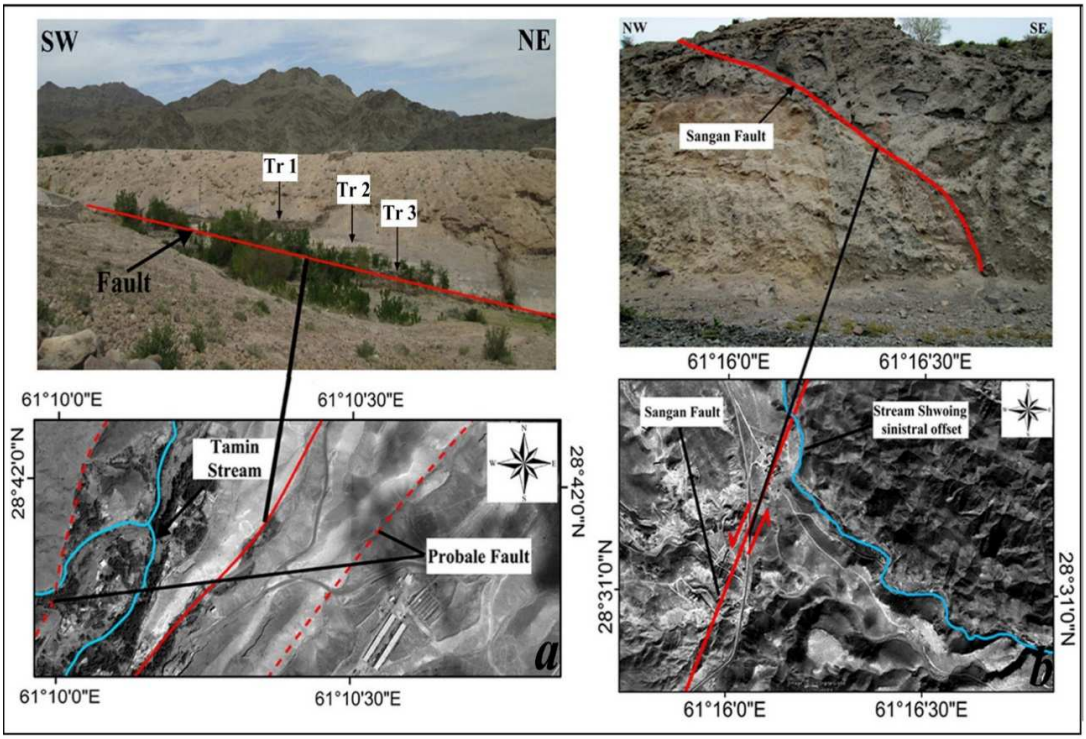

Fig. 12. Landsat Satellite images illustrate some active tectonic evidence. a) River traces near this area Tamin Village on the northeast of Taftan volcano, b) Effect of Sangan Fault in dug tranche wall in the southeast of Taftan volcano.

Conclusion

The amounts gained from calculating the indices on the basis of the relative active tectonic category have been integrated and concluded that neotectonic plays an important role in evolving area tectonic. Regarding the new-tectonic insights, the presence of active structures in the study area such as folds and faults has been caused into changes in this region which (these changes) are visible as uplifts. Three tectonic areas are recognizable in the area: Area with high relative tectonic action found in sub-basins of 4-B and 9-C. An area with high relative tectonic activities has been found in sub-basins of 4-B and 9-C. An area with moderate relative tectonic activities has been found in wide areas such as Dargiaban and Sa'adabad faults located on the northwest part. An area with low relative tectonic action activities has been found in a small area. Sub-basins of 4-B and 9-C have high relative tectonic activity affected by moving young faults and active tectonic structures located on both sub-basins. Sub-basins of 1-A, 1-B, 1-C, 1-E, 2, 3-A, 4-A, 4-B, 5-A, 5-B, 6, 7, 9-A, 9-B have moderate relative tectonic activities**,** and 8 and 5-C have low relative tectonic activities. By calculating the tectonic indices, it was found that in the broad range of the study area, the level of tectonic activities is moderate. In the boundary of Taftan volcano cone which was the result of the accumulation of magma over the past times due to the existence of high resistance rocks, the values obtained from the calculation of tectonic indices indicate this active area. However, near the boundaries of the volcanic cone which mainly consists of flake deposits and metamorphic rocks, the tectonic activities, as well as structures such as the faults of Saravan and Mirjaveh, Khan Mohammad Chah, Sa'ad Abad, Dagiaban, and the folds resulted from these activities, can be controlled. Additionally, as the result of these tectonic movements, the morphometric parameters of this region have changed.

References

Aghanabati , A.: Iran Geology. *Geological Survey of Iran, 2004.*

Alipoor R., Poorkermani M., Zare M., El-Hamdouni R.: Active tectonic assessment around Rudbar Lorestan dam site, High Zagros Belt (SW of Iran), *Geomorphology, 128, p.1-14, 2011.*

Azor A., Keller E.A., Yeats R.S.: Geomorphic indicators of active fold growth: South Mountain-Oak Ridge Ventura basin, southern California, *Geol Soc Am Bull, 114, p.745–753, 2002.*

Bagha N., Arian M., Ghorashi M., Pourkermani M., El-Hamdouni R., Solgi A.: Evaluation of relative tectonic activity in the Tehran basin, central Alborz, northern Iran, *J Geomorph, 213, p.66–87, 2014.*

Biabangard, H.: Petrography, geochemistry, geocronology and volcanic activity (Taftan volcano) located in the Makran belt, PhD thesis, *Shahid Bahonar University of Kerman. 2009.*

Bull W.B., McFadden L.D.: Tectonic geomorphology north and south of the Garlock fault, California. Proceedings of the 8th Annual Geomorphology Symposium on Geomorphology in Arid Regions, *State University of New York, Binghamton, Sept, 272, p.23–24, 1977.*

Bull W.B.: Tectonic geomorphology of mountains, a new approach to Paleoseismology, Malden, Massachusetts, *Black well Publishing, 2007, 316 p.*

Cloetingh S., Cornu T., Ziegler P.A., Beekman F., Group, E.: Neotectonics and intraplate continental topography of the northern Alpine Foreland, *Earth-Sci, Rev, 74, p.127–196, 2006.*

Chen Y.C., Sung Q., Cheng K.Y.: Along-Strike variations of morphotectonic Feature in the Western Foothill of Taiwan: tectonic implications based on Stream-Gardient and Hypso metric analysis, *Geomorphology, 56, p.109–137, 2003.*

Dehbozorgi M., Porkermani M., Arian M., Matkan A.A., Motamedi D., Hosseiniasl, A.: Quantitative analysis of relative tectonic activity in the Sarvestan area, central Zagros, Iran, *Geomorphology, 121, p.329–341, 2010.*

Eftekhar Nejad J., and Aghanabati A.: The geological map of Khash. *Geol surv of iran, 1994.*

El-Hamdouni R., Irigaray C., Fernández T., Chacón J., Keller E.A.: Assessment of relative active tectonics, southwest border of the Sierra Nevada (southern Spain), *Geomorphology, 96, p.150–173, 2008.*

Faghih A., Nourbakhsh A.: Implication of Surface Fractal Analysis to Evaluate the Relative Sensitivity of Topography to Active Tectonics, Zagros Mountains, Iran, *J Mt Sci, 12, p.177–185, 2015.*

Ganser, A.: The Taftan volcano (Southeast Iran). *Eclogae geol helv, 64, 319-334, 1971.*

Han Z., Wu L., Ran Y., Ye Y.: The concealed active tectonics and their characteristics as revealed by drainage density in the North China plain (NCP), *J asian earth sci, 21, p.989–998, 2003.*

Hare P.W., Gardner T.W.: Geomorphic indicators of vertical neotectonism along converging plate margins, Nicoya Peninsula, Costa Rica. Proceedings of the 15th Annual Binghamton Geomorphology Symposium on Tectonic Geomorphology, *Allen and Unwin, Boston, p.123–134, 1985.*

Keller E.A.: Investigation of active tectonics: use of surficial Earth processes. In: Wallace, R.E. (ed.), Active Tectonics, Studies in Geophysics, *National Academy Press, Washington DC, 1986, 280 p.*

Keller E.A., Pinter N.: Active Tectonics: Earthquakes, Uplift, and Landscape, *Prentice Hall, Upper Saddle River, 2002, 362 p.*

Mahmood S.A., Gloaguen R.: Appraisal of active tectonics in Hindu Kush: Insights from DEM derived geomorphic indices and drainage analysis, *Geosci Front, 3, p.407–428, 2012.*

Memarian, H.: Geology for Engineers*, University of Tehran, p.49 -126. 2001*

Molin P., Pazzaglia F.J., Dramis F.: Geomorphic expression of active tectonics in a rapidly-deforming forces, sila massif, Calabria, southern Italy, *J Am Sci, 304, p.559–589, 2004.*

Pedrera A., Pérez-Peña J.V., Galindo-Zaldívar J., Azañón J.M., Azor A.: Testing the sensitivity of geomorphic indices in areas of low-rate active folding (eastern Betic Cordillera, Spain), *Geomorphology, 105, p.218–231, 2009.*

Pike R.J., Wilson S.E.: Elevation-relief ratio, hypsometric integral and geomorphic area-altitude analysis, *J Geol Soc Am Bull, 82, p.1079–1084, 1971.*

Pérez-Peña J.V., Azor A., Azañón J.M, Keller E.A.: Active tectonics in the Sierra Nevada (Betic Cordillera, SE Spain): Insights from geomorphic indexes and drainage pattern analysis, *Geomorphology, 119, p.74–87, 2010.*

Ramirez-Herrera M. T.: Geomorphic assessment of active tectonics in the Acambay Graben, Mexican volcanic belt. Earth Surf. Process, *Landf., 23, p.317–332, 1998.*

Rockwell T.K., Keller E.A., Johnson D.L.: Tectonic geomorphology of alluvial fans and mountain fronts near Ventura, California. In: Morisawa, M. and Hack, J.T. (eds.), Tectonic Geomorphology, *George Allen and Unwin, Boston, 1985, 183–207 p.*

Silva P.G., Goy J.L., Zazo C., Bardajm T.: Fault generated mountain fronts in Southeast Spain: geomorphologic assessment of tectonic and earthquake activity, *Geomorphology, 250, p.203–226, 2003.*

Strahler A.N.: Hypsometric (area-altitude) analysis of erosional topography, *Geol Soc Am Bull, 63, p.1117–1142, 1952.*

Vernant P., Nilforoushan F., Hatzfeld D., Abbassi M.R., Vigny C., Masson F., Nankali H., Martinod J., Ashtiani A., Bayer R., Tavakoli F., Chery J.: Present-day crustal deformation and plate kinematics in the Middle East constrained by GPS measurements in Iran and northern Oman, *J Geophysical Inter, 157, p.381–398, 2004.*

Wells S,G., Bullard T.F., Menges T.M., Drake P.G., Karas P.A., Kelson K.I., Ritter J.B., Wesling J.R.: Regional variations in tectonic geomorphology along segmented convergent plate boundary, Pacific coast of Costa Rica, *Geomorphology, 1, p.239–265, 1988.*

Zovoili, E., konstantinidi, W., koukouvelas, I. K., (2004), Tectonic geomorphology of escarment The Cases of kompotades and Nea Anchialos Faults. Bulletin of the Geological Society of Greece 63: 1716 – 1725.

The conditions for implementing a circular economy in the Czech Republic

Šárka Vilamová[1], Anežka Podlasová[2], Marian Piecha[3], Kamila Janovská[1], Petr Šikýř[2], Drahomír Foltan[2], Martin Šanda[2], Karel Bařinka[2] *and* ***Roland Grosoš[4]***

In July 2018, measures of the European Commission regarding the Circular Economy Package (CEP) came into force. All EU Member States have two years since to implement these measures into their national legislations. The aim of the authors is, using available resources, to evaluate current conditions in the Czech Republic in the areas affected by this legislation. It is primarily the area of waste management, which has set values within the CEP that must be achieved within those two years. The article offers an analysis of the circular economy penetration into the Czech legislation. The procedure for introducing changes in legislation is presented through the Waste Management Plan (WMP) for the period 2015-2024. The aim of the article is to verify whether the Czech Republic is able to meet the EU and WMP's requirements in the current development of waste management. The authors are first to use the analysis of secondary data from national and transnational sources, from which they created unique and original outcomes for the given issue. After the analysis, they introduced the measures that could be used for the greater motivation of the target groups in order to meet the goals of the Czech Republic. The authors address the concrete impacts of CEP implementation within the Czech Republic and also present Czech examples of good practice.

Keywords: *Circular Economy; Circular Economy Package; Waste Management Plan; Legislation; Czech Republic; European Union*

Introduction

In recent years, the term circular economy has been repeatedly debated not only in the European states. A circular economy as a counter for a linear economy that has been used all over the world. The purpose of the circular economy is to transform waste into resources, i.e. waste that can be reused is transformed and then returned to the production process. This will reduce state dependence on primary resources, which must very often be imported from very distant and often politically unstable countries. In addition, there are savings of primary resources, which are mostly mineral raw materials characterized by their non-renewable nature, i.e. their reserves are exhaustible in the long run. For this reason, it is necessary, as Šimková (2016) suggests, focusing on strategies leading to the responsible use of raw materials.

The need to implement the circular economy has been foreseen by the European Union, respectively by the European Commission, which on the 3 December 2015 adopted the so-called Circular Economy Package. Over the following three years, talks have been taking place on the final values to be achieved across all Member States. The given values were approved by the Member States on 22 May 2018 under the Circular Economy Package, which came into force on 4 July of the same year.

The Circular Economy Package and the related environmental legislation at European Union level is a field of expertise of Wysokińska (2017), who lists individual strategic plans and their aims. In particular, the Strategic Plan 20/20/20 is de facto a document setting goals to be achieved by 2030. The aim of this plan is recovering from the crisis and preparing the European economy for the next decade, i.e. period until 2030. The whole strategy is based on promoting the knowledge-based economy, participating in the labour market, eliminating poverty and more resource-efficient production (Bilan, 2013). Furthermore, national strategies shall be linked to the right corporate strategies that can provide additional funding and reduce the cost of implementing the legislative obligation. Chlopecký (2018) shows such cooperation using the example of mining companies and highlights the importance of econometric models of mining and subsequent prediction models of mining.

Stahel (2017) states that the circular economy and the Circular Economy Package are a result of an industrial economy and consist of two parts: industrial goods (technological cycle) and food and water (biological cycle). Both of these cycles need to focus on zero waste system and prevention of waste. Bartl (2015) presumes that the Circular Economy Package focuses too much on recycling and not enough on prevention of waste production. However, the Circular Economy Package is not all that the European Union introduces within the field of waste management. On 16 January 2018, the so-called Strategy for Plastics was announced by the European Commission saying that by 2030 only plastic that is either reusable or recyclable shall be used and that

[1] *Šárka Vilamová, Kamila Janovská,* VSB-Technical University of Ostrava, Faculty of Materials Science and Technology, 17. listopadu 2172/15, 708 00 Ostrava – Poruba, Czech Republic, *sarka.vilamova@vsb.cz, kamila.janovska@vsb.cz*

[2] *Anežka Podlasová, Petr Šikýř, Drahomír Foltán, Martin Šanda, Karel Bařinka*, VSB-Technical University of Ostrava, Faculty of Mining and Geology, 17. listopadu 2172/15, 708 00 Ostrava – Poruba, Czech Republic, *anezka.podlasova.st@vsb.cz, petr.sikyr.st@vsb.cz, drahomir.foltan.st@vsb.cz, martin.sanda.st@vsb.cz, karel.barinka.st@vsb.cz*

[3] *Marian Piecha,* Ministry of Industry and Trade Czech Republic, Na Františku 32, 110 15 Praha 1, Czech Republic, *piecha@mpo.cz*

[4] *Roland Grosoš,* Technical University of Košice, Technical University of Košice, Faculty of Mining, Ecology, Process Control and Geotechnology, Letná 9, 042 00, Košice, Slovak republic, *roland.grosos@tuke.sk*

it is necessary to lower the pollution of plastic, especially microplastics, into the environment. As one of the main benefits of recycling plastics EU considers the fact that its members will be less dependent on the import of fossil fuels (Ministry of Industry and Trade of the Czech Republic, 2018).

Another step leading towards lowering the amount of plastic waste, based on the Strategy for Plastics, is the European Parliament and Council Directive on the Limitation of the Impact of Certain Plastic Products on the Environment of 28 May 2018. This Directive prohibits the production of certain plastic products for which there are available and affordable alternatives. The ban applies specifically to the following products: plastic cotton buds, cutlery, plates, straws, stirrer sticks, balloon sticks that have to be replaced with sustainable materials. Disposable plastic drinking beverage containers will only be allowed on the market if their caps and lids remain attached to the container. The ban on the distribution of these products will apply from 2021. In addition, by 2025, Member States will have to ensure the collection of 90% of disposable plastic bottles of beverages (Treti ruka, 2018).

Circular Economy Package in Czech Legislation

From the time when the Circular Economy Package came into force, the Member states have 24 months to implement its content into their national legislations. That means that all EU Member States must have a valid legislative until the 5 July 2020, including the following directives:

- Directive 2018/851 / EU amending the Waste Directive,
- Directive 2018/852 / EU amending the Packaging Directive,
- Directive 2018/850 / EU amending the Landfill Directive;
- Directive 2018/849 / EU amending Directive 2000/53 / EC on end-of-life vehicles, 2006/66 / EC on batteries and accumulators and waste batteries and accumulators and 2012/19 / EU on waste electrical and electronic equipment.

In the Czech Republic, it mainly concerns updating Act no. 185/2001 Coll., On Waste and Act no. 477/2001 Coll., On Packaging and the introduction of the law on end of life products. Kozel (2015) deals with selected aspects of Czech legislation in relation to the environment and above all, the solution of environmental needs by means of appropriate legislation. Similar problems are also addressed by Slovak authors. Horodníková (2008) shows the importance of legislative by the implementation of new technological solutions in using renewable energy sources. Khouri (2016) deals with a system approach to solving the problems of re-use of metallurgical brownfields, as a potential tool to support further regional development, accepting the valid legal regulations, as well as the principles of sustainable environmental development.

Given that the process of endorsement of the Circular Economy Package was relatively extensive and the values changed over the years, the legislation in this area could not be adopted earlier. In 2015, the plan was to achieve the following three goals in the field of waste management: reaching 65% rate of the municipal waste recycling, 75% of packaging waste recycling and also that within the European Union only 10% of all waste will be landfilled. (European Commission, 2015) Recently it has been understood that the Commission is proposing to ban landfills altogether and the Parliament aims to increase the recycling rate of municipal waste to 70% and packaging waste to 80%. The landfilling should not exceed 5% rate (Vosecký, 2017).

The final values that shall be achieved are as follows: by 2035, as previously planned, the recycling of municipal waste rate shall go up to 65%, given that by 2025 it should be up to 55% and 5 years later it should reach 60%. For packaging waste, a recycling rate of 70% is expected to be achieved by 2030. The specific values for the individual types of materials are shown in Figure 1. Besides, it is set that after 2035 less than 10% of all municipal waste shall be landfilled as intended in the year 2015 (European Commission, 2018).

In 2015, even though there were no exact figures, the Czech Government, in response to the adoption of the Circular Economy Package approved the new Waste Management Plan (WMP) for the period 2015–2024. This plan already counts on limiting the amount of mixed municipal waste and landfilling. Given that the exact values to be achieved are still not known today, it is not possible to say with certainty whether by fulfilling the national targets the Czech Republic had set, the requirements of the European Union can be met.

The Czech Waste Management Plan is divided into four parts: introduction, evaluation of the current state of waste management in the Czech Republic, and binding and indicative parts. The binding part is issued as a government order due to the possibility of legal enforceability. The binding part of the current Waste Management Plan is a part of the Government Decree No. 352/20014 Coll., On the Waste Management Plan of the Czech Republic for the period 2015–2024. Waste Management Plans of individual regions and the Waste Management Plans of individual cities follow the national Waste Management Plan.

The most important and the most striking objective, that the Czech Republic puts forward by 2024 is the landfill ban of municipal, recycling and reusable waste. Nevertheless, this step has only been legally enacted in the Government Order on the Waste Management Plan as the amendment to Act No. 185/2001 Coll., On Waste that would regulate it, despite several attempts to date, have not been adopted yet. However, measures are known

to achieve this goal. It is assumed that the fee for dumping the waste that will be banned after 2024 will increase. According to the existing Waste Act (Act no. 185/2001 Coll.), the actual standard fee for municipal and mixed waste is 500 CZK/t and 1700 CZK/t for dangerous waste per one calendar year. It is apparent that increasing this fee would result in increasing the fee for municipal waste paid by citizens and therefore they will try to recycle as much as possible in order to avoid that. The fundamental problem with landfill ban is the fact that it has not yet been solved how to proceed in case that the landfills will be banned after the year 2023 and the banned waste will continue to be landfilled there. It is also necessary to figure out how to prevent illegal landfills of this waste. With regards to landfill ban, one of the goals of the WMP 2015–2024 is above all the energy utilization of waste after the removal of the materials of use, hazardous components and biodegradable waste.

Other types of waste and goals that should be met in the year 2020 are also addressed in the binding part of the WMP. In the Czech Republic, the overall level of preparation for re-use and recycling should be increased to at least 50% by weight, for waste from plastic, paper, glass and metal originating in households, or for wastes which are similar to those wastes, but which are of different origin.

In the area of packaging waste, the recycling rate should increase to 70% by 2020. The specific percentages for each type of packaging waste are given in the following table (Table 1).

Tab. 1. Packaging recycling

Packaging waste	Recycling [%]	Overall recovery [%]
Paper and cardboard	75	
Glass	75	
Plastic	50	
Metal	55	
Wooden	15	
Consumer sales	50	55
Total	**70**	**80**

Source: Ministry of Environment, 2014, p. 108.

It is known that glass and metals can be recycled basically over and over again, so in the case that they are sorted out of the municipal waste, it should not be a problem to achieve the values mentioned in Table 1. Plastic packaging recycling is, however, quite problematic and not only in the conditions of the Czech Republic. The process of recycling plastic waste is resource-intensive, primarily for water and energy, but also finance, because recycling costs are high. A very important element of recycling is the process of collecting waste in a form that allows its further sorting and pre-treatment processes to produce a secondary raw material that is subsequently recycled. As a result of legislation, it is virtually impossible to meet the legislative targets of recycling and recovery without proper infrastructure and logistics of waste collection. A very important role in meeting the objectives in the field of municipal waste is played by consumer communication, which represents one of the key elements of influencing the citizens to handle their waste responsibly, i.e. so as to meet the objectives of recycling and recovery. As an example, residents sort their waste into containers for recycling or bring used batteries to take-back points, which could be, for example, points of sale of these batteries. None of that would have happened without effective and continual communication.

In the category of sorting electrical and electronic equipment waste, the aim is also to increase the level of sorting this waste and, consequently, the rate of recovery, recycling and preparation for re-use. In the Czech Republic, in accordance with EU legislation, legal and natural persons placing those products on the market are obliged to ensure their take back. Citizens also have the possibility to put small electrical appliances in special containers, but there are not enough of them in the Czech Republic. In this waste category, meeting the goals is partly set for August 2018. Individual target values will be stated in the next chapter (Table 3).

An important goal of the Waste Management Plan 2015–2024 is also reducing biodegradable waste that ends in landfills. The problem of sorting biodegradable waste lies primarily in the fact that citizens have only a few options to store this type of waste even though they are required to sort it from 2015 onwards.

In terms of the Czech Republic, the circular economy is also reflected in the Secondary Raw Materials Policy, which is a part of the Raw Material Policy of the Czech Republic. On 15th April 2014, the government approved the Secondary Raw Materials Policy as the Government Resolution No. 755. This is the first document of the Czech Republic, creating a strategic framework for the efficient use of secondary raw materials. Its slogan is "Waste conversion to resources". In the analysis, ten commodities and sources of secondary raw materials were formed on the basis of which the Policy was then prepared. These include metals, paper, plastics, glass, construction and demolition materials, energy by-products, end-of-life vehicles (wrecks), waste electrical and electronic equipment, used tires and waste rubber, waste batteries and accumulators.

The Policy sets out five strategic goals and sixteen measures. These goals are:

1) Increasing the self-sufficiency of the Czech Republic in raw material sources by replacing primary sources with secondary raw materials.

2) Promoting innovation securing the acquisition of secondary raw materials in a quality suitable for further use in industries.
3) Promoting the use of secondary raw materials as a tool for reducing the energy and material demands of industrial production while eliminating negative impacts on the environment and human health.
4) Supporting the education of qualified workers in the field of secondary raw materials as an endorsement of the competitiveness of the Czech Republic.
5) Updating the scope of the statistical survey for the processing of material accounts, enabling the mass balance of secondary raw materials to be processed in the Czech economy (Ministry of Industry and Trade of the Czech Republic, 2015).

The ability of the Czech Republic to meet the requirements of the Circular Economy Package and the Waste Management Plan 2015-2024

In order to determine whether the state is able to meet the waste recycling requirements, it is first and foremost necessary to take into account the very definition of the basic concepts of waste management, such as recycling, as defined by a specific state.

For a specific process of determining whether the Czech Republic is able to meet the requirements of the Waste Management Plan that are already set until 2024, it is necessary to use data from previous years. There are two sets of data available in the Czech Republic, collected by different institutions. One of them is the Czech Statistical Office and the second one, the Ministry of Industry and Trade of the Czech Republic. It is now being discussed that the data related to the environment should be collected by a single methodology.

As already stated above, the Czech Republic plans to put forward the so-called landfill ban of the communal, recyclable and recoverable waste by 2024. At present, it can be stated that dumping has a declining trend, but if the landfills are to be banned completely, dumping must be radically reduced. In 2016, according to EUROSTAT data, 50 per cent of waste was landfilled; ten years earlier, it was 77 per cent (2006) - see Table 2. In the past ten years, it has dropped by only 27 per cent, and it is now necessary to reduce dumping by a total of 50 per cent in the following six years. So if the Czech Republic does not implement significant changes in waste management, the criteria (< 10 %) of the European Union will not be met.

Tab. 2. Dumping in the Czech Republic in the years 2006 – 2016 [%]

2006	2007	2008	2009	2010	2011	2012	2013	2014	2015	2016
77	75	75	73	68	65	56	56	56	53	50

Source: Eurostat, 2017.

Undoubtedly, alternatives to waste disposal are also needed in the context of diversion from landfill. This is mainly the energy recovery of waste in ZEVO (waste incineration plant, generally incineration plant), i.e. the production of electric and thermal energy. In the Czech Republic, there are four incineration plants: in Prague, Brno, Liberec and in Chotíkov u Plzně. The last facility, which is also the latest, have been a subject to many disputes and it has long been unsure of whether it will ever be possible to put it into operation. There are many opponents to new ZEVO in the Czech Republic. In particular, they are mostly eco-activists and locals who do not want similar facilities near their homes.

Nevertheless, the area of energy use of mixed municipal waste in ZEVO is supported by the state. Baránková (2013) found grounds for supporting the ZEVO system in her article, where she compared two similar cities, in regard of size and number of citizens (Ostrava and Brno), with a different approach to waste disposal (dumping vs ZEVO). The calculated economic indicators reached significantly different values in favour of the energy use of mixed municipal waste.

Straka (2018) tried to find out, using computer simulation, the volume of the environmental impact of waste incineration processes within a particular region. The aim was to find ways to reduce the impact on the environment of the combustion process in the Slovak Republic. The simulation results show that incineration during a one-year period produces about 15,266 tons of plastic and electrical components, and will release about 590,000 GJ of energy and about 199,000 tons of steam and 287 tons of other emissions with only 3 milligrams of dioxins.

In the field of packaging recycling, the Waste Management Plan sets the overall recycling rate at 70%. According to the Circular Economy Package, the rate is 70 per cent. In 2017, according to data from EKO-KOM, the total recycling rate was 74%. Figure no.1 shows that the Czech Republic has already met the objectives of the Waste Management Plan 2015–2024 both for the overall recycling of packaging waste and for each type of packaging material. At the same time, the Czech Republic already meets the EU requirements of the Circular Economy Package.

The Czech Republic's waste management strategy should be both motivating and realistic. It also should not burden Czech citizens or the industries any more than it burdens citizens and industries of other European

countries. The state should also actively develop and support tools that would help to meet the objectives of the future European legislation.

Kozel (2018) dealt with ways to motivate citizens to recycle. He sees potential in information technology and as the most attractive considers the use of RFID chips, thanks to which it is possible to see how full are individual waste containers. This way, it would be possible to eliminate situations when the containers are filled up, and citizens are therefore less willing to recycle. Zapletal (2017) emphasises the link between motivation and specific financial measures. As an incentive tool for businesses, he sets out a system of allowances that the heavy industrial enterprises in the EU face from the beginning of the millennium. This system has threats associated with the emission-trading obligation. Significant factors are the number of allowances granted to the business for free and the price of emissions for different types of permits.

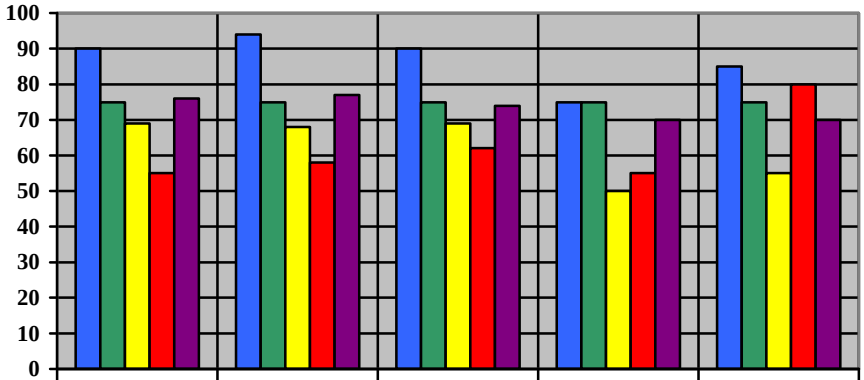

	2015	2016	2017	WMP 2020	CEP 2030
Paper and cardboard	90	94	90	75	85
Glass	75	75	75	75	75
Plastic	69	68	69	50	55
Metal	55	58	62	55	80
Total	76	77	74	70	70

Fig. 1. Packaging recycling rate in 2015-2017 and values according to WMP and Circular Economy Package
WMP 2020 = Waste Management Plan 2015–2024; CEP 2030 = Circular Economy Package
Source: own processing according to the Ministry of Environment, 2014; EKO-KOM 2016, 2017, 2018 and European Commission, 2018.

Companies participating in the adoption of the Circular Economy Package in the Czech Republic

There are companies in the Czech Republic, which are trying to point out both: the issues of waste management and the circular economy. Probably the best-known waste company is the only authorized packaging company in the Czech Republic EKO-KOM, a.s. Company.

Industrial companies producing packaged goods in 1997 as a non-profit joint-stock company founded the EKO-KOM. The purpose of establishing EKO-KOM Company was to create one umbrella organization, which would provide the take-back of packaging and the utilization of waste from the packaging for its contractual partners, whereas the contractual partners are those entities who, according to Act No. 477/2001 Coll. are obligated to perform these two activities. The system, at present, includes more than 20,000 companies and more than 6,000 Czech municipalities. (EKO-KOM)

The scope of the company's activities lies not only with the above stated, but it also helps its clients with other issues related to waste management and especially it focuses on the field of awareness and education. Awareness and education are undoubtedly particularly important for citizens to realize the importance of recycling. Unless the citizens are able to sort their waste the best they can, the system of a circular economy cannot work effectively.

The EKO-KOM Company uses most of the media to educate the citizens. There are TV campaigns bearing the claim “Má to smysl, třiďte odpad” (It’s worth it, sort your waste”) pointing out the importance of recycling. The campaigns are extended to the online environment, specifically to several websites run by the Company. There are also Facebook and Instagram pages supporting the campaign.

Another company that addresses pretty much all of the target groups influenced by the impacts of the new legislation is the Institute of Circular Economy. This non-governmental organization, established in 2015, is dedicated to spreading ideas about the circular economy, both between businesses and government authorities, as well as citizens. The Institute organizes seminars, conferences and workshops to educate those interested in the

circular economy. For municipalities and their leadership that will indisputably also be affected by the adoption of the package, it annually organizes the Waste Management Conference, where it explains the benefits of the transition to the circulator economy (Institute of Circular Economy).

The Impact of Adopting the Circular Economy Package

It is apparent from the previous text that the adoption of the Circular Economy Package at the level of the European Union and its subsequent incorporation into state legislation will have an impact on all the involved target groups, i.e.:

- Individual states,
- Their entrepreneurs and
- Their citizens.

At the state level, it is necessary to adopt such legislative measures so that Czech legislative is in line with those of the European ones. An amendment to Act No. 185/2001 Coll., On Waste (effective from 1 January 2018) was approved in 2017, however, from the point of view of the circular economy, there were no significant changes. Even though there were points on changes to the circular economy in the draft, the lobby finally won, and the proposals were not enforced (Drábková, 2017). However, as stated above, the Czech Republic must implement the Circular Economy Package into its legislation within 24 months of CEP's entry into the force.

In connection with the transition to the circular economy, it is essential that all target groups companies and institutions are involved. The government should adopt not only new legislation that is in line with the law of the European Union, but also create optimal conditions so the entire circular economy system can work efficiently. This includes especially removing all the obstacles related to the production of new products as well as the transfer of waste (resources) to others for further processing. For smooth transition to circular economy, it is also vital to create a special plan, i.e. so-called circular roadmap, which would provide a long-term concept involving the implementation of circular economy principles into legislation, finding key and priority areas, mapping the current situation and, above all, steps to be taken in individual phases (Drábková, 2017).

The Ministry of Industry and Trade is trying to promote the circular economy through various competitions. For example, at the beginning of this year, a nationwide competition called the "Transformation of waste to resources" took place, where production and construction enterprises, public administration of municipalities and towns, university students and colleges of secondary schools, vocational schools, elementary schools and facilities for leisure activities could participate (Ministry of Industry and Trade, 2017).

And it should be the production companies and enterprises placing the packaged products on the market that should eliminate the amount of waste. The Eco-design should become a trend as its main objective is to lower the impacts of products on the environment during the whole product life cycle. In the field of the circular economy, it is important that the products can be continually used even after the end of their life cycle. And that is precisely why it is appropriate to use materials that can be recycled or otherwise used while using technological procedures that do not prevent their further use. As far as packaging is concerned, it is also advisable to select such materials for their manufacture, which can be further utilised, and, in particular, it is important to consider whether it is necessary to use such quantities of packaging. These are in particular consumer packages, which are often totally unnecessary, as the goods are essentially stored in two packages (for example, perfumes). Supporting Eco-design is also one of the waste prevention objectives enshrined in Act No. 185/2001 Coll., On Waste. Under this law, Eco-design means systematic incorporation of environmental aspects into the design of the product in order to improve the environmental impact of the product throughout its life cycle.

The amendment to the Act no. 477/2001 Coll., On Packaging, which responds to the relevant EU Directive and came into effect on 1st January 2018, can be considered an innovation in packaging. Since this day, it is forbidden to provide a plastic bag to a consumer for free. Some of the retailers have already prepared for this regulation and are currently selling bags for a certain amount, or they have switched to paper bags or those that can be used repeatedly.

At the same time, it is necessary to realize that the adopted legislation for introducing the circular economy is also manifested outside the waste management and brings the need for new legislation in other areas. An example may be Act No. 181/2014 Coll. The Cyber Security Law, which regulates the rights and obligations of individuals and the powers of public authorities in cybersecurity. (Moravec, 2017) For example, heating plants produce, on the one hand, a significant amount of hazardous waste and are therefore directly affected by the fulfilment of EU (or CEP) conditions. On the other hand, the legislation of the circular economy is also reflected in the cybersecurity of businesses and carries the cost of implementing regulations in companies.

There is an increasing trend of recycling among citizens. It is even reported that in the overall recycling we are in second place in Europe - after Belgium (EKO-KOM, 2017). But, if we look at the amount of waste that could be sorted and is still in the mixed municipal waste, the citizens of the Czech Republic have still a lot to

learn. From this point of view, the awareness and education that are in the scope of activities of, for example, the EKO-KOM Company and the Institute of Circular Economy, are very important.

Lastly, Czech citizens very often do not realise how they recycle as other people do not as well, or they are not really thorough in doing so. Many citizens do not recycle at all as it seems of no significance to them. And some go to extremes such as littering, i.e. throwing away garbage anywhere.

In the Czech Republic, although Act No. 185/2001 Coll., On Waste obliges everyone to recycle, yet, there is currently no system to sanction those who breach it. However, the absence of such a system that to some extend commonly works in other European countries, limits the development of other forms of waste recovery and recycling. Particularly, when the state is planning the landfill ban, it is necessary to think about this problem and, in particular, in a suitable way, implement a system of sanctions for citizens. Many cities have been trying to motivate the citizens to sort their waste by reducing or cancelling the fee for municipal waste, but once again there must be a system that will be able to recognise whether the citizens actually do sort their waste.

Though, there are few cities in the Czech Republic that have been implementing systems to monitor recycling. They provide their citizens with special bar codes used to hold together or tie their waste and thus the municipality knows precisely how they recycle.

Examples of Good Practice in Waste Management in the Czech Republic

Nowadays, in connection with the transition to the circulatory economy, the so-called “Urban mining” is being discussed, which is the mining of valuable raw materials directly in the cities. The Smolo Ostrava waste company has been addressing this option. This company is trying to find new ways how to get raw materials. Since Ostrava was a heavily industrial area, there are a large number of old industrial buildings waiting for demolition. The Smolo Company sees them as sources of raw materials they can get and offer them further. For example, they can create a certified product from old buildings using crushers and screeners. These could be different fractions of aggregate, asphalt or reinforced concrete (Czech Waste Management Association, 2017).

Companies that are in waste collection business very often come across an issue of route planning. Such an issue belongs to the problems called TSP- Travelling Salesman Problem. These are computationally complex combinatorial tasks and, in addition, different local specifics such as one-way streets, different service capacities, and so on, shall be taken into consideration. The problem is also to convert map data into the format appropriate for these algorithms. This is why experts from two faculties at VŠB-TU Ostrava are now working on a project, the output of which will be the design of acceptable routes and their implementation into specialized maps, primarily for verifying the proposed methodology, secondary for individual partners from practice. Project co-workers work with several companies in the field of waste management (Kozel, 2014).

Another example of good practice is the IKEA Czech Republic, which has decided to introduce a system of furniture take back. The service called "Second Life" was launched in 2017 as a pilot project of one of Prague's stores. IKEA's customers have the opportunity to return furniture they do no longer want, simply taking a picture of it, uploading it to a website with a price they wish to sell it for. IKEA either agrees with the price or proposes its own, according to the degree of wear, and then negotiates with the customer the final take back. The customer then receives a voucher in the agreed amount to buy a new product in IKEA, and the company offers the furniture to other customers. The aim of this service is most of all, reducing waste (IKEA, 2017).

As a perfect example that the initiative in the field of the circular economy does not necessarily have to come from businesses, but may also come from citizens is the good practice at Palacký University in Olomouc (Univerzita Palackého v Olomouci, 2017). In 2016, an association Sustainable Palacký was founded aiming at lowering the amount of waste produced within the University grounds. Students who saw great potential in this field established the association. They, for example, placed the sorting bags of EKO-KOM Company into student's dormitories. Last year, students created the so-called Freeshop where not only students, who are leaving the dormitories, can leave the things they no longer need. And it also works the other way around – students who are moving in can come and take such things or buy them for a voluntary contribution. The Freeshop originated in response to a number of functional products that ended year after year in the garbage bin on the dormitories because students needed to get rid of them. Thanks to this initiative, things can keep serving their purpose.

In connection with the reduction of the amount of plastic waste, we can exemplify the good practice of the campaign "Dost bylo plastu” (“Done with Plastic”) realized by the Ministry of Environment of the Czech Republic. The campaign's principle is the conclusion of voluntary agreements between the Ministry of Environment and companies willing to commit themselves to reduce the consumption of plastics and disposable tableware at their premises. The idea is to create alternatives for customers that will not have environmental or wallet impacts. Among the well-known organizations involved in the project are: the Czech Railways, Bageterie Boulevard, UGO, Costa Coffee, Lidl Czech Republic, Czech University of Life Sciences, Starbucks, Benzina, Leo Express, CrossCafe, Ikea Czech Republic, Frutisimo, Relay, Hello or Mr. Baker (Ministry of Environment of the Czech Republic, 2018).

Conclusions

The adoption of the so-called Circular Economy Package at the EU level and the resulting obligations will affect all Member States, and the Czech Republic is no exception. The Circular Economy Package was adopted in 2015, but its specific form was not approved by the European Commission until 22 May 2018 and had entered into force on 4 July 2018.

The Circular Economy Package includes values for recycling and storage of municipal waste, which must be achieved by individual Member States by 2030 at the latest. The final values were approved together with the package in May 2018. Notwithstanding this, the Czech Republic reacted to the adopted Circular Economy Package already in 2015, when it adopted the new Waste Management Plan for 2015-2024. It contains several targets that the Czech Republic has to achieve in the area of waste management by 2024, i.e. six years before it will have to reach the European Union's standards.

The assessment, made by the authors, has shown that the objectives set out in the Waste Management Plan had been, in fact, already met at the time the new Waste Management Plan was issued. These include both packaging recycling and recycling, re-use and the use of waste electrical and electronic equipment. Why the goals are set, so that they are already greatly exceeded, remains a question. At the same time, however, we must not forget the balance of the economic level and the efficiency of the whole process.

The authors of this article, therefore, incline to think that there are two main problems in putting the new legislation into practice. This is mainly about the inconsistency of the methodology of data collection and a lack of a functional motivation system. Given that there is no single EU-wide guideline on how to collect data and make a variety of waste management calculations, objective results cannot be achieved. To ensure that all target groups affected by the new legislation are motivated to handle waste more efficiently, an adequate system must be put in place to penalize those, who do not comply with the legislation and, on the contrary, favour those who do comply and exceed their obligations.

Acknowledgement: *The article was supported by specific university research by the Ministry of Education, Youth and Sports of the Czech Republic No. SP2017/17 Creating system for analysing internal and external environment of industrial enterprises and No. SP2018/22 Risk Management Study of Industrial Enterprises in the Czech Republic.*

References

Baránková, L. and Baránek, P. (2013). Cost-Benefit Analysis of the Current Municipal Waste Management in the Cities od Ostrava and Brno. In *Proceedings of Knowledge for Market Use 2013*, pp. 8-21.

Bartl, A. (2015). Withdrawal of the circular economy package: A wasted opportunity or a new challenge? *Waste Management*, 44 (2015) pp. 1–2.

Bilan, Y. (2013). Sustainable Development of a Company: Building of New Level Relationship with the Consumers of XXI Century. *Amfiteatru Economic*, 15 (7), pp. 687–701.

The Czech Waste Management Association (ČAOH). (2017). *iDnes: Urban Mining - těžba cenných surovin přímo v městech.* [online] Available at: <http://www.caoh.cz/odborne-clanky-a-aktuality/idnes-urban-mining-tezba-cennych-surovin-primo-v-mestech.html> [Accessed 15 December 2018].

Drábková, J. a Jonášová, S. (2017). *Oběhové hospodářství vyžaduje spolupráci, ne boj různých lobby*. [online] Available at: <http://www.businessinfo.cz/cs/clanky/sona-jonasova-obehove-hospodarstvi-vyzaduje-spolupraci-ne-boj-ruznych-lobby-90301.html> [Accessed 15 December 2018].

EKO-KOM. *O společnosti.* [online] Available at: <http://www.ekokom.cz/cz/ostatni/o-spolecnosti/system-eko-kom/o-systemu> [Accessed 14 December 2018].

EKO-KOM. (2016). *Výsledky třídění a recyklace v systému EKO KOM za rok 2015.* [online] Available at: <www.ekokom.cz/uploads/news/id524/TZ_vysledky_trideni_2015.docx> [Accessed 14 December 2018].

EKO-KOM. (2017). *Výsledky třídění a recyklace v systému EKO-KOM za rok 2016*. [online] Available at: <http://www.ekokom.cz/cz/ostatni/o-spolecnosti/media/tiskove-zpravy> [Accessed 15 December 2018].

EKO-KOM. (2018). *Výsledky systému EKO-KOM za rok 2017.* [online] Available: <http://www.ekokom.cz/uploads/news/id655/TZ_V%C3%BDsledky_2017_p%C5%99%C3%ADloha_1.pdf> [Accessed 22 June 2018].

European Commission. (2015). *Otázky a odpovědi k balíčku o oběhovém hospodářství.* [online] Available at: <http://europa.eu/rapid/press-release_MEMO-15-6204_cs.htm> [Accessed 14 December 2018].

European Commision. (2018). *Circular Economy: New rules will make EU the global front-runner in waste management and recycling*. [online] Available at: <http://europa.eu/rapid/press-release_IP-18-3846_en.htm> [Accessed 22 June 2018].

Eurostat. (2017). *Database.* [online] Available at: <http://ec.europa.eu/eurostat/data/database> [Accessed 14 December 2017].

Horodníková, J., Khouri, S., Rybár, R. and Kudelas, D. (2008). TESES rules as a tool of analysis for chosen OZE projects. *Acta Montanistica Slovaca*, 13 (3), pp. 350-356.

Chlopecký, J., Pawliczek, A., Vilamová, Š., Moravec, L., Hubáček, J. and Ameir, O. (2018). Strategic risk management of an enterprise depending on external conditions. In *International Multidisciplinary Scientific GeoConference Surveying Geology and Mining Ecology Management, SGEM*, 18 (1.3), pp. 855-861.

IKEA. (2017). *IKEA dává nábytku druhý život.* [online] Available at: <http://www.ikea.com/cz/cs/about_ikea/newsitem/druhy_zivot_nabytku> [Accessed 15 December 2018].

Institut cirkulární ekonomiky. *O nás.* [online] Available at: <https://incien.org/o-nas/> [Accessed 14 December 2018].

Khouri, S., Pavolová, H., Cehlár, M. and Bakalár, T. (2016) Metallurgical brownfields re-use in the conditions of Slovakia - A case study. *Metalurgija*, 55 (3), pp. 500-502.

Kozel, P., Michalcová, Š. and Friedrich, V. (2014). The using of linear programming for solving the municipal waste collection problem. In *Proceedings of 32nd International Conference on Mathematical Methods in Economics (MME 2014)*, pp. 483-488.

Kozel, R., Podlasová, A., Šikýř, P. and Smelik, R. (2018). Innovations in Waste Management. In *IDIMT 2018: Strategic Modeling in Management, Economy and Society - 26th Interdisciplinary Information Management Talks*, pp. 119-126.

Kozel, R., Vilamová, Š., Király, A., Hawrysz, L. and Hys, K. (2015). Legal aspects of environmental issues in the Czech Republic. In *International Multidisciplinary Scientific GeoConference Surveying Geology and Mining Ecology Management, SGEM*, 2 (5), pp. 703-709.

Ministry of Industry and Trade of the Czech Republic. (2015). *Politika druhotných surovin České republiky schválená vládou ČR dne 15. 9. 2014.* [online] Available at: <https://www.mpo.cz/dokument153352.html> [Accessed 15 December 2018].

Ministry of Industry and Trade of the Czech Republic. (2017). *Celostátní soutěž Ministerstva průmyslu a obchodu Přeměna odpadů na zdroje.* [online] Available at: <https://www.mpo.cz/cz/prumysl/politika-druhotnych-surovin-cr/celostatni-soutez-ministerstva-prumyslu-a-obchodu-premena-odpadu-na-zdroje--221269/> [Accessed 15 December 2018].

Ministry of Industry and Trade of the Czech Republic. (2018). *Evropská komise zveřejnila Strategii pro plasty a další dokumenty k oběhovému hospodářství.* [online] Available at: <https://www.mpo.cz/cz/prumysl/politika-druhotnych-surovin-cr/evropska-komise-zverejnila-strategii-pro-plasty--234763/> [Accessed 19 February 2019].

Ministry of Environment of the Czech Republic. (2014). *Plán odpadového hospodářství 2015–2024.* [online] Available at: <https://www.mzp.cz/cz/plan_odpadoveho_hospodarstvi_cr> [Accessed 14 December 2018].

Ministry of Environment of the Czech Republic. (2018). *Kampaň Dost bylo plastu*. [online] Available at: <https://www.mzp.cz/cz/kampan_dost_bylo_plastu> [Accessed 19 February 2019].

Moravec, L., Danel, R. and Chlopecký, J. (2017). Application of the Cyber Security Act in Havířovská teplárenská společnost, a.s. In *SMSIS 2017 - Proceedings of the 12th International Conference on Strategic Management and its Support by Information Systems 2017*, pp. 425-433.

Nařízení vlády ze dne 22. prosince 2014 o Plánu odpadového hospodářství České republiky pro období 2015-2024. In Sbírka zákonů České republiky. 2014, částka 141, s. 4650**.**

Stanel, W. R. (2017). Analysis of the structure and values of the European Commission's Circular Economy Package. In *Proceedings of the Institution of Civil Engineers - Waste and Resource Management*, 170(1), pp. 41-44.

Straka, M., Rosová, A., Malindžáková, M., Khouri, S. and Čulková, K. (2018). Evaluating the waste incineration process for sustainable development through modelling, logistics, and simulation. *Polish Journal of Environmental Studies*, 27 (6), pp. 2739-2748.

Šimková, Z., Cehlár, M. and Pavolová, H. (2016). Strategy of point out relevance of responsible exploitation of mineral resources. *Acta Montanistica Slovaca*, 21 (3), pp. 208-216.

Třetí ruka. (2018). *Plasty*: *Komise navrhuje pravidla pro deset druhů jednorázových plastových výrobků.* [online] Available at: <https://www.tretiruka.cz/news/plasty-komise-navrhuje-pravidla-pro-deset-druhu-jednorazovych-plastovych-vyrobku/> [Accessed 19 February 2019].

Palacký University in Olomouc. (2017). *Na Univerzitě Palackého vznikl v tuzemsku ojedinělý studentský Freeshop*. [online] Available at: <https://www.upol.cz/nc/zpravy/zprava/clanek/na-univerzite-palackeho-vznikl-v-tuzemsku-ojedinely-studentsky-freeshop/> [Accessed 15 December 2018].

Vosecký, V. (2017). *Institut Cirkulární Ekonomiky: Cirkulární ekonomika a co se děje v Bruselu.* [online] Available at: <http://ekolist.cz/cz/zpravodajstvi/tiskove-zpravy/cirkularni-ekonomika-a-co-se-deje-v-bruselu> [Accessed 14 December 2018].

Wysokińska, Z. (2016). The "New" Environmental Policy Of The European Union: A Path To Development Of A Circular Economy And Mitigation Of The Negative Effects Of Climate Change. *Comparative Economic Research*, 19 (2), pp. 57–73.

Zákon ze dne 15. května 2001 o odpadech a o změně některých dalších zákonů. In Sbírka zákonů České republiky. 2001, částka 71, s. 4074.

Zákon ze dne 4. prosince 2001 o obalech a o změně některých zákonů (zákon o obalech). In Sbírka zákonů České republiky. 2001, částka 172, s. 9948.

Zapletal, F., Ministr, J. and Rehacek, P. (2017). Management of emissions permits: Threats of the European emissions trading system. *Scientific Papers of the University of Pardubice, Series D: Faculty of Economics and Administration*, 24 (41), pp. 217- 229.

Exploration of Disparities in Environmental Activities of European Countries from Year 2006 to Year 2016

***Beata Gavurova*[1], *Viliam Kovac*[2], *Peter Drabik*[3] *and* *Marian Gomory*[1]**

The main aim of the study is to investigate and to evaluate the disparities in the environmental activities of the European countries in the time period from the year 2006 to the year 2016. The data from the Eurostat database is applied. Regarding the character of the data and the target orientation of the study, the cluster analysis is selected in order to reveal the desired relations. The analysis outcome point to several interesting facts. The distribution of the countries among the clusters is very uneven. The participants behave considerably differently. For instance, Austria belongs to the largest clusters in all but one explored fields, although its output is not very similar to the remaining countries. This reveals inefficiency that should be a subject of further research. The obtained findings enable to carry out a structural analysis of the environmental activities under investigation and to define causal relationships and research trajectories that would reflect the extent of economic and legislative measures in place in each country, the demographic structure impacts on environmental activities, and economic subsystems in the country, causes of environmental disparities within countries, etc. The results of the study are particularly relevant for national and international environmental policymakers, as well as for the concept of regional development plans and the development of monitoring and evaluation mechanisms.

Keywords: *environmental activity, environmental indicator, environmental protection, cluster analysis, dendrogram, Euclidean distance.*

Introduction

The environmental indicators are usually applied to assess efficiency and effectiveness of the environmental activities in the individual countries. They support the processes of planning, setting strategic goals as well as developing measures and instruments in the regional development concepts of the countries. The environmental indicators are part of the monitoring and decision-making mechanisms and systems. Their important role also lies in signalling economic, social and environmental threats. Many international organisations focus on developing indicator groups to assess the environmental aspects and to implement them into practice as, for instance, the Organisation for Economic Co-operation and the United Nations. The first published indicator group is the Organisation for Economic Co-operation Core Set of Indicators for Environmental Performance in the year 1993 (Organisation for Economic Co-operation, 1993). It was later innovated in the year 2001 (Organisation for Economic Co-operation, 2001) and in the year 2003 (Organisation for Economic Co-operation, 2003). Gradually, the groups of the indicators were developed for transport, energy, agriculture, and household consumption. Another group of the indicators of this institution are the indicators derived from the environmental accounting consists of the three parts, which pollution abatement and control expenditure, natural resource accounts, and environmental accounting belong among. By introducing these indicators, it is possible to monitor and to evaluate developments in these environmental areas and to compare the achievements in the individual Organisation for Economic Co-operation member countries over the previous two decades. The further development of the environmental indicators is accompanied by the adoption of the new strategies. For instance, the so-called green growth strategy from the year 2009 is adopted to support the economic growth and development of the countries while providing ecosystem services (Organisation for Economic Co-operation, 2011). It underlines the need for investment and innovation support as well as for competition that has a positive impact on sustainable growth and the creation of new labour positions usually. Green growth provides both a policy strategy for economic transition and a monitoring framework with a proposed set of indicators. It connects the economic and environmental context (Guštafíková et al., 2014). All the activities in the field of environmental protection by the year 2020 emphasise the importance of the transition to a greener and more cyclical economy. The development of the new groups of the indicators is often complicated, and this construction of the composite indicators impede international comparison, which may also reveal the reasons for the national disparities in some environmental areas. Therefore, it is important to continuously develop national and international registers that would contain retrospective as well as up-to-date data declaring the current state in the environmental policies of the countries and the effectiveness of the intervention measures. This also allows causal relationships between changes in the environmental characteristics of the individual geographical areas and their impact on the economic and social spheres. This is also an incentive to carry out the introduced research, which is based on the data from Eurostat, in order to analyse and to evaluate the disparities in the environmental activities of the European countries in the time period from the year 2006 to the year 2016.

[1] *Beata Gavurova, Marian Gomory*, Technical University of Košice, Faculty of Mining, Ecology, Process Control and Geotechnologies, Slovak Republic, *beata.gavurova@tuke.sk, marian.gomory@tuke.sk*
[2] *Viliam Kovac*, Technical University of Košice, Faculty of Economics, Slovak Republic, *viliam.kovac@tuke.sk*
[3] *Peter Drabik*, University of Economics in Bratislava. Faculty of Commerce, Slovak Republic, *peter.drabik@euba.sk*

The structure of the study is as follows – the literature review of the research studies is focused on the exploration of the use the environmental indicators – whether separately, or in groups – in order to assess the individual areas of the environment and the implications in the several types of the policies. This allows defining the research framework. In order to process the values of the indicators aimed at assessing the environmental activities of the individual countries, the cluster analysis is applied to demonstrate the disparities between the countries in the examined areas. The analysis outcome creates a platform for formulating the discussion framework and the research conclusions. Also, the ideas for the potential subsequent research in this area are specified.

Literature Review

Many national and international types of research focus on monitoring and assessing the environmental activities in particular countries with specific causal links to the socio-economic and demographic spheres of interest. The environmental activities are carried out in the legislative frameworks, which also create a platform for setting up regulatory and stabilisation mechanisms in the area of environmental, economic and social policies.

The available research studies dealing with the explored issue are largely heterogeneous in their content, which is determined by the aim of the presented researches, the aspects examined as well as the methodological backgrounds. Most of them have a strongly implied nature with links to many types of policies and thus, encouraging not only research teams to carry out the following research, but they also create the supporting mechanisms for a more in-depth examination of the various environmental determinants.

Wang et al. (2020) focus in their study on the performance of municipal solid waste management in Nottingham by analysing the material flows as well as the appropriately selected indicators based on the concept of the waste hierarchy and the objectives set out in the waste management regulations. The authors analyse improvements in waste reduction, material recycling, energy recovery and landfill prevention. The results of the study declare the fulfilment of the high ambitious goals set by the local government, while the authors call for the creation of the new improvement programmes. These can be achieved by setting up an education system as well as through promotion of public waste separation. The environmental activities are often linked to the competitiveness of a particular country as well as business performance (Rajnoha et al., 2017). Agovino et al. (2020) examine the relationship between the recycling rates achieved and the competitiveness of the enterprises operating in the circular economy sectors. The results of the study clearly declare the positive impact between packaging recycling, electronic and biological waste recycling rates and the competitiveness of the companies involved. The authors examined this research trajectory across the 17 European countries through the data from the period from the year 2010 to the year 2016. The results show the clear differences between the countries too. Some authors evaluate environmental aspects not only separately, but also in the form of the composite indicators, monitoring related indicators respectively. Kikas et al. (2018) explore the possibility of using an expert system for mapping high nature value agricultural land in Estonia. The authors selected the 20 suitable indicators from the four thematic groups. Their methodology is also applicable in the other countries, and the map created should benefit agricultural policymakers to identify zones of high biodiversity where the suitable environmental schemes can be used. The study has a strong implication output for a policymaking process. Also, in the study by Biasi et al. (2019), the analytical trajectories are aimed at supporting the environmental policies. The authors point out the objectives of the national governments to promote the responsible management of natural capital. Therefore, in their study, they propose an extended version of the genuine saving macroeconomic indicator to account for water and soil depletion (Hamilton, 2000). As natural capital is spatially heterogeneous, the selected indicator is estimated for Italy for the period from the year 2000 to the year 2015 at the regional level. Although the study is conducted in Italy, the methodological framework is generally applicable to other countries as well. The methodological contribution suggests that genuine saving can support policymakers in developing the targeted policies for sustainable growth. Also, Tasser et al. (2019) deal with regional development and biodiversity protection. Agricultural, environmental, and climate measures create a central tool of the European Union to support its biodiversity conservation policy. In their study, the authors show a system for assessing agricultural land through a set of indicators related to the various aspects of biodiversity. They apply the evaluation system to the selected 44 farms in Austria, France, Germany, Italy, and Switzerland. The proposed system can serve as a tool to detect differences in biodiversity resulting from land-use practices. The results have an impact on the setting up of educational activities and agricultural advisory services.

Ribeiro et al. (2015) deal with the issue of the removal of organic micropollutants in the environment. In this study, the analytical methods are presented for the trace quantification of the 37 micropollutants including the priority substances meaning the substances of the recent watch list and the contaminants of emerging concern, which pesticides, multiclass pharmaceuticals, metabolites, estrogens and other industrial compounds belong among. The validated method is applied to wastewater treatment plant samples that assess the concentration of micropollutants after secondary biological and tertiary ultraviolet treatment. The results of the

study also create a platform for potential following research and networking of international research teams in sharing experience in the application of the selected analytical methods to achieve the best performance in the removal of most of the determined micropollutants. McMahon et al. (2019) address in their study the recycling processes and their relevance in the framework of the emerging waste and recycling management legislation. The nature of many raw materials for the production of electrical and electronic equipment is critical and classified as hazardous waste. The authors use the results of interviews with the stakeholders of the involved enterprises on the reuse of waste electrical and electronic equipment in the year 2006 in Austria, Belgium, France, and the United Kingdom, where these systems are used and considered very successful. Even in Ireland, this system has evolved, but it has not yet been implemented. Spain as the first country in the European Union to have deemed preparation for reuse targets separate to those ones which are aimed at recycling in a necessary way. The authors define the elementary factors of the successful preparation for reuse in general involving social enterprise. Hermoso et al. (2020) explore alternative regional planning scenarios at the European Union level in the area of green infrastructure. The European Union Strategy on Green Infrastructure aims at developing a strategically planned network of natural areas to support the maintenance of ecosystem services and thus, to connect protected areas by promoting in this way through multifunctional landscapes. The authors test the two alternative spatial planning scenarios for the design of the network that would ensure support for the maintenance of the ecosystem services and the integration of protected areas. The results highlight the benefits of international cooperation in regional planning and the need to develop appropriate policy instruments to support ecosystem services as well as their integration into sectoral policies and funding systems. In addition to the studies dealing with separate environmental aspects or process areas directly linked to the environmental characteristics of the countries, some authors examine the efficiency of the countries in the terms of environmental efficiency (Zofio and Prieto, 2001; Zhou et al., 2007; Zhou et al., 2016; Gavurova et al., 2017). Halkos and Petrou (2019) examine the environmental efficiency of the 28 European Union member countries for the years 2008, 2010, 2012, and 2014 through the data envelopment analysis and the directional distance function to tackle the undesirable outputs. The eight parameters are applied – namely municipal solid waste generation, employment rate, capital formation, gross domestic product, population density and for the first time sulphur oxide, nitrogen oxide, and greenhouse gases emissions from the waste sector for the relevant countries. The results demonstrate that the most efficient countries are Germany, Ireland, and the United Kingdom. This outcome is reviewed against the recycling rate of each country for the examined time periods. The recycling rate actually depicts the data envelopment analysis results. Especially, more efficient countries seem to have a higher recycling rate too. Moreover, its efficiency results are contrasted to the overall treatment options used in the countries under consideration. Overall, it is noticed that countries employing all four treatment options with high use of more sustainable treatment and decrease in the use of landfill are the ones that also prove to be efficient according to the data envelopment analysis. As the authors point out, these results demonstrate a reflection of the financial crisis that forces countries to look for ways to move to a circular economy and to set production processes to minimise waste generation. The study has valuable outputs for policymakers, both nationally and internationally. It offers a platform to modify the European Union legislation and the directives in order to achieve a strategic direction for the European countries to the circular economy. The importance of investigating the effects of the environmental factors is not only related to economic and socio-economic areas. The population health directly affects the economic system of the country not only through the productivity indicators but also through the social indicators. The sustainability of the health and the social systems in the demographic ageing processes of the countries is also addressed. For this reason, in the last decade, many research teams have quantified the impact of the environmental factors on the population health and thus, to seek to economically assess the ecological burden of the particular country, including the impact on the health indicators and their causal links.

Alguquerque et al. (2017) examine the impact of industrial and agricultural activities on soil quality in their study. The authors report that potentially toxic elements pose a threat to public health and the environment. According to them, the strict definition of the critical areas requiring restore is crucial. Kupiec et al. (2019) investigate soil contamination with trace elements and fluoride in the selected location in Poland, where economic activity has historically been associated with the use of trace metals. The results of the study point to the fact that land in the places of extinct metalworking enterprises can still be an important source of trace metals. The research done has also shown an increased concentration of fluoride in the surface layers of soil. Mataloni et al. (2016) examine the health impacts associated with staying near landfills. They evaluate the possible effects of the concentration of hydrogen sulphide from landfills on the health of the population in the central part of Italy. There are the 9 landfill sites available; the analysed group is located within 5 km of the landfills. Šedová (2016) link the determinants of illegal landfilling to the economic and socio-economic indicators. She investigated illegal landfills at the regional level in Slovakia. The results of the study show that a higher level of the expected waste production results in a higher rate of illegal landfills and also their higher volume. Higher-income has a positive impact on the illegal landfill rate, whilst poverty affects them negatively. Higher levels of education do not lead to more responsible waste management. The results of this study clearly

correlate with the results of Martuzzi et al. (2009), whose aim is to assess the possible adverse health effects of uncontrolled landfills in Italy. The authors point out the negative health impacts of the environmental exposures related to waste in the region of Campania, paying attention to the 9 causes of death and the 12 types of the congenital anomalies. The increased risks of cancer deaths for both sexes are identified. The congenital anomalies of the urogenital system and central nervous system are reported too. Festin et al. (2019) confront the impacts of mining on landscape changes related to the discharge of large quantities of waste, which have an impact on environmental pollution and harm to human health. Their study confirms the fact that over the last two decades, there has been an increase in interest in research into the recovery of the land after mining, which several techniques have been examined in. The authors point out the significant regional disparities in the knowledge base and in the implementation of the procedures aimed at the recovery of the mining sites. Insufficient attention focused on the elimination of these disparities may have significant negative economic and noneconomic impacts in the future – for instance, related to health, population migration, etc.

Data and Methodology

The applied methodological approaches are selected in order to obtain the desired aim set to carry out the analysis.

Data. The data comes from Eurostat – the statistical office of the European Union. The data set Production of environmental protection services of general government by economic characteristics marked env_ac_pepsgg serves as the source data set for the analysis (Eurostat, 2020). It describes a situation in the 31 countries throughout the period beginning in the year 2006 and ending in the year 2016 from a yearly perspective. The start of the observed period is determined by the accessibility of the data. This year is available almost for all the then European Union member countries. The remaining participate countries possess a shorter time period. Also, because of this fact, in order to achieve the same conditions for all the participants, the mean value of the explored dimensions is applied in the further analytical process. The observed data set to cover the data for all the environmental activities and for all the sections of the environmental activities too.

These six sections involve subsequent fields:

- protection of air, climate, soil, water and against noise, vibration, and radiation;
- wastewater management;
- waste management;
- protection of biodiversity and landscapes;
- environmental research and development;
- other environmental protection activities.

For all the mentioned sections, the following dimensions are observed:

- output;
- market output;
- nonmarket output;
- gross fixed capital formation and acquisitions;
- compensation of employees.

All the numbers are expressed in a money form denominated in the euro currency.

The explored countries are marked by the abbreviations according to the International Organization for Standardization 3166 standard Codes for the representation of names of countries and their subdivisions – the two-letter alpha-2 codes are applied particularly: AT – the Republic of Austria, BE – the Kingdom of Belgium, BG – the Republic of Bulgaria, CH – the Swiss Confederation, CZ – the Czech Republic, DE – the Federal Republic of Germany, DK – the Kingdom of Denmark, EE – the Republic of Estonia, ES – the Kingdom of Spain, FI – the Republic of Finland, FR – the French Republic, GB – the United Kingdom of Great Britain and Northern Ireland, GR – the Hellenic Republic, HR – the Republic of Croatia, HU – Hungary, IE – the Republic of Ireland, IT – the Italian Republic, LT – the Republic of Lithuania, LU – the Grand Duchy of Luxembourg, LV – the Republic of Latvia, MT – the Republic of Malta, NL – the Kingdom of the Netherlands, NO – the Kingdom of Norway, PL – the Republic of Poland, PT – the Portuguese Republic, RO – Romania, RS – the Republic of Serbia, SE – the Kingdom of Sweden, SI – the Republic of Slovenia, SK – the Slovak Republic, and TR – the Republic of Turkey (International Organization for Standardization).

Methodology. The main technique applied in the analysis is cluster analysis. The hierarchical clustering approach is applied (Hartigan, 1975; Hartigan, 1983). Its outcome is visualised in the form of the matrix of the mutual distances of the individual pairs of the explored countries that expresses their similarities and in the form of the dendrogram that illustrates the similarity of the produced clusters. The similarity is quantified by the Euclidean distance method.

The number of clusters is determined by the tau index (Rohlf, 1974; Milligan, 1981). The same number is applied in all the clustering process in the analysis. It is based upon the whole data set.

The elementary formula of the tau index is as follows:

$$\tau = \frac{CC - DC}{\sqrt{\frac{D(D-1)}{2(2-C)}}} \tag{1}$$

where the involved variables mean:

- τ – a tau value;
- CC – a number of the concordant comparisons;
- DC – a number of the disconcordant comparisons;
- D – the total distances;
- C – a number of the comparisons when two pairs of the points representing comparison within the cluster or between the clusters.

Analysis

The whole analysis is divided into seven sections. The first section is the fundamental section based on an analysis of the whole data set, covering all the environmental protection activities. Then, all the environmental protection activities are next. Successively, the six sections involving the particular fields mentioned in the Data and Methodology section follow.

Overall View. Firstly, an overall view of the scrutinised topic is offered. This serves as a reference outcome for the subsequent analysis.

The following table demonstrates the similarities between the analysed countries based on all the sections of the environmental protection activities.

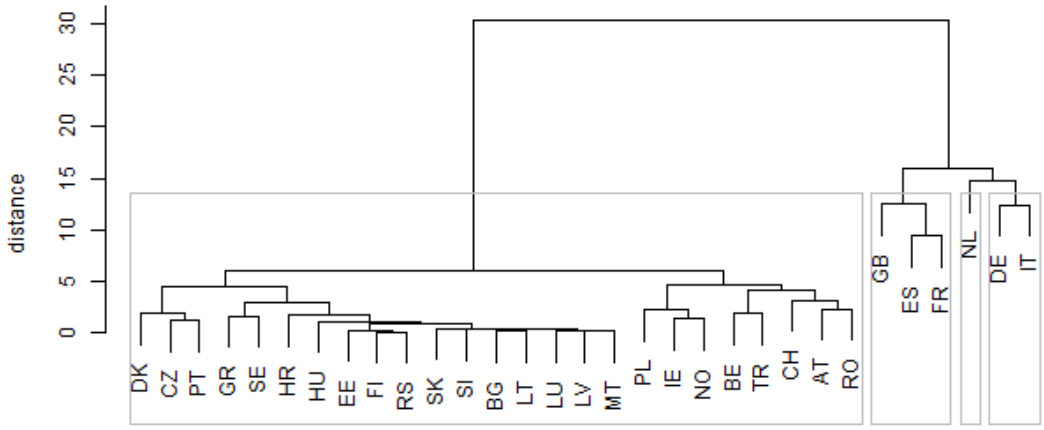

Fig. 1: The Dendrogram of All the Individual Sections
Source: own elaboration by the authors.

As it is seen from the figure, the division of the countries is uneven. The largest cluster involves the 25 countries – as they are illustrated by the dendrogram Denmark, Czechia, Portugal, Greece, Sweden, Croatia, Hungary, Estonia, Finland, Serbia, Slovakia, Slovenia, Bulgaria, Lithuania, Luxembourg, Latvia, Malta, Poland, Ireland, Norway, Belgium, Turkey, Switzerland, Austria, and Romania. The second cluster consists of the three countries where the United Kingdom of Great Britain and Northern Ireland, Spain, and France belong. The third cluster is created by only a sole country – the Netherlands. The fourth cluster involves the two countries – Germany and Italy. The whole division of the countries is considerably unproportional. This is caused by very high disparities between the well-developed countries and the remaining ones. Also, there is visible a very sharp patter in the first cluster. At a level of distance of approximately over five Euclidean units, this cluster could be divided into to two groups unconditionally. But, as the disparities among the observed countries are high, this inequality is not so high in order to distinguish the separate clusters. The same note can be applied to the further classification of the countries within these imaginary groups.

Tab. 1: The similarity Matrix of the Explored Countries

Country	AT	BE	BG	CH	CZ	DE	DK	EE	ES	FI	FR	GB	GR	HR	HU	IE	IT	LT	LU	LV	MT	NL	NO	PL	PT	RO	RS	SE	SI	SK	TR
AT	0	2.74	2.25	2.44	2.98	2.84	14.50	2.25	6.99	2.67	15.09	11.51	2.66	2.13	2.30	2.58	14.02	2.22	2.21	2.16	2.24	13.39	3.08	3.18	3.51	2.36	2.68	2.40	2.02	2.13	3.19
BE	2.74	0	4.08	2.91	3.62	3.47	13.14	3.29	5.83	4.34	14.05	10.07	3.64	2.85	3.92	4.17	12.48	4.13	4.10	4.07	4.16	12.05	3.56	3.38	4.13	3.67	2.98	3.00	4.05	3.04	1.95
BG	2.25	4.08	0	3.79	1.52	2.71	15.56	0.46	7.82	0.73	15.66	12.32	1.75	1.36	0.64	2.32	13.86	0.22	0.35	0.31	0.27	14.30	2.60	2.81	2.80	2.26	0.42	1.87	0.35	0.34	2.77
CH	2.44	2.91	3.79	0	3.44	3.64	14.67	3.95	5.65	3.96	10.06	10.99	3.32	3.85	3.55	3.68	15.59	3.84	3.93	3.90	3.93	11.73	3.48	3.57	3.42	3.51	4.26	2.53	3.72	3.65	3.40
CZ	2.98	3.62	1.52	3.44	0	1.76	15.96	1.86	6.85	1.72	11.91	12.76	2.14	2.39	1.17	2.83	14.72	1.60	1.62	1.69	1.67	13.46	2.60	2.65	1.22	2.93	1.80	1.99	1.54	1.60	2.33
DE	2.84	3.47	2.71	3.64	1.76	0	14.45	2.54	6.81	2.02	14.68	11.86	3.22	2.64	2.60	3.34	12.64	2.69	2.62	2.66	2.71	13.09	3.32	3.06	1.81	3.36	1.75	2.34	2.54	2.55	2.43
DK	14.50	13.14	15.56	14.67	15.96	14.45	0	15.57	12.43	16.65	12.32	14.73	15.29	14.83	15.25	14.65	12.46	15.55	15.56	15.59	15.64	13.24	14.04	13.58	15.08	15.04	16.28	15.73	15.53	15.35	15.68
EE	2.25	3.29	0.46	3.95	1.86	2.54	15.57	0	7.55	0.14	15.50	11.59	1.61	1.40	1.01	1.89	14.78	0.41	0.34	0.40	0.35	14.73	2.63	3.13	2.87	2.58	0.30	2.05	0.48	0.53	2.88
ES	6.99	5.83	7.82	5.65	6.85	6.81	12.43	7.55	0	7.87	9.47	9.99	7.06	7.31	7.55	7.47	10.40	7.99	7.78	7.88	7.90	11.77	6.60	6.91	6.88	7.92	7.11	6.04	7.87	7.16	5.32
FI	2.67	4.34	0.73	3.96	1.72	2.02	16.65	0.14	7.87	0	12.88	13.32	2.27	1.61	1.17	2.66	15.42	0.64	0.68	0.66	0.69	14.08	3.02	2.95	1.24	2.72	0.11	2.03	0.70	0.47	2.87
FR	15.09	14.05	15.66	10.06	11.91	14.68	12.32	15.50	9.47	12.88	0	13.41	15.24	15.32	15.28	15.17	15.31	15.65	15.80	15.77	15.83	15.62	14.58	13.76	15.07	15.62	15.14	10.90	15.65	15.25	11.08
GB	11.51	10.07	12.32	10.99	12.76	11.86	14.73	11.59	9.99	13.32	13.41	0	10.96	11.25	12.14	12.25	14.43	12.57	12.43	12.43	12.45	15.56	11.59	11.58	11.95	12.34	10.23	11.48	12.41	11.23	10.95
GR	2.66	3.64	1.75	3.32	2.14	3.22	15.29	1.61	7.06	2.27	15.24	10.96	0	2.03	1.64	2.84	13.64	1.89	1.90	1.90	1.89	14.04	2.68	3.08	3.10	2.77	1.77	1.63	1.89	1.31	2.57
HR	2.13	2.85	1.36	3.85	2.39	2.64	14.83	1.40	7.31	1.61	15.32	11.25	2.03	0	1.42	2.09	14.61	1.33	1.32	1.31	1.37	14.94	2.75	2.82	3.29	2.65	1.23	2.12	1.39	1.30	2.39
HU	2.30	3.92	0.64	3.55	1.17	2.60	15.25	1.01	7.55	1.17	15.28	12.14	1.64	1.42	0	2.32	13.55	0.75	0.84	0.86	0.84	14.10	2.42	2.52	2.79	2.24	1.20	1.69	0.73	0.79	2.65
IE	2.58	4.17	2.32	3.68	2.83	3.34	14.65	1.89	7.47	2.66	15.17	12.25	2.84	2.09	2.32	0	13.63	1.56	2.35	2.32	2.34	13.23	1.45	2.40	3.47	3.12	1.30	2.48	2.33	1.73	3.10
IT	14.02	12.48	13.86	15.59	14.72	12.64	12.46	14.78	10.40	15.42	15.31	14.43	13.64	14.61	13.55	13.63	0	14.05	13.78	13.86	13.89	15.06	13.21	12.80	13.24	13.73	16.21	15.85	13.83	14.48	15.23
LT	2.22	4.13	0.22	3.84	1.60	2.69	15.55	0.41	7.99	0.64	15.65	12.57	1.89	1.33	0.75	1.56	14.05	0	0.31	0.22	0.24	13.98	2.35	2.80	2.82	2.33	0.33	1.94	0.34	0.35	2.80
LU	2.21	4.10	0.35	3.93	1.62	2.62	15.56	0.34	7.78	0.68	15.80	12.43	1.90	1.32	0.84	2.35	13.78	0.31	0	0.24	0.20	14.32	2.70	2.91	2.76	2.30	0.22	1.99	0.40	0.43	2.84
LV	2.16	4.07	0.31	3.90	1.69	2.66	15.59	0.40	7.88	0.66	15.77	12.43	1.90	1.31	0.86	2.32	13.86	0.22	0.24	0	0.18	14.29	2.70	2.88	2.79	2.30	0.25	2.00	0.35	0.40	2.85
MT	2.24	4.16	0.27	3.93	1.67	2.71	15.64	0.35	7.90	0.69	15.83	12.45	1.89	1.37	0.84	2.34	13.89	0.24	0.20	0.18	0	14.36	2.72	2.94	2.81	2.31	0.19	2.01	0.37	0.43	2.88
NL	13.39	12.05	14.30	11.73	13.46	13.09	13.24	14.73	11.77	14.08	15.62	15.56	14.04	14.94	14.10	13.23	15.06	13.98	14.32	14.29	14.36	0	12.82	12.85	13.10	13.45	15.54	13.83	14.14	14.64	13.89
NO	3.08	3.56	2.60	3.48	2.60	3.32	14.04	2.63	6.60	3.02	14.58	11.59	2.68	2.75	2.42	1.45	13.21	2.35	2.70	2.70	2.72	12.82	0	1.79	3.55	3.20	2.10	2.85	2.64	2.43	2.97
PL	3.18	3.38	2.81	3.57	2.65	3.06	13.58	3.13	6.91	2.95	13.76	11.58	3.08	2.82	2.52	2.40	12.80	2.80	2.91	2.88	2.94	12.85	1.79	0	3.61	3.23	2.86	3.00	2.81	2.88	3.12
PT	3.51	4.13	2.80	3.42	1.22	1.81	15.08	2.87	6.88	1.24	15.07	11.95	3.10	3.29	2.79	3.47	13.24	2.82	2.76	2.79	2.81	13.10	3.55	3.61	0	3.55	1.31	1.53	2.71	2.90	2.47
RO	2.36	3.67	2.26	3.51	2.93	3.36	15.04	2.58	7.92	2.72	15.62	12.34	2.77	2.65	2.24	3.12	13.73	2.33	2.30	2.30	2.31	13.45	3.20	3.23	3.55	0	3.16	3.24	2.23	2.47	3.72
RS	2.68	2.98	0.42	4.26	1.80	1.75	16.28	0.30	7.11	0.11	15.14	10.23	1.77	1.23	1.20	1.30	16.21	0.33	0.22	0.25	0.19	15.54	2.10	2.86	1.31	3.16	0	2.25	0.49	0.49	2.39
SE	2.40	3.00	1.87	2.53	1.99	2.34	15.73	2.05	6.04	2.03	10.90	11.48	1.63	2.12	1.69	2.48	15.85	1.94	1.99	2.00	2.01	13.83	2.85	3.00	1.53	3.24	2.25	0	1.98	1.69	2.22
SI	2.02	4.05	0.35	3.72	1.54	2.54	15.53	0.48	7.87	0.70	15.65	12.41	1.89	1.39	0.73	2.33	13.83	0.34	0.40	0.35	0.37	14.14	2.64	2.81	2.71	2.23	0.49	1.98	0	0.51	2.90
SK	2.13	3.04	0.34	3.65	1.60	2.55	15.35	0.53	7.16	0.47	15.25	11.23	1.31	1.30	0.79	1.73	14.48	0.35	0.43	0.40	0.43	14.64	2.43	2.88	2.90	2.47	0.49	1.69	0.51	0	2.51
TR	3.19	1.95	2.77	3.40	2.33	2.43	15.68	2.88	5.32	2.87	11.08	10.95	2.57	2.39	2.65	3.10	15.23	2.80	2.84	2.85	2.88	13.89	2.97	3.12	2.47	3.72	2.39	2.22	2.90	2.51	0

Source: own elaboration by the authors.

The following figure demonstrates a division of the countries according to all environmental protection activities that are covered by the explored data set.

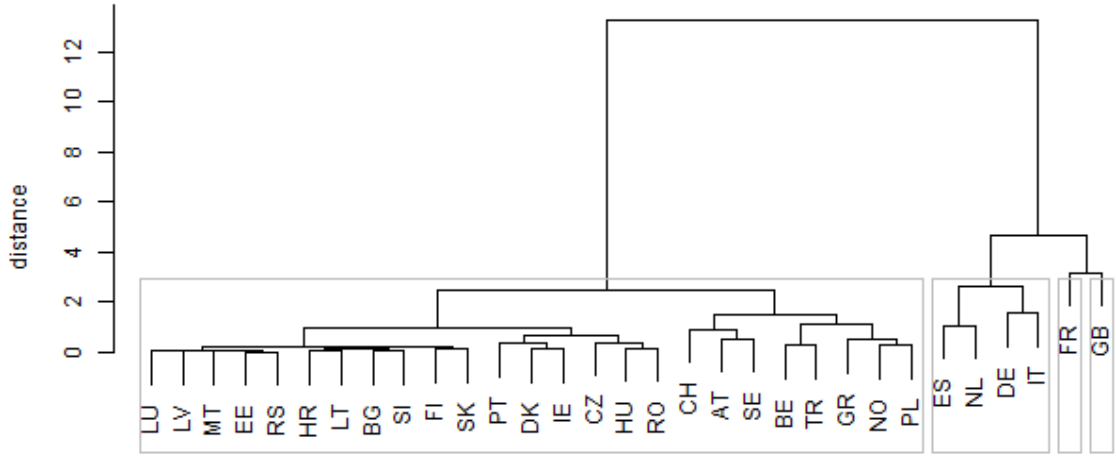

Fig. 2: The Dendrogram of All the Environmental Protection Activities
Source: own elaboration by the authors.

Comparing the dendrogram of all environmental protection activities to the first one devoted to all the individual sections of the environmental protection activities, the differences are seen. A basement of the distribution of the participated countries has a similar pattern – the same more developed countries are kept together. The first cluster is the substantial, and it involves the 25 countries – Luxembourg, Latvia, Malta, Estonia, Serbia, Croatia, Lithuania, Bulgaria, Slovenia, Finland, Slovakia, Portugal, Denmark, Ireland, Czechia, Hungary, Romania, Switzerland, Austria, Sweden, Belgium, Turkey, Greece, Norway, and Poland. The second cluster is created by the four countries which Spain, the Netherlands, Germany, and Italy belong among. The last two clusters involve the sole countries – France and the United Kingdom of Great Britain and Northern Ireland separately.

Protection of Air, Climate, Soil, Water and Against Noise, Vibration, and Radiation. The first partial clustering process is applied in a field of protection of air, climate, soil, water and against noise, vibration, and radiation.

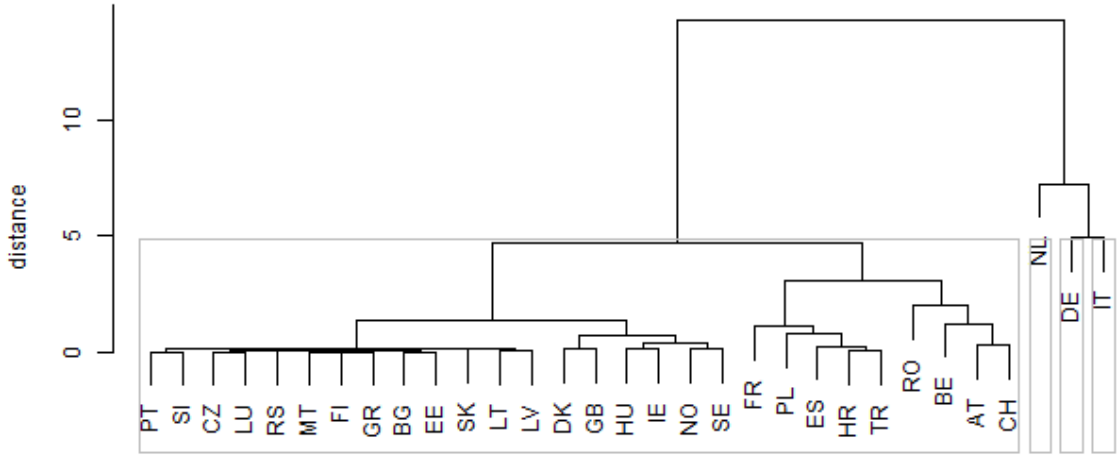

Fig. 3: The Dendrogram of Protection of Air, Climate, Soil, Water and Against Noise, Vibration, and Radiation
Source: own elaboration by the authors.

The uneven division is also confirmed in a field of protection of air, climate, soil, water and against noise, vibration, and radiation. The first cluster represents a substantial part of the whole data set, because it covers the 28 countries – Portugal, Slovenia, Czechia, Luxembourg, Serbia, Malta, Finland, Greece, Bulgaria, Estonia, Slovakia, Lithuania, Latvia, Denmark, the United Kingdom of Great Britain and Northern Ireland, Hungary, Ireland, Norway, Sweden, France, Poland, Spain, Croatia, Turkey, Romania, Belgium, Austria, and Switzerland. The two-part and also the four-part distinction of this cluster is clearly visible. The second, the third, and the fourth cluster are created only by the sole countries – successively, the Netherlands, Germany, and Italy.

Wastewater Management. The second partial clustering process is devoted to a field of wastewater management, and it is pictured on the succeeding dendrogram.

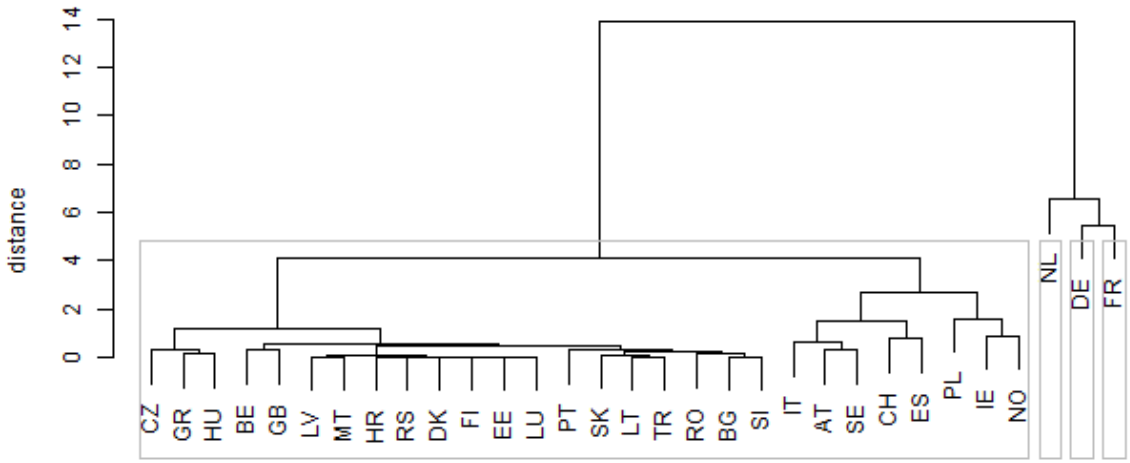

Fig. 4: The Dendrogram of Wastewater Management
Source: own elaboration by the authors.

Again, the very strong disproportion is seen in a clustering outcome distribution. The first cluster involves all the countries except for the three countries that create the separate clusters. The substantial cluster consists of the 28 countries which Czechia, Greece, Hungary, Belgium, the United Kingdom of Great Britain and Northern Ireland, Latvia, Malta, Croatia, Serbia, Denmark, Finland, Estonia, Luxembourg, Portugal, Slovakia, Lithuania, Turkey, Romania, Bulgaria, Slovenia, Italy, Austria, Sweden, Switzerland, Estonia, Poland, Ireland, and Norway belong among. The Netherlands, Germany, and France represent the three individual clusters.

Waste Management. The third partial clustering process covers a field of waste management which is illustrated by the following dendrogram.

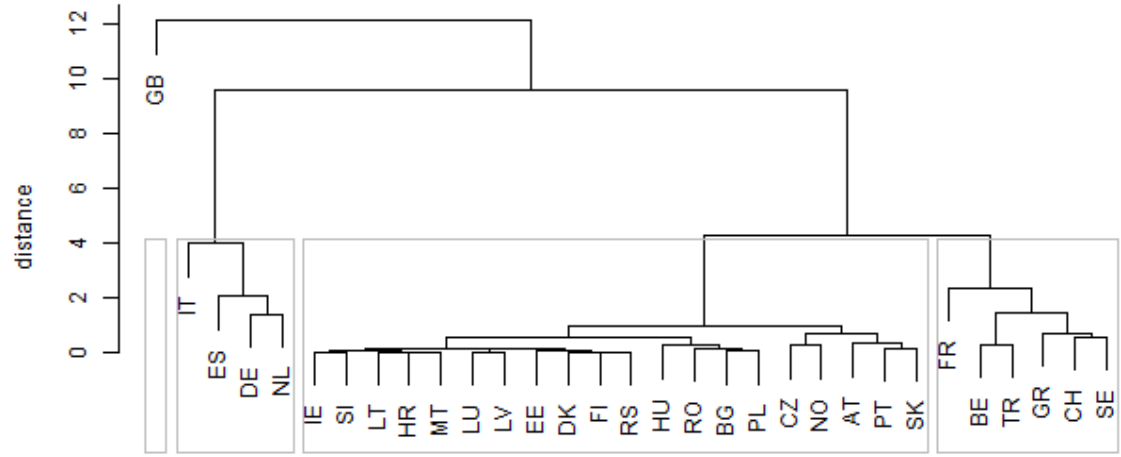

Fig. 5: The Dendrogram of Waste Management
Source: own elaboration by the authors.

Although the distribution of the countries is not so solid, the first cluster involves only a sole country – the United Kingdom of Great Britain and Northern Ireland. The second cluster covers the countries that are usually in the clusters characterised by a very low number of the participants. These are Italy, Spain, Germany, and the Netherlands. The third cluster presents the fundamental group which involves Ireland, Slovenia, Lithuania, Croatia, Malta, Luxembourg, Latvia, Estonia, Denmark, Finland, Serbia, Hungary, Romania, Bulgaria, Poland, Czechia, Norway, Austria, Portugal, and Slovakia. The fourth cluster covers the territories of France, Belgium, Turkey, Greece, Switzerland, and Sweden.

Protection of Biodiversity and Landscapes. The fourth partial dendrogram visualises a situation in a field of protection of biodiversity and landscapes.

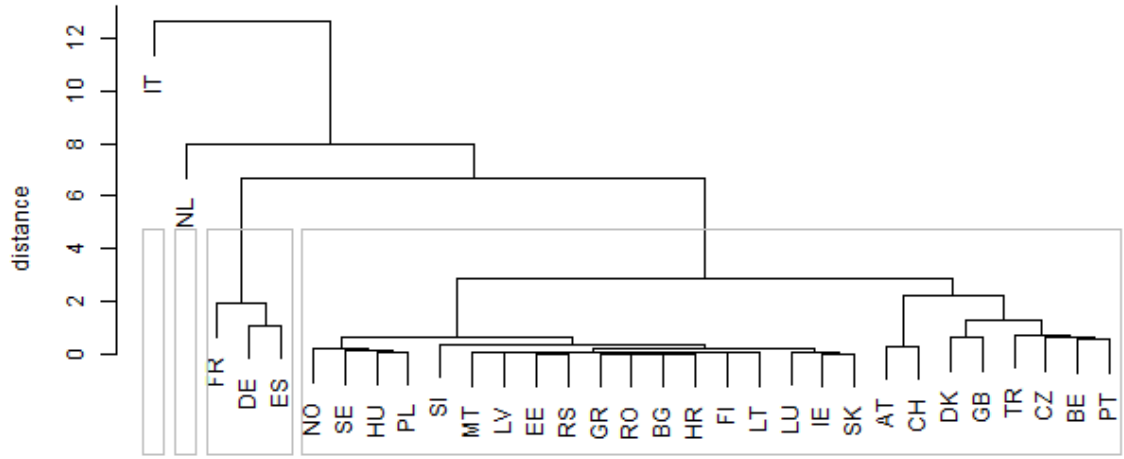

Figô 6: The Dendrogram of Biodiversity and Landscapes
Source: own elaboration by the authors.

The key pattern of this clustering distribution is very similar to the first and the second partial dendrograms. Italy and the Netherlands represent the individual clusters, whilst the latter one repeats its role from the previous case. The third cluster consists of the three countries – France, Germany, and Spain. All the remaining countries, where Norway, Sweden, Hungary, Poland, Slovenia, Malta, Latvia, Estonia, Serbia, Greece, Romania, Bulgaria, Croatia, Finland, Lithuania, Luxembourg, Ireland, Slovakia, Austria, Switzerland, Denmark, the United Kingdom of Great Britain and Northern Ireland, Turkey, Czechia, Belgium, and Portugal belong, create the fourth cluster. Also, it is visible a potential separation within this cluster here.

Environmental Research and Development. The fifth fractional dendrogram envisages a situation in a field of environmental research and development.

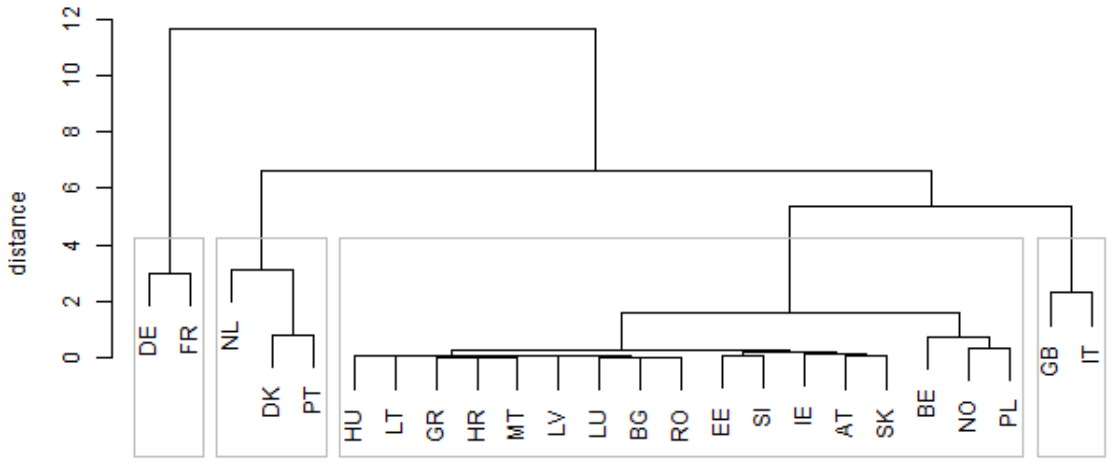

Fig. 7: The Dendrogram of Environmental Research and Development
Source: own elaboration by the authors.

Though there is no cluster with a sole country, the two of them involve only the two countries. The first cluster is created by Germany and France. The second cluster includes the Netherlands, Denmark, and Portugal. The third cluster is the largest one covering the 17 countries – Hungary, Lithuania, Greece, Croatia, Malta, Latvia, Luxembourg, Bulgaria, Romania, Estonia, Slovenia, Ireland, Austria, Slovakia, Belgium, Norway, and Poland. The fourth cluster covers the United Kingdom of Great Britain and Northern Ireland and Italy. There is to note that the seven countries, which Switzerland, Czechia, Spain, Finland, Serbia, Sweden, and Turkey belong among, are avoided in this clustering process because of the lack of the data in a field of the environmental research and development.

Other Environmental Protection Activities. The sixth partial clustering process illustrates the distribution of countries according to the data on the other environmental protection activities.

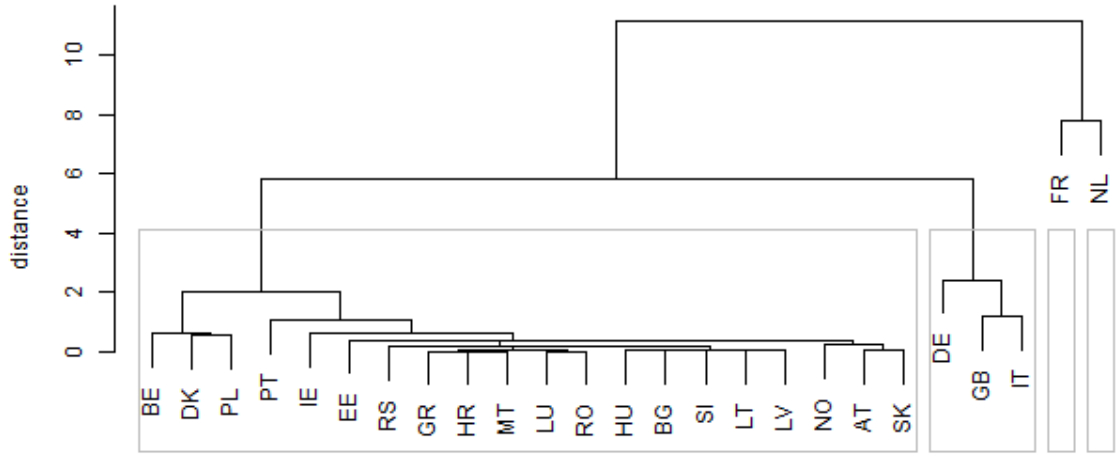

Fig. 8: The Dendrogram of Other Environmental Protection Activities
Source: own elaboration by the authors.

The other environmental protection activities data is represented by a very similar pattern as it is in the previous sections. The elementary pattern is clearly visible – a very large cluster and besides it the clusters with a very low number of the countries. The main cluster covers the territories of Belgium, Denmark, Poland, Portugal, Ireland, Estonia, Serbia, Greece, Croatia, Malta, Luxembourg, Romania, Hungary, Bulgaria, Slovenia, Lithuania, Latvia, Norway, Austria, Slovakia. The second cluster involves Germany, the United Kingdom of Great Britain and Northern Ireland, and Italy. The last two countries – France and the Netherlands – create their own individual clusters. As in the previous case, there is to note that the six countries, which Switzerland, Czechia, Spain, Finland, Sweden, and Turkey belong among, are removed from the clustering process because of the lack of the data in a field of the other environmental protection activities.

Differences Between the Explored Fields. The elementary differences between the individual dendrograms can be illustrated by the distances between the created clusters. The following table demonstrates the main intermediate distance between the pairs of the clusters in the second column successively, in the third column, the distance between the first cluster and the second cluster; and in the fourth column the distance between the third cluster and the fourth cluster.

Tab. 2: The Similarities of the Countries Within the Analysed Fields

Field	Intermediate distance	The first cluster to the second cluster distance	The third cluster to the fourth cluster distance
all the individual sections	30.2830	5.9855	16.0444
all the environmental protection activities	13.2181	2.4957	4.6271
protection of air, climate, soil, water and against noise, vibration, and radiation	14.2579	not applicable	4.9263
wastewater management	13.8662	not applicable	5.4581
waste management	12.0861	not applicable	3.9884
protection of biodiversity and landscapes	12.6225	not applicable	6.6814
environmental research and development	11.6445	not applicable	5.3683
other environmental protection activities	11.1278	5.8091	7.7733

Source: own elaboration by the authors.

There is to note that all the numbers are rounded to four decimal places mathematically. For all the cases of all the individual sections, all the environmental protection activities, and the other environmental protection activities, the involved countries are divided into the two hierarchical steps into the four clusters directly. The remaining cases are represented by the successive distribution into the particular clusters. Hence, the column of the first cluster to the second cluster distance is not available in these cases. It could be measured through the other distance, but this is not a substantial point in order to make a conclusion from this analytical approach.

As it is seen in the previous table, there are the very high numbers of the intermediates distances between the clusters. It is the most visible in a case of all the individual sections, where the Euclidean distance between the splits of the clusters reach a level of 30.2830. For all the other cases, this position is kept the numbers over a two-digit level from 11.1278 up to 14.2579. Besides these differences, there are visible the quite considerable dissimilarities also between the separate clusters. In a case of all the individual sections, there is the highest distance between the two particular neighbouring clusters at a level of 16.0444. This is a more dissimilar situation than all of the intermediate relations for all the other explored fields.

Differences Between the Clusters Participants. The large disparities within the whole data set are also demonstrated by the following table that shows the numbers of the countries participating in the cluster where the particular country lies.

Tab. 3: The Numbers of the Co-participants Within the Particular Clusters

Country	Individual fields	All fields	Field 1	Field 2	Field 3	Field 4	Field 5	Field 6	Average value of fields
AT	25	25	28	28	20	26	17	20	23.17
BE	25	25	28	28	6	26	17	20	20.83
BG	25	25	28	28	20	26	17	20	23.17
CH	25	25	28	28	6	26	17	20	20.83
CZ	25	25	28	28	20	26	17	20	23.17
DE	2	4	1	1	4	3	2	3	2.33
DK	25	25	28	28	20	26	3	20	20.83
EE	25	25	28	28	20	26	17	20	23.17
ES	3	4	28	28	4	3	17	20	16.67
FI	25	25	28	28	20	26	17	20	23.17
FR	3	1	28	1	6	3	2	1	6.83
GB	3	1	28	28	1	26	2	3	14.67
GR	25	25	28	28	6	26	17	20	20.83
HR	25	25	28	28	20	26	17	20	23.17
HU	25	25	28	28	20	26	17	20	23.17
IE	25	25	28	28	20	26	17	20	23.17
IT	2	4	1	28	4	1	2	3	6.5
LT	25	25	28	28	20	26	17	20	23.17
LU	25	25	28	28	20	26	17	20	23.17
LV	25	25	28	28	20	26	17	20	23.17
MT	25	25	28	28	20	26	17	20	23.17
NL	1	4	1	1	4	1	3	1	1.83
NO	25	25	28	28	20	26	17	20	23.17
PL	25	25	28	28	20	26	17	20	23.17
PT	25	25	28	28	20	26	3	20	20.83
RO	25	25	28	28	20	26	17	20	23.17
RS	25	25	28	28	20	26	17	20	23.17
SE	25	25	28	28	6	26	17	20	20.83
SI	25	25	28	28	20	26	17	20	23.17
SK	25	25	28	28	20	26	17	20	23.17
TR	25	25	28	28	6	26	17	20	20.83

Source: own elaboration by the authors.

The average value is rounded to the two decimal places mathematically. The fields are numbered according to their order stated in the methodology section. The numbers of the coparticipants in the particular clusters clearly demonstrate which countries can be classified as almost the sole ones in the individual clusters. The absolutely lowest average value of coparticipants is reached by the Netherlands at a level of 1.83, whilst this country reaches the individual cluster as its sole participant for four times. The second position with an average value of 2.33 is occupied by Germany. It creates its own individual cluster for two times. The third place with a little offset is kept by Italy at a level of 6.5. Again, its own individual cluster is created for two times. Just right behind it, France follows on the fourth position with an average value of 6.83 and completing two own individual clusters. After these four countries, there is a considerable offset followed by the United Kingdom of Great Britain and Northern Ireland with an average value of 14.67. It is the country with the highest average value of the coparticipants in the clusters that creates its own individual cluster, although only for once. The sixth place is held by Spain with an average value of 16.67. All the remaining countries keep their average values over a twenty-coparticipant threshold.

Discussion

The analysis demonstrates the considerable differences between the explored participating countries. This is the fact that should be investigated further. The aim of this paper is to point out there are the significant inconsistencies among the European Union member countries, the European Free Trade Association and the other countries that act as the potential European Union member candidates. It is a crucial point which has to be revealed in order to implement the regulations which would lead to more efficient spending of the financial resources in a field of the environmental protection services generally. Here, it is observed from an angle of view of the governments of the explored countries and therefore, it is perceived from the population of these countries more sensitively.

Policy plays an important role in environmental issues. Whether it is related to air, climate, soil, water, or waste, it is the key element in the process of protection environment for future life. Besides all the partial fields,

environmental research and the development activities in this research perform very considerably too, along with the other environmental protection activities.

Mitigation and adaptation are the two mainstreamed policy fields that are required to be integrated into the existing sectoral policies. A key aim of jointly institutionalising mitigation and adaptation should be ready to reduce conflicts, ambiguity and inconsistencies how to handle the current issues in combination with the other policy contents. In a case of the climate change adaptation, administration related to it is considerably difficult. The climatic issues should be included in daily practice by the consistent actions with the existing sectoral policies. As the analysis carried out for this paper demonstrates, climate with the other air and similars issues possesses an existence of the individually positioned clusters itself, which the Netherlands, Germany, and Italy among. Processes and means aimed at a reduction of the coherence problems between the sectoral policies and the climate policies have to be introduced (Göpfert et al., 2019).

Nowadays, there is an urgent need for integrated modelling studies. Here, a potential platform is offered to be created in order to develop a further investigation of the new issues not only in a field of water and soil together. The general circulation model is one of the possible solutions of such hydrologic question. Unambiguously, the representation of land usage change caused by the climate alteration throughout the certain period is interpreted in a more comprehensive way than in the past, since the indirect impact of land usage caused by this climate alteration is more substantial in comparison with the direct impacts (Li and Fang, 2016). A large variety of inputs can perform in the mentioned succession (Purakayastha et al., 2019). Similarly, it is very demanding on an opinion of each involved government.

A country perspective is an important part of the whole gear train. In a field of the soil issues multiplicatively. There are still the countries that have no regulations for soil protection – Austria and Sweden mainly, whilst Ireland and Slovenia only partially, and France merely indirectly. On the other hand, Germany, Italy, the Netherlands, Portugal, Romania, Slovakia, and a little bit unexpectedly Luxembourg regarding its area and geographical conditions apply plenty of the legal acts in this field. Bulgaria, Croatia, Czechia, Denmark, Estonia, Finland, Greece, Hungary, Latvia, Lithuania, Malta, Poland, Spain, and the United Kingdom of Great Britain and Northern Ireland have the regulation that stands at a national level (Ronchi et al., 2019). Their positions in the cluster analysis are influenced by this naturally.

These findings constitute a strong platform for potential subsequent research in this area. They contribute to the larger system individually (Schönhart et al., 2018). The research ambition is to conduct a structural analysis of the investigated environmental activities and hence, to define causal relationships and research trajectories that reflect the extent of the economic and legislative measures in the individual countries, the impact of the demographic structure on the environmental activities, the impact of the environmental burdens on economic and social causes of the environmental disparities within these countries, etc.

Conclusion

Ensuring a sustainable environment as well as protecting natural resources represent the key environmental policy objectives that require actions at all the levels of management. Environmental protection is directly linked to the competitiveness of the individual country. The environmental policy supports labour position creation, investment promotion and innovation development. Environmental indicators are applied to measure the efficiency and effectiveness of the environmental activities, which are now part of many decision-making mechanisms. Their important role is also informative. Many international institutions assess countries from the perspective of environmental activities and also assess the impacts of industry, transport and construction. An impact evaluation of legislative, economic and incentive instruments is also important, which encourages the linking of economic, social and environmental policies. The evaluation systems require the accessibility of the international databases containing the indicators quantifying the several environmental activities of the European countries. They create a space for the multivariate comparative analyses. This is also the motive to carry out our research, which is aimed at analysing and evaluating the disparities in the environmental activities of the selected countries in the time period from the year 2006 to the year 2016. The cluster analysis is applied in order to process the available data. The six areas are examined – namely protection of air, climate, soil, water and against noise, vibration, and radiation, wastewater management, waste management, protection of biodiversity and landscapes, environmental research and development, and other environmental protection activities. The outcome shows the significant disparities in the environmental areas of the individual countries. As it is seen from the distribution of the countries among the clusters, there are the sole countries, which behave considerably dominantly often. Also, among the most numerous clusters, the countries with the larger outputs appear beside the other similar countries. This reveals partial inefficiency that should be a subject of the further research – for instance, France and the United Kingdom in protection of air, climate, soil, water and against noise, vibration, and radiation, Austria and the United Kingdom in wastewater management, Austria in waste management, Austria and the United Kingdom in biodiversity and landscapes, Austria and Belgium in environmental research and development, and these two countries also in the other environmental activities too. The results of the

analyses represent a valuable platform for national policymakers as well as for developing national and international benchmarking indicators in this area.

Acknowledgements: *This work is supported by the Scientific Grant Agency of the Ministry of Education, Science, Research, and Sport of the Slovak Republic and the Slovak Academy Sciences as part of the research project VEGA 1/0797/20 Quantification of Environmental Burden Impacts of the Slovak Regions on Health, Social and Economic System of the Slovak Republic.*

References

Agovino, M., Matricano, D., and Garofalo, A. (2020). Waste management and competitiveness of firms in Europe: A stochastic frontier approach. Waste Management, 102: 528–540. ISSN: 0956-053X. DOI: 10.1016/j.wasman.2019.11.021. Available online: https://www.sciencedirect.com/science/article/pii/S0956053X19307172.

Albuquerque, M. T. D., Gerassis, S., Sierra, C., Taboada, J., Martín, J. E., Antunes, I. M. H. R., and Gallego, J. R. (2017). Developing a new Bayesian Risk Index for risk evaluation of soil contamination. Science of the Total Environment, 603: 167-177. ISSN: 0048-9697. DOI: 10.1016/j.scitotenv.2017.06.068. Available online: https://www.sciencedirect.com/science/article/pii/S0048969717314729.

Biasi, P., Ferrini, S., Borghesi, S., Rocchi, B., and Di Matteo, M. (2019). Enriching the Italian Genuine Saving with water and soil depletion: National trends and regional differences. Ecological Indicators, 107: 105573. DOI: 10.1016/j.ecolind.2019.105573. Available online: https://www.sciencedirect.com/science/article/abs/pii/S1470160X19305655.

Eurostat (2020). Production of environmental protection services of general government by economic characteristics. Available online: http://appsso.eurostat.ec.europa.eu/nui/show.do?dataset=env_ac_pepsgg.

Festin, E. S., Tigabu, M., Chileshe, M. N., Syampungani, S., and Odén, P. C. (2019). Progresses in restoration of post-mining landscape in Africa. Journal of Forestry Research, 30 (2): 381–396. ISSN: 1993-0607. DOI: 10.1007/s11676-018-0621-x. Available online: https://link.springer.com/article/10.1007/s11676-018-0621-x.

Gavurová, B., Behúnova, A., Tkáčová, A., Peržeľová, I. (2017). The mining industry and its position in the economic cycle of the EU countries. Acta Montanistica Slovaca, 22 (3): 278–286. ISSN: 1335-1788. Available online: https://actamont.tuke.sk/pdf/2017/n3/6gavurova.pdf.

Göpfert, C., Wamsler, C., and Lang, W. (2019). Institutionalizing climate change mitigation and adaptation through city advisory committees: Lessons learned and policy futures. City and Environment Interactions: 1: 100004. DOI: 10.1016/j.cacint.2019.100004. Available online: https://www.sciencedirect.com/science/article/pii/S2590252019300042.

Guštafíková, T., Adamkovičová, A., Baranovičová, Z., Baďurová, D., Hericová, D., Kapusta, P., Koreňová, Ľ., Kročková, B., Lieskovská, Z., Škantárová, K., Štibrányiová, T., Štroffeková, S., and Vall, J. (2014). Vybrané indikátory zeleného rastu v Slovenskej republike – Selected Green Growth Indicators in the Slovak Republic. Banská Bystrica, Slovak Republic: Slovenská agentúra životného prostredia.
Available online: https://www.oecd.org/greengrowth/Green%20Growth%20Indicators%20in%20the%20Slovak%20Republic.pdf.

Halkos, G., and Petrou, K. N. (2019). Assessing 28 EU member states' environmental efficiency in national waste generation with DEA. Journal of Cleaner Production, 208: 509–521. ISSN: 0959-6526. DOI: 10.1016/j.jclepro.2018.10.145. Available online: https://www.sciencedirect.com/science/article/pii/S0959652618331615.

Hamilton, K. (2000). Genuine Saving as a Sustainability Indicator. Environment Department Papers, 77. Washington, United States of America: The World Bank Environment Department. Available online: http://documents.worldbank.org/curated/en/908161468740713285/pdf/multi0page.pdf.

Hartigan, J. A. (1975). Clustering Algorithms. New York, United States of America: John Wiley & Sons. ISBN: 0-471-35645-X. Available online: https://people.inf.elte.hu/fekete/algoritmusok_msc/klaszterezes/John%20A.%20Hartigan-Clustering%20Algorithms-John%20Wiley%20&%20Sons%20(1975).pdf.

Hartigan, J. A. (1983). Bayes Theory. New York, United States of America: Springer-Verlag. ISBN: 978-1-4613-8242-3. DOI: 10.1007/978-1-4613-8242-3. Available online:

https://people.inf.elte.hu/fekete/algoritmusok_msc/klaszterezes/(Springer%20Series%20in%20Statistics)%20J.%20A.%20Hartigan%20(auth.)-Bayes%20Theory-Springer-Verlag%20New%20York%20(1983).pdf.

Hermoso, V., Morán-Ordóñez, A., Lanzas, M., and Brotons, L. (2020). Designing a network of green infrastructure for the EU. Landscape and Urban Planning, 195: 103732. ISSN: 0169-2046. DOI: 10.1016/j.landurbplan.2019.103732.

International Organization for Standardization. International Organization for Standardization 3166 standard – Codes for the representation of names of countries and their subdivisions. Genève, Swiss Confederation: International Organization for Standardization. Available online: https://www.iso.org/obp/ui/#search/code/.

Kikas, T., Bunce, R. G. H., Kull, A., and Sepp, K. (2018). New high nature value map of Estonian agricultural land: Application of an expert system to integrate biodiversity, landscape and land use management indicators. Ecological Indicators, 94 (2): 87–98. ISSN: 1470-160X. DOI: 10.1016/j.ecolind.2017.02.008. Available online: https://www.sciencedirect.com/science/article/abs/pii/S1470160X17300560.

Kupiec, M., Pieńkowski, P., Bosiacka, B., Gutowska, I., Kupnicka, P., Prokopowicz, A., Chlubek, D., and Baranowska-Bosiacka, I. (2019). Old and New Threats—Trace Metals and Fluoride Contamination in Soils at Defunct Smithy Sites. International Journal of Environmental Research and Public Health, 16 (5): 819. ISSN: 1660-4601. DOI: 10.3390/ijerph16050819. Available online: https://www.mdpi.com/1660-4601/16/5/819/htm.

Li, Z., and Fang H. (2016). Impacts of climate change on water erosion: A review. Earth-Science Reviews: 163, 94–117. ISSN: 0012-8252. DOI: 10.1016/j.earscirev.2016.10.004. Available online: https://www.sciencedirect.com/science/article/pii/S0012825216303555.

Martuzzi, M., Mitis, F., Bianchi, F., Minichilli, F., Comba, P., and Fazzo, L. (2009). Cancer mortality and congenital anomalies in a region of Italy with intense environmental pressure due to waste. Occupational and Environmental Medicine, 66 (11): 725–732. DOI: 10.1136/oem.2008.044115.

Mataloni, F., Badaloni, C., Golini, M. N., Bolignano, A., Bucci, S., Sozzi, R., Forastiere, F., Davoli, M., and Ancona, C. (2016). Morbidity and mortality of people who live close to municipal waste landfills: a multisite cohort study. International Journal of Epidemiology, 45 (3): 806–815.

DOI: 10.1093/ije/dyw052. Available online: https://academic.oup.com/ije/article/45/3/806/2572780.

McMahon, K., Johnson, M., and Fitzpatrick, C. (2019). Enabling preparation for re-use of waste electrical and electronic equipment in Ireland: Lessons from other EU member states. Journal of Cleaner Production, 232: 1005–1017. ISSN: 0959-6526. DOI: 10.1016/j.jclepro.2019.05.339.

Milligan, G. W. (1981). A monte carlo study of thirty internal criterion measures for cluster analysis. Psychometrika, 46 (2): 187–199. DOI: 10.1007/BF02293899.

Organisation for Economic Co-operation (1993). OECD Core Set of Indicators for Environmental Performance. Paris, French Republic: Organisation for Economic Co-operation. Available online: http://www.oecd.org/officialdocuments/publicdisplaydocumentpdf/?cote=OCDE/GD(93)179&docLanguage=En.

Organisation for Economic Co-operation (2001). OECD Environmental Indicators – Towards Sustainable Development. Paris, French Republic: Organisation for Economic Co-operation. Available online: https://www.oecd.org/site/worldforum/33703867.pdf.

Organisation for Economic Co-operation (2003). OECD Environmental Indicators – Development, Measurement and Use. Paris, French Republic: Organisation for Economic Co-operation. Available online: http://www.oecd.org/environment/indicators-modelling-outlooks/24993546.pdf.

Organisation for Economic Co-operation (2011). Towards green growth – A summary for policy makers. Paris, French Republic: Organisation for Economic Co-operation. Available online: https://www.oecd.org/greengrowth/48012345.pdf.

Purakayastha, T. J., Pathak, H., Kumari, S., Biswas, S., Chakrabarty, B., Padaria, R. N., Kamble, K., Pandey, M., Sasmal, S., and Singha A. (2019). Soil health card development for efficient soil management in Haryana, India. Soil and Tillage Research: 191, 394–305. DOI: 10.1016/j.still.2018.12.024. Available online: https://www.sciencedirect.com/science/article/pii/S0167198718311152.

Rajnoha, R., Lesníková, P., and Krajčík, V. (2017). Influence of Business Performance Measurement Systems and Corporate Sustainability Concept to Overall Business Performance: "Save the Planet and Keep Your Performance". E+M Ekonomie a Management, 20 (1): 111–128. DOI: 10.15240/tul/001/2017-1-008. Available online: https://dspace.tul.cz/bitstream/handle/15240/19859/EM_1_2017_08.pdf.

Ribeiro, A. R., Pedrosa, M., Moreira, N. F. F., Pereira, M. F. R., and Silva, A. M. T. (2015). Environmental friendly method for urban wastewater monitoring of micropollutants defined in the Directive 2013/39/EU and Decision 2015/495/EU. Journal of Chromatography A, 1418: 140–149.

DOI: 10.1016/j.chroma.2015.09.057.

Rohlf, F. J. (1974). Methods of Comparing Classifications. Annual Review of Ecology and Systematics, 5: 101–113. DOI: 10.1146/annurev.es.05.110174.000533.

Ronchi, S., Salata, S., Arcidiacono, A., Piroli, E., and Montanarella, L. (2019). Policy instruments for soil protection among the EU member states: A comparative analysis. Land Use Policy: 82, 763–780. ISSN: 0264-8377. DOI: 10.1016/j.landusepol.2019.01.017. Available online: https://www.sciencedirect.com/science/article/pii/S0264837718307622.

Schönhart, M., Trautvetter, H., Parajka, J., Blaschke, A. P., Hepp, G., Kirchner, M., Mitter, H., Schmid, E., Strenn, B., and Zessner, M. (2018). Modelled impacts of policies and climate change on land use and water quality in Austria. Land Use Policy: 76, 500–514. ISSN: 0264-8377. DOI: 10.1016/j.landusepol.2018.02.031. Available online: https://www.sciencedirect.com/science/article/pii/S0264837717311134.

Šedová, B. (2016). On causes of illegal waste dumping in Slovakia. Journal of Environmental Planning and Management, 59 (7): 1277–1303. DOI: 10.1080/09640568.2015.1072505.

Tasser, E., Rudisser, J., Plaikner, M., Wezel, A., Stockli, S., Cincent, A., Nitsch, H., Dubbert, M., Moos, V., Walde, J., and Bogner, D. (2019). A simple biodiversity assessment scheme supporting nature-friendly farm management. Ecological Indicators, 107: 105649. DOI: 10.1016/j.ecolind.2019.105649. Available online: https://orgprints.org/36372/1/1-s2.0-S1470160X19306417-main.pdf.

Wang, D., Tang, Y. T., Long, G., Higgitt, D., He, J., and Rovinson, D. (2020). Future improvements on performance of an EU landfill directive driven municipal solid waste management for a city in England. Waste Management, 102: 452–463. DOI: 10.1016/j.wasman.2019.11.009. Available online: https://www.sciencedirect.com/science/article/pii/S0956053X19307056.

Zhou, P., Poh, K. L., and Ang, B. W. (2007). A non-radial DEA approach to measuring environmental performance. European Journal of Operational Research, 178 (1): 1–9. DOI: 10.1016/j.ejor.2006.04.038. Available online: https://www.sciencedirect.com/science/article/pii/S0377221706003407.

Zhou, P., Poh, K. L., Ang, B. W. (2016). Data Envelopment Analysis for Measuring Environmental Performance. International Series in Operations Research & Management Science, 239 – Handbook of Operations Analytics Using Data Envelopment Analysis: 31–49. Boston, United States of America: Boston. DOI: 10.1007/978-1-4899-7705-2_2.

Zofio, J. L., and Prieto, A. M. (2001). Environmental efficiency and regulatory standards: the case of CO_2 emissions from OECD industries. Resource and Energy Economics, 23 (1): 63–83. DOI: 10.1016/S0928-7655(00)00030-0. Available online: https://www.sciencedirect.com/science/article/pii/S0928765500000300.

Shield Support Monitoring System – operation during the support setting

Dariusz Jasiulek[1], Sławomir Bartoszek[1], Karel Perůtka[2], Aleksandr Korshunov[3], Jerzy Jagoda[1] *and* ***Marek Płonka[4]***

The paper presents the results of testing the geometry measurement system of powered roof support using inclinometers that meet the requirements of the ATEX directive. Mechanized longwall system is most often used for coal mining. The longwall system includes basic machines, such as a longwall shearer, AFC and powered roof support that protects the roof. The powered roof support consists of the units that are hydraulically or electro-hydraulically controlled and are equipped with pressure sensors in the selected places of the hydraulic system and displacement sensors for selected actuators. One of the challenges associated with controlling and monitoring the parameters of the powered roof support is the mapping of its geometry and arrangement of individual components. KOMAG Institute of Mining Technology designed and manufactured the geometry monitoring system based on inclinometers that meet the requirements of the ATEX Directive. The system was tested on a real object in the laboratory. Impact of the structure of the powered roof support on the accuracy of geometry measurement and mapping was determined based on the test results. The results of the tests will be used during the implementation of the system in real conditions.

Keywords: *powered roof support geometry; ATEX directive; inclinometer; battery.*

Introduction

In 2017 KOMAG Institute of Mining Technology started realization of PRASS III (Productivity and safety of shield support) project (PRASS III project website). The project is co-financed from the Research Fund for Coal and Steel (RFCS) as well as from the Ministry of Science and Higher Education. The project is realized by the international consortium consisting of the companies from Poland (GIG Central Mining Institute, KOMAG Institute of Mining Technology, Jastrzębska Coal Company S.A., Becker Warkop Sp. z o.o.), from Germany (DMT GmbH & Co. KG), Great Britain (University of Exeter) and Spain (Geocontrol S.A.). Development of the measuring system dedicated to powered roof supports as well as the system for rockfall prediction is the main project objective.

The work carried out within the PRASS III project is aimed at developing the monitoring system allowing for visualization and assessment of operational parameters of powered roof supports. The most innovative functions of the Shield Support Monitoring System (SSMS) include measuring the width of the tip-to-face path and monitoring the geometry of the powered roof supports. These parameters are important for the stability of the longwall and correct interaction between the roof support and the rock mass, and in certain conditions, they may affect the possibility of damage to the roof support components.

In the Polish mining industry, mechanised shield support is rarely monitored, unlike other machines in the longwall complex. The effectiveness and safety of mining operations depend on shield support. Aspects related to the cooperation between mechanised shield support and rock mass, which affect the proper maintenance of the roof, have a significant impact on the effectiveness and safety of hard coal mining. The stability of the roof is affected, among others, by the tip to face distance, the support parameters of the shield support (initial and working support), the control system and the height of longwall (Bronya, Wiklund et al., 2011).

A lot of research work is carried out in the world, related to modelling the behaviour of a mechanized shield supports and the roof. This modelling is carried out on the basis of actual data recorded during mining or on the basis of theoretical assumptions (Bronya Wiklund et al., 2011, Langosch et al., 2003). The results of the model work unequivocally indicate that the proper operation of the powered roof support is necessary from the point of view of the effectiveness and safety of coal production. Supporting the operator and preventing potential mistakes made by the operator is possible only in the case of monitoring the basic parameters of the shield support operation and analysing their changes and trends in real-time.

Work is underway to develop algorithms for prediction of roof behaviour in a mechanized longwall complex. The paper (Herezy et al., 2018) presents an algorithm for prediction of the behaviour of shield support based on

[1] *Dariusz Jasiulek, Sławomir Bartoszek, Jerzy Jagoda,* KOMAG Institute of Mining Technology, ul. Pszczyńska 37, 44-101 Gliwice, Poland, *djasiulek@komag.eu, sbartoszek@komag.eu, jjagoda@komag.eu*

[2] *Karel Perůtka,* Tomas Bata University in Zlin, Faculty of Applied Informatics, T.G.Masaryka 5555, Zlin, Czech Republic, *KPerutka@utb.cz*

[3] *Aleksandr Korshunov*, Federal State Budgetary Institution of Science «Udmurt Federal Research Center of the Ural Branch of the Russian Academy of Sciences» Institute of Mechanics, T. Baramzinoy str., 34, Izhevsk, Udmurt Republic, Russia, *maguser_kai@mail.ru*

[4] *Marek Płonka*, GIG Central Mining Institute, Plac Gwarków 1, 40-166 Katowice, Poland, *mplonka.@gig.eu*

pressure in hydraulic cylinders and the position of a mining machine in a longwall. The prediction of the roof behaviour is most often performed on the basis of changes in the pressure in hydraulic cylinders caused by the character of the powered roof support operation and the influence of the rock mass. The results of works related to the analysis of pressure changes are presented in the paper (Wang et al., 2018) in relation to coal seams in the Shendong coalfield, located in the northwest of China. In work (Jingyi Cheng et al., 2018) present software package SSRI, to analyze monitoring data from leg pressure. The paper (Verma et al., 2016) presents the use of artificial neural networks to determine the working pressure of hydraulic cylinders in the shield support. Work in the field of co-operation between the shield support and the rock mass is the subject of many analyses (Jing Xuan Yang et al., 2017). The results of this work are used at the stage of designing shield support for specific mining and geological conditions but are not taken into account in the process of control.

The geometry measurement can also be used to obtain information about the load of the shield support. It will be an indirect measurement, but direct measurement of the load is technically difficult in real conditions, as indicated by the results of work (Witek and Prusek, 2016, Kalentev et al., 2017). The authors presented the results of the GEOSOFT project, in which complex tests of the shield support unit in various support conditions were performed.

The inclinometers should be installed primarily in newly designed support units. In the design process (Yang et al., 2018, Swedish et al., 2016, Siegfried, 2013) it is possible to introduce full geometry information and to install inclinometers to ensure their safe use.

Justification for monitoring the geometry of shield support

Operation of the roof support with the correct geometry, understood as the parallelism of the canopy and the base, is important for the interaction of the roof support with the rock mass. This fact is particularly important in the case of weak rocks in the roof or in the case of mining the longwall under the rockfall zone. In such conditions it is important to operate the powered roof supports properly, so as not to create a linear contact between the canopy and the roof, which may cause damage to the structure of roof rocks. Roof fall risk in longwall coal faces is presented in work (Prusek et al., 2016).

Operation of the roof support with incorrect geometry also affects the distribution of base pressure on the floor. This problem was illustrated by the method used in the Department of Extraction Technologies and Mining Support at GIG and with software for the analysis of geometry and distribution of forces in roof support nodes (Płonka, 2009). For example, lifting the canopy of powered roof support results in changing the distribution of pressures on the floor (Płonka and Rajwa, 2018). In the case of raising the canopy, the highest pressure on the floor occurs closer to the coal face, which may lead to the roof support tendency of sinking into the floor and in extreme cases leading to loss of stability.

The analysis of the forces at the powered roof support structure nodes should be taken into account when considering the impact of the roof support design on its failure (Fig. 1). This problem is described in the publication (Płonka and Rajwa, 2018) where, based on the case study, it is described how the lifting of the canopy end affected the increase in strength at the point of connection between the canopy and the caving shield. It was determined that the forces in the roof support construction nodes might differ significantly from the model usually used in the Operational Manual for the horizontal position of the canopy and base. It was found that the changes in forces in the joint node of the canopy with the caving shield depend mainly on the specific form of kinematics and then on the inclination between the canopy and base and on the load to the caving shield of the roof support.

In the mathematical models, it was confirmed that for the specified lifting angles of the canopy by 8° and 12° (inclinations found in a particular longwall), the forces at the connection between the canopy and the caving shield are significantly higher than the forces calculated in the case of operation with the horizontal canopy (Płonka and Rajwa, 2018, Rajwa et al., 2017).

Work on inclinometers is carried out by DOH Centrum Hydrauliki company, among others. The inclinometers have their own battery power supply and are adapted to work on the shield support (Szurgacz and Brodny, 2019). The paper (Prusek et al., 2016) presents measurements of shield support geometry; however, they were performed in laboratory conditions.

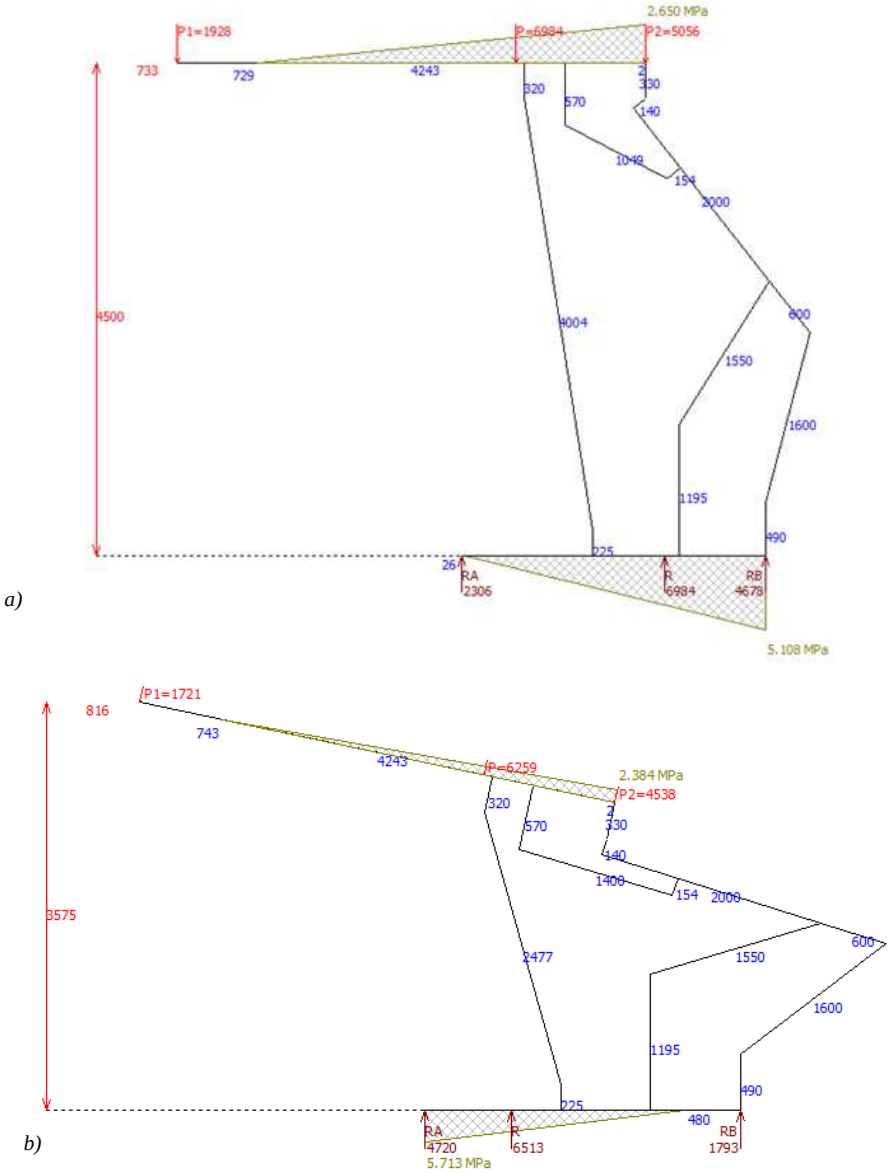

Fig. 1. Distribution of pressure on the roof and floor depending on the shield support geometry: a) canopy parallel to the floor; b) canopy raised at an angle of 12°. (Płonka and Rajwa, 2018)

System design

The models and prototypes of system components were developed within the PRASS III project, and then they were certified in accordance with the ATEX Directive and tested in real conditions. The shield support monitoring system consists of the following three modules (Fig. 1):

- SSMS-C - central unit for communication with individual modules, power supply, archiving and data transmission.
- SSMS-I - two-axis inclinometer.
- SSMS-S – "tip to face" sensor, a module that detects the distance between the mechanized housing section and the longwall face.

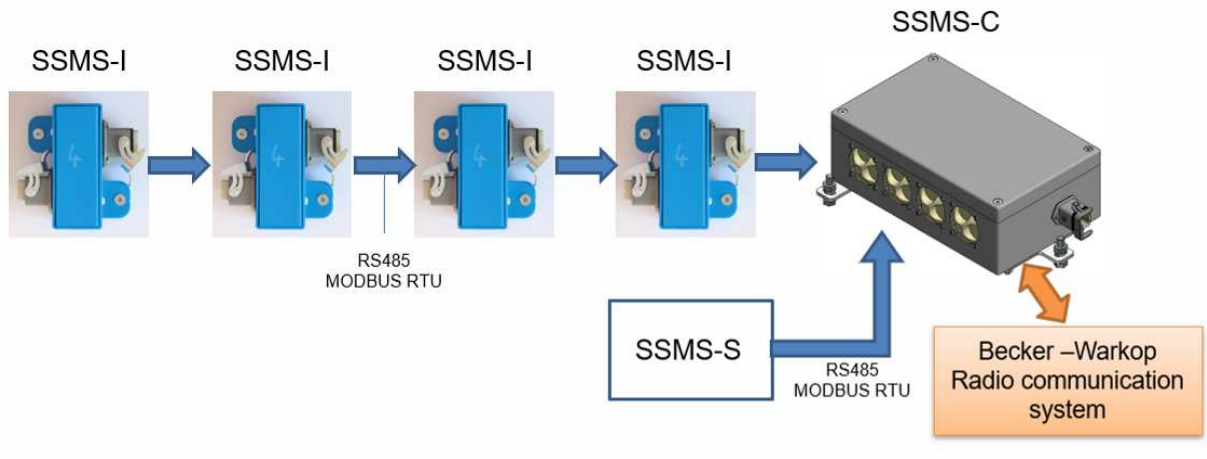

Fig. 2. SSMS system design.

Each module of the SSMS is placed on the powered roof support components (Fig. 3). In order to be able to place each SSMS-I inclinometer module in appropriate places in the powered roof support (to ensure correct reading of measurement data), the dimensions of the device enclosure were minimized. In order to reduce the size of the SSMS-I module, each inclinometer system did not have its own power source; it was power supplied from the SSMS-C central unit (which was located on the canopy of roof support, this place allows to install this device).

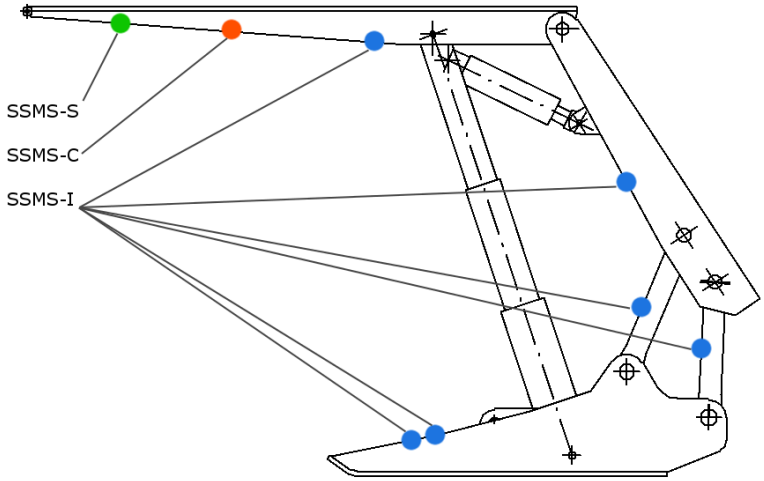

Fig. 3. Arrangement of SSMS components on the powered roof support

To simplify the communication system and ensure adequate radio visibility, the module responsible for communication of all system components for single powered roof support was placed in the SSMS-C central unit. On the slope, there is also an SSMS-S track measurement module, which has an independent battery circuit and data from the module are sent by cable to the SSMS-C central unit. Communication between SSMS-C units will be based on distributed algorithms (Stankiewicz, 2018; Baranov et al., 2017).

SSMS-C module

The SSMS-C central unit module (Fig. 4) is used for power supply, communication, archiving and data transmission. It is equipped with 4 primary cells of a capacity 70mAh enabling the system to operate for at least one year. The unit is adapted to be mounted on powered roof support and connected with SSMS-I inclinometer modules and SSMS-S path sensor. Data are transmitted using the MODBUS-RTU protocol. Data collected from each module are initially processed, archived in non-volatile memory and sent by radio to the superior unit.

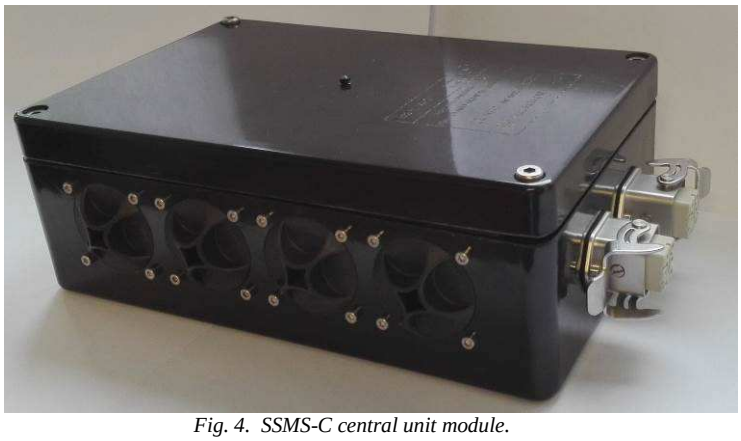

Fig. 4. SSMS-C central unit module.

During the designing process of the unit, it was necessary to provide IP65 protection level of the unit enclosure against dust and water ingress. The device is designed to operate on the powered roof support of a longwall system in conditions of an underground hard coal mine. Working conditions in longwall faces are characterized by a high level of airborne dust. To reduce dust concentration, water spraying systems are used, which means that the equipment working in this place should have a high level of protection against water penetration.

In order to ensure IP protection level of 65, the ROSE company selected an enclosure with the manufacturer's declaration of IP65 protection level. Selected battery compartments also had the IP 67 protection level provided by the manufacturer. Selected Harting connector for data transmission and power supply of individual modules of the system had IP 67 protection level. All screwed fittings were equipped with the appropriate seal to ensure the required protection level (Qazizada and Pivarčiová, 2018).

The requirements of the working environment in which the device will operate also require that the device operates in the temperature range from –20 °C to +50 °C. This requirement is met by selecting the enclosure components that meet these criteria. Also, all electronic components were selected to ensure safe working temperature (in accordance with the ATEX Directive), taking into account the operating temperature of the device.

Due to the requirements of the ATEX Directive, the short-circuit current from the cells had to be limited. It was also important to connect the batteries to ensure a sufficiently high voltage supplied to the device. The batteries were therefore connected in series-parallel. The connection of two cells in series ensures that the power supply voltage is increased by doubling the voltage coming from a single cell and affects the reduction of short circuit current (in its calculation we take into account the double value of the cell internal resistance).

SSMS-C is characterized by the following operational parameters:

- ATEX parameters: I M1 Ex ia I Ma
- Ambient temperature: Ta = –20 °C ¸ +50 °C
- Protection class: IP65
- Power of the transmitter: 17 dBm (50 mW)
- Capacity: 4 x 3.6 V 17Ah.

SSMS-I module

Two-axis inclinometer SSMS-I (Fig. 5) is designed to be mounted on the components of powered roof support. The inclinometers are battery-powered (from the SSMS-C central unit, which is placed on each roof support), so there is no need to run power cables between the roof supports. Up to 6 inclinometers can be installed on one roof support.

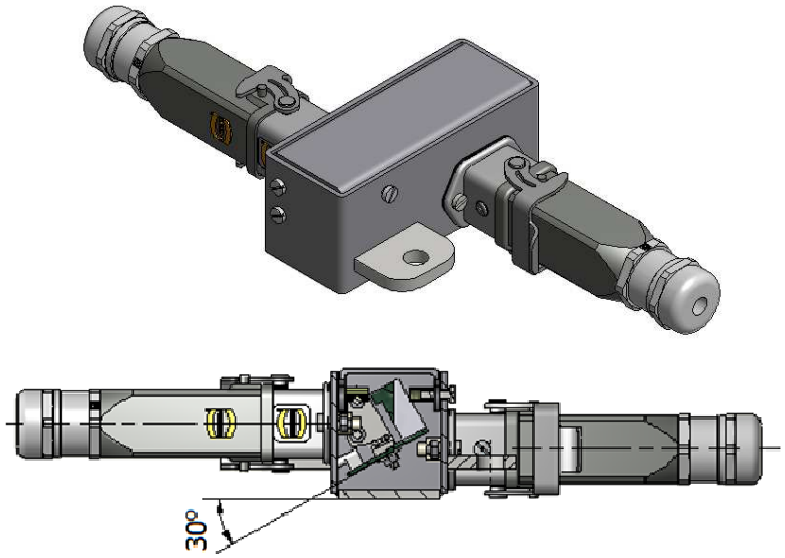

Fig. 5. SSMS-I inclinometer module

As in the case of the SSMS-C central unit, it was necessary to provide IP65 protection of the inclinometer enclosure against dust and water ingress, as it is designed to operate in underground mine conditions.

In order to increase the mechanical resistance, the inclinometer enclosure is made of steel. In order to ensure that the enclosure is waterproof and dust-proof, the SSMS-I enclosure was additionally sealed. The filler also acts as a heat dissipator for individual electronic components. The applied electronic components have been selected so as to meet the requirements of the ATEX Directive for equipment applied in the operating temperature range from –20 °C to +50 °C.

The use of a two-axis inclinometer allows determining the position of the enclosure assembly in two axes. One of them is the side tilting of the enclosure (the enclosure of the longwall complex is never horizontal). The inclination is an important parameter to determine the supporting capacity, which is determined in a direction parallel to the gravity force.

The analysis of the mechanized enclosure geometry showed that in some designs, during the operation, the bracket angle of inclination exceeded 90 °. In order to avoid such a situation, the printed circuit board with built-in inclinometers was inclined at the angle of 30 ° (Fig. 6). This also improves the measuring accuracy of the inclinometer. The SSMS-I inclinometer, designed and manufactured in this way, is shown in Figure 6.

Fig. 6. SSMS-I inclinometer module.

SSMS-I is characterized by the following operating parameters:

- ATEX parameters: I M1 Ex ia I Ma;
- Ambient temperature: Ta = –20 °C ¸ +50 °C;
- Protection class: IP65.

Tests

JZR 13/28 POZ shield support was tested (Fig. 7). Inclinometers were installed on the shield support using the magnetic mounting. Four SSMS-I inclinometers were installed – on the base, on the canopy, on the goaf shield and on the lemniscate linkage. Places of the inclinometers installation are presented in Figure 8. Data from the inclinometers were recorded using the computer programme developed especially for the tests. Sampling frequency was 500 ms.

Fig. 7. JZR 13/28 POZ shield support

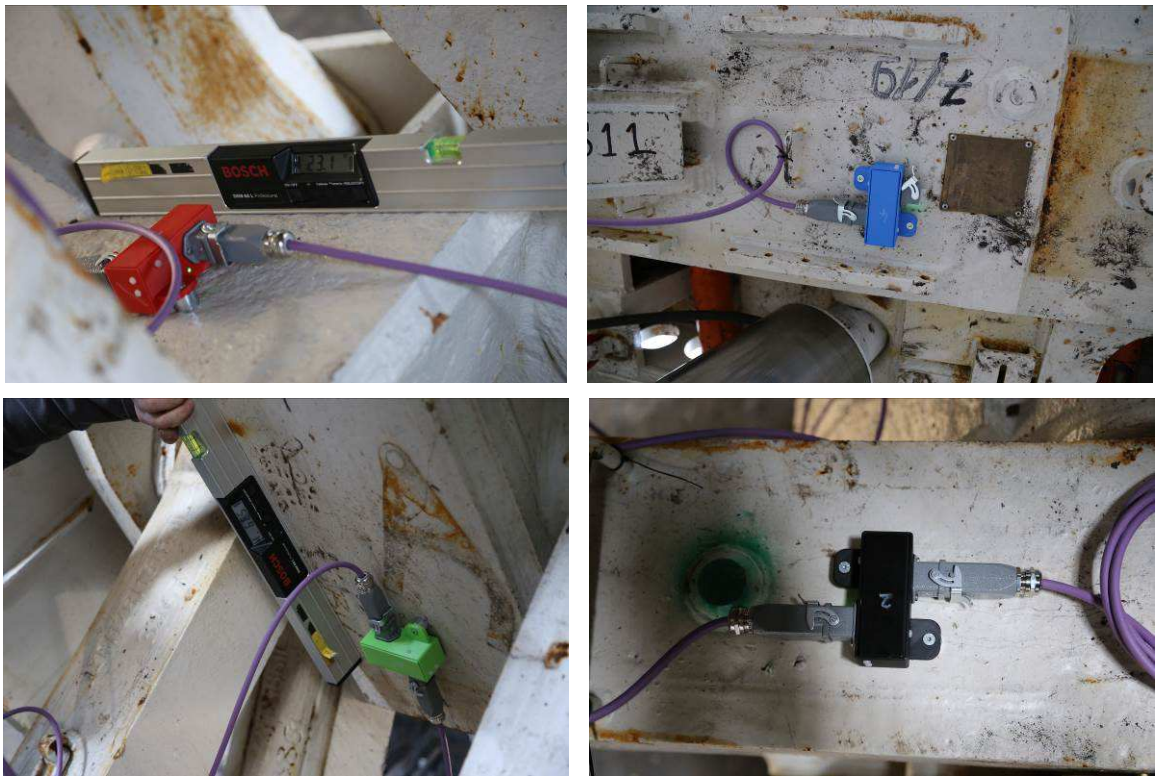

Fig. 8. Model of SSMS-I inclinometers: a) on the base, b) on the canopy, c) on the goaf shield, d) on the lemniscate linkage

Fig. 9. Test rig

The main purpose of the tests was to verify the correctness of inclinometer measurements in conditions close to real ones. The test rig was used for functional analysis of powered roof supports (Fig. 9). The test rig enables simulations of the roof support operation in inclined seams (up to 40 degrees), and roof support set up keeping the working pressure. The roof of the test rig is set up to the selected height and is locked with bolts, which creates a rigid frame structure in which the roof support is set up. The test's objective was to verify the correctness of readings in the case of roof support being set up against a rigid roof.

This process is associated with the elimination of backlash on powered roof support pins and roof locks (this process is often dynamic).

Figures 9, 10, 11 and 12 show the angles of the individual components of the shield support during the tensile test in the test rig - the nominal pressure in cylinders was assumed to be 24 MPa. The tests were started at the canopy placed in parallel to the rig roof in the distance of 20 cm.

The tests were conducted in five stages:

- Stage 1 - the shield support without any resistance travels through the empty space between the rig roof and the canopy (time period from 110th to 142nd seconds).
- Stage 2 - the time period between the canopy edge contact with the floor (142nd second) and the whole canopy plane contact (145th second).
- Stage 3 - pressing the canopy to the rig roof (145th second).
- Stage 4 – elimination of clearances - rapid adjustment of the shield support components (153rd second)
- Stage 5 - the shield support stabilization (153rd – 170th seconds).

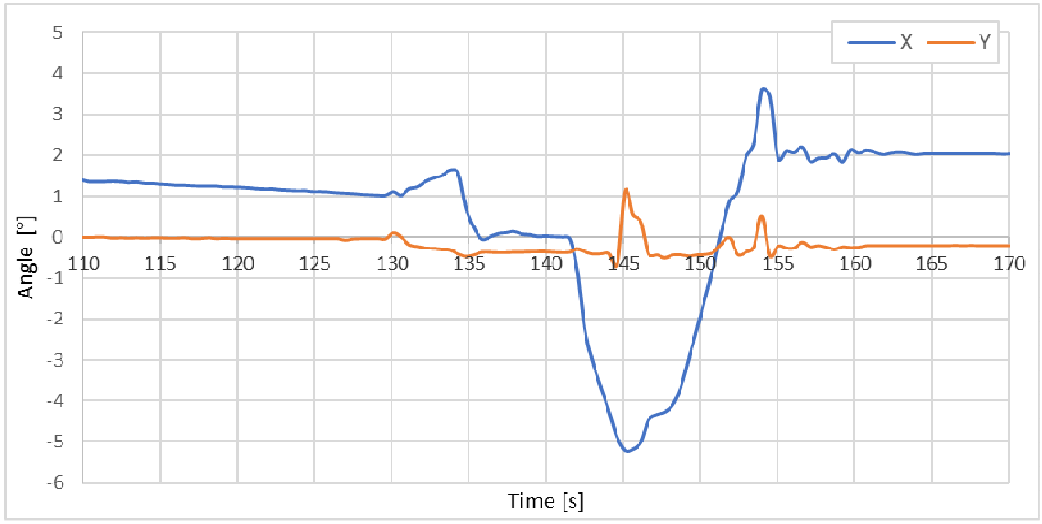

Fig. 9. The angle of the canopy during the tests

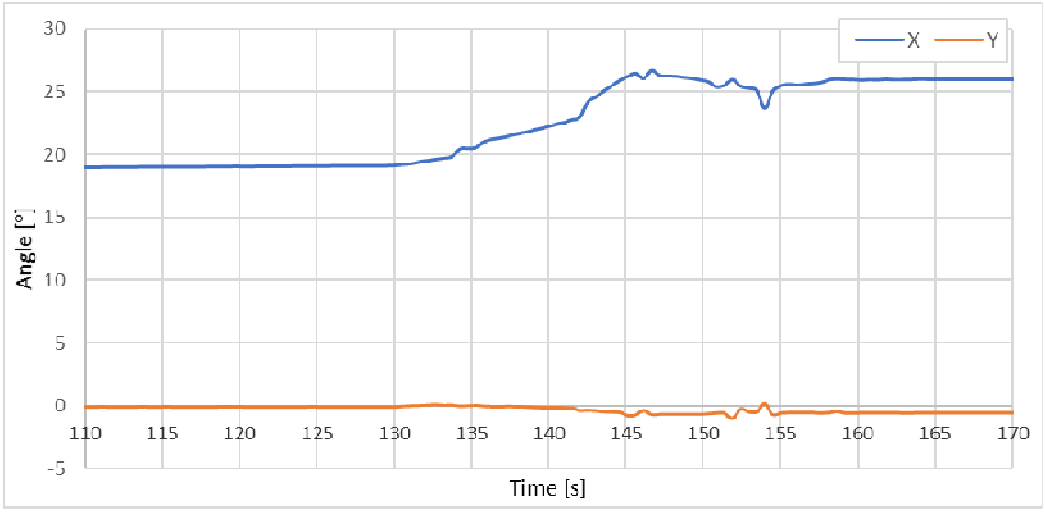

Fig. 10. The angle of the goaf shield during the tests

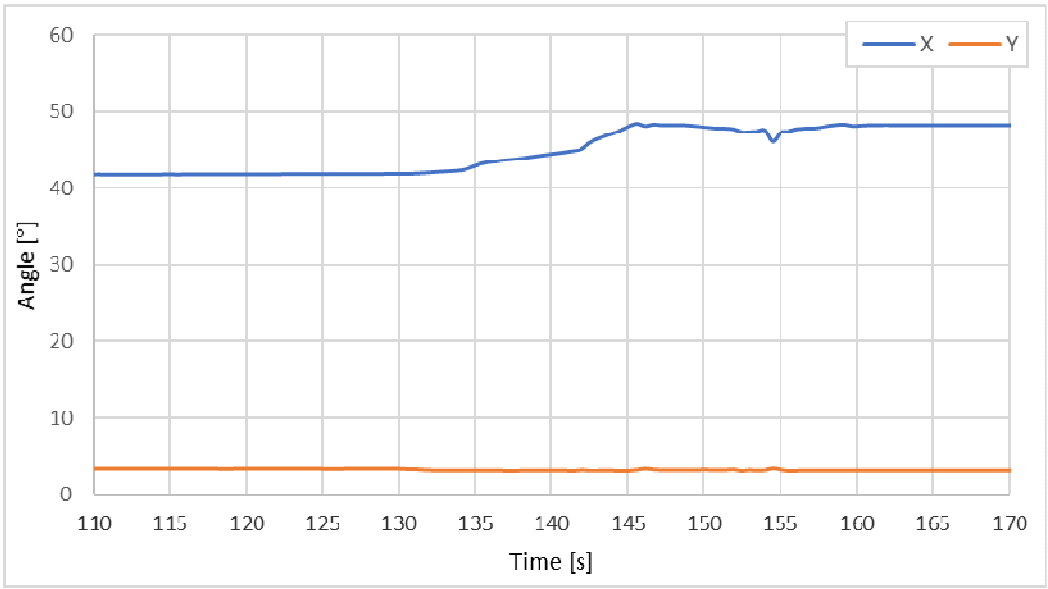

Fig. 11. The angle of the lemniscate linkage during the tests

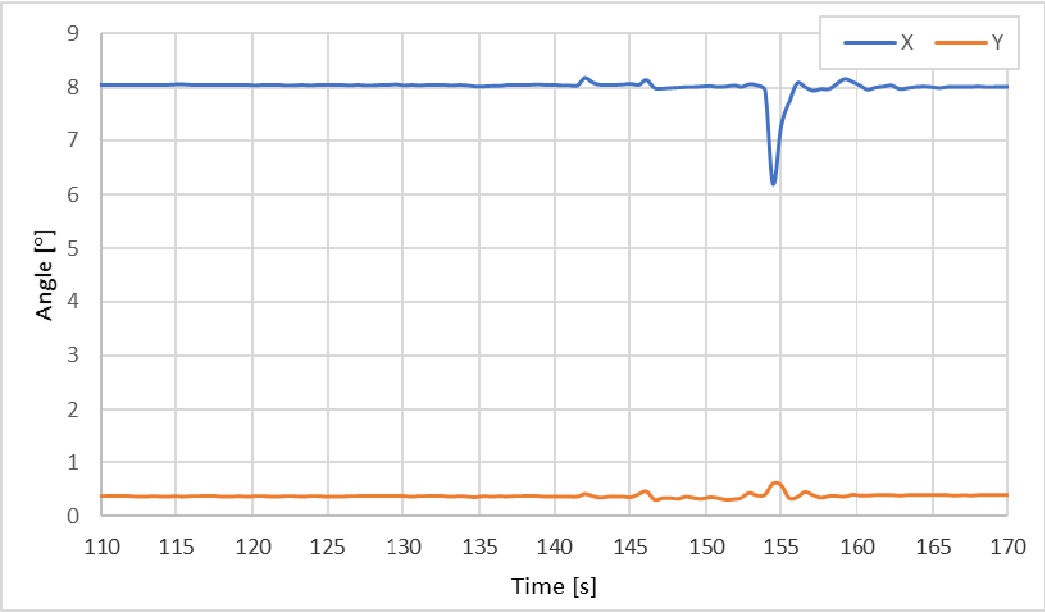

Fig. 12. The angle of the base during the tests

The results of the tests confirmed that the design of inclinometers and the applied algorithms of signal filtering are correct and resistant to dynamic phenomena. The measurement results presented on the chart were averaged through a low pass filter. There are no oscillations after the angle change and no vibrations from the dynamic removal of backlash in the tests of the powered roof supports.

Summary

It was assumed that monitoring and analysis of powered roof support operational parameters in real-time using SSMS enable to predict the hazards associated with the fall of roof rock. The KOMAG Institute of Mining Technology designed and made a geometry monitoring system based on inclinometers that meet the requirements of the ATEX Directive. System tests were carried out on a real object in laboratory conditions. The tests confirmed the correct operation of the SSMS system. The next step will be to make the prototype and install it in real mining conditions. The tests of the impact of clearances in structural nodes on the accuracy of the measurement system will also be carried out.

The aim of the research was to determine whether the applied filtration algorithms will allow monitoring the geometry in shield support in the case of dynamic changes. During the contact between the shield support canopy and the roof of the test rig, changes in the position of shield support components, resulting from an adjustment to the roof, took place and the shield support eliminated clearances on the connecting components (pins). In the case of monitoring the shield support geometry during operation, the support unit advancing process will be omitted - these changes will not affect long-term trends and can be regarded as interference.

Funding: *The research work undertaken in PRASS III (Productivity and safety of shield support), grant 752504 (2017) was supported by EU Research Fund for Coal and Steel (RFCS) as well as the Ministry of Science and Higher Education.*

References

ATEX Directive 2014/34/EU

Baranov, M., Bozek, P., Prajova, V., Ivanova, T., Novokshonov, D., and Korshunov, A. (2017). Constructing and calculating of multistage sucker rod string according to reduced stress. Acta Montanistica Slovaca, Vol. 22, Issue: 2, p 107-115

Bronya Wiklund, Mahmet S. Kizil, Ismet Canbulat (2011). Development of s cavity prediction model for longwall mining. Coal Operators' Conference 10-11 Ferbuary 2011. s.48-59

Herezy, Ł., Janik, D. and Skrzypkowski, K. (2018). Powered Roof Support – Rock Strata Interactions on the Example of an Automated Coal Plough System. Studia Geotechnica et Mechanica, 40(1): 46–55.

Jing Xuan Yang, Chang You Liu and Bin Yu (2017). The interaction between face support and surrounding rock and its rib weakening mechanism in hard coal seam. Acta Montanistica Slovaca Volume 22, number 1, 67-78

Jingyi Cheng, Zhijun Wan, and Yinlin Ji, (2018). Shield-Roof Interaction in Longwall Panels: Insights from Field Data and Their Application to Ground Control. Advances in Civil Engineering, vol. 2018, Article ID 3031714, 18 pages. https://doi.org/10.1155/2018/3031714.

Kalentev, E., Vaclav, S., Bozek, P., Tarasov, V. and Korshunov, A. (2017). Numerical analysis of the stress-strain state of a rope strand with linear contact under tension and torsion loading conditions. ADVANCES IN SCIENCE AND TECHNOLOGY-RESEARCH JOURNAL, Vol. 11, Issue: 2, p 231-239

Langosch, U., Ruppel, U., Wyink, U. (2003). Longwall roof control by calculation of the shield support requirements. In: Proceedings of the Coal Operators' Conference, 162–172

Qazizada, E. Pivarčiová, E. (2018). Reliability of parallel and serial centrifugal pumps for dewatering in mining process. Acta Montanistica Slovaca, Vol. 23, Issue 2, p. 141-152

Płonka, M. (2009). Zmienność obciążenia sekcji obudowy w ścianie zawałowej. Prace naukowe GIG Górnictwo i środowisko, kwartalnik, nr 1/2009. p. 41-49

Płonka, M. and Rajwa, S. (2018). Utrudnienia w prowadzeniu sekcji obudowy zmechanizowanej obserwowane podczas pracy w dolnym zakresie jej wysokości roboczej, Mining – Informatics, Automation and electrical Engineering 4 (536) 2018 p. 55-64

PRASS III project website: www.prass3.komag.eu

Prusek, S., Płonka, M. and Walentek, A. (2016). Applying the ground reaction curve concept to the assessment of shield support performance in longwall faces. Arab J Geosci. 9: 167. https://doi.org/10.1007/s12517-015-2171-2

Prusek, S., Rajwa, S., Wrana, A. and Krzemień, A. (2017). Assessment of roof fall risk in longwall coal mines, International Journal of Mining, Reclamation and Environment, 31:8, 558-574, DOI: 10.1080/17480930.2016.1200897

Rajwa, S., Prusek, S., Szuścik, J. and Gąska, R. (2017). Prowadzenie ściany pod gruzowiskiem zawałowym w warunkach zmiennej grubości pozostawionej warstwy przyspągowej, Przegląd Górniczy 6/2017 p. 33-37

Stankiewicz, K. (2018). Górnicze systemy sterowania i automatyzacji rozproszonej. Journal of Machine Construction and Maintenance. Nr 2/2018 (109). s. 117-122.

Szurgacz, D. and Brodny, J. (2019). Tests of Geometry of the Powered Roof Support Section. Energies, 12, 3945. https://doi.org/10.3390/en12203945

Szweda, S., Szyguła, M. and Mazurek, K. (2016). Czynniki wpływające na postać konstrukcyjną i parametry techniczne sekcji ścianowej obudowy zmechanizowanej. Część 1. Monografia Instytut Techniki Górniczej KOMAG, Gliwice 2016.

Szyguła, M. (2013). Rozwój konstrukcji sekcji obudowy zmechanizowanej w górnictwie węgla kamiennego w Polsce. Maszyny Górnicze nr 2/2013. s. 30-38.

Wang, J., Ning, J., Jiang, L., Jiang, J-Q., and Bu, T.. (2018). Structural characteristics of strata overlying of a fully mechanized longwall face: a case study. Journal of the Southern African Institute of Mining and Metallurgy, 118(11), 1195-1204. https://dx.doi.org/10.17159/2411-9717/2018/v118n11a10

Witek, M., Prusek, S. (2016). Numerical calculations of shield support stress based on laboratory test results. Computers and Geotechnics 72, p. 74–88

Verma, A.K., Kishore, K. and Chatterjee, S. (2016). Prediction Model of Longwall Powered Support Capacity Using Field Monitored Data of a Longwall Panel and Uncertainty-Based Neural NetworkGeotech. Geol Eng 34: 2033. https://doi.org/10.1007/s10706-016-0081-z

Yang, Y., Zeng, Q., Zhou, J., Wan, L., and Gao, K. (2018). The design and analysis of a new slipper-type hydraulic support. PLoS ONE 13(8):e0202431. https://doi.org/10.1371/journal.pone.0202431

Testing the selected parameters of conical picks

Beata Grynkiewicz-Bylina[1], Bożena Rakwic[1], Aleksey Shchenyatsky[2]

Conical picks are characterized by the structural and material parameters, affecting the effectiveness of mechanical mining of coal and rock with roadheaders and longwall shearers in mining plants. Unsatisfying the specific technical parameters of cutting tools by manufacturers, especially pick length and not proper type and quality of materials used for their manufacture may result in excessive asymmetric wear, break of holding part or fall out what means a necessity of their frequent replacement. There is no standardized method for assessing the cutting picks quality and durability. That is why, to reduce conical picks rate of wear, the scientific organizations have undertaken the research projects on new designs of cutting picks and materials for their manufacture as well as on the development of laboratory and computational methods for determination of conical picks rate of wear. Results of testing the cutting picks, used in roadheaders and longwall shearers, conducted according to the unique author's procedure, are presented. The test results indicate for the need of improving the methods for assessing the quality of cutting picks, especially in the scope of testing the connection of sintered carbide with a body of a cutting tool.

Keywords: *Conical picks, Sintered carbides, assessment of the quality*

Introduction

Mechanical mining based on the direct action of cutting drums of mining machines on solid coal is one of the methods for hard coal mining. Conical picks fixed to the drum of roadheaders and longwall shearers are commonly used (Kotwica, 2018; Krauze et al., 2009). The body of a cutting tool consists of a pick holder and a conically shaped working part with a carbide tip soldered to it. Cutting picks are exposed to high mechanical stresses and temperature, generated in the areas, where the cutting tool contacts the mined rock. This leads to relatively rapid wear, causing changes in both the geometrical shape and loss in sintered carbide mass and the working part (Barker et al., 1981; Krauze and Mucha, 2016; Baranov et al., 2017). It is also important to select the proper cutting picks for the specific design of mining drums, where inappropriate manufacturing and improper operation may contribute to mechanical damages, including excessive, and uneven abrasion as well as falling off or cracking the sintered carbide – Fig. 1.

Fig 1. Examples of conical picks used in the cutting drum of a roadheader withdrawn from operation

Such a failure causes a roadheader's break in the operation due to a replacement of cutting picks what results in significant financial losses in the mining plants (Biały and Beno, 2016; Biały, 2017; Biały and Fries, 2019; Bołoz, 2018).

In order to obtain proper durability of conical picks, the selection of their shape and type of the material used for their manufacture should be based on the analysis of geological and physical-mechanical properties of rocks (Biały, 2013; Biały, 2014), parameters and conditions of the cutting process and the cutting tool design (Gospodarczyk, 2013; Krauze and Bołoz, 2015).

[1] *Beata Grynkiewicz-Bylina, Bożena Rakwic*, Laboratory of Material Engineering and Environment, ITG KOMAG, Pszczyńska 37, 44-100 Gliwice, Poland, *bbylina@komag.eu, brakwic@komag.eu*
[2] *Aleksey Shchenyatsky*, Kalashnikov Izhevsk State University, Izhevsk, Russian Federation, *bkkupol@istu.ru*

The conical picks are made of sintered carbides of various grades, having high hardness, compressive strength as well as resistance to abrasion, to brittle fracture and high temperature (Ścieszka and Filipowicz, 2001). The bodies of the picks are made of steel of high impact strength by an increased content of manganese, molybdenum, chromium, nickel and boron. The steels are subjected to heat treatment, consisting of hardening and tempering to obtain hardness above 40 HRC and thus high resistance to abrasion. In the case of conical picks and working parts of the cutting tool bodies, their resistance to abrasion increases by padding the outer conical surface with abrasion-resistant materials (Krauze et al., 2016; Qazizada and Pivarčiová, 2018). It is also important to ensure the declared linear and angular parameters.

Due to the lack of a standardized method for assessing the quality and durability of conical picks, various test procedures were used, including those developed by the AGH University of Science and Technology and implemented in the selected mining plants (Krauze and Kotwica, 2007; Krauze et al., 2015; 2017b). Scientific papers focus on the design solutions of conical tool holders and methods for testing the rate of the tools' wear on the laboratory testing stands, as well as applying computational methods using the neural networks (Kotwica, 2015; Krauze et al., 2014; 2017a; Gajewski and Jonak, 2009; Božek and Pivarčiová, 2013). One of them (Bołoz, 2018) presents the results of the quality assessment of conical picks delivered to six mining plants in the form of public tender. They show the high quality of the conical picks as well as single cases of failure to meet the requirements of geometric parameters. The hardness of the pick holder and content of carbon, chromium and manganese in the material of the tools' bodies are the most common parameters that do not meet the requirements. There are, however, no literature data on the assessment of sintered carbide parameters, i.e. the degree of filling the soldering gap with solder and the embedment depth from the edge of the working part, having an important impact on the durability of carbide fixation in the cutting tool's holder.

The results of research work on assessing the geometrical parameters of conical picks and the properties of the materials used to manufacture them carried out at the KOMAG Institute (Grynkiewicz-Bylina and Rakwic, 2019), are given. They complement the state-of-the-art in the above-mentioned scope. The assessment of the degree of filling the soldering gap with solder and of the embedment depth of the sintered carbides from the edge of the working part is also presented.

Material and Methods

The research work was realized in four stages. In the first stage, the documentation from the conical picks tests, carried out in the KOMAG accredited Laboratory of Material Engineering and Environment within the years 2006-2017, was analyzed. The focus was on the conical picks. The geometrical parameters and properties of the materials used for their manufacture were tested. The assessment covered 10 types of conical picks, with sintered carbides of diameters from 18 to 25 mm and cutting tool lengths from 140 to 195 mm. The conical picks were delivered by six manufacturers, marked from A to F, and they were intended to be used in roadheaders (three types) and longwall shearers (seven types) – Fig. 2. In total 23 sets of conical picks, including twenty one-step and three two-step tools, were tested.

a/ conical pick used in cutting drum of a longwall shearer

b/ conical pick used in a roadheader's cutterhead

Fig. 2. Conical picks used in cutterheads of longwall shearers and roadheaders

In the second stage, on the basis of the test documentation, the following technical parameters of the conical picks, important for an assessment of their manufacture quality and durability, were specified:

- geometric parameters of the cutting tool, its working part and pick holder as well as of the sintered carbide,
- hardness, impact strength KCU/energy of impact test KV and tensile strength Rm of the working part,
- hardness and embedment depth of the sintered carbide from the edge of the working part and the degree of filling the soldering gap with solder.

The geometrical parameters of the cutting tool are marked in Fig. 3.

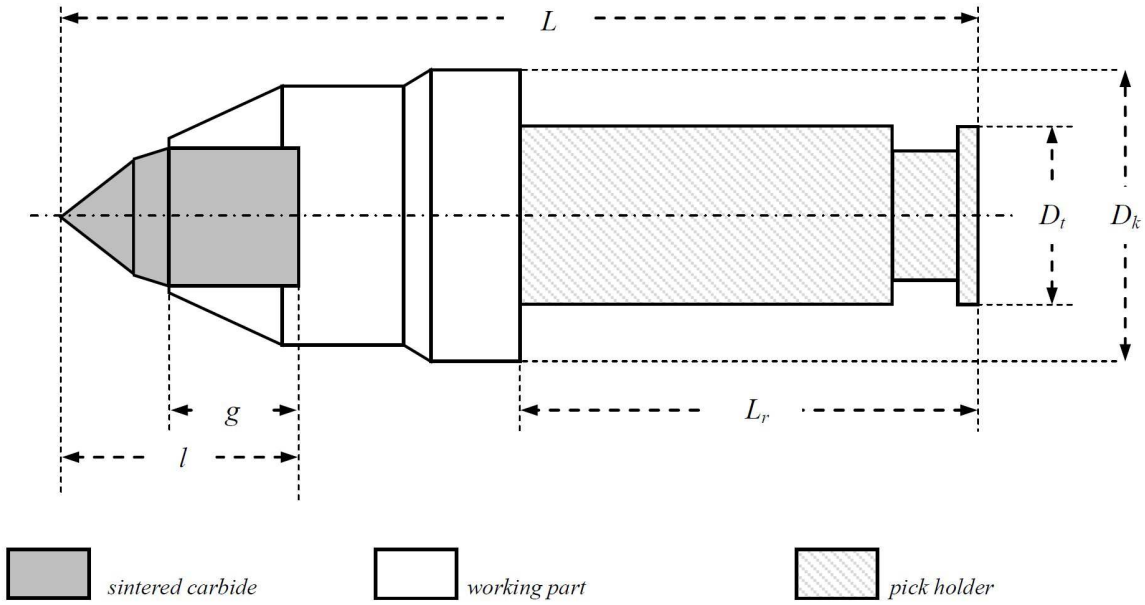

Fig. 3. The geometrical parameters of the cutting tool in the roadheader's cutterheads

In the third stage, the criteria for the assessment of conical picks were defined based on the analysis of the manufacturer's specifications and the requirements of the mining plants – Table 1.

Tab. 1. Criteria for the assessment of technical parameters of conical picks

Conical picks/pick component	**Technical parameters**		**Criteria for the assessment of technical parameters**
Conical pick	total length, L		deviation from the nominal dimension: ±1 mm
Working part of the pick body	length, L_r		
	flange diameter, D_k		
	hardness		from 40 to 46 HRC
	impact resistance / energy of impact	*KCU*	> 28 J/cm^2
		KV	> 25 J
	tensile strength R_m		> 1250 MPa
Pick holder	diameter, D_t		deviation from the nominal dimension: ±0.2 mm
Sintered carbides tip	degree of filling the soldering gap with a solder		> 90%
	embedment depth of the sintered carbide from the edge of the working part, g		> 22 mm for the sintered carbide insert of 25 mm dia
			> 19 mm for the sintered carbide insert of 22 mm dia
			> 12 mm for the sintered carbide insert of 18 mm dia
	length, l		> 37 mm for the sintered carbide insert of 25 mm dia
			> 34 mm for the sintered carbide insert of 22 mm dia
			> 27 mm for the sintered carbide insert of 18 mm dia
	hardness		> 1000 HV_{30}

The criteria for the assessment of geometric dimensions, including L, L_r, D_k, D_t and strength parameters, i.e. hardness of the working part of the body and the carbide as well as *KCU*, *KV* and R_m, were the same for all the tested conical picks. In the case of sintered carbide parameters, l and g, the criteria for their assessment depend on the sintered carbide diameter.

In the fourth stage, the results of the cutting tool tests were assessed. The tests were carried out in the KOMAG Laboratory and the following cooperating laboratories: Baildonit and ZDT-GLIMAG (Grynkiewicz-

Bylina and Rakwic, 2019; Božek and Pokorný, 2014). The testing procedure was developed by the paper authors – Fig. 4.

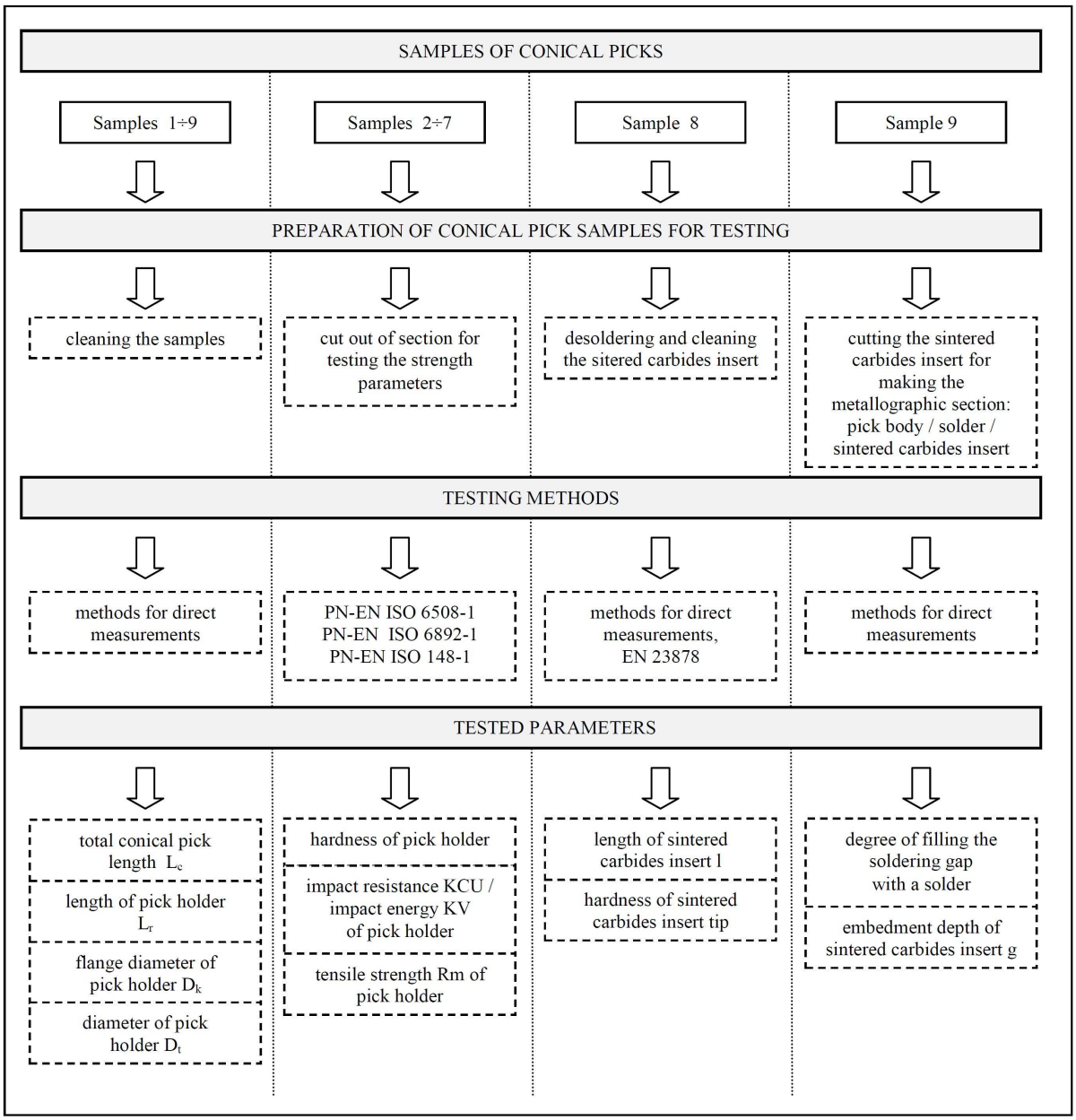

Fig. 4. Algorithm of the testing procedure of conical picks used in longwall shearers and roadheaders

Quality tests of each type of cutting tool were carried out on nine cutting tool samples marked by numbers from 1 to 9. Before taking measurements of the geometrical parameters of the tool's body, the samples were cleaned with petroleum ether. A 10 mm thick disc was cut from the working part of the sample No. 2. Then the sample was ground to obtain two parallel cross-section planes for measuring the hardness of the body material. For the tensile strength tests, two sections of dimensions according to the PN-EN ISO 6892-2 Standard were cut off from the working part of samples No. 3 and 4, and three sections with a notch U or V were cut off according to the PN-EN 148-1 Standard from the samples 5÷7 for impact resistance/energy of impact tests. For measurements of geometrical parameters (length and diameter) and hardness, the sintered carbide was desoldered from the sample No. 8 and cleaned from the solder.

For testing the degree of filling the soldering gap with solder and the embedment depth of sintered carbide from the edge of the working part of the cutting tool's body, a metallographic section of the cutting tool, solder and sintered carbide connection, obtained after cutting the sample No. 9 along its axis, were prepared.

The measurements of geometrical parameters of the bodies of conical picks and sintered carbides were taken using the direct methods. The degree of filling the solder gap was determined as the percentage share of the solder surface area in the solder gap surface area, subtracting the surface of the technological void. The surface area of the solder, voids and solder gap were calculated based on their edge length and their width, obtained from the stereoscopic microscope measurements. Measurement results for metallographic microsections of connection between the pick holder, solder and sintered carbides inserts made on two perpendicular cross-sections of the sample No. 9 along the symmetry axis, were averaged.

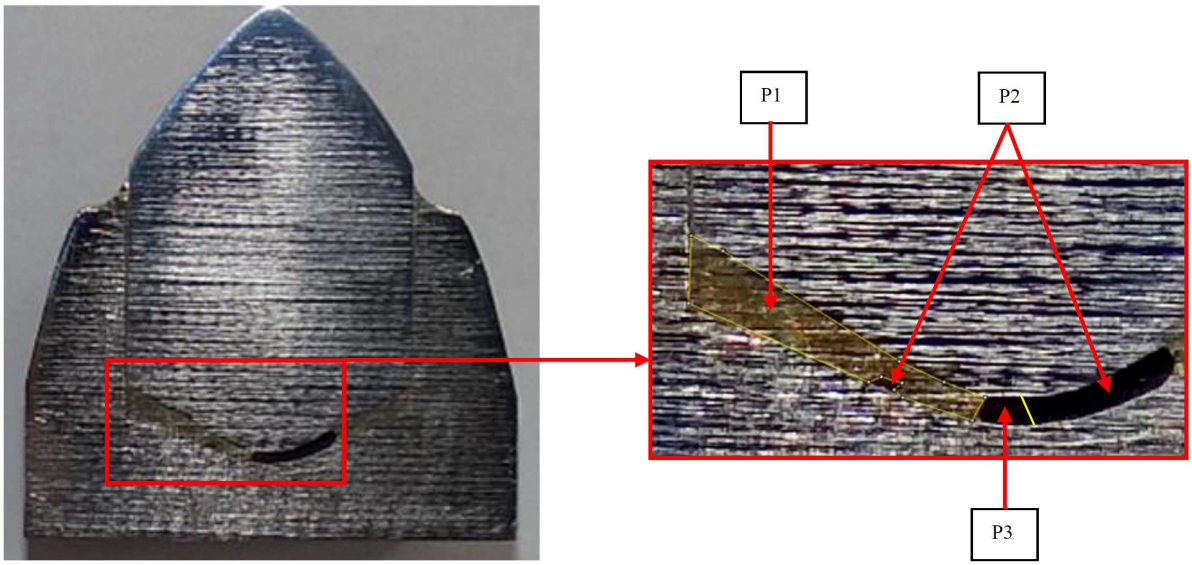

Fig. 5. Sample cross-section of roadheader's cutting tool used for determination of the degree of filling the solder gap symbols: P1 – solder, P2 – lack of solder, P3 – technological void

Tests of material properties of the conical picks holders and sintered carbides were conducted using the standardized methods. Hardness of the holder's material was measured according to the PN-EN ISO 6508-1 Standard using the Rockwell method, hardness of the sintered carbide was determined according to the EN 23878 Standard using the Vickers method, the tensile test was carried out according to the PN-EN ISO 6892-1 Standard, and the *KCU* impact test or the *KV* energy of impact test was conducted according to the PN-EN ISO 148-1 Standard.

The test results were assessed in Stage 4 according to the criteria set out in Stage 2. Based on the analysis of the results, the parameters of conical picks, which require a correction were pointed out.

Results and discussion

The tests showed that geometric parameters in the majority of samples of conical picks holders did not differ from the criteria specified in stage 2. Single cases which did not meet the accepted deviation in the total length of a cutting tool and in its working part as well as in the flange diameter and holding part for the manufacturers A and C, were reported.

Individual cases of failure to meet the above criteria were also found for the depth of sintered carbide embedment from the working edge. Two reported cases concerned the F cutting tool manufacturer.

The detailed results of testing the strength parameters of pick holders, hardness and length of sintered carbides and the degree of solder filling of the solder gap are presented in Table 2.

Tab. 2. Results of testing the strength parameters of conical picks, their hardness and length of combined carbides as well as the degree of solder filling of the solder gap

Markings of the conical picks				**Results of testing the pick holders**				**Results of testing the sintered carbides inserts**		
				strength to the tensile force R_m	**impact resistance *KCU***	**impact energy *KV***	**hardness**	**hardness**	**length**	**degree of solder gap-filling of the solder gap**
				[MPa]	[J/cm^2]	[J]	[HRC]	[HV30]	[mm]	[%]
Ø22 146/70/58/38/1	X	I	A	**1099.5**	-	**17.2**	45.0	1190	35.0	-
Ø22 146/70/58/38/2	X	I	A	**1046.5**	-	**17.5**	44.5	1240	35.0	-

Ø22 140/65/48/38/30/1	X	II	B	1435.5	-	45.0	44.0	1010	35.0	92.6
Ø18 169/89/48/30 /1	Y	I	B	1358.0	-	**14.0**	40.4	1010	27.7	90.2
Ø18 169/89/48/30 /2	Y	I	B	1310.5	-	28.7	43.6	1020	**25.4**	**83.3**
Ø25 147/70/58/38 /1	X	I	A	1260.0	39.7	-	47.6	1020	-	-
Ø22 144/64/48/30/1	X	I	C	**1119.5**	29.7	-	**38.0**	**950**	**32.0**	**39.1**
Ø22 189/92/59/38/1	X	I	C	**688.0**	40.4	-	**21.8**	**940**	**29.2**	**60.5**
Ø22 186/92/59/38/1	X	I	C	**1211.0**	32.7	-	**37.6**	**980**	**27.5**	**77.9**
Ø22 186/92/59/38/2	X	I	C	**1195.5**	-	**22.0**	**35.1**	1170	**25.6**	100.0
Ø22 144/64/48/30/2	X	I	B	1477.0	**25.8**	-	**46.6**	1200	35.1	99.0
Ø20 165/89/65/38/30/1	Y	II	A	**1161.5**	36.7	-	43.4	1120	-	99.5
Ø25 146/70/58/38/1	X	I	D	**1007.5**	37.5	-	**32.6**	1200	-	99.2
Ø18 195/102/55/35/1	Y	I	E	1695.5	39.8	-	44.0	1040	**24.0**	99.1
Ø22 189/92/59/38/2	X	I	A	1389.5	35.1	-	**51.2**	1230	34.3	93.4
Ø18 195/102/55/35/2	Y	I	F	1408.5	48.2	-	44.0	1030	27.1	98.5
Ø20 165/89/65/38/30/2	Y	II	A	**1224.0**	40.7	-	**38.6**	1000	-	92.1
Ø22 144/64/48/30/3	X	I	B	1300.5	50.8	-	42.6	1180	35.4	93.7
Ø22 189/92/59/38/3	X	I	A	1324.0	36.6	-	41.8	1130	35.3	91.9
Ø22 189/92/59/38/4	X	I	F	1544.5	**22.7**	-	46.5	1120	34.2	95.2
Ø22 189/92/59/38/5	X	I	F	**1143.0**	46.1	-	**33.5**	1110	**31.1**	98.7
Ø22 189/92/59/38/6	X	I	F	**1140.0**	**23.5**	-	**35.5**	1150	**31.1**	97.4
Ø22 189/92/59/38/7	X	I	F	**1068.5**	53.3	-	**34.1**	1150	34.3	**74.2**

Symbols: X – conical picks for roadheaders, Y – conical picks for shearers, I – one-step conical picks, II – two-step conical picks, A÷F – manufacturers.

The tests showed that:

- materials for conical picks had high tensile strength from 688.0 MPa to 1695.5 MPa, impact resistance from 22.7 to 50.8 J/cm^2, the energy of impact test from 14 to 45 J and hardness from 21.8 to 51.2 HRC,
- the hardness of sintered carbides varied from 940 to 1240 HV,
- length of sintered carbides varied from 24.0 to 35.4 mm,
- degree of solder filling of the solder gap varied from 39.1 to 100.0%.

The analysis of the test results showed that:

- materials for pick holders in 52% of the tested conical picks did not meet the required tensile strength, in 18% - impact resistance, in 67% – energy of impact test,
- 39% of tested pick holders had hardness below the required one and 9% above it,
- 13% of tested sintered carbides did not meet the criteria regarding the hardness, 44% regarding the length and 25% regarding the degree of solder filling of the solder gap.

The inconsistencies mentioned above concerned the conical picks of all manufacturers.

Conclusions

Technical parameters of conical picks, including the geometric ones as well as types and properties of materials used for their manufacture, specified at the cutting drums designing stage, have a decisive impact on their life during rocks cutting.

Excessive and uneven abrasion as well as falling out of sintered carbides are the most frequent mechanical damages to conical picks. These disadvantages can be caused by the insufficient hardness of the pick holder material, improper length of sintered carbides and their embedment depth from the working edge as well as by the insufficient degree of solder filling of the solder gap. The authors' test results confirm (Bołoz, 2018; Kalentev et al., 2017) that the manufacturers control geometric parameters of pick holders. However, the problem is with meeting the requirements concerning the properties of the materials used for the manufacture of conical picks, especially their hardness. Thus, it is indispensable to extend the scope of controlling the quality of conical picks manufacture by the control of materials, delivered by steel and sintered carbides manufacturers, in the independent laboratories and to avoid assessing them based only on the materials attestation approvals.

The authors show that the procedures for assessing the quality of conical picks, implemented in the mining plants, including the method developed at the AGH University of Science and Technology, should be complemented by an assessment of the parameters of the connection between sintered carbide and pick holder. Especially the solder filling degree of the solder gap should be assessed. For that purpose, the method, suggested by the authors in their testing procedure, can be implemented.

References

Baranov M., Božek P., Prajová V., Ivanova T., Novokshonov D. and Korshunov A. (2017). Constructing and calculating of multistage sucker rod string according to reduced stress. Acta Montanistica Slovaca Volume 22, number 2, 107-115

Barker R.H., Jones G.J., Hardman D.R. (1981). An Assessment of Pick Wear and its Effect of Continuous Miner Performance. Chamber of Mines of South Africa.

Biały W. (2013) New devices used in determining and assessing mechanical characteristics of coal. 13th SGEM GeoConference on Science and Technologies In Geology, Exploration and Mining, SGEM2013 Conference Proceedings, June 16-22, 2013, Vol. 1, BUŁGARIA ISBN 978-954-91818-7-6/ISSN 1314-2704. s. 547-554.

Biały W. (2014) Coal cutting force measurment systems – (CCFM). 14th SGEM GeoConference on Science and Technologies In Geology, Exploration and Mining, SGEM2014 Conference Proceedings, June 17-26, 2014, Vol. III, BUŁGARIA ISBN 978-619-7105-09-4/ISSN 1314-2704. s. 91-98.

Biały W. and Beno P. (2016). Application of quality engineering in assessment of mining technical equipment failure. Mm Science Journal 2016(04):1127-1133. DOI: 10.17973/MMSJ.2016_10_201682

Biały W. (2017) Application of quality management tools for evaluating the failure frequency of cutter-loader and plough mining systems. Archives of Minning Sciences, Volume 62, issue 2, 2017. pp. 243-252. ISSN 0860-7001. DOI 10.1515/amsc-2017-0018

Biały, W. and Fries, J. (2019) Computer systems supporting the management of machines/equipment in hard coal mines Case study. Management Systems in Production Engineering, 27(3), pp. 138-143.

Bołoz Ł. (2018). Results of a study on the quality of conical picks for public procurement purposes. Proceedings of the international conference on Human safety in work environment: operating machinery and equipment: integrated management systems: quality - environment - safety 23-27 October 2018 Gdańsk – Nynashamn - Sztokholm – Tallin – Sztokholm – Nynashamn – Gdańsk pp. 687-693. DOI: https://doi.org/10.2478/ntpe-2018-0087

Božek P. and Pivarčiová E.(2013). Flexible manufacturing system with automatic control of product quality. StrojarstvoVolume 55, Issue 3, April 2013, pp. 211-221

Božek P. and Pokorný P. (2014). Analysis and evaluation of differences dimensional products of production system. Applied Mechanics and Materials, Volume 611, 2014, Pages 339-345.

Gajewski J. and Jonak J. (2009). Research on rotating tangent cutters wear. Motrol 11c p40-50 (in Polish).

Gospodarczyk P., Kotwica K., Stopka G. (2013). A new generation mining head with head with disc tool of complex trajectory. Arch. Min. Sci., 58 (4) (2013), pp. 985-1006. DOI: 10.2478/amsc-2013-0069

Grynkiewicz-Bylina B. and Rakwic B. (2019). Testing the conical picks. Research project (Gliwice: KOMAG Institute of Mining Technology) (not published).

Kalentev, E., Václav, Š., Božek, P., Korshunov, A. and Tarasov, V. (2017). Numerical analysis of the stress-strain state of a rope strand with linear contact under tension and torsion loading conditions. In Advances in Science and Technology Research Journal. Vol. 11, iss. 2, pp. 231-239.

Kotwica K. (2015). New solutions of mining tools and rotary-tangential picks holders for roadheaders mining heads. Napędy i sterowanie 4 pp122-127 (in Polish).

Kotwica K. (2018). Atypical and innovative tool, holder and mining head designed for roadheaders used to tunnel and gallery drilling in hard rock. Tunnelling und Underground Space Technology 82 (2018) 493-503. https://doi.org/10.1016/j.tust.2018.08.017.

Krauze, K. and Kotwica, K. (2007). Selection and underground tests of the rotary tangential cutting picks used in cutting heads of the longwall and roadway miners. Archives of Mining Sciences, 2007, Vol. 52, No. 2, pp. 195-217. ISSN 0860-7001. https://pdfs.semanticscholar.org/e922/389078db4d1c5c68e3ffbfaa75c5415a5058.pdf

Krauze K. and Bołoz Ł. (2015). Cutting head used for mechanical mining of hard rocks. Cuprum – Czasopismo Naukowo-Techniczne Górnictwa Rud 4(77) pp. 169-180.

Krauze K., Bołoz Ł., Stopka G. and Wydro T. (2009). Use of new cutting tools for mining of hard rock grades Problems of safety in manufacture and operation of mining machines and equipment in the underground mining industry. Monograph ed K Krauze (Lędziny Kraków: Centrum Badań i Dozoru Górnictwa Podziemnego Sp. z o.o.) chapter 7 pp 95-105 (in Polish).

Krauze K., Bołoz Ł. and Wydro T. (2015). Parametric factors for the tangential-rotary picks quality assessment Arch.Min.Sci. 60(1) pp. 265-281. DOI: 10.1515/amsc-2015-0018

Krauze K., Bołoz Ł. and Wydro T. (2017a). Quality assessment of tangential-rotary picks with parametric factors Polish Mining Review T.73 nr 6 pp1-8 (in Polish).

Krauze K., Bołoz Ł., Wydro T. and Mucha K. (2017b). Durability testing of tangential-rotary picks made of different materials Mining – Informatics, Automation and Electrical Engineering No. 1(529) pp. 68-76. DOI: dx.doi.org/10.7494/miag.2017.1.529.68

Krauze K., Kotwica K. and Bołoz Ł. (2014). Determination of parameters for impact and rotation picks in the aspects of hazard reduction during mining of cohesive hard rocks Mechanization, automation and robotization in the mining industry. Monograph ed K Krauze (Lędziny Kraków: Centrum Badań i Dozoru Górnictwa Podziemnego Sp. z o.o.) chapter 14 pp 143-154 (in Polish).

Krauze K. and Mucha K. (2016). The increasing wear resistance of cutting picks Polish Mining Review T.72 nr 1 pp 63-67 (in Polish).

Krauze K., Skowronek T. and Mucha K. (2016). Influence of the hard-faced layer welded on tangential-rotary pick operational part on to its wear rate Arch.Min. Sci. 61(4) pp. 779-792. DOI: 10.1515/amsc-2015-0018.

Qazizada E. and Pivarčiová E. (2018). Reliability of parallel and serial centrifugal pumps for dewatering in mining process. Acta Montanistica Slovaca Volume 23 (2018), number 2, 141-152.

Ścieszka S. F. and Filipowicz K. (2001). Materials for mining tools – New trends in testing technology Monograph (Gliwice: Wydawnictwo Politechniki Śląskiej) (in Polish).